DIGITAL ACCESS TO SCHOLARSHIP AT HARVARD
DASH.HARVARD.EDU

HARVARD LIBRARY
Office for Scholarly Communication

The Role of Catalyst-Catalyst Interactions in Asymmetric Catalysis with (salen)Co(III) Complexes and H-Bond Donors

Citation

Ford, David Dearborn. 2013. The Role of Catalyst-Catalyst Interactions in Asymmetric Catalysis with (salen)Co(III) Complexes and H-Bond Donors. Doctoral dissertation, Harvard University.

Permanent link

http://nrs.harvard.edu/urn-3:HUL.InstRepos:11169772

Terms of Use

This article was downloaded from Harvard University's DASH repository, and is made available under the terms and conditions applicable to Other Posted Material, as set forth at http://nrs.harvard.edu/urn-3:HUL.InstRepos:dash.current.terms-of-use#LAA

Share Your Story

The Harvard community has made this article openly available.
Please share how this access benefits you. Submit a story .

Accessibility

The Role of Catalyst-Catalyst Interactions in Asymmetric Catalysis with (salen)Co(III) Complexes and H-Bond Donors

A dissertation presented

by

David Dearborn Ford

to

The Department of Chemistry and Chemical Biology

in partial fulfillment of the requirements

for the degree of

Doctor of Philosophy

in the subject of

Chemistry

Harvard University

Cambridge, Massachusetts

August 2013

© 2013 David Dearborn Ford

All rights reserved.

Dissertation Advisor: Eric N. Jacobsen *David Dearborn Ford*

The Role of Catalyst-Catalyst Interactions in Asymmetric Catalysis with (salen)Co(III) Complexes and H-Bond Donors

Abstract

In asymmetric catalysis, interactions between multiple molecules of catalyst can be important for achieving high catalyst activity and stereoselectivity. In Chapter 1 of this thesis, we introduce catalyst-catalyst interactions in the context of the classic Kagan nonlinear effect (NLE) experiment, and present examples of the strengths and drawbacks of the NLE experiment. For the remainder of the thesis, we explore catalyst-catalyst interactions in the context of two different reactions. First, in Chapter 2, we apply a combination of reaction kinetics and computational chemistry to a reaction that is well known to require the cooperative action of two molecules of catalyst: the (salen)Co(III)-catalyzed hydrolytic kinetic resolution (HKR) of terminal epoxides. In our investigation, we demonstrate that stereoselectivity in the HKR is achieved through catalyst-catalyst interactions and provide a model for how high selectivity and broad substrate scope are achieved in this reaction. In Chapter 3, we focus our attention on the thiourea-catalyzed enantioselective alkylation of α-chloroethers with silyl ketene acetal nucleophiles, a reaction that was not known to require the cooperative action of two molecules of catalyst at the outset of our investigation. By using a wide range of physical organic chemistry tools, we established that the resting state of the optimal thiourea catalyst is dimeric under typical reaction conditions, and that two molecules of catalyst work cooperatively to activate the α-chloroether electrophile. The implications of this mechanism for catalyst design are discussed.

Table of Contents

Acknowledgements

First of all, I would like to thank Eric Jacobsen for providing a wonderful environment to perform mechanistic research. The Jacobsen group is an incredibly intellectually rich environment. Over the past five years, Eric has taught me much about how to think about and perform science. I thank him for giving me the level of freedom to pursue the research presented in this thesis, even when it didn't seem like it was leading anywhere. I also want to thank Nicole Minotti for keeping the lab running smoothly. No mean feat to be sure!

I would also like to thank my committee members, Tobias Ritter and Ted Betley. Prof. Ritter has had a way of asking great questions during my GAC meetings that kept me on my toes and forced me to challenge assumptions in my research. I want to thank Prof. Betley for providing me candid career advice and for making himself available for discussions about the electronic structure of (salen)Co(III) complexes. His insights allowed me to approach the study presented in Chapter 2 of this thesis with a level of rigor that I am very happy with.

I was inspired to pursue my graduate studies by the wonderful experiences I had doing research as an undergrad. My first experience with research was in Mike Imperiale's lab at the University of Michigan, working with Johanna Abend, a graduate student in his lab. They both taught me a lot about biology and about science in general. My experiences in the Imperiale lab led me to decide to go to graduate school. My second experience with research was at the Molecular Foundry at Lawrence Berkeley National Lab, where I worked for Ron Zuckermann. Ron really took an interest in helping me learn about chemistry, and for that I am deeply appreciative. Two postdocs from the Bertozzi lab, Kamil Godula and Ramesh Jasti, set a great example for me and my fellow undergrad Adam Weinstein, and they went out of their way to

make sure we were learning as much as possible. It's been inspiring to watch them pursue their careers.

I have had the pleasure of sharing my time in the Jacobsen group with a number of extremely talented graduate students. There is no chance that I will be able to do justice to all of them in this acknowledgement. You are all amazing. That said, I do want to acknowledge a few people specifically. First, I would like to thank Stephan Zuend, with whom I overlapped for the first year of my time at Harvard. By teaching and by example, Stephan showed me how to attack mechanistic problems using experiment and calculations. I would also like to thank Lars Nielsen, who, along with Stephan Zuend, did the beautiful work that set the stage for the computational analysis presented in Chapter 2 of this thesis. I also learned a great deal about mechanistic study from Chris Uyeda, who was my baymate from my rotation in the group until his graduation. We also shared teaching fellow responsibilities for the physical-organic class Chem 205 during my second year here, and that was a fantastic experience for me as a junior graduate student. Meredeth McGowan, Rebecca Loy, and Bekka Klausen rounded out the corps of senior graduate students when I joined, and I learned a lot from all of them.

I want to thank the members of my class, Jim Birrell and Song Lin, and the members of the class above us, Adam Brown and Naomi Rajapaksa. The five of us were very close for all of our time in graduate school, and in addition to being Adam's and Jim's roommate for two years each, all five of us spent a lot of time together inside lab and out. Andreas Rötheli is another honorary member of our class who joined at the beginning of my second year. I don't really want to contemplate what grad school would have been like if I hadn't shared it with this cohort. I am excited to see where their talents take them. I am also looking forward to seeing where the younger students in the group take it in the years to come.

I have also had the pleasure of working with a number of extremely talented post-doctoral researchers in our group. In particular, Dan Lehnherr has been my collaborator for nearly three years now. His relentless enthusiasm has been a real boon to the project presented in Chapter 3 of this thesis, and I am excited to see where his efforts in the development of linked thiourea catalysts will lead. I have been impressed by his ability to absorb so much of the knowledge in our group. Other post-docs who made a particularly big impact on my time here include Cheyenne Brindle, Ellie Beck, Noah Burns, Jean-Nicolas Desrosiers, Eric Fang, Sean Kedrowski, Rob Knowles, Corinna Schindler, Dave Stuart, Gemma Veitch, and Mary Watson. The extremely high caliber of the postdocs in the Jacobsen group is a big part of what makes the lab run at such a high level and I am indebted to each of them for sharing their knowledge with me.

I have also greatly enjoyed interacting with students and postdocs in other groups in my time at Harvard. Eugene Kwan has been a great sounding board for ideas about science, and we've enjoyed climbing and skiing a great deal as well. I have greatly enjoyed exchanging ideas and drinking craft beers with Dave Powers. I've also enjoyed blowing off steam by climbing and skiing with Jon Mortison and Jessica Wu.

Finally, I would like to thank my girlfriend Nicole and my family for their love and support. Getting through graduate school would have been much, much more difficult without them.

List of Abbreviations

Ac	acetyl
atm	atmosphere
ATR	attenuated total reflectance
AU	atomic units; Hartrees for energies
B3LYP	Hybrid DFT functional using Becke 88 for exchange and the LYP correlation functional
BINAP	2,2'-Bis(diphenylphosphino)-1,1'-binaphthyl
BINOL	1,1'-bi-2-napthol
Boc	*t*-butyl carbamate
BP86	DFT functional using the Becke 88 exchange functional and the Perdew 86 correlation functional
Bu	butyl
c-Hex	cyclohexyl
DET	diethyl tartrate
DFT	density functional theory
DIPEA	diisopropylethylamine
DKEE	dynamic kinetic enantiomeric enhancement
DKR	dynamic kinetic resolution
DMAP	4-dimethylaminopyridine
DMPU	1,3-dimethyl-3,4,5,6-tetrahydro-2(1*H*)-pyrimidinone
EDC•HCl	1-3(dimethylamino)propyl)-3-ethyl-carbodiimide hydrochloride
ee	enantiomeric excess
EPR	electron paramagnetic resonance
er	enantiomeric ratio
ESI	electrospray ionization
Et_2O	diethyl ether
Et_3N	triethylamine
EtOAc	ethyl acetate

equiv	equivalents
EXSY	EXchange SpectroscopY
FTIR	Fourier-transform infrared
GC	gas chromatography
H-bond	hydrogen bond
HBTU	*O*-(Benzotriazol-1-yl)-*N,N,N′,N′*-tetramethyluronium hexafluorophosphate
HKR	hydrolytic kinetic resolution
HPLC	high performance liquid chromatography
HR	high-resolution
KIE	kinetic isotope effect
LC	liquid chromatography
LR	low-resolution
LYP	the Lee–Yang–Parr correlation functional
M05, M06	two of Truhlar's Minnesota functionals
Me	methyl
MO	molecular orbital
MS	mass spectrometry
NLE	nonlinear effect
NMR	nuclear magnetic resonance
NaOMe	sodium methoxide
NOESY	Nuclear Overhauser Effect SpectroscopY (an NMR experiment)
OLYP	DFT functional using the OPTX exchange functional and the LYP correlation functional
Ph	phenyl
Pr	propyl
PW91	the Perdew–Wang 91 DFT functional
RMSD	root-mean-square deviation
RO-DFT	restricted open shell DFT
rt	room temperature

salen	ligand formed by the condensation of two equiv of a salicylaldehyde derivative with a diamine
SCF	self-consistent field
SIR	selective inversion-recovery
TBHP	*tert*-butyl hydroperoxide
TBME	*tert*-butylmethyl ether
TBS	*tert*-butyldimethylsilyl
THF	tetrahydrofuran
TMAC	tetramethylammonium chloride
TMS	trimethylsilyl
TPSSh	hybrid DFT functional based on the Tao–Perdew–Staroverov–Scuseria functional
TOCSY	TOtal Correlation SpectroscopY
TOF	time-of-flight
Ts	toluenesulfonyl; tosyl
U-DFT	unrestricted DFT

Chapter 1

Beyond Nonlinear Effects: Deconvoluting Catalyst-Catalyst Interactions in Asymmetric Catalysis

1.1 Introduction

In 1986, Kagan and coworkers demonstrated that interactions between catalyst molecules can lead to a nonlinear relationship between the enantiomeric purity of the product of a catalytic reaction and the enantiomeric purity of the catalyst itself.[1] They termed this phenomenon a nonlinear effect (NLE) and since then, determining the relationship between catalyst e.e. and product e.e. has been used extensively as a probe for catalyst-catalyst interactions.[2] NLEs come in two basic forms: a *positive nonlinear effect* describes a situation in which enantioselectivity lies above the linear relationship, whereas a *negative nonlinear effect* describes the opposite situation. The presence of an NLE is a versatile readout for stereochemically dependent interactions between catalyst molecules, and critically, it tests for these interactions regardless of

[1] Puchot, C.; Samuel, O.; Dunach, E.; Zhao, S.; Agami, C.; Kagan, H. B. *J. Am. Chem. Soc.* **1986**, *108*, 2353–2357.

[2] (a) Girard, C.; Kagan, H. B. *Angew. Chem. Int. Ed.* **1998**, *37*, 2922–2959. (b) Kagan, H. B. *Synlett* **2001**, 888–899. (c) Satyanarayana, T.; Abraham, S.; Kagan, H. B. *Angew. Chem. Int. Ed.* **2009**, *48*, 456–494.

whether they are in the catalyst resting state, or the turnover-limiting transition state. This feature is valuable because it allows a chemist to assay for unexpected catalyst-catalyst interactions without having any preconceived notion of what they might be. There is a flipside to the unbiased nature of the NLE, however: it can be difficult to use the data to gain understanding of the underlying catalyst-catalyst interactions.

Drawing conclusions about the nature of the catalyst-catalyst interactions based on a NLE and incomplete mechanistic data is particularly tempting in situations where there is an accepted mechanism for how catalysts might interact with one another, but this practice can lead to misleading results. For example, a positive NLE in proline-catalyzed aldol reactions was long thought to support a theory of cooperative action of two molecules of proline.[1,3] It was later shown through the use of kinetics experiments that only one molecule of proline is involved and that the NLE observed initially was the result of incomplete dissolution of the proline catalyst.[4] The proline crystals that did not dissolve consisted of a 1:1 mixure of L- and D-proline, leading to an increased e.e. of proline in solution, and an increase in the enantioselectivity of the reaction.[5] No NLE is observed under homogeneous reaction conditions.[4,5] In another example, the (tartrate)Ti-catalyzed enantioselective oxidation of sulfides was thought to involve an active catalyst with the stoicheometry $Ti_2(tartrate)_4$. The presence of a distinctive relationship between diethyl tartrate e.e. and sulfoxide product e.e. that fit this model was taken as evidence in support of this theory.[1,3] It was later shown that the observed NLE in the sulfide oxidation is due to a kinetic resolution of the sulfoxide product to form the corresponding sulfone. This results in an

[3] Guillaneux, D.; Zhao, S. H.; Samuel, O.; Rainford, D.; Kagan, H. B. *J. Am. Chem. Soc.* **1994**, *116*, 9430–9439.

[4] Hoang, L.; Bahmanyar, S.; Houk, K. N.; List, B. *J. Am. Chem. Soc.* **2003**, *125*, 16–17.

[5] Klussmann, M.; Iwamura, H.; Mathew, S. P.; Wells, D. H.; Pandya, U.; Armstrong, A.; Blackmond, D. G. *Nature* **2006**, *441*, 621–623.

upgrade in e.e. at the expense of yield of sulfoxide. No NLE is observed for sulfoxide formation if the reaction is quenched before sulfone is observed.[6] Furthermore, the presence of an NLE does not prove that catalyst-catalyst interactions play a role in preparative reactions performed with enantiopure catalyst.[7]

Considering these examples and others, one must be very careful to ascribing an NLE to a specific catalyst-catalyst interaction without experimental evidence for the presence of that interaction. It is critical to determine the resting state stoichiometry of the catalyst as well as the kinetic order in the catalyst before drawing any conclusions about the origin of an NLE.[8] In this chapter, we present examples of the basic ways that two molecules of catalyst can interact with one another under the conditions of asymmetric catalysis. In addition, we discuss the physical-organic tools that can be used to distinguish between these possibilities, which we have organized according to the molecularity of the catalyst resting state and of the turnover-limiting transition structure. While all of the reactions discussed below exhibit nonlinear effects, we do not focus our attention on the quantitative models to fit those NLEs, as this topic has received attention elsewhere.[2,8] In this chapter we focus our attention on systems with demonstrable catalyst-catalyst interactions under preparative conditions with enantiopure catalyst.

[6] Newhouse, T. R.; Li, X.; Blewett, M. M.; Whitehead, C. M. C.; Corey, E. J. *J. Am. Chem. Soc.* **2012**, *134*, 17354–17357.

[7] For an example of a reaction in which a nonlinear effect is due to catalyst-catalyst interactions in the heterochiral pathway alone, see: (a) Kitamura, M.; Okada, S.; Suga, S.; Noyori, R. *J. Am. Chem. Soc.* **1989**, *111*, 4028–4036. (b) Noyori, R.; Kitamura, M. *Angew. Chem. Int. Ed. Engl.* **1991**, *30*, 49–69.

[8] Blackmond, D. G. *Acc. Chem. Res.* **2000**, *33*, 402–411.

1.2 Resting State Monomer, Dimer in the Turnover-Limiting Step

A striking way that catalyst-catalyst interactions play a role in a mechanism is if the catalyst is a monomer in the resting state and two molecules of catalyst work cooperatively in the turnover-limiting step. The (salen)metal-catalyzed asymmetric ring-opening reactions follow this general mechanism: one molecule of catalyst serves as a Lewis acid to activate the electrophile while a second molecule of catalyst activates the nuclophile.[9] These complexes react with one another in a turnover-limiting, bimetallic ring-opening step. For the purposes of this discussion, we will focus on the case of the (salen)Co(III)-catalyzed hydrolytic kinetic resolution (HKR) of terminal epoxides (Scheme 1.1).[10] This transformation has been used extensively in industrial and academic settings to efficiently access terminal epoxides and the corresponding 1,2-diols in high enantiomeric purity.[11] Like other (salen)metal-catalyzed asymmetric ring-opening reactions, HKR reactions exhibit a second-order kinetic dependence on the concentration of catalyst.[12]

Scheme 1.1. The hydrolytic kinetic resolution (HKR) of terminal epoxides

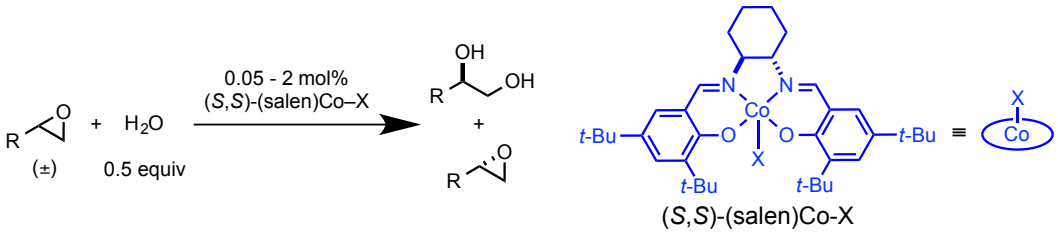

[9] Jacobsen, E. N. *Acc. Chem. Res.* **2000**, *33*, 421–431.

[10] (a) Tokunaga, M.; Larrow, J. F.; Kakiuchi, F.; Jacobsen, E. N. *Science* **1997**, *277*, 936–938. (b) Schaus, S. E.; Brandes, B. D.; Larrow, J. F.; Tokunaga, M.; Hansen, K. B.; Gould, A. E.; Furrow, M. E.; Jacobsen, E. N. *J. Am. Chem. Soc.* **2002**, *124*, 1307–1315.

[11] For reviews of applications of the (salen)Co(III)-catalyzed HKR reaction in industrial and natural products synthesis, see: (a) Larrow, J. F.; Hemberger, K. E.; Jasmin, S.; Kabir, H.; Morel, P. *Tetrahedron: Asymmetry* **2003**, *14*, 3589–3592. (b) Schneider, C. *Synthesis* **2006**, 3919–3944. (c) Kumar, P.; Naidu, V.; Gupta, P. *Tetrahedron* **2007**, *63*, 2745–2785. (d) Furukawa, Y.; Suzuki, T.; Mikami, M,.; Kitaori, K.; Yoshimoto, H. *J. Synth. Org. Chem. Japan* **2007**, *65*, 308–319. (e) Kumar, P; Gupta, P. *Synlett* **2009**, 1367–1382. (f) Pellissier, H. *Adv. Synth. Catal.* **2011**, *353*, 1613–1666.

[12] (a) Nielsen, L. P. C.; Stevenson, C. P.; Blackmond, D. G.; Jacobsen, E. N. *J. Am. Chem. Soc.* **2004**, *126*, 1360–1362. (b) Nielsen, L. P. C.; Zuend, S. J.; Ford, D. D.; Jacobsen, E. N. *J. Org. Chem.* **2012**, *77*, 2486–2495.

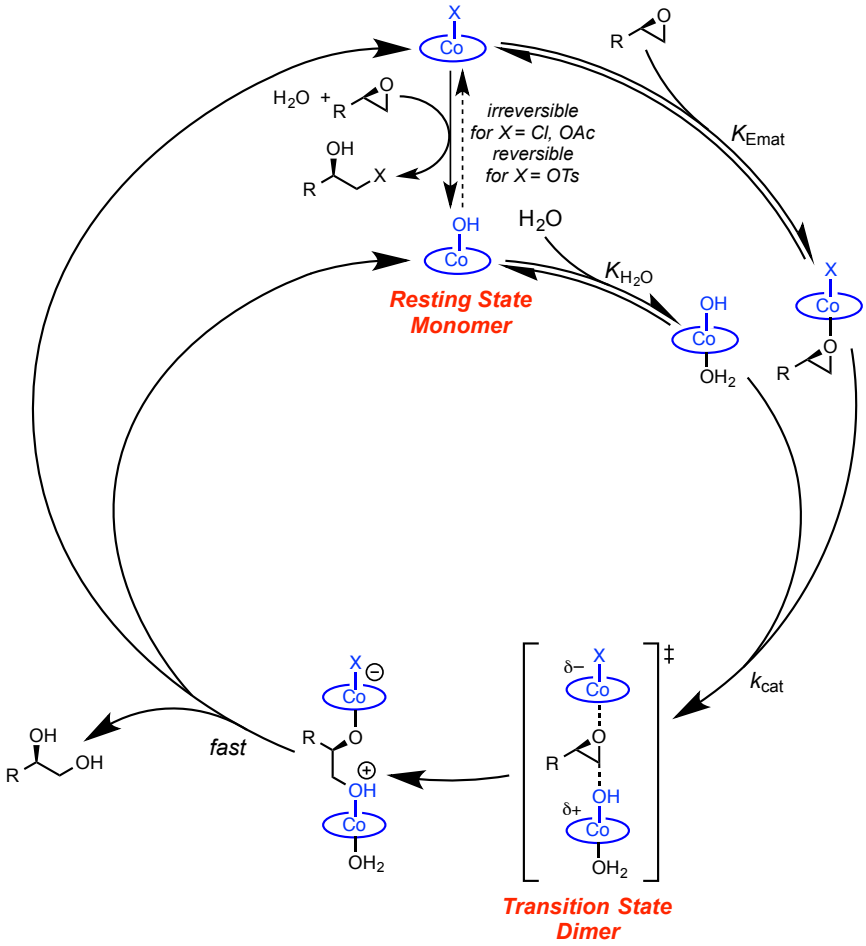

Figure 1.1. Currently accepted catalytic cycle of the (salen)Co(III)-catalyzed hydrolytic kinetic resolution of terminal epoxides.

The HKR displays a strong positive NLE,[13] and in spite the challenges associated with measuring NLEs in kinetic resolutions,[14] these NLE data show clearly that the two molecules of (salen)Co(III) catalyst that act together must interact in a stereochemically dependent fashion.

[13] Johnson, D. W.; Singleton, D. A. *J. Am. Chem. Soc.* **1999**, *121*, 9307–9312. Because the enantiomeric purity of the product of a kinetic resolution is a function of conversion, this analysis required the development of an alternative expression for stereoselectivity.

[14] Blackmond, D. G. *J. Am. Chem. Soc.* **2001**, *123*, 545–553.

Still, the question of whether one of the two catalyst molecules plays a greater role than the other in inducing stereoselectivity in the HKR remained. To determine whether there is an appreciable rate associated with a bimetallic epoxide-opening pathway employing one molecule of each enantiomer of (salen)Co(III), an alternative formaulation of the NLE experiment was devised.[15] Instead of measuring the selectivity of kinetic resolution with respect to catalyst e.e., the relationship between catalyst e.e. and the rate of hydrolysis of enantiopure epoxide was studied. These experiments led to the unambiguous conclusion that both molecules of catalyst must be stereochemically matched to each other and to the epoxide for any measurable rate of hydrolysis to occur. Furthermore, related experiments showed that catalyst-catalyst interactions mediated by the canted conformation of the salen ligand are responsible for stereoselectivity. In combination with a detailed computational chemistry analysis, these insights led to a model for the broad substrate scope of the HKR.

Bringing two molecules of catalyst together imposes a significant entropic penalty on the reaction. By linking catalyst molecules, this penalty need not be paid with every catalyst turnover because it has already been paid in the catalyst-linking step. Efforts to develop highly active linked Co(III) catalysts for the HKR drew on earlier work on linked analogs of (salen)Cr(III) catalysts developed for epoxide opening with azide.[16] The application of a related linking strategy to the HKR reaction led to the development of macrocyclic oligomers that are dramatically more active catalysts than the monomer.[17] Not only are these oligomers superlative

[15] Ford, D. D.; Nielsen, L. P. C.; Zuend, S. J.; Jacobsen, E. N. *Submitted for publication.* See Chapter 2 of this thesis.

[16] Konsler, R. G.; Karl, J.; Jacobsen, E. N. *J. Am. Chem. Soc.* **1998**, *120*, 10780–10781.

[17] (a) Ready, J. M.; Jacobsen, E. N. *J. Am. Chem. Soc.* **2001**, *123*, 2687–2688. (b) Ready, J. M.; Jacobsen, E. N. *Angew. Chem. Int. Ed.* **2002**, *41*, 1374–1377. (c) White, D. E.; Jacobsen, E. N. *Tetrahedron: Asymmetry* **2003**, *14*, 3633–3638.

epoxide hydrolysis catalysts, they catalyze other asymmetric ring opening reactions that are difficult or not possible with the monomeric catalyst.[18]

1.3 Inactive Resting State Dimer, Monomer in Turnover-Limiting Step

In the preceding section, we considered the HKR of terminal epoxides, a reaction in which catalyst-catalyst interactions are responsible for high activity and stereoselectivity. The antithesis of that scenario would be a reaction in which catalyst-catalyst interactions limit activity, such as if the catalyst forms an inactive dimer and which must dissociate before productive catalysis can occur. The (binap)Rh(I)-catalyzed 1,4-addition of boronic acid nucleophiles to α,β-unsaturated ketones developed by Hayashi and coworkers (Scheme 1.2) is an example of such a reaction.[19]

Scheme 1.2. Rhodium-catalyzed 1,4-addition of boronic acids to cyclic enones.

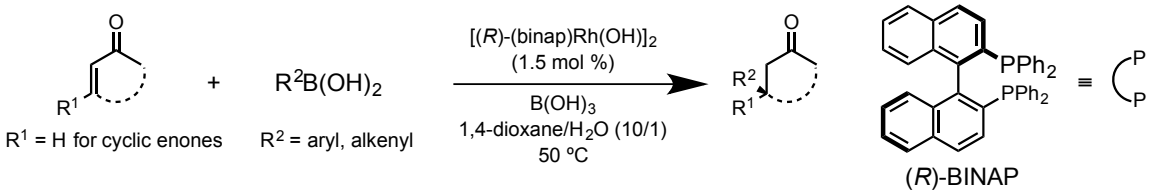

The preferred pre-catalyst for this reaction is the μ-hydroxo-bridged dimer $[(binap)Rh(OH)]_2$, and this species is also the catalyst resting state during the 1,4-addition reaction.[20] This dimer lies off the catalytic cycle: it must dissociate to form a monometallic (binap)Rh(OH) solvato complex before undergoing rate-determining transmetallation with the boronic acid substrate to form the corresponding (binap)Rh(I) aryl or alkenyl complex. As a result of the dimeric resting state, followed by rate-determining transmetallation of a

[18] (a) Loy, R. N.; Jacobsen, E. N. *J. Am. Chem. Soc.* **2009**, *131*, 2786. (b) Birrell, J. A.; Jacobsen, E. N. *Org. Lett.* **2013**, *15*, 2895. See Ref. 17 for additional examples.

[19] Takaya, Y.; Ogasawara, M.; Hayashi, T.; Sakai, M.; Miyaura, N. *J. Am. Chem. Soc.* **1998**, *120*, 5579–5580.

[20] Kina, A.; Iwamura, H.; Hayashi, T. *J. Am. Chem. Soc.* **2006**, *128*, 3904–3905.

monometallic rhodium(I) complex, the rate law has a first-order dependence on the concentration of arylboronic acid, a half-order dependence on total rhodium concentration, and a zero-order dependence on the concentration of α,β-unsaturated ketone.

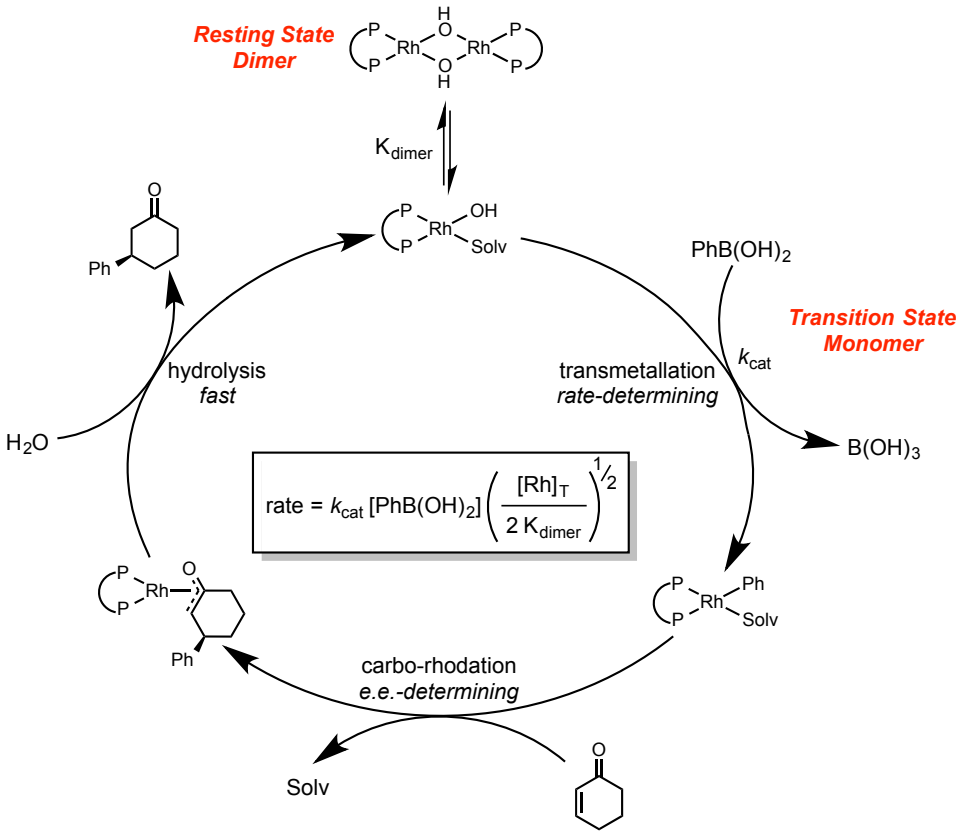

Figure 1.2. Currently accepted catalytic cycle for the (binap)Rh(I)-catalyzed 1,4-addition of boronic acids to α,β-unsaturated ketones.

Because transmetallation is rate-determining, there is no direct way to study the subsequent steps, one of which must determine the enantioselectivity of the reaction. The reactivity of the rhodium(I) aryl species was studied by analyzing stoichiometric reactions of the related complex (binap)Rh(Ph)(PPh_3) by NMR spectroscopy.[21] This complex undergoes rapid migratory insertion into 2-cyclohexenone to form an oxa-π-allyl species. This species is formed

[21] Hayashi, T.; Takahashi, M.; Takaya, Y.; Ogasawara, M. *J. Am. Chem. Soc.* **2002**, *124*, 5052–5058.

as a single diastereomer, suggesting that this is the e.e.-determining step under catalytic conditions. Hydrolysis of this species provides the 1,4-addition product in 99% e.e.

Given the involvement of a resting state dimer, Hayashi and coworkers examined the effect of ligand e.e. on enantioselectivity and reaction rate.[20] They found a negative NLE on product e.e. and that catalyst prepared from enantiopure ligand was slower than catalyst prepared from racemic ligand. Additionally, they observed no difference in the ^{31}P NMR spectra of catalyst prepared from racemic or enantiopure BINAP, suggesting that there is no measurable quantity of the *meso* dimer. Fitting a kinetic model that only included homochiral dimeric resting states to the NLE data and the dependence of rate on ligand e.e. allowed them to extract a self-dimerization constant K_{dimer} of 800 M^{-1}.

1.4 Active Resting State Dimer

A resting state dimer is not always detrimental to reactivity; dimers are sometimes the active catalyst themselves. The asymmetric epoxidation of allylic alcohols with *tert*-butyl hydroperoxide (TBHP) under Ti(IV) catalysis developed by Sharpless (Scheme 1.3) is a classic example of a reaction that is catalyzed by a dimeric species.[22] This reaction is remarkably general and has been applied broadly.[23] The active catalyst is generated *in situ* from a 1:1 mixture of titanium(IV) isopropoxide and a dialkyl tartrate ester. The solid-state structure determined by X-ray crystallography revealed that the catalyst can adopt a dimeric structure of stoichiometry $[(tartrate)Ti(OR)_2]_2$ wherein the two titanium centers are bridged by the hydroxo groups of the tartrate ligand.[24] A solution-phase molecular weight determination by Signer's

[22] Katsuki, T.; Sharpless, K. B. *J. Am. Chem. Soc.* **1980**, *102*, 5974–5976.

[23] Katsuki, T.; Martin, V. S. *Org. React.* **1996**, *48*, 1–299.

[24] Williams, I. D.; Pedersen, S. F.; Sharpless, K. B.; Lippard, S. J. *J. Am. Chem. Soc.* **1984**, *106*, 6430–6431.

method[25] indicated that the average stoichiometry in CH_2Cl_2 is a dimer.[26] The average stoichiometry in pentane is trimeric, and trimers and tetramers of Ti-tartrate complexes have been observed in the solid state.[27]

Scheme 1.3. The (tartrate)Ti(IV)-catalyzed epoxidation of allylic alcohols.

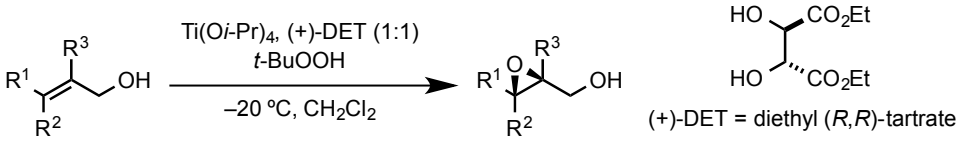

A reaction kinetics study conducted in CH_2Cl_2 under pseudo-first-order conditions revealed the rate law shown in Figure 1.3.[28] The reaction rate obeys a first-order dependence on the concentration of Ti-tartrate over a tenfold range of concentrations, suggesting that the dominant dimeric species in solution is the active catalyst. Notably, if the analysis is conducted in pentane, which favors higher order aggregates, the reaction rate obeys a half-order dependence on Ti-tartrate, implying a mechanism that requires dissociation into dimers prior to productive catalysis. The detailed structure of the dinuclear complex of TBHP and allylic alcohol immediately prior to O-atom transfer has eluded researchers for over 30 years. It has proven difficult to determine which species is active because (tartrate)Ti(IV) complexes undergo dynamic ligand exchange and the coordination mode of the tartrate ligand is fluxional at room temperature.[26] Perhaps more secrets of this reaction will be revealed as new techniques and instrumentation are developed.

[25] Clark, E. P. *Ind. Eng. Chem.* **1941**, *13*, 820–821.

[26] Finn, M. G.; Sharpless, K. B. *J. Am. Chem. Soc.* **1991**, *113*, 113–126.

[27] Pedersen, S. F.; Dewan, J. C.; Eckman, R. R.; Sharpless, K. B. *J. Am. Chem. Soc.* **1987**, *109*, 1279–1282.

[28] Woodard, S. S.; Finn, M. G.; Sharpless, K. B. *J. Am. Chem. Soc.* **1991**, *113*, 106–113.

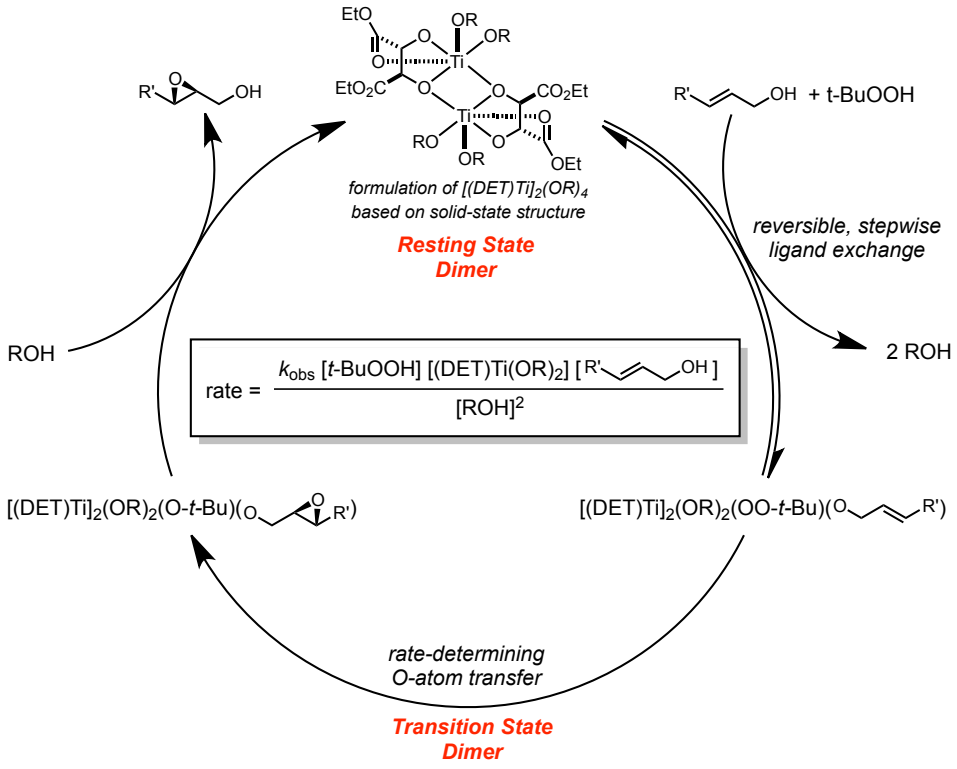

Figure 1.3. Currently accepted catalytic cycle of the Sharpless asymmetric epoxidation reaction. The detailed structures of the species on the catalytic cycle are unknown because the catalyst rapidly samples several different isomeric conformations and coordination modes.

1.5 Resting State Dimer, *Different* Dimer in the Turnover-Limiting Step

A final scenario to consider is one in which two molecules of catalyst form an inactive dimer, which must dissociate to form monomeric catalyst, which then dimerizes to form a second, active dimeric structure en route to the turnover-limiting step. This mechanism would give a first-order kinetic dependence on the concentration of catalyst for the same reason as in the preceding section, but critically *the resting state dimer is not active for catalysis.* These two scenarios are very difficult to distinguish between and one typically needs a detailed understanding of the reaction to definitively say that the resting state dimer is not the dimer that is responsible for catalysis. Furthermore, as discussed above, the first-order dependence of rate

on catalyst concentration can misleadingly suggest a simple one-catalyst mechanism from a resting state monomer.

The mechanism of the thiourea-catalyzed asymmetric Mukaiyama-type alkylation of 1-chloroisochroman derivatives (Scheme 1.4) is consistent with this scenario.[29] This mechanism is discussed in detail in Chapter 3 of this thesis. The reaction obeys a first-order kinetic dependence in both the silyl ketene acetal nucleophile and the 1-chloroisochroman electrophile. Based on an inverse secondary kinetic isotope effect for the hydrogens at the α-position of the silyl ketene acetal (k_H/k_D = 0.88), and a lack of a strong rate dependence on the identity of the silyl group, the C–C bond forming step has been proposed to be turnover-limiting. While this reaction exhibits a first order kinetic dependence on catalyst concentration at high catalyst concentration (over ca. 5 mM), at low concentrations catalyst activity drops off sharply, suggesting a more complicated mechanism.

Scheme 1.4. Thiourea-catalyzed asymmetric alkylation of 1-chloroisochroman

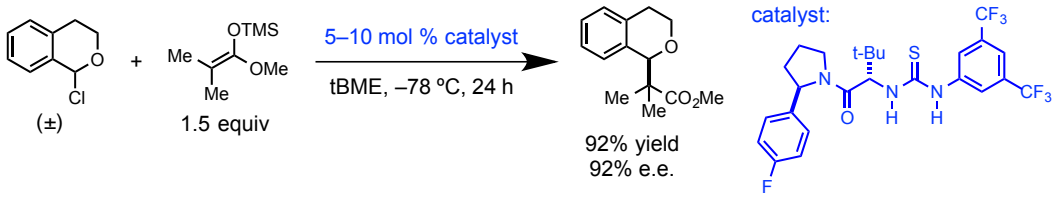

Detailed studies of catalyst structure using ^{1}H-^{1}H NOESY experiments as well as ^{1}H NMR dilution experiments, led to the conclusion that at high catalyst concentration, the catalyst is a resting state head-to-tail dimer in which the thiourea moiety of one molecule of catalyst is hydrogen-bonded to the amide moiety of the second molecules of catalyst (Figure 1.4). The fact

[29] This kinetic scenario has also recently been shown to be operative in the context of a (salen)Co(III)-catalyzed epoxide fluorination reaction. The mechanism is thought to be similar to the other (salen)metal-catalyzed ARO reactions, except that the catalyst resting state is an inactive bimetallic complex that must dissociate prior to productive catalysis: Kalow, J. A.; Doyle, A. G. *J. Am. Chem. Soc.* **2011**, *133*, 16001–16012.

that the resting state of the catalyst is dimeric means that the first-order kinetic dependence at those concentrations is evidence for two molecules of catalyst being present in the rate-determining C–C bond forming step (Figure 1.4). This mechanism also describes the sharp dependence of rate on catalyst concentration at low catalyst concentration: if the catalyst resting state is monomeric at those concentrations, there should be a second order kinetic dependence on the concentration of catalyst. Notably, it is highly unlikely that the resting state dimer itself is active for catalysis because the mode of dimerization requires participation of the hydrogen bond donor moieties.

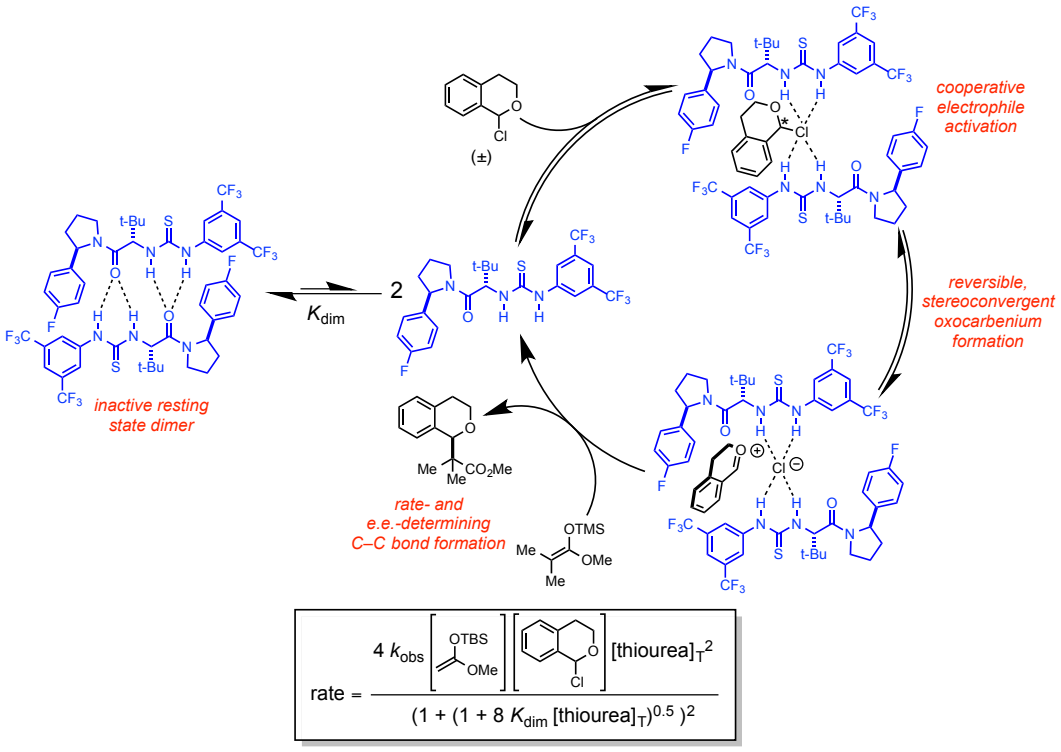

Figure 1.4. Recently proposed catalytic cycle for the thiourea-catalyzed asymmetric Mukaiyama-type alkylation of 1-chloroisochroman derivatives with silyl ketene acetals.

This mechanism provides an explanation for why this reaction performs so poorly at low catalyst loadings: if the reaction obeys a second-order kinetic dependence on the concentration of catalyst, a twofold decrease in catalyst concentration leads to a fourfold decrease in rate. It also

raises the question of whether, as in the context of the HKR (Section 1.2), linking catalyst molecules could lead to a rate enhancement. While this idea is attractive, any linked catalyst design will need to tread a fine line to favor the mode of cooperative electrophile activation shown in Figure 1.4 while discouraging the formation of an intramolecularly aggregated dimer. This strategy has shown promise, and additional catalyst development is ongoing.

1.6 Conclusion

In the nearly thirty years since Kagan and coworkers had the key insight that catalyst-catalyst interactions can lead to a nonlinear dependence of enantioselectivity on the enantiopurity of the catalyst, chemists have discovered that a wide variety of circumstances can lead to an NLE. In the preceding sections, we presented examples of four different mechanisms by which two catalysts can interact. Each of the reactions displays an NLE, but as discussed in the introduction, an NLE is not conclusive evidence for catalyst-catalyst interactions in reactions performed with enantiopure catalyst, and the NLE does not reveal the identity of the catalyst-catalyst interactions themselves.

To determine the mechanistic basis for the NLE, we must determine the resting state stoichiometry of the catalyst and determine the order of the rate law with respect to catalyst concentration. The additional information comes at a price: collecting this data is much more difficult and time-consuming than performing a nonlinear effect experiment. For this reason, practitioners of asymmetric catalysis should think of the NLE experiment as a rapid but preliminary test for catalyst-catalyst interactions in complex settings. After observing an NLE, careful mechanistic investigation can provide a great deal of insight into those catalyst-catalyst interactions, and it can also facilitate rational improvement of catalytic methods: each of the scenarios discussed above has distinct implications for catalyst design and reaction optimization.

Hence, these tools are complimentary in their use for deconvoluting complex mechanisms in asymmetric catalysis.

1.7 A Note on the Kinetics of Asymmetric Catalytic Reactions

In the reactions presented above, kinetics data were essential for determining the nature of the catalyst-catalyst interactions. To provide a framework for our discussion, we offer a brief discussion of using reaction kinetics to dissect complex catalytic mechanisms. The relationship between rate and concentration can be quite complicated, but in the simplest case, a power law equation can accurately describe the kinetics of a reaction. In eq 1.1, we present a power law rate equation for a hypothetical reaction between reagents A and B that is promoted by a catalyst.

$$\frac{d[\mathrm{P}]}{dt} = k_{\mathrm{obs}}[\mathrm{A}]^{a}[\mathrm{B}]^{b}[\mathrm{cat}]^{c} \qquad (1.1)$$

In the power law, the exponents *a*, *b*, and *c* give the kinetic order in each reagent or catalyst. The *different excess experiment* developed by Blackmond is a convenient way to determine these parameters from a minimal number of experiments.[30] The kinetic order of a reaction with respect to catalyst or reagent concentration reflects the *change in stoichiometry* between the resting state and the transition state. To reach a conclusion about the stoichiometry of the catalyst in the transition state, we need to have information about the stoichiometry of the catalyst resting state. Unlike reaction kinetics, which is generally performed using a handful of methods, there are dozens of methods that we can bring to bear on the question of resting state structure. The selection of the proper methods for this task will depend strongly on the identity of the species in question and the strength of the interaction between units of an aggregate. The examples below should serve as examples for how this can be accomplished.

[30] Blackmond, D. G. *Angew. Chem. Int. Ed.* **2005**, *44*, 4302–4320.

Another important issue for practitioners of kinetics is that experiments should be performed under conditions that mimic preparative reaction conditions as closely as possible. In asymmetric catalysis, e.e. is an excellent probe for whether modifications made for convenient kinetics analysis cause a significant change to the mechanism: the formation of high e.e. product during the kinetics experiments is good evidence that the mechanism is the same as in the preparative conditions. Another pitfall of analyzing the kinetics of catalytic reactions is that the pre-catalyst added to a reaction mixture often undergoes a series of modifications to generate the active catalyst. This can lead to an induction period in which the reaction rate depends both on the rate at which active catalyst is formed and on the intrinsic activity of that species.[31] An initial-rates kinetics investigation would give misleading results and would be inappropriate in such a situation. This problem can be avoided in large part by analyzing data over full course of the reaction in "rate vs. conversion" form, the application of "same excess" type experiments developed by Blackmond[30] and by verifying that any proposed rate equation is valid over a range of conversions.

A final issue is one of whether proposed mechanisms are *kinetically distinguishable* from one another. This can be challenging, because once we determine the stoichiometry of the resting state or the turnover-limiting transition state, we must use our chemical intuition combined with structure-activity relationships to infer detailed structure. Some kinetically indistinguishable mechanisms can be very difficult to differentiate from one another, so it is important to keep an open mind with respect to these possibilities while collecting data and drawing conclusions. Consider the hypothetical reaction between substrates A and B. In this reaction, the catalyst is a

[31] (a) Kiener, C. A.; Shu, C. T.; Incarvito, C.; Hartwig, J. F. *J. Am. Chem. Soc.* **2003**, *125*, 14272–14273. (b) Shekhar, S.; Ryberg, P.; Hartwig, J. F.; Mathew, J. S.; Blackmond, D. G.; Strieter, E. R.; Buchwald, S. L. *J. Am. Chem. Soc.* **2006**, *128*, 3584–3591. (c) Shen, Z. M.; Dornan, P. K.; Khan, H. A.; Woo, T. K.; Dong, V. M. *J. Am. Chem. Soc.* **2009**, *131*, 1077–1091.

resting state monomer and the rate law is first order in each substrate and second order in catalyst. Two possible mechanisms are presented in Figure 3.1. These mechanisms are indistinguishable on the basis of kinetics alone. Additional experiments would be necessary to distinguish between these mechanisms.

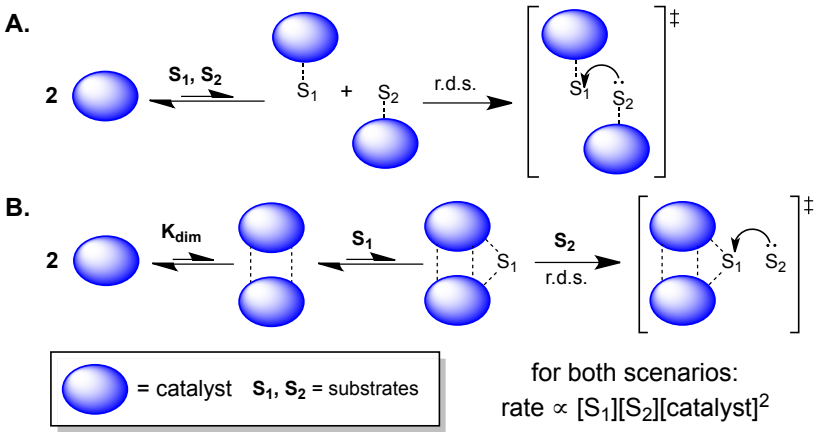

Figure 1.5. Two hypothetical catalytic mechanisms that are kinetically indistinguishable. While kinetics experiments can reveal the stoichiometry of the rate-limiting transition state, they cannot provide us with details of the connectivity between catalysts and substrates or the order of the equilibria that precede the slow step.

Chapter 2

The Mechanistic Basis for High Selectivity and Broad Substrate Scope in the (salen)Co(III)-Catalyzed Hydrolytic Kinetic Resolution of Terminal Epoxides[1]

2.1 Introduction

The (salen)Co(III)-catalyzed hydrolytic kinetic resolution (HKR) is a powerful and widely-used method for accessing enantiomerically pure terminal epoxides (Scheme 2.1).[2,3] One of the most remarkable features of the HKR is the consistently high stereoselectivity obtained in the hydrolysis of a wide range of terminal epoxides, with $k_{rel} > 500$ for some substrates and

[1] This work was performed in collaboration with Lars P. C. Nielsen and Stephan J. Zuend. Portions of this work have been presented in article form: Ford, D. D.; Nielsen, L. P. C.; Zuend, S. J.; Jacobsen, E. N. *J. Am. Chem. Soc.* In Press, DOI: 10.1021/ja408027p. Experimental details about the kinetics experiments presented in this chapter can be found in Dr. Nielsen's thesis: Nielsen, L. P. C. Ph. D. Thesis, Harvard University, Cambridge, MA, November, 2006.

[2] (a) Tokunaga, M.; Larrow, J. F.; Kakiuchi, F.; Jacobsen, E. N. *Science* **1997**, *277*, 936–938. (b) Schaus, S. E.; Brandes, B. D.; Larrow, J. F.; Tokunaga, M.; Hansen, K. B.; Gould, A. E.; Furrow, M. E.; Jacobsen, E. N. *J. Am. Chem. Soc.* **2002**, *124*, 1307–1315. (c) Stevenson, C. P.; Nielsen, L. P. C.; Jacobsen, E. N.; McKinley, J. D.; White, T. D.; Couturier, M. A.; Ragan, J. *Org. Synth.* **2006**, *83*, 162–169.

[3] For reviews of applications of the HKR reaction in industrial and natural products synthesis, see: (a) Larrow, J. F.; Hemberger, K. E.; Jasmin, S.; Kabir, H.; Morel, P. *Tetrahedron: Asymmetry* **2003**, *14*, 3589–3592. (b) Schneider, C. *Synthesis* **2006**, 3919–3944. (c) Kumar, P.; Naidu, V.; Gupta, P. *Tetrahedron* **2007**, *63*, 2745–2785. (d) Furukawa, Y.; Suzuki, T.; Mikami, M,.; Kitaori, K.; Yoshimoto, H. *J. Synth. Org. Chem. Japan* **2007**, *65*, 308–319. (e) Kumar, P; Gupta, P. *Synlett* **2009**, 1367–1382. (f) Pellissier, H. *Adv. Synth. Catal.* **2011**, *353*, 1613–1666.

> 100 for almost all examined.[2b,4] Kinetic analyses of the HKR and related asymmetric ring-opening reactions have revealed a strict second-order rate dependence on the concentration of catalyst, indicating that two (salen)Co(III) molecules are involved the rate-limiting transition structure and thereby implicating a cooperative, bimetallic mechanism for epoxide ring opening.[5,6] Subsequent analyses of the HKR using a broad assortment of kinetic and structural probes have all led to a mechanistic picture wherein the rate- and stereoselectivity-determining step involves one Co(III) complex acting as a Lewis acid to activate epoxide while another serves to activate water as a nucleophile via a (salen)Co–OH complex (Scheme 2.2).[7,8] The rate of this step, and therefore of the overall reaction, depends strongly on the identity of the counterion in the (salen)Co–X precatalyst.[7,9] In contrast, the stereoselectivity in the HKR was shown to be quite insensitive to counterion effects.[7]

[4] Throughout this chapter, we will refer to the property of the HKR catalysts to differentiate between substrate enantiomers as "stereoselectivity". Stereoselectivity in any kinetic resolution is most unambiguously defined by the relative rate of reaction with the two enantiomers of the substrate (k_{rel}). We choose this term instead of "enantioselectivity", which is applied more commonly to describe chiral catalysts, but generally refers to the enantiomer ratio (e.r.) or enantiomeric excess (e.e.) obtained from an achiral or rapidly-racemizing substrate.

[5] (salen)Cr(III): Hansen, K. B.; Leighton, J. L.; Jacobsen, E. N. *J. Am. Chem. Soc.* **1996**, *118*, 10924–10925.

[6] Jacobsen, E. N. *Acc. Chem. Res.* **2000**, *33*, 421–431.

[7] (a) Nielsen, L. P. C.; Stevenson, C. P.; Blackmond, D. G.; Jacobsen, E. N. *J. Am. Chem. Soc.* **2004**, *126*, 1360–1362. (b) Nielsen, L. P. C.; Zuend, S. J.; Ford, D. D.; Jacobsen, E. N. *J. Org. Chem.* **2012**, *77*, 2486–2495.

[8] Ready, J. M.; Jacobsen, E. N. *J. Am. Chem. Soc.* **2001**, *123*, 2687–2688

[9] (a) Jain, S.; Zheng, X.; Jones, C. W.; Weck, M.; Davis, R. J. *Inorg. Chem.* **2007**, *46*, 8887–8896. (b) Jain, S.; Venkatasubbaiah, K.; Jones, C. W.; Davis, R. J. *J. Mol. Catal. A: Chem.* **2010**, *316*, 8–15.

Scheme 2.1. Hydrolytic kinetic resolution of terminal epoxides catalyzed by (salen)Co(III) complexes.

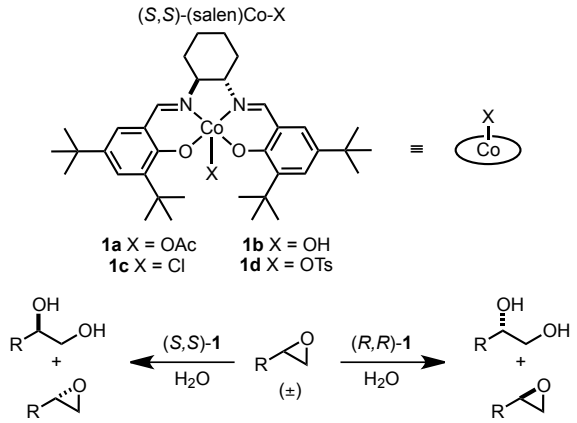

Scheme 2.2. Proposed catalytic mechanism for epoxide hydrolysis by (salen)Co(III) complexes.

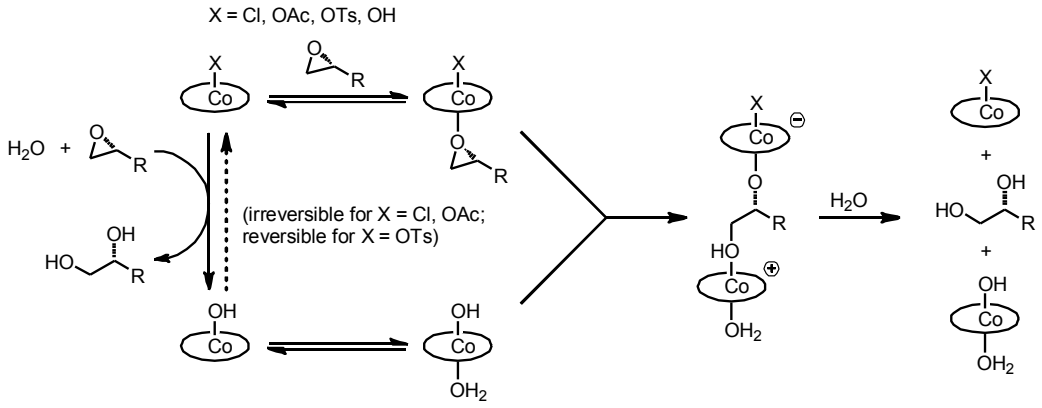

While the mechanistic model in Scheme 2 presents a striking example of cooperativity in a catalytic reaction,[10] it does not answer the fundamentally and practically significant question of how the HKR achieves the sometimes contradictory goals of high stereoselectivity and broad substrate scope. In this chapter, we analyze the stereoselectivity of the HKR using a combination

[10] Selected reviews of other cooperative catalysis schemes: on *synergistic catalysis:* (a) Allen, A. E.; MacMillan, D. W. C. *Chem. Sci.* **2012**, *3*, 633–658, *bifunctional/multifunctional catalysis*: (b) Breslow, R.; *J. Mol. Catal.* **1994**, *91*, 161–174. (c) Shibasaki, M.; Yoshikawa, N. *Chem. Rev.* **2002**, *102*, 2187–2209. (d) Paull, D. H.; Abraham, C. J.; Scerba, M. T.; Alden-Danforth, E.; Lectka, T. *Acc. Chem. Res.* **2008**, *41*, 655–663. (e) Shibasaki, M.; Kanai, M.; Matsunaga, S.; Kumagai, N. *Acc. Chem. Res.* **2009**, *42*, 1117–1127, and *metal–organic cooperative catalysis*: (f) Park, Y. J.; Park, J.-W.; Jun, C.-H. *Acc. Chem. Res.* **2008**, *41*, 222–234. The HKR and other related (salen)metal-catalyzed asymmetric ring-opening reactions stand apart from the above categories of cooperative catalysis because one catalyst serves to activate each reaction partners individually, and these activated species then react with one another in a bimetallic ring-opening step.

of experimental and computational methods. We show that asymmetric induction in epoxide opening is imparted by both chiral complexes working cooperatively rather than by either complex alone. We provide evidence that stereochemical communication between the chiral complexes is mediated by the chiral, stepped conformation of the ligands. Finally, we advance a complete transition structure analysis for the epoxide ring-opening step in the HKR, wherein the relative geometries between the two (salen)Co(III) complexes in the epoxide ring-opening event account for the observed high stereoselectivity and broad substrate scope.

2.2 Stereochemical Cooperativity in the HKR

A fundamental question underlying the mechanism of the HKR is whether stereoselectivity is controlled by the Lewis acidic complex that activates the epoxide, by the (salen)Co-OH complex that delivers the nucleophile, or in a coordinated manner by both complexes (Figure 2.1).[11] Non-linear-effect studies have been applied extensively in analyses of asymmetric catalytic reactions to probe whether interactions between chiral catalysts play any role in an asymmetric reaction of interest: a non-linear dependence of product e.e. on catalyst e.e. may be ascribed to a stereochemically-dependent interaction between catalysts, either in a resting state or the stereoselectivity-determining transition state.[12] Interpretation of non-linear effects in kinetic resolutions is inherently more challenging than in enantioselective reactions of prochiral substrates, because in a kinetic resolution the e.e. of both product and starting material

[11] For a recently reported effort at addressing this question, see: Key, R. E.; Venkatasubbaiah, K; Jones, C. W. *J. Mol. Catal. A: Chem.* **2013**, *366*, 1–7.

[12] (a) Girard, C.; Kagan, H. B. *Angew. Chem., Int. Ed.* **1998**, *37*, 2922–2959. (b) Satyanarayana, T.; Abraham, S.; Kagan, H. B. *Angew. Chem., Int. Ed.* **2009**, *48*, 456–494.

are conversion-dependent.[13] Nonetheless, Johnson and Singleton succeeded in evaluating non-linear effects in the HKR by evaluating what they termed the Differential Kinetic Enantiomeric Enhancement (DKEE = $(k_R - k_S)/(k_R + k_S)$) as a constant measure of stereoselectivity in kinetic resolutions. By plotting DKEE against the catalyst e.e., they observed positive non-linear effects in the (salen)Co(III)-catalyzed hydrolysis of terminal epoxides, thereby demonstrating that the (salen)Co complexes do indeed interact in a stereochemically dependent manner in the HKR.[14] However, the mechanistic basis for this non-linear effect has never been elucidated.[13c]

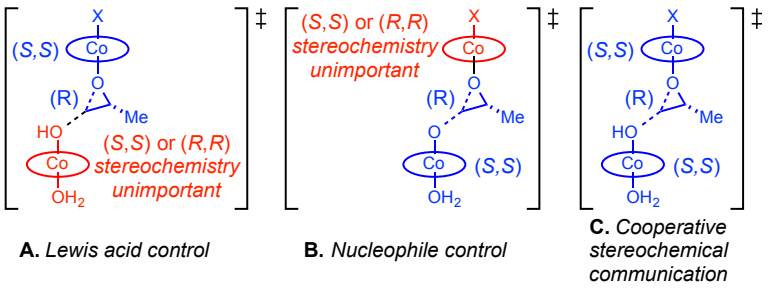

Figure 2.1. Limiting models for stereoinduction in the bimetallic mechanism include: (A) The stereochemistry of the Lewis acidic complex determines stereoselectivity, with the stereochemistry of the nucleophile-delivery agent (salen)Co–OH being inconsequential; (B) The stereochemistry of the nucleophilic (salen)Co–OH complex controls stereoselectivity, with that of the Lewis acidic complex being unimportant; (C) High stereoselectivity is contingent on a matched relationship between the stereochemistry of both catalysts.

In order to analyze the role of stereochemical cooperativity between (salen)Co(III) catalysts in the HKR, we sought to evaluate all eight stereochemically distinct bimetallic pathways that could lead to epoxide hydrolysis (Figure 2.2). Evaluation of the rate constants for each of these pathways would provide a direct measure of the importance of stereochemistry of each of the catalyst components in the HKR. Kinetic analysis of the HKR is complicated by the dynamic nature of catalyst partitioning between (salen)Co–X and (salen)Co–OH (Scheme 2.2), rendering

[13] (a) Ismagilov, R. F. *J. Org. Chem.* **1998**, *63*, 3772–3774. (b) Luukas, T. O.; Girard, C.; Fenwick, D. R.; Kagan, H. B. *J. Am. Chem. Soc.* **1999**, *121*, 9299–9306. (c) Blackmond, D. G. *J. Am. Chem. Soc.* **2001**, *123*, 545–553.

[14] Johnson, D. W. Jr.; Singleton, D. A. *J. Am. Chem. Soc.* **1999**, *121*, 9307–9312.

the catalytic rate law a "moving target" that changes over the duration of the reaction.[7] However, this complication is lifted if X = OH, that is if the Lewis acid component in the HKR is the (salen)Co–OH complex **1b**. This catalyst is more than tenfold less reactive than more Lewis acidic complexes such as (salen)Co–OAc or (salen)Co–OTs.[7a] However, as noted above, while the identity of the counterion X has a strong effect on the rate of epoxide hydrolysis, it has very little effect on the stereoselectivity of the HKR. Accordingly, analysis of the HKR using (salen)Co–OH complex **1b** alone allows straightforward rate studies uncomplicated by counterion effects, and can provide the same information about the basis of stereoselectivity as the more reactive (salen)Co–X derivatives. For these reasons, all analyses described in this study were carried out using complex **1b**.

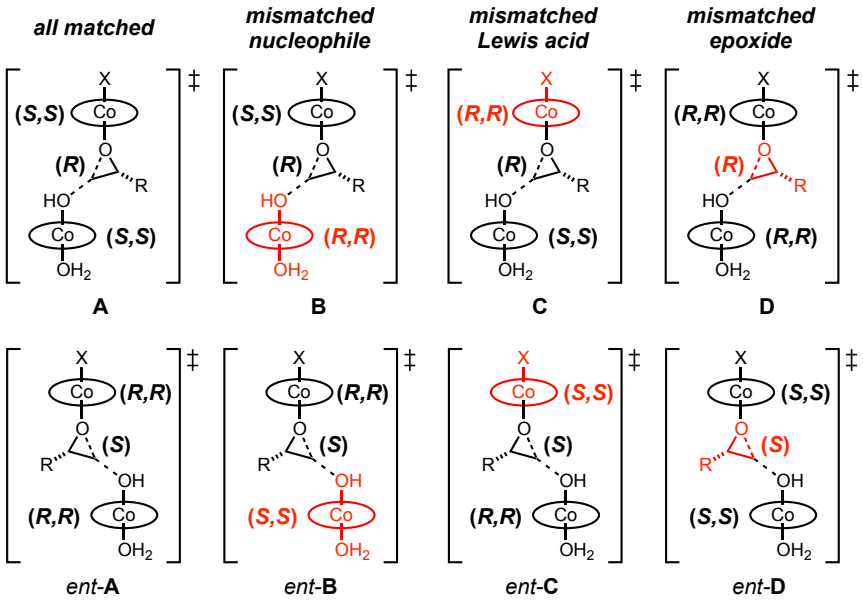

Figure 2.2. The eight possible stereochemically distinct pathways in a (salen)Co(III)-catalyzed hydrolysis of a terminal epoxide. In each case, the reaction component that is "mismatched" with respect to the other two components is shown in red.

The pathways in Figure 2.2 can be divided into four diastereomeric pathways with a given epoxide enantiomer (**A**–**D**), each of which has an equienergetic mirror-image counterpart (pathways *ent*-**A**–*ent*-**D**). Because the enantiomeric pathways are necessarily identical in

energy, we can simplify the analysis by performing kinetic experiments with enantiopure epoxide, thereby limiting the number of possible pathways to four. The stereoselectivity in the kinetic resolution of any racemic terminal epoxide using enantiopure catalyst arises from the difference in rate between Pathway **A** and Pathway *ent*-**D** (or the difference in rate between Pathways *ent*-**A** and **D**). Since enantiomeric pathways are identical in rate, the difference in rate between Pathways **A** and *ent*-**D** must be identical to the difference in rate between Pathways **A** and **D**. As noted, the HKR is highly stereoselective ($k_{rel} > 100$) for almost all terminal epoxides examined to date, so from a kinetic standpoint Pathway **D** is almost negligible relative to Pathway **A**.

Pathways **B** and **C** each require a cooperative reaction between the opposite enantiomers of catalyst. If either of these pathways can compete effectively with Pathway **A**, then adding the mismatched enantiomer of **1b** to a reaction mixture containing enantiopure epoxide and matched catalyst would be expected to accelerate the rate of epoxide hydrolysis. Accordingly, the viability of Pathways **B** and **C** was evaluated through kinetic experiments conducted with non-enantiopure mixtures of catalyst **1b**.

The rate of hydrolysis of (*R*)-1,2-epoxyhexane catalyzed by (*S*,*S*)-**1b** alone and with mixtures of (*S*,*S*)- and (*R*,*R*)-**1b** was determined by reaction calorimetry (Figure 2.3). As established previously, 1,2-epoxyhexane is a convenient substrate for kinetic studies of the HKR due to its relatively low volatility and favorable solubility properties, in addition to the fact that it undergoes kinetic resolution with very high stereoselectivity ($k_{rel} > 300$ using either the (salen)Co–OAc precatalyst **1a** or the (salen)Co–OH catalyst **1b** generated *in situ*).[2b] Comparison of the rates with enantiopure catalyst (solid red curves) and mixtures of catalyst enantiomers (dashed blue curves) reveals that the mismatched catalyst (*R,R*)-**1b** has no detectable effect on

the rate of hydrolysis of (*R*)-1,2-epoxyhexane. Thus, there is no appreciable rate for epoxide hydrolysis involving two different enantiomers of catalyst working cooperatively (Pathways **B** and **C** in Figure 2.2). For epoxide hydrolysis to occur, the absolute stereochemistry of both the nucleophilic and Lewis acidic (salen)Co(III) complexes must therefore be the same and be matched to the absolute stereochemistry of the epoxide (Pathway **A**). As such, the question is resolved as to which of the two chiral (salen)Co(III) complexes is necessary for controlling the stereoselectivity in the HKR (Figure 2.1). The answer is that both are essential.[15]

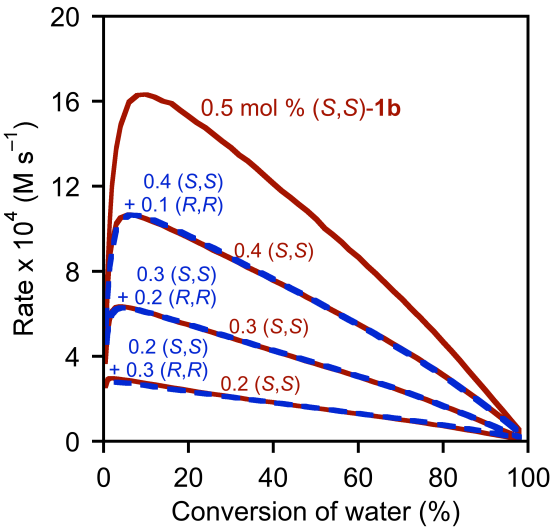

Figure 2.3. Dependence of the loading of matched catalyst (*S*,*S*)-**1b** and mismatched catalyst (*R*,*R*)-**1b** on the rate of hydrolysis of (*R*)-1,2-epoxyhexane ([epoxide]$_i$ = 6.6 M) in 1,2-hexanediol. The reaction rate is plotted as a function of conversion, with water ([H_2O]$_i$ = 2.8 M) as the limiting reagent. In order to generate the (salen)Co–OH complex **1b** quantitatively, the (salen)Co–Cl complex (*S*,*S*)-**1c** and/or (*R*,*R*)-**1c** (0.1–0.5 mol%) was added to the mixture of epoxide and diol and was aged for 60 min prior to addition of water (ref. 7).

2.3 The Salen Step as the Basis for Stereochemical Communication in the HKR

While the experiments described above demonstrate that there is a strong stereochemical interaction between both molecules of (salen)Co(III) complex and the epoxide in the HKR ring-opening event, they do not answer the question of why stereoselectivity in the HKR is so high.

[15] This conclusion receives further validation from computational analyses described later in this chapter (Sections 2.7 and 2.8).

Metal complexes of the salen ligand in **1** have been applied successfully in a wide range of asymmetric catalytic reactions,[16] and understanding how this privileged ligand induces high enantioselectivity has been a topic of analysis for over two decades.[17,18] One of the key insights to emerge from studies of certain other (salen)metal-catalyzed reactions is the importance of the stepped conformation of the salen ligand as a selectivity-determining element.[19,20] The salen step is the result of a tilt of the salicylaldimine aryl rings relative to the equatorial plane of the metal complex. This is illustrated clearly in the (salen)Co(III) bisaziridine complex characterized by X-ray crystallography by Chin and coworkers (Figure 2.4).[21]

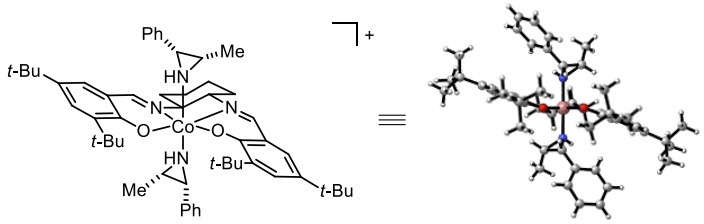

Figure 2.4. Chiral, stepped conformation of a cationic (salen)Co(III) bis(aziridine) complex. Figure generated from data retrieved from the Cambridge Structural Database, submission number CCDC 185815 and ref. 21. The counterions (a 1:1 mixture of chloride and acetate) and solvent (methylene chloride) are omitted for clarity.

The existence and absolute stereochemistry of the salen step are tied directly to the staggered conformation of the 1,2-diamine backbone in the ligand (Figure 2.5). The step itself

[16] Larrow, J. F.; Jacobsen, E. N. *Topics Organomet. Chem.* **2004**, *6*, 123–152.

[17] (a) Initial report and analysis of stereoinduction: Jacobsen, E. N.; Zhang, W.; Muci, A. R.; Ecker, J. R.; Deng, L. *J. Am. Chem. Soc.* **1991**, *113*, 7063–7064. (b) For a comprehensive review, see: (a) McGarrigle, E. M.; Gilheany, D. G. *Chem. Rev.* **2005**, *105*, 1563–1602.

[18] Yoon, T. P.; Jacobsen, E. N. *Science* **2003**, *299*, 1691–1693.

[19] For discussions of the step-like conformation of (salen)Mn(V) oxo complexes, see: (a) Cavallo, L. Jacobsen, H. *Chem. Eur. J.* **2001**, *7*, 800–807. (b) Katsuki, T. *Adv. Synth. Catal.* **2002**, *344*, 131–147. (c) El-Bahraoui, J.; Wiest, O.; Feichtinger, D.; Plattner, D. A. *Angew. Chem., Int. Ed.* **2001**, *40*, 2073–2076. (d) Cavallo, L.; Jacobsen, H. *J. Org. Chem.* **2003**, *68*, 6202–6207. For the crystal structure of an achiral, stepped (salen)Cr(V) oxo complex, see: (e) Samsel, E. G.; Srinivasan, K.; Kochi, J. K. *J. Am. Chem. Soc.* **1985**, *107*, 7606–7617.

[20] In contrast, little deviation from planarity is observed in crystal structures of (salen)Mn(III) complexes: Pospisil, P. J.; Carsten, D. H.; Jacobsen, E. N. *Chem. Eur. J.* **1996**, *2*, 974–980.

[21] Bobb, R.; Alkahimi, G.; Studnicki, L.; Lough, A.; Chin, J. *J. Am. Chem. Soc.* **2002**, *124*, 4544–4545.

possesses a chirality element, and by analogy to Fox's work with (salen)Ni(II) complexes,[22] we use the helical chirality descriptors *P* and *M* to describe the absolute stereochemistry of the step in the salen structures (Figure 2.5). In the case of *trans*-1,2-diaminocyclohexane-derived salen ligands such as in **1**, the backbone is locked in a single staggered chiral conformation, thereby setting the absolute stereochemistry of the helical chirality element in the salen step.[23] In order to define the interactions responsible for high stereoselectivity in the HKR, we sought to probe whether it is the shape of the chiral diamine-derived backbone or the step chirality of the salen framework that plays the more dominant role. In order to accomplish this, we required a strategy to decouple these closely interconnected chirality elements.

[22] (a) Zhang, F.; Bai, S.; Yap, G. P. A.; Tarwade, V.; Fox, J. M. *J. Am. Chem. Soc.* **2005**, *127*, 10590–10599. (b) Dong, Z.; Karpowicz, R. J., Jr.; Bai, S.; Yap, G. P. A.; Fox, J. M. *J. Am. Chem. Soc.* **2006**, *128*, 14242–14243. (c) Dong, Z.; Yap, G. P. A.; Fox, J. M. *J. Am. Chem. Soc.* **2007**, *129*, 11850–11853. (d) Fisher, L. A.; Zhang, F.; Yap, G. P. A.; Fox, J. M. *Inorg. Chim. Acta* **2010**, *364*, 259–260. (e) Dong, Z.; Plampin, J. N. III; Yap, G. P. A.; Fox, J. M. *Org. Lett.* **2010**, *12*, 4002–4005. (f) Dong, Z.; Bai, S.; Yap, G. P. A.; Fox, J. M. *Chem. Commun.* **2011**, *47*, 3781–3783.

[23] In a series of elegant studies, Fox and coworkers have shown that the match between the sense of helical chirality in a metal salen complex and the absolute stereochemistry of the diamine backbone can be overturned in the context of (salen)Ni(II) metallofoldamers by introducing stereogenic end-groups at the salicylidene 3-position (ref. 21). While Fox's work raises the possibility that a similar phenomenon might occur in (salen)Co(III) structures, i.e. that diastereomeric complexes (*P*,*S*,*S*)- and (*M*,*S*,*S*)-**1b** could both be present in HKR reaction mixtures, an examination of the crystal structures of the (salen)Ni(II)-derived metallofoldamers reveal a conformation of the salen ligand that is distinct from the (salen)Co(III) step structures that are the focus here. In the (salen)Ni(II) structures, the ligand appears to be twisted out of planarity into a helix, as opposed to adopting the salen step. Indeed, a crystal structure of (salen)Ni(II) complexes with the same ligand as in complexes **1** reveals no salen step, instead, the ligand takes on a slight twist (see: Shimazaki, Y.; Tani, F.; Fukui, K.; Naruta, Y.; Yamauchi, O. *J. Am. Chem. Soc.* **2003**, *125*, 10512–10513). For the purpose of our analysis of (salen)Co(III) complexes, we make the assumption that there is only a single energetically accessible diastereomer of **1b**, with the step absolute stereochemistry matched to the diamine absolute stereochemistry.

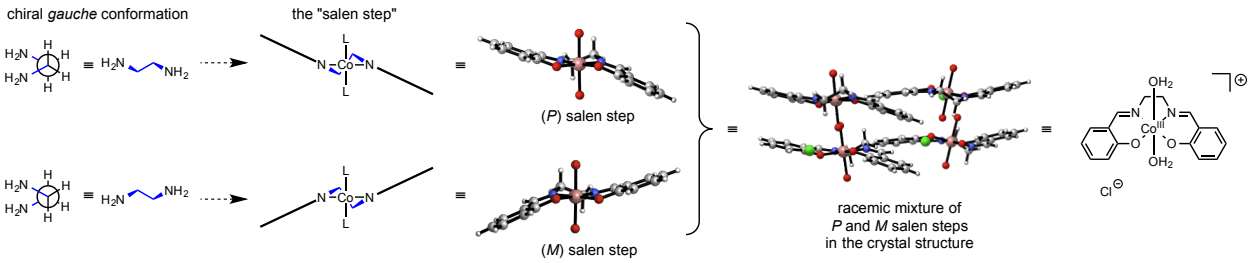

Figure 2.5. The salen step is an element of chirality in metal salen complexes. The structure shown is derived from single crystal X-ray diffraction data from ref. 25. The structure on the right is the unit cell, containing two complexes of each enantiomeric conformer.

The question of which chirality element of the salen ligand plays the more dominant role in stereoinduction has been addressed in an elegant and compelling manner in the context of (salen)Mn(III)-catalyzed epoxidation reactions. Salen complexes derived from achiral 1,2-diamines such as 1,2-ethylenediamine can still adopt a chiral stepped conformation, but they exist as a racemic mixture of conformers (eq 2.1, $K_{eq} = 1$). In the presence of chiral additives such as amines, pyridine *N*-oxides, or BINOL-derived phosphates, these complexes have been shown to function as enantioselective epoxidation catalysts.[24]

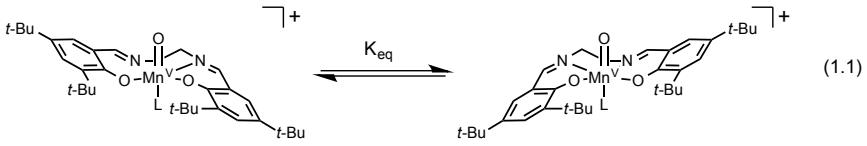

(1.1)

L = Neutral Lewis base, solvent, or anionic ligand.
$K_{eq} = 1$ if L is achiral, may be $\neq 1$ if L is chiral

The chiral additives were assumed to bind directly to the metal center trans to the oxo ligand, so direct stereochemical communication from the chiral additive in the epoxidation event was considered unlikely. Instead, the catalysts have been proposed to induce enantioselectivity by undergoing reaction selectively from one of the diastereomeric stepped conformers. The observation of high enantioselectivity in some cases with systems consisting of an achiral salen

[24] a) Hashihayata, T.; Ito, Y.; Katsuki, T. *Synlett* **1996**, 1079–1081; b) Hashihayata, T.; Ito, Y.; Katsuki, T. *Tetrahedron* **1997**, *53*, 9541–9552; c) Miura, K.; Katsuki, T. *Synlett* **1999**, 783–785; d) Liao, S.; List, B. *Angew. Chem. Int. Ed.* **2010**, *49*, 628–631.

ligand with a chiral axial ligand has been taken as evidence that the salen step alone is sufficient for high stereoselectivity in (salen)Mn(III)-catalyzed epoxidation reactions.[24c,d]

An analogous strategy of employing chiral axial ligands would not lend itself to a straightforward analysis of stereoselectivity in the HKR because of the complex ligand exchange phenomena and cooperative reactivity that are associated with this reaction (Scheme 2.2).[7,11,25] Instead, we considered whether we might be able to apply a kinetic analysis of epoxide hydrolysis reactions catalyzed by achiral (salen)Co(III) complexes to shed light on the question of whether the salen step or the shape of the chiral diamine play the principal role in stereoinduction. This strategy was based on the fact that the salen step is a feature of (salen)Co(III) complexes whether or not the ligands are derived from chiral diamines. For example, the Co(III) complex of a 1,2-diaminoethane-derived salen ligand crystallizes as a racemic mixture of stepped chiral conformations (Figure 2.5).[26]

Optimized, computed structures of neutral (salen)Co(III) complexes derived from both chiral and achiral 1,2-diamines and using a range of computational methods are depicted in Figures 2.6 and 2.7. Each of these complexes is computed to be most stable in the low spin, closed-shell configuration (see Section 2.5). The similarity in the stepped structures of these

[25] In the recently discovered (salen)Co(III)-catalyzed epoxide fluorination reaction, there is a strong matched/mismatched relationship between the absolute stereochemistry of a chiral amine additive and the absolute stereochemistry of the salen ligand. In addition, modest levels of selectivity can be achieved using ethylene diamine-derived (salen)Co–OTs catalyst **2d** in conjunction with these chiral additives. These effects may be attributed to the chiral additive serving as a axial ligand on the (salen)Co(III) complex, thereby favoring one chiral salen step conformer over the other, but the complexity of the mechanism of these reactions would make it difficult to determine the precise stereochemical role of the chiral additive. (a) Kalow, J. A.; Doyle, A. G. *J. Am. Chem. Soc.* **2010**, *132*, 3268–3269. (b) Kalow, J. A.; Doyle, A. G. *J. Am. Chem. Soc.* **2011**, *133*, 16001–16012.

[26] van den Bergen, A. M.; Fallon, G. D.; West, B. O. *Private communication to the Cambridge Crystallographic Database* **1999**, deposition number CCDC 136763.

complexes is particularly noteworthy, and consistent with reported crystal structures of (salen)Co(III) complexes.[27,28,29]

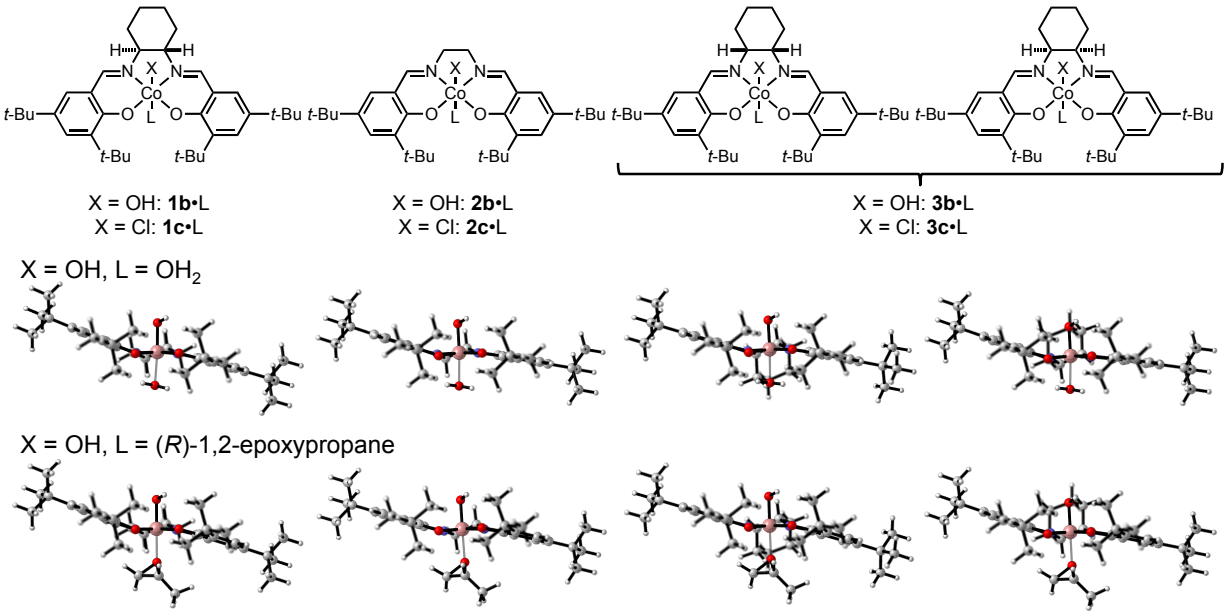

Figure 2.6. Optimized structures of neutral (salen)Co(III) complexes calculated as closed-shell singlets at the B3LYP/6-31G(d) level.

[27] For crystal structures of cationic (salen)Co(III) complexes possessing only L-type axial ligands, see: (a) Bobb, R.; Alkahimi, G.; Studnicki, L.; Lough, A.; Chin, J. *J. Am. Chem. Soc.* **2002**, *124*, 4544–4545. (b) Huang, Y.; Iwama, T.; Rawal, V. H. *J. Am. Chem. Soc.* **2002**, *124*, 5950–5951. (c) Hutson, G. E.; Dave, A. H.; Rawal, V. H. *Org. Lett.* **2007**, *9*, 3869–3872.

[28] For crystal structures of neutral (salen)Co(III) complexes possessing an X-type axial ligand, see: (a) Ready, J. M.; Jacobsen, E. N. *J. Am. Chem. Soc.* **2001**, *123*, 2687–2688. (b) Hong, J. Ph. D. Thesis, Harvard University, Cambridge, MA, October, 2001. (c) Cohen, C. T.; Thomas, C. T.; Peretti, K. L.; Lobvoksky, E. B.; Coates, G. W. *Dalton Trans.* **2006**, 237–249.

[29] For a compilation of crystal structures of (salen)metal complexes, see: Nielsen, L. P. C. Ph. D. Thesis, Harvard University, Cambridge, MA, November, 2006, Appendix 1. The complete text of this document is available via the internet through Proquest (http://www.proquest.com).

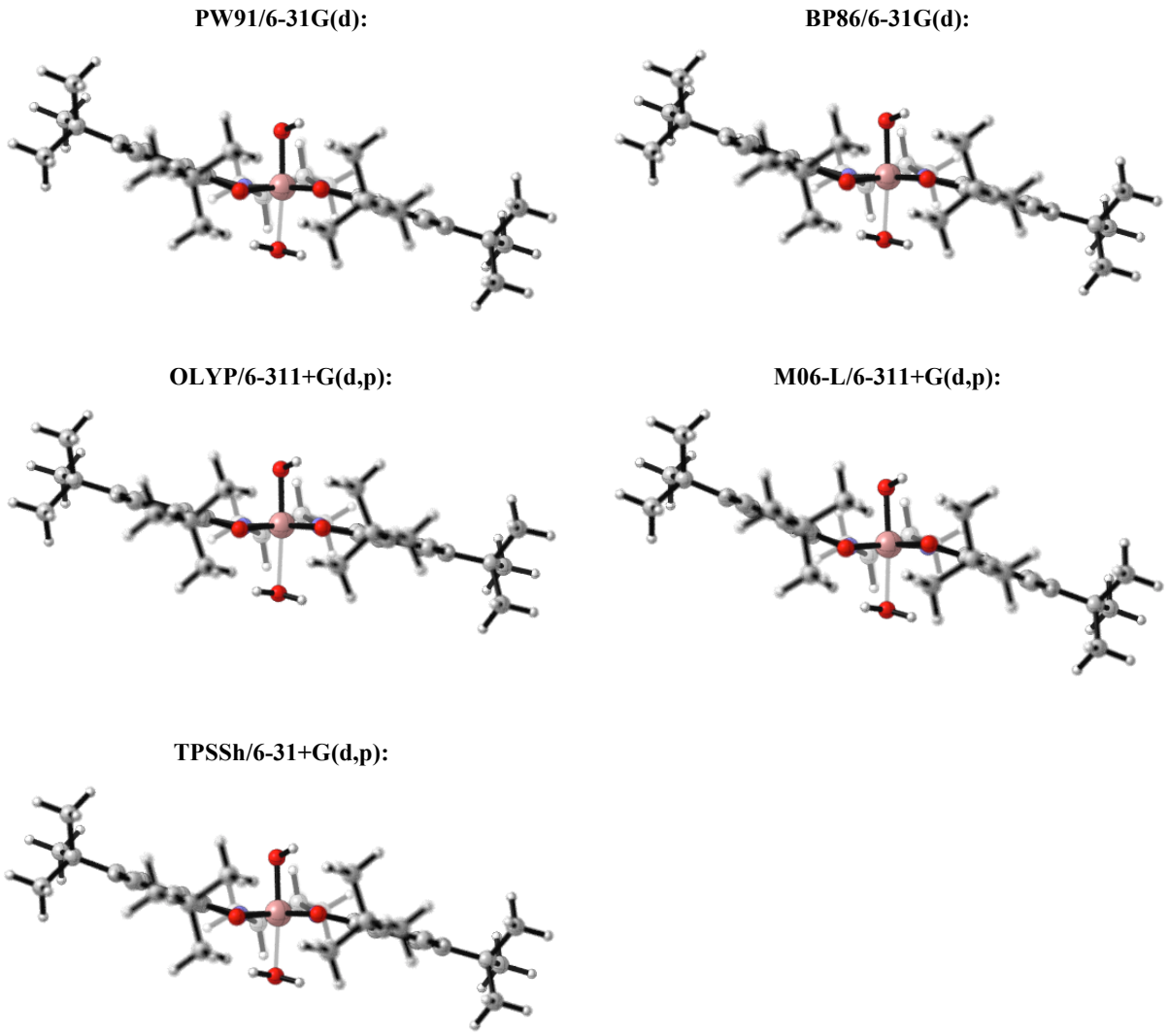

Figure 2.7. To test whether the stepped conformation of the salen ligand was a robust feature of these complexes, we fully optimized the structure of (salen)Co(OH)(OH_2) using a variety of levels of theory. The resulting geometries demonstrate clearly that the stepped conformation is predicted over a range of DFT methods and basis sets.

If the salen step alone were responsible for stereochemical communication between (salen)Co(III) complexes in the HKR, the different complexes depicted in Figure 2.6 with similar step structures but different backbone structures should participate comparably in cooperative catalysis either alone or with one another (Figure 2.8). We undertook a kinetic analysis of the achiral (salen)Co(III) complexes depicted in Figure 2.6 in epoxide hydrolysis reactions in order

to determine whether this is the case.[30] The achiral (salen)Co–Cl complex derived from 1,2-diaminoethane (**2c)** is a competent catalyst, but was found to undergo significant deactivation during the course of epoxide hydrolysis reactions, thereby precluding a meaningful rate comparison to **1b**.

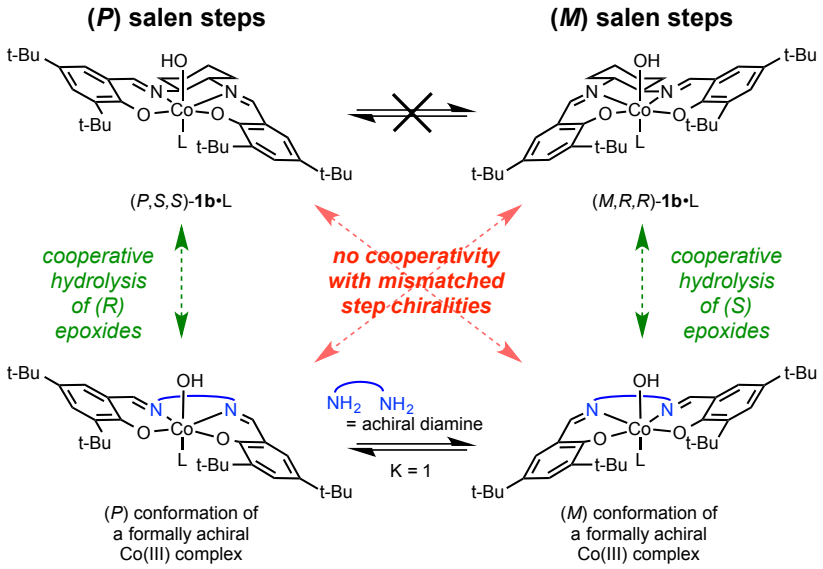

Figure 2.8. Summary of possible pathways for **1b** to engage in cooperative catalysis with a Co(III) complex of an achiral salen ligand. If the salen step mediates stereochemical communication, each (salen)Co(III) complex would only be able to undergo cooperative catalysis with another identical complex or with a different (salen)Co(III) complex of the same absolute step stereochemistry. L = H_2O or epoxide.

In contrast, the meso (salen)Co–Cl complex derived from *cis*-1,2-diaminocyclohexane (**3c**) was shown to be an effective and kinetically well-behaved precatalyst for the hydrolysis of 1,2-epoxyhexane. Previous kinetics studies have demonstrated that (salen)Co–Cl **1c** aged with epoxide is converted quantitatively to the corresponding hydroxo compound **1b** upon addition of water. The meso (salen)Co(III) analog **3c** behaves in an identical manner, supporting the assumption that (salen)Co–OH **3b** is also generated quantitatively and is the active catalyst under

[30] The achiral (salen)Co(III) complexes in Figure 2.6 exist in chiral conformations that may or may not undergo racemization rapidly on the time scale of the epoxide hydrolysis reactions. For the purposes of this analysis, the only important issue is that they exist as 50:50 mixtures of the stepped, chiral conformers.

these conditions. As we observed previously with compound **1b**, compound **3b** catalyzes hydrolysis of 1,2-epoxyhexane with a second-order dependence on the concentration of catalyst (Figure 2.9). Given the similar kinetic behavior of **1b** and **3b**, we conclude that hydrolysis reactions catalyzed by Co(III) complexes **1b** and **3b** occur by analogous bimetallic mechanisms.

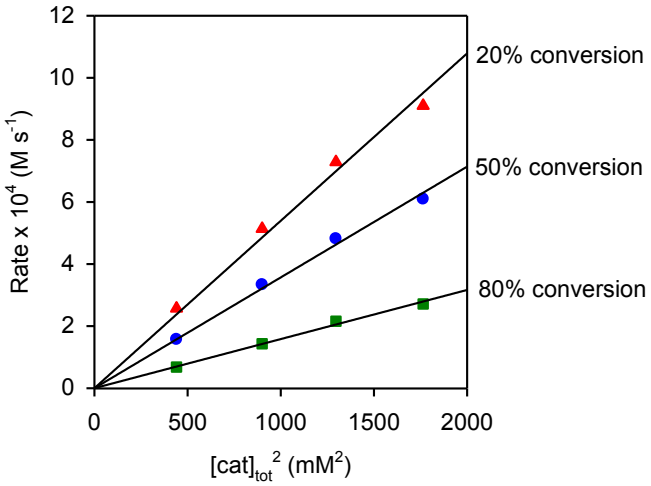

Figure 2.9. Plots of the rate of hydrolysis of (*R*)-1,2-epoxyhexane ([epoxide]$_i$ = 6.0 M) versus [**3c**]$_{initial}^2$ in 1,2-hexanediol ([diol]$_i$ = 1.74 M) at different %-conversion of water ([H_2O]$_i$ = 3.41 M). The catalyst **3b** was generated by aging **3c** in epoxide for 1 h before addition of water. The black curves represent least-squares fits to $f(x) = a$ x, 20 % conversion, $a = 0.54 \pm 0.01$ M^{-1} s^{-1}; 50 % conversion, $a = 0.356 \pm 0.007$ M^{-1} s^{-1}; 80 % conversion, $a = 0.159 \pm 0.003$ M^{-1} s^{-1}.

Having established that **3b** and **1b** have similar step but different diamine backbone structures (Figure 2.6), and that both catalyze epoxide hydrolysis by a second-order mechanism (Figure 2.9), we were in a position to address which chirality elements mediate stereochemical communication between (salen)Co(III) catalysts in the key epoxide ring-opening step. If (*P*)-**3b** were kinetically indistinguishable from (*P,S,S*)-**1b** and (*M*)-**3b** were kinetically indistinguishable from (*M,R,R*)-**1b**, we would expect that hydrolysis of *R*-1,2-epoxyhexane catalyzed by (*P,S,S*)-**1b** (matched with respect to epoxide) would proceed at the same rate as a reaction catalyzed by twice the concentration of **3b** (which consists of 50% (*P*)-**3b**). The rates of these reactions were determined using reaction calorimetry, and indeed reactions carried out with **1b** or **3b** ([(*P,S,S*)-**1b**] = [**3b**]/2) proceed at very similar rates (Figure 2.10). The curves in Figure 2.10 should

overlay perfectly only if (*P*,*S*,*S*)-**1b** were kinetically indistinguishable from (*P*)-**3b** and if (*M*)-**3b** were completely incapable of promoting the hydrolysis (*R)*-1,2-epoxyhexane (no catalysis through mechanisms analogous to Pathways B, C or D in Figure 2.2). The similarity of the kinetic behavior of catalysts **1b** and **3b** shown in Figure 2.10 is therefore taken as support for the hypothesis that the salen step plays the dominant role in mediating stereoinduction in epoxide hydrolysis and that catalysis by **3b** occurs by a mechanism very similar to Pathway A shown in Figure 2.2.[31]

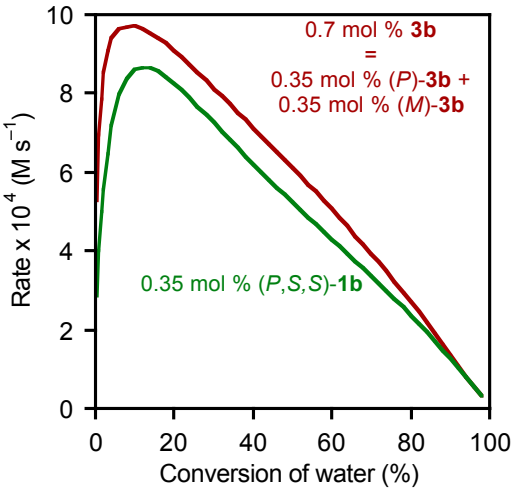

Figure 2.10. Comparison of rate of epoxide hydrolysis catalyzed by **3b** (0.7 mol %) and (*P,S,S*)-**1b** (0.35 mol %). The rates of hydrolysis of (*R*)-1,2-epoxyhexane ([epoxide]$_i$ = 6.0 M) in 1,2-hexanediol as a function of conversion of the limiting reagent ([H_2O]$_i$ = 3.4 M). In each experiment, **3c** or (*R*,*R*)-**1c** was added to the reaction mixture and aged for 60 min, followed by water to generate **3b** or **1b**, respectively, *in situ*.

To further probe the question of the stereochemical requirements for **3b** to participate in catalysis, we assayed for cooperative reactivity between **3b** and **1b**. Hydrolysis of (*R*)-1,2-epoxyhexane catalyzed by mixtures of **3b** and (*M*,*R*,*R*)-**1b** (mismatched with respect to epoxide)

[31] The small rate difference between **1b** and **3b** (at double the concentration) was reproduced with several different batches of catalysts. It can be ascribed to several factors, including the fact that the step conformations are similar but not identical in the two catalysts (Figure 7), and/or that the concentrations of (*P*)-**3b** and (*M*)-**3b** are not necessarily identical in the presence of the chiral epoxide.

was found to proceed at nearly identical rates to reactions catalyzed by **3b** alone (Figure 2.11).[32] The hydrolysis of (*R*)-1,2-epoxyhexane catalyzed by mixtures of **3b** and the matched chiral catalyst, (*P,S,S*)-**1b** provides a strikingly different result, with clear evidence of cooperativity between the two complexes (Figure 2.12).

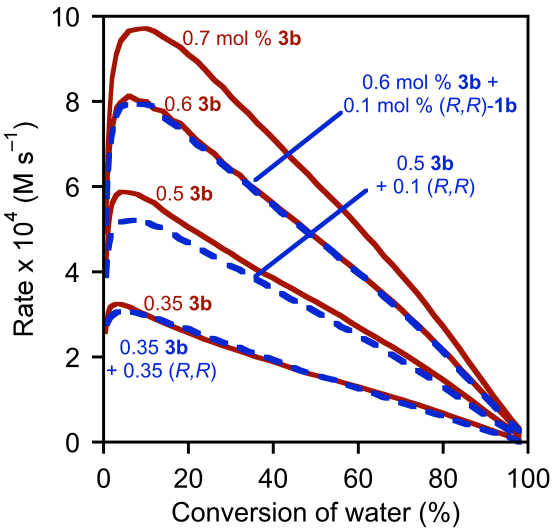

Figure 2.11. Rate dependence on amount of **3b** and (*R*,*R*)-**1b** catalyst. Plot of the rates of hydrolysis of (*R*)-1,2-epoxyhexane ($[epoxide]_i$ = 6.0 M) in 1,2-hexanediol versus conversion of water ($[H_2O]_i$ = 3.4 M) in 1,2-hexanediol. In each experiment, **3c** and/or (*R*,*R*)-**1c** (0.35–0.70 mol%) was added to the reaction mixture and aged for 60 min, followed by water to generate **3b** or **1b**, respectively, *in situ*.

[32] The "0.5 mol % **3c**" and "0.5 mol % **3c** + 0.2 mol % (R,*R*)-**1c**" curves are not perfectly superimposable. Although this effect is small (< 10% difference in rate), it appears to be reproducible.

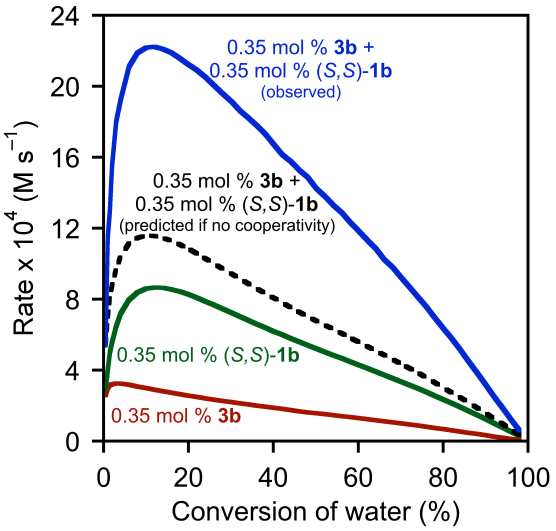

Figure 2.12. Rate dependence on amount of **3b** and (*P*,*S*,*S*)-**1b**. Plot of the rates of hydrolysis of (*R*)-1,2-epoxyhexane ($[epoxide]_i$ = 6.0 M) in 1,2-hexanediol versus conversion of water ($[H_2O]_i$ = 3.4 M) in 1,2-hexanediol. In each experiment, **3c** and/or (*S*,*S*)-**1c** (0.35 mol%) was added to the reaction mixture and aged for 60 min, followed by water. The dotted black curve represents the rate of hydrolysis expected from the mixture of **3b** and (*P*,*S*,*S*)-**1b** if no cooperative catalysis between these two catalysts occurred.

The results of both experiments are consistent with the proposal that the stepped conformation of the salen ligand, rather than the shape of the chiral diamine backbone, is responsible for stereochemical induction in epoxide hydrolysis. In the experiment depicted in Figure 2.11, the observed epoxide hydrolysis can be attributed entirely to catalysis by the (*P*) conformer of **3b**, and no cooperative reactivity is observed with (*M*,*R*,*R*)-**1b** because the latter is mismatched with respect the epoxide absolute stereochemistry. In the experiment depicted in Figure 2.12, cooperative reactivity between **1b** and **3b** is observed, and this can be ascribed to the fact that the (*P*) conformer of **3b** and (*P*,*S*,*S*)-**1b** have the same step stereochemistry, matched to that of the epoxide. Thus, catalysts with structurally different diamine backbones that still possess similar salen step features can operate cooperatively in epoxide hydrolysis only if the salen step absolute stereochemistries are matched and matched to the stereochemistry of the epoxide. Such reactivity patterns would not be expected if the shape of the chiral diamine played

an important role in recognition between catalysts in Pathway A. We conclude that the salen step is the dominant factor mediating stereochemical communication in the HKR.

2.4 Computed Structure of (salen)Co(III)•Epoxide Complexes

The experimental data described above provides strong evidence that stereoselectivity in the HKR is tied directly to the chiral, stepped nature of both (salen)Co(III) complexes in the epoxide ring-opening event. We turned to a computational analysis in order to glean a clearer understanding of how this stereochemical cooperativity leads to the remarkably high selectivity factors and broad substrate scope that are characteristic of the HKR. We chose the B3LYP density functional theory method,[33] with a relatively small 6-31G(d) basis set, as the primary method due to the level of success with which it has been applied to other transition metal-based systems.[34] Given the state of the art in high performance computing hardware and electronic structure theory software, the choice of a relatively small basis set was critical to the feasibility of this analysis given the fact that the ring-opening transition structures shown schematically in Figure 2 have ca. 700 electrons and 90 heavy atoms. Conscious of the well documented limitations of B3LYP,[35] we repeated several key calculations at higher levels of theory, both with

---

[33] (a) Becke, A. D. *Phys. Rev. A* **1988**, *38*, 3098–3100. (b) Lee, C.; Yang, W.; Parr, R. G. *Phys. Rev. B*. **1988**, *37*, 785–789. (c) Becke, A. D. *J. Chem. Phys*. **1993**, *98*, 1372–1377. (d) Stephens, P. J.; Devlin, F. J.; Chabalowski, C. F.; Frisch, M. J. *J. Phys. Chem*. **1994**, *98*, 11623–11627.

[34] Selected examples of the application of B3LYP in quantum chemical calculations of transition metal structure and reactivity: (a) Strassner, T.; Taige, M. A. *J. Chem. Theory Comput*. **2005**, *1*, 848–855. (b) Jenkins, D. M.; Di Bilio, A. J.; Allen, M. J.; Betley, T. A.; Peters, J. C. *J. Am. Chem. Soc*. **2002**, *124*, 15336–15350. (c) Takaoka, A.; Peters, J. C. *Inorg. Chem*. **2012**, *51*, 16–18. (d) Shakya, R.; Imbert, C.; Hratchian, H. P.; Lanznaster, M.; Heeg, M. J.; McGarvey, B. R.; Allard, M.; Schlegel, B.; Verani, C. N. *Dalton Trans*. **2006**, 2517–2525. (e) Araujo, C. M.; Doherty, M. D.; Konezny, S. J.; Luca, O. R.; Usyatinsky, A.; Grade, H.; Lobkovsky, E.; Soloveichik, G. L.; Crabtree, R. H.; Batista, V. S. *Dalton Trans*. **2012**, *41*, 3562–3573. (f) Wang, T.; Brudvig, G.; Batista, V. S. *J. Chem. Theory Comput*. **2010**, *6*, 755–760.

[35] Selected examples of studies documenting the drawbacks of B3LYP: Zhao, Y.; Truhlar, D. G. *J. Chem. Phys*. **2006**, *124*, 224105. See also ref. 44.

and without continuum solvent modeling.[36] The results obtained using these higher levels of theory were qualitatively similar to those found with B3LYP/6-31G(d), and support fully the conclusions drawn in this study. A summary of those calculations is provided in Section 2.11.4 and Figure 2.7.

As a first step in the computational analysis of the HKR, we sought to evaluate the geometries of epoxide complexation to the chiral (salen)Co(III) complex, and the extent to which these might depend on the absolute stereochemistry of the epoxide. In particular, the energetic cost of varying the O–Co–O–C dihedral angle θ in epoxide-(*S,S*)-**1b** complexes was evaluated systematically with (*R*)-1,2-epoxypropane (matched with respect to (*S,S*)-**1b**), (*S*)-1,2-epoxypropane (mismatched) and ethylene oxide (Figure 2.13).[37] This analysis reveals a strong preference for epoxide binding within a narrow range of dihedral angles θ regardless of epoxide stereochemistry, with θ = 40º as the global minimum for the three epoxides examined.[38] Comparison of the lowest energy computed structures of (*S,S*)-(salen)Co–OH with bound (*R*)- and (*S*)-1,2-epoxyhexane reveals only a 0.52 kcal/mol preference for binding of (*R*)-epoxypropane (Figure 2.14). This result is consistent with kinetic analyses of HKR reactions[7a] and binding studies performed using ^{1}H NMR,[39] which showed that both enantiomers of epoxide

[36] We performed calculations with B3LYP, OLYP, TPSSh, BP86, PW91, and M06L, using basis sets as large as 6/311+G(d,p) and ccPVTZ.

[37] As would be expected for a six-coordinate d^6 Co(III) complex, the **1b•**epoxide complexes are all most stable as closed-shell singlets. A more detailed discussion of spin state in (salen)Co(III) complexes can be found in the next Section.

[38] Nearly identical binding geometries are observed in two crystal structures of *cis*-disubstituted aziridines bound to cationic (salen)Co(III) complexes, with θ = 40–52º (Figure 4 and ref 17). These values represent a range of six values of θ culled from two crystal structures. Each cationic (salen)Co(III) unit has two bound aziridines, and in one of the crystal structures, there are two crystallographically distinct (salen)Co(III) units. The similarities in the binding geometries of epoxides and aziridines to (salen)Co(III) are striking given the different electronic and steric properties of these ligands.

[39] Kemper, S.; Hrobárik, P.; Kaupp, M.; Schlörer, N. E. *J. Am. Chem Soc.* **2009**, *131*, 4172–4173.

bind rapidly and reversibly to chiral (salen)Co(III) complexes such as **1b**, and with approximately equal affinity. Taken together, the experimental and computational data reveal that that epoxides are bound in a well-defined orientation with respect to the (salen)Co(III) complex independent of the stereochemistry of the epoxide, but that differential epoxide complexation is not responsible for stereoselectivity in the HKR

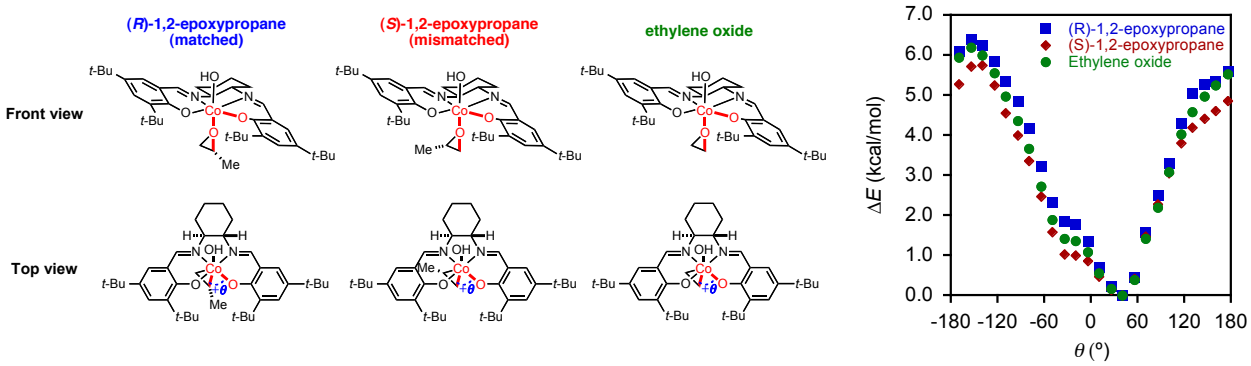

Figure 2.13. Plot of relative energy versus O–Co–O–C dihedral angle θ in a neutral (*S*,*S*)-(salen)Co(III) complex with bound (*R*)-1,2-epoxypropane (blue squares), (*S*)-1,2-epoxypropane (red diamonds) and ethylene oxide (green circles), calculated as closed-shell singlets at the B3LYP/6-31G(d) level. Each point represents the relative uncorrected electronic energy of an optimization performed with θ frozen and all other degrees of freedom permitted to relax. The minimum for each epoxide was set to ΔE = 0 kcal/mol.

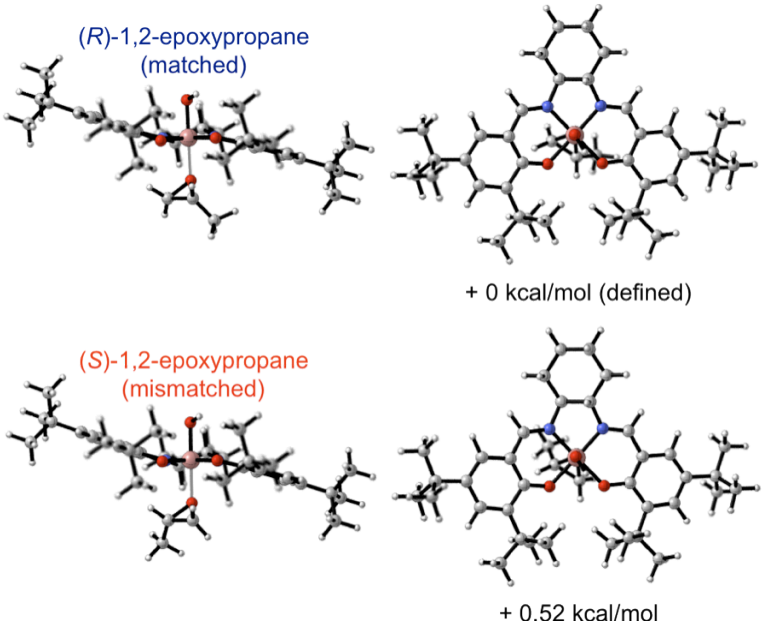

Figure 2.14. Structures of neutral (*S*,*S*)-(salen)Co–OH complexes with bound (*R*)-1,2-epoxypropane and (*S*)-1,2-epoxypropane, calculated as closed-shell singlets at the B3LYP/6-31G(d) level.

2.5 Computational Characterization of the Nucleophilic (salen)Co–OH Complex. Together with the epoxide complex analyzed in Part C, the other critical reacting partner in the HKR is the nucleophilic (salen)Co–OH complex, so we also sought to characterize this intermediate computationally. In particular, we were interested in defining the coordination geometry and spin state of the most reactive (salen)Co–OH complex. A hexacoordinate, low spin (salen)Co(OH_2)(OH) complex (^{1}**1b**•H_2O, S = 0)[40] has been implicated as the reactive nucleophilic species in the HKR based on kinetic analyses.[7] These species have been shown to be nucleophilic: hexacoordinate Co(III) hydroxo complexes studied as metalloprotease mimics are competent nucleophiles in the hydrolysis of pendant ester groups of *N*-coordinated amino ester ligands.[41]

Recently, an alternative, pentacoordinate, intermediate spin (salen)Co–OH complex (^{3}**1b**, S = 1) was proposed in a separate study as a potentially reactive species on the basis of the assignment of ^{3}**1c** ((salen)Co–Cl) in CH_2Cl_2 solution by magnetic susceptibility measurements.[39] In this analysis, the authors found that in donor solvents such as THF, there is an equilibrium between diamagnetic and paramagnetic species. This led us to consider whether ^{3}**1b** and ^{1}**1b**•H_2O might both be accessible under the conditions of the HKR reaction, and, if so, which of those is the active nucleophile in the epoxide ring-opening. Based on a superficial analysis, the triplet ^{3}**1b** might be expected to be more reactive, as low spin, octahedral d^6 complexes such as ^{1}**1b**•H_2O are typically inert to ligand substitution reactions.[42]

---

[40] For the purposes of this discussion, compound numbers are labeled with their spin multiplicity. For example $^{2S+1}$**1**, refers to an electronic configuration of compound **1** with a total spin quantum number of S.

[41] Sutton, P. A.; Buckingham, D. A. *Acc. Chem. Res.* **1987**, *20*, 357–364.

[42] (a) The kinetic non-lability of six-coodinate Co(III) complexes is well established: Crabtree, R. H. *The Organometallic Chemistry of the Transition Metals*, 4th ed.; John Wiley & Sons: Hoboken, 2005; pp 11–12. (b) The effect is illustrated in a dramatic way by the fact that hexaaminecobalt(III) chloride can be purified by

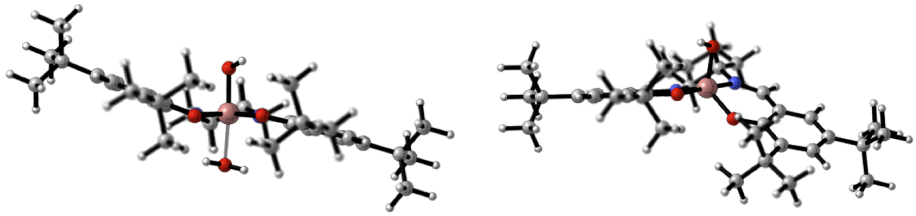

^{1}1b•H_2O *singlet spin state* **^{3}1b** *triplet spin state*

Figure 2.15: Structures of potential nucleophilic catalysts **^{3}1b** and **^{1}1b**•H_2O optimized at the B3LYP/6-31G(d) level of theory.

Optimized, computed structures of **^{1}1b**•H_2O and **^{3}1b** are presented in Figure 2.15.[43] Six-coordinate **^{1}1b**•H_2O adopts a pseudo-octahedral geometry with a distinct step conformation as discussed in Section B, whereas five-coordinate **^{3}1b** adopts a distorted square pyramidal geometry.[44] The calculations predict that **^{3}1b** is stable as a five-coordinate complex and has very little affinity for water, while **^{1}1b**•H_2O is most stable as a six-coordinate complex and therefore binds water tightly. While different levels of theory provided subtly different results, the general picture that emerges is that the lowest energy five-coordinate complexes are triplets while the lowest energy six-coordinate complexes are singlets.[45] After examining individual Co(III)

---

recrystallization from concentrated hydrochloric acid in high yield: Bjerrum, J.; McReynolds, J. P. *Inorg. Synth.* **1946**, *2*, 216–221.

[43] In both five- and six-coordinate complexes, the quintet (S = 2) spin state was higher in energy (see Supporting Information), and it was not considered further.

[44] We also considered the valence tautomer of **^{3}1b** in which cobalt is in the +II oxidation state (S_{Co} = 3/2) and the salen ligand is oxidized by one electron and is antiferromagnetically coupled to the metal center (S_{salen} = –1/2), but these species do not appear to be stable: no structures of this type were located. Nevertheless, as others have observed, the computed structure of **^{3}1b** appears to have a resonance contribution from a Co(II)–phenoxyl representation. Spin density maps and molecular orbitals relevant to our analysis are presented in Section 1.11. A detailed analysis of cationic (salen)Co$(OH_2)^+$ yielded EPR and magnetic susceptibility data that support significant Co(II)–phenoxyl character: Kochem, A.; Kanso, H.; Baptiste, B.; Arora, H.; Philouze, C.; Jarjayes, O.; Vezin, H.; Luneau, D.; Orio, M.; Thomas, F. *Inorg. Chem.* **2012**, *51*, 10557–10571. In contrast, further one-electron oxidation of (salen)Co(III) complexes occurs on the ligand to generate the Co(III)–phenoxyl. For a detailed discussion of ligand-centered redox behavior in (salen)Co complexes, see: (a) Vinck, E.; Murphy, D. M.; Fallis, I. A.; Strevens, R. R.; Van Doorslaer, S. *Inorg. Chem.* **2010**, *49*, 2083–2092. For examples with other, related complexes, see: (b) Ray, K.; Begum, A.; Weyhermüller, T.; Piligkos, S.; van Slageren, J.; Neese, F.; Wieghardt, K. *J. Am. Chem. Soc.* **2005**, *127*, 4403–4415. (c) Smith, A. L.; Hardcastle, K. I.; Soper, J. D. *J. Am. Chem. Soc.* **2010**, *132*, 14358–14360.

[45] Key calculations were repeated using other exchange functionals that have been used to reproduce spin state preferences for Co(III) complexes correctly. For evaluations of DFT performance with Co(III) spin state ordering, see: (a) Wasbotten, I. H.; Ghosh, A. *Inorg. Chem.* **2007**, *46*, 7890–7896. (b) Takatani, T.; Sears, J. S.; Sherrill, C. D.

complexes in the ground state, we extended our analysis of spin state to the bimetallic epoxide ring-opening transition structures (Figure 2.16).

In a comparison of the calculated barriers to ring-opening transition structures of 1,2-epoxypropane (**TS-1**), we found that ^{1}**1b**•H_2O is in fact more nucleophilic than ^{3}**1b**: the barrier for epoxide opening in the singlet manifold is 1.4 kcal/mol lower than what is calculated for the triplet manifold (Figure 2.16).[46, 47] These calculations demonstrate that the hydroxo ligand in this six-coordinate Co(III) complex ^{1}**1b**•H_2O is in fact highly nucleophilic.

J. Phys. Chem. A **2009**, *113*, 9231–9236. (c) Jensen, K. P.; Cirera, J. *J. Phys. Chem. A* **2009**, *113*, 10033–10039. (d) Ghosh, A. *J. Biol. Inorg. Chem.* **2006**, *11*, 712–724.

[46] The data presented in Figure 15 show that the epoxide ring-opening step has a higher activation barrier, but is considerably more favorable thermodynamically when the (salen)Co–OH complex undergoes reaction from the triplet spin state instead of the singlet spin state. Calculations repeated with implicit solvent modeling show that this difference in energy is predominantly an artifact of the penalty for charge separation in the gas phase: whereas pre-complex ^{3}**SM-1** and transition structure ^{3}**TS-1**, have unpaired spin density localized to the nucleophile-delivering (salen)Co(III) complex, the bimetallic product of reaction from the triplet manifold is predicted computationally to undergo disproportionation to a Co(II)/Co(IV) complex to minimize this charge separation. This behavior is not observed when solvation models are applied. However, this effect becomes significant only after the rate- and selectivity-determining transition structure. Accordingly, we opted to conduct the remainder of our analyses using gas phase calculations, which were found to converge more rapidly and consistently than calculations carried out with solvent correction. See Section 1.11 for additional details.

[47] We are mindful not to draw too strong of a conclusion from an energy difference of this magnitude involving structures of two different spin states, especially with a fairly primitive DFT method. The important conclusion is that the hydroxo ligand can react as a nucleophile with an activated epoxide without dissociating from the Co(III) center and that the barrier to this reaction is comparable to the hydroxo in ^{3}**1b**. A survey of other computational methods reveals that some functionals predict ^{3}**1b** to be slightly more nucleophilic than ^{1}**1b**•H_2O, making it difficult to draw a conclusion about the absolute nucleophilicities of these hydroxo complexes (see Section 1.11). Nonetheless, the computational models all show that ^{1}**1b**•H_2O is both stable and highly nucleophilic.

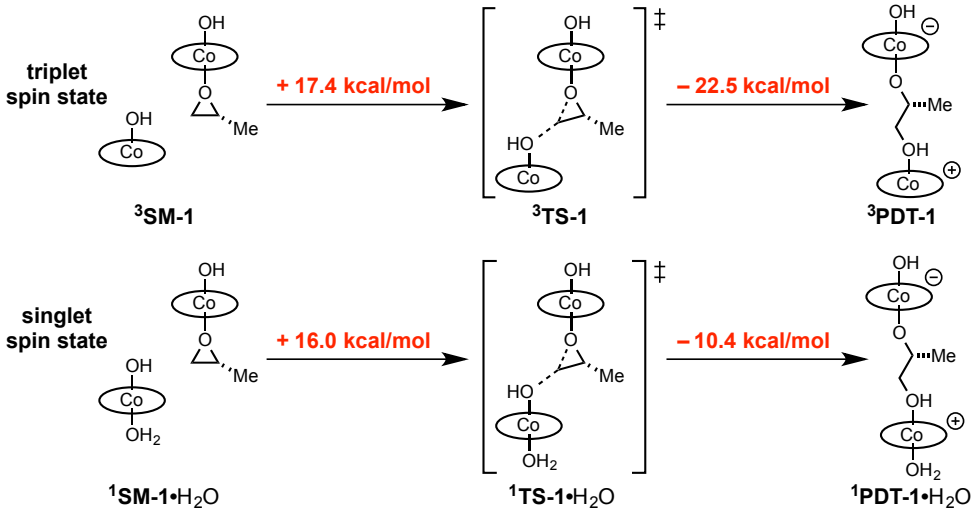

Figure 2.16. Electronic configuration preferences in the epoxide-opening transition structure for (salen)Co–OH at the B3LYP/6-31G(d) level in the gas phase. Structures in the singlet spin state were calculated as closed-shell configurations. Energies reported as the difference in uncorrected electronic energy.

An analysis of the computed transition structures (Table 2.1) provides a potential explanation: the epoxide ring-opening transition state comes early on the reaction coordinate, with the hydroxo ligand still fully associated to the Co(III) center. As such, nucleophilicity is not tied to the coordinative stability or lability of the hydroxo ligand, but rather to its nucleophilicity when bound to cobalt. We note the possibility that crossover to the triplet manifold plays a role in achieving catalyst turnover after the rate-determining epoxide ring-opening step. On the basis of this analysis and the previously reported kinetic analysis, we conclude that ^{1}**1b**•H_2O is indeed the nucleophilic partner in the HKR, and we use this structure in the remainder of the calculations in this chapter.

Table 2.1. Key bond lengths on the reaction coordinate from **1b** to **PDT-1** for the singlet and triplet spin states at the B3LYP/6-31G(d) level of theory.

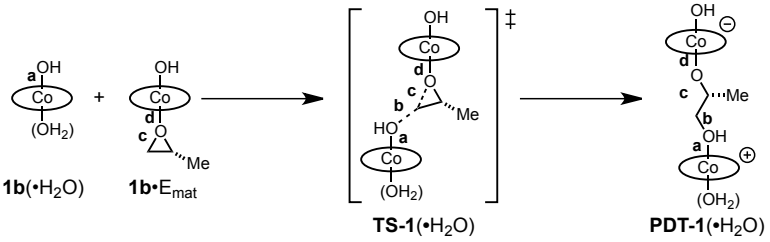

Bond Length (Å)	^{3}**1b**	^{1}**1b**•H_2O	^{1}**1b**•E_{mat}	^{1}**TS-1**•H_2O	^{3}**TS-1**	^{1}**PDT-1**•H_2O	^{3}**PDT-1**
a	1.82	1.82	–	1.86	1.91	1.92	2.35
b	–	–	–	1.97	1.96	1.49	1.44
c	–	–	1.45	1.88	1.90	2.30	2.35
d	–	–	2.09	1.98	1.97	1.94	1.83

2.6 Cooperative Stereochemical Communication in Epoxide Ring Opening

Having elucidated the most salient features of the structure of both the (salen)Co-epoxide complex and the reactive (salen)Co–OH complex that participate in the HKR reaction, we sought to establish how these catalysts achieve stereoselectivity in the epoxide ring-opening reaction. The experimental results described in Section 2.2 demonstrate that a stereochemical match is required between the epoxide and the two molecules of (salen)Co(III) in the epoxide ring-opening reacton, and determining whether this requirement could be reproduced computationally was a logical starting point for our analysis. Specifically, we sought to compare the calculated transition structure energies of the "all matched" **TS-1**•H_2O with diastereomeric transition structures corresponding to Pathways **B**, **C** and *ent*-**D** introduced in Figure 2.2.

To more effectively model dispersive interactions that the B3LYP functional tends to underestimate, single point calculations were performed on the B3LYP-optimized geometries using Truhlar's M06-L meta-GGA functional and the larger 6-31+G(d,p) basis set, which performs well in benchmarks for a range of noncovalent interactions.[48] The related Minnesota

[48] Zhao, Y.; Truhlar, D. G. *Theor. Chem. Acc.* **2008**, *120*, 215–241.

functional M05-2X has been shown to accurately predict catalyst structure-enantioselectivity relationships in reactions that are dominated by noncovalent interactions, although this method sometimes overestimates the magnitude of these selectivity trends.[49] Calculations with both the B3LYP and M06-L methods described above show that changing the absolute stereochemistry of either molecule of (salen)Co(III) catalyst or the epoxide resulted in a significantly higher transition structure energy (Figure 2.17). These data show that the stereochemical match required in HKR reactions is reproduced remarkably well with the chosen DFT methods.

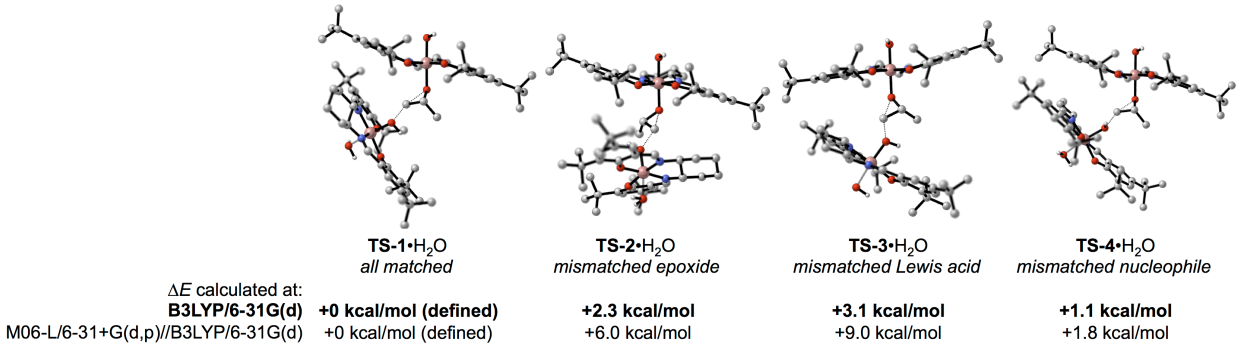

Figure 2.17. Epoxide ring-opening transition structures optimized at the B3LYP/6-31G(d) level of theory are presented along with the difference in energy between each structure and **TS-1**•H_2O. The selectivity was also calculated from single-point energies at the M06-L/6-31+G(d,p) level of theory with the B3LYP/6-31G(d) geometry. C–H bonds are omitted for clarity.

[49] (a) Zuend, S. J.; Jacobsen, E. N. *J. Am. Chem. Soc.* **2009**, *131*, 15358–15374. (b) Uyeda, C.; Jacobsen, E. N. *J. Am. Chem. Soc.* **2011**, *133*, 5062–5075.

Table 2.2. Diastereomeric transition structures for epoxide opening.

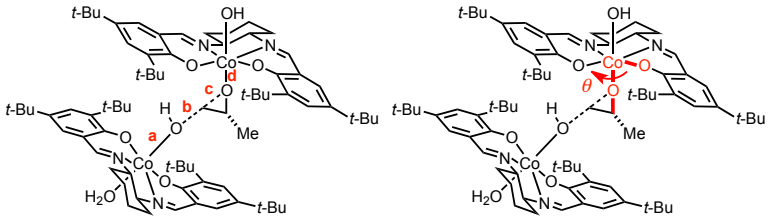

	TS-1•H_2O	**TS-2**•H_2O	**TS-3**•H_2O	**TS-4**•H_2O
Lewis Acid **Epoxide** **Nucleophile**	(*S*,*S*) (R) (S,S)	(*S*,*S*) (***S***) (*S*,*S*)	(***R***,***R***) (*R*) (*S*,*S*)	(*S*,*S*) (*R*) (***R***,***R***)
a	1.86	1.86	1.86	1.86
b	1.97	1.95	1.98	1.96
c	1.88	1.89	1.89	1.88
d	1.98	1.98	1.99	1.98
θ	54.4°	51.8°	8.3°	44.8°

Comparison of **TS-1**•H_2O and **TS-2**•H_2O is of particular interest, because the difference in energy between these two transition structures corresponds to the stereoselectivity of the kinetic resolution of a racemic epoxide with enantiopure catalyst (i.e. the HKR reaction). Inspection of **TS-2**•H_2O reveals that the nearest contact between the two (salen)Co(III) complexes is between the *tert*-butyl group at the salicylidene 5-position of the Lewis acidic complex and backbone cyclohexane ring on the nucleophile-delivering catalyst. Superficially, invoking such a contact as playing a role in stereoinduction seems to be inconsistent with the results presented in Section 2.3 that showed that the salen step mediates the stereochemical match between catalysts, and that the shape of the backbone plays a less significant role. The precise interpretation of the kinetics data presented in Section 2.3 is more subtle, however: the data only show that the "all matched" Pathway A proceeds at comparable rates for **1b** and **3b** (Figure 2.10) and that other pathways are too slow to detect by reaction calorimetery. The data

are not sufficient to conclude whether the interactions that destabilize Pathways B–D for **1b** are the same as those that destabilize the analogous pathways for **3b**.

To test the effect of ligand bulk at the salicylidene 5-position experimentally, we prepared a series of substituted catalysts and determined each catalyst's stereoselectivity in (±)-1,2-epoxyhexane hydrolysis (Table 2.3).[50] The data reveal that the size of the substituent indeed has a significant effect on stereoselectivity of epoxide hydrolysis, with larger substituents generally resulting in more selective catalysts.[51,52,53,54]

[50] For examples of electronic or steric tuning of chiral (salen)metal complexes by variation of the salicylidene 5-substituent, see: (a) Palucki, M.; Finney, N. S.; Pospisil, P. J.; Guler, M. L.; Ishida, T.; Jacobsen, E. N. *J. Am. Chem. Soc.* **1998**, *120*, 948–955. (b) Doyle, A. G.; Jacobsen, E. N. *Angew. Chem., Int. Ed.* **2007**, *46*, 3701–3705.

[51] Kinetic analyses with some of these catalysts also reveal an approximately second order dependence on catalyst loading, suggesting that these catalysts promote hydrolysis via a cooperative, bimetallic mechanism. In this analysis, we have also found that catalysts that induce higher enantioselectivity are also generally more reactive. Although the basis for this rate acceleration effect is not known, it is possible that different degrees of solvation of the largely hydrophobic catalyst in a hydrophilic reaction mixture may play a role.

[52] The enantioselectivity trends determined by GC analysis are reproduced well by reaction calorimetry experiments in which the rates of hydrolysis of (*R*)- and (*S*)-1,2-epoxyhexane were measured independently. See the Supporting Information for details.

[53] The measured selectivity factor for R = *t*-Bu is larger than the selectivity factor obtained previously from analogous experiments: ref 2b. Measuring selectivity factors of this magnitude is technically challenging. For a discussion of the factors that might limit accuracy and precision in the determination of selectivity factors in the HKR, see: ref 1b. The experimental procedure used for the determination of selectivity factors is included in the Supporting Information.

[54] The data also suggest there is a leveling effect with very large substituents, and substituents larger than *tert*-butyl appear to induce slightly lower enantioselectivity (i.e., R = trimethylsilyl induces lower enantioselectivity than R = *t*-Bu). Preliminary calorimetry experiments using (salen)Co–Cl complexes with substituents larger than trimethylsilyl (i.e., triethylsilyl and tripropylsilyl) indicate that this trend continues.

Table 2.3. Selectivity factors in epoxide hydrolysis with substituted catalysts.

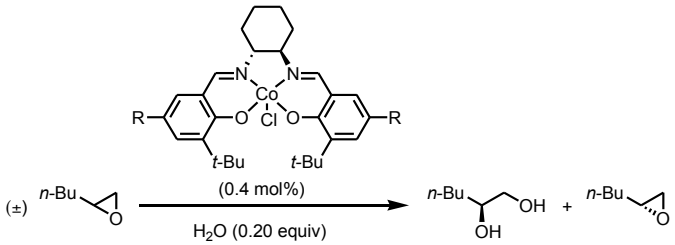

Entry	R	Selectivity factor*
1	H	62 ± 5
2	Me	82.14 ± 0.04
3	Et	146.5 ± 0.4
4	*i*-Pr	368 ± 1
5	*t*-Bu	620 ± 40
6	$SiMe_3$	524 ± 9

*Average of two independent experiments ± 1 standard deviation. Determined by chiral GC analysis of acetylated 1,2-hexanediol recovered from the reaction mixture.

To test whether this close contact could play a role in destabilizing **TS-2**•H_2O, we used DFT methods to locate transition structures analogous to **TS-1**•H_2O and **TS-2**•H_2O with different substituents at the 5 and 5' (*para*) positions of the salen ligand (Figure 2.18). When the 5,5'-*t*-Bu groups in **1b** are replaced with Me or H, the geometry of the bimetallic epoxide ring-opening transition structure relaxes somewhat, most significantly in the analogs of **TS-2**•H_2O (mismatched epoxide). The fact that the transition structure that is more sensitive to this effect leads to the minor pathway in epoxide hydrolysis reactions catalyzed by **1b** is consistent with the hypothesis that this effect plays a role in stereochemical communication. While the B3LYP/6-31G(d) energies do not predict an increase in selectivity with increasing steric bulk (indeed, they predict a decrease), single point calculations at the M06-L/6-31+G(d,p) level predict a significant increase in selectivity with bulkier ligands.

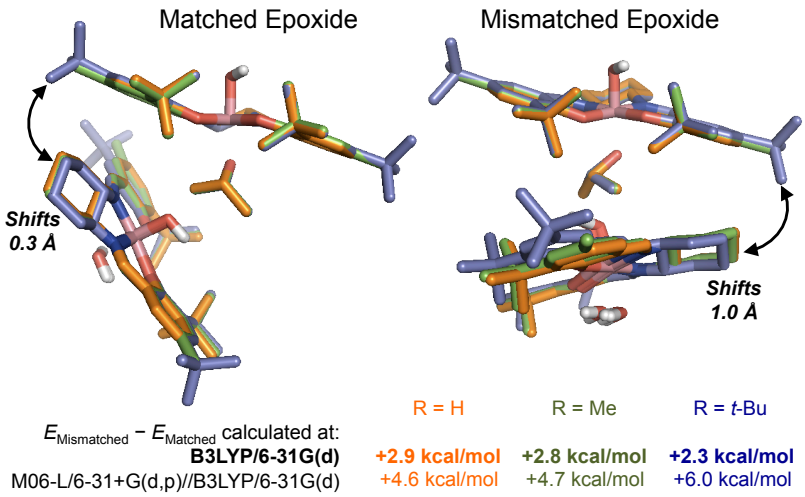

Figure 2.18. Proposed interaction responsible for stereochemical communication between (salen)Co(III) catalysts in the HKR. Transition structures for epoxide ring-opening with analogs of **1b** substituted at the 5,5' (*para*) positions were optimized at the B3LYP/6-31G(d) level of theory in the gas phase and overlaid by minimizing the RMSD between the six atoms in the Lewis acidic Co(III) center's coordination sphere. The structures are annotated with the amount that the nucleophile-delivering complex's backbone six-membered ring shifts when the ligand is changed from R = H to R = *t*-Bu.

2.7 Intrinsic Stereoselectivity of (salen)Co–OH as a Lewis Acid

As demonstrated above, DFT calculations of HKR transition structures provide good agreement with experimental stereoselectivities and even served to uncover a specific steric interaction that is important for selectivity. Our resulting confidence in the utility of these calculations prompted us to consider addressing questions related to the HKR computationally that are not readily addressable experimentally. These include the intrinsic stereoselectivity of (salen)Co–OH complex **1b** as both a Lewis acid for epoxide activation and as a nucleophile-delivery agent.

As established in Section 2.2, a stereochemical match between the two (salen)Co(III) complexes is necessary for epoxide ring opening to occur. However, the question remains unanswered as to whether the Lewis acid complex alone is capable of inducing high stereoselectivity in epoxide ring opening. As illustrated in Figure 2.13, both enantiomers of epoxide bind to the (salen)Co(III) complex in the same orientation with respect to the salen step.

As such, approaching nucleophiles attacking the less substituted carbon of the epoxide experience different steric interactions with the Lewis acid catalyst depending on the stereochemistry of the epoxide (Figure 2.19).

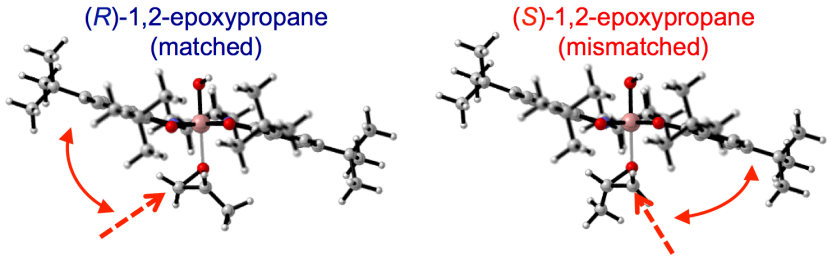

Figure 2.19. While the epoxide ring is held in the same orientation with respect to the catalyst for both enantiomers of epoxide, an incoming nucleophile attacking the less substituted epoxide carbon is expected to experience different steric interactions with the stepped conformation of the catalyst depending on the stereochemistry of the epoxide (red arrows).

As discussed in Section 2.2, it is impossible to isolate the two roles of the (salen)Co(III) complex – epoxide activation and nucleophile delivery – experimentally because of the rapid ligand exchange that is characteristic of this system.[11] On the other hand, computational analysis is well suited to address this question because the composition of the calculated structure can be controlled precisely. To evaluate whether (salen)Co–OH could be a highly stereoselective Lewis acid in the absence of a chiral nucleophile-delivery agent, we investigated the hypothetical reaction of ammonia with epoxides activated by (salen)Co–OH. We chose ammonia for its lack of charge, its small size, and its symmetry about the forming C–N bond – all desirable properties for a straightforward computational investigation. The results demonstrate that the Lewis acidic (salen)Co(III) catalyst alone does not activate epoxide stereoselectively: the calculated stereoselectivity of 0.35 kcal/mol for 1,2-epoxypropane actually represents an erosion of selectivity from the calculated ground state preference of 0.52 kcal/mol for binding the matched enantiomer of epoxide (Table 2.4).

Table 2.4: Transition structures for the hypothetical reaction of ammonia with epoxides activated by (*S,S*)-(salen)Co–OH calculated as closed-shell singlets at the B3LYP/6-31G(d) level.

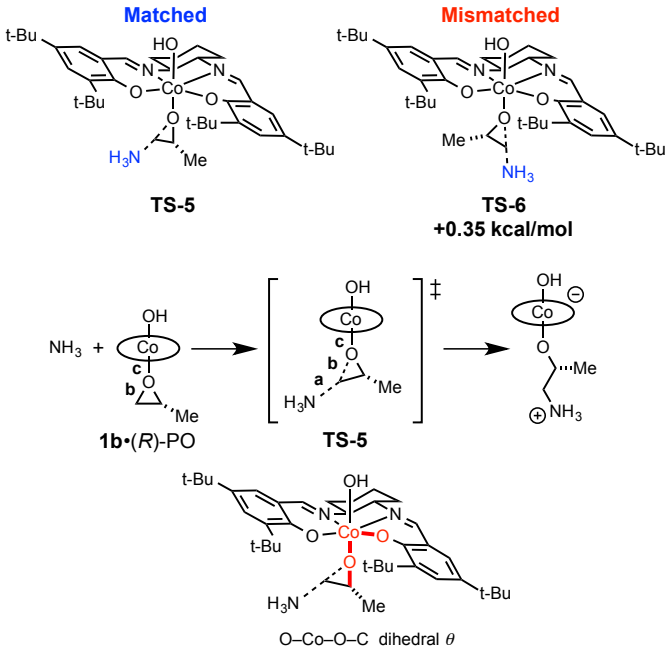

Bond Length (Å) or Angle	**1b**•(*R*)-PO	**1b**•(*S*)-PO	**TS-5**	**TS-6**
a	–	–	2.00	2.00
b	1.45	1.45	1.94	1.93
c	2.09	2.09	1.99	2.00
θ	40.5°	40.2°	48.9°	42.6°

2.8. Intrinsic Stereoselectivity of (salen)Co(OH)(OH_2) as a Nucleophile

Having established the calculated selectivity in our DFT model does not arise from (salen)Co–OH selectively activating the matched enantiomer of epoxide for attack, we set out to address the alternative possibility that (salen)Co(OH)(OH_2) (**1b**•H_2O) alone might be a highly stereoselective nucleophile-delivering agent that can discriminate between enantiomers of epoxide. If this were so, **1b**•H_2O should be able to discriminate between two enantiomers of an epoxide bound to an achiral Lewis acid. We selected borane as the Lewis acid for computational analysis of this hypothetical reaction for reasons analogous to those that led us to chose ammonia

as our test nucleophile: borane is small, neutral and symmetrical. However, this analysis is considerably more nuanced than the reaction of **1b•**(epoxide) with ammonia, as the nucleophilic oxygen atom of **1b•**H_2O might be reactive in a variety of trajectories. After thoroughly examining possible trajectories for nucleophilic addition to epoxide, we determined that in the lowest energy pathway there is actually a slightly lower barrier to opening the "mismatched" enantiomer of epoxide (Table 2.5). The analyses in this and the preceding sections allow us to conclude that neither (salen)Co complex alone is responsible for the high stereoselectivity in the HKR, and that instead catalyst-catalyst interactions must be responsible. The remainder of this article endeavors to elucidate the precise basis for this remarkable cooperative effect.

Table 2.5: Transition structures for the hypothetical reaction of (*S,S*)-(salen)Co–OH with borane-activated 1,2-epoxypropane calculated as closed-shell singlets at the B3LYP/6-31G(d) level.

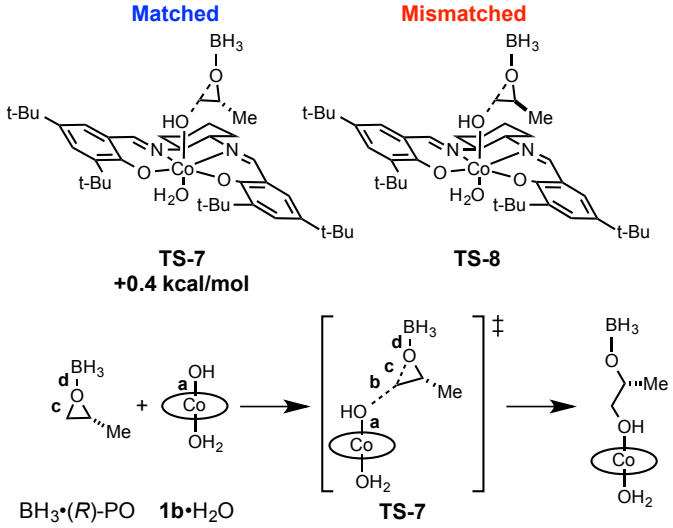

Bond Length (Å) or Angle	**1b•**H_2O	BH_3•(*R*)-PO	**TS-7**	**TS-8**
a	1.82	–	1.86	1.86
b	–	–	2.03	2.02
c	–	1.46	1.84	1.83
d	–	1.67	1.57	1.57

2.9. A Stereochemical Model for the HKR

As noted in the introduction, consistently high stereoselectivities are obtained in (salen)Co(III)-catalyzed kinetic resolutions of terminal epoxides. For this reason, any meaningful stereochemical model for the HKR should shed light on why the steric properties of the epoxide substituent have so little impact on the stereoselectivity of the ring-opening reaction.

A visual inspection of lowest energy transition structure **TS-1**•H_2O (Figure 2.17) suggests a possible explanation: the epoxide substituent (in this case, methyl), which is the element that can be varied without negative impact on reaction stereoselecitivity, projects into a large open space between the two Co(III) complexes. We evaluated whether this is the case in the HKR of a variety of different epoxides by optimizing matched epoxide-opening transition structures analogous to **TS-1**•H_2O and mismatched transition structures analogous to **TS-2**•H_2O for epoxides with different steric and electronic properties. Each of the epoxides subjected to this analysis undergoes hydrolysis with high stereoselectivity under (salen)Co(III) catalysis.

Both "matched" and "mismatched" transition structure geometries remain remarkably unchanged upon changing the epoxide substituent in **TS-1**•H_2O from methyl to *tert*-butyl, cyclohexyl or phenyl (Figure 2.20).[55] These structures give a striking perspective on a molecular assembly that is at once highly selective in epoxide kinetic resolution and remarkably promiscuous in accommodating a broad range of terminal epoxides: the epoxide substituent does not participate in any significant interactions in the stereoselectivity-determining transition

[55] We note that while the selectivities predicted for these epoxides do not follow the experimental trends—*tert*-butyl and phenyl substituents lead to lower selectivities than cyclohexyl or methyl[1b]—these epoxide are all excellent substrates for the HKR and our calculations predict high selectivities for each of them. It seems likely that differences in selectivity between these epoxides are driven by weak dispersion interactions, which B3LYP is not well suited to accurately reproduce.

structure, but rather its primary role is only to determine the position of the more reactive less-substituted position of the epoxide with respect to the chiral salen ligand.

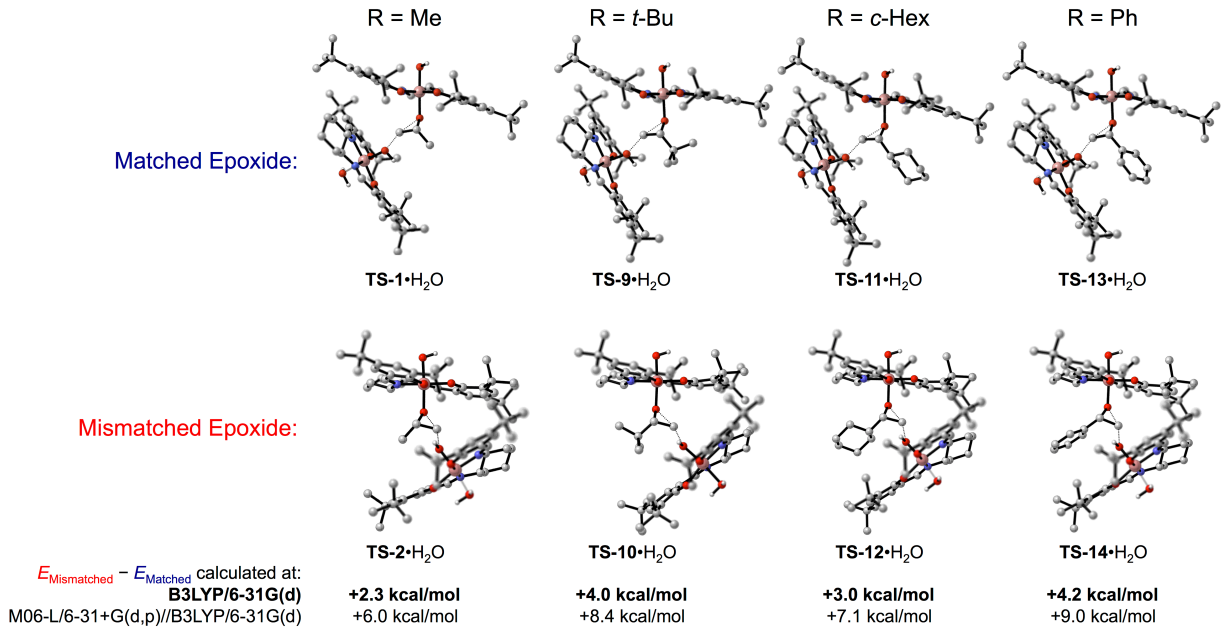

Figure 2.20. The effect of the epoxide substituent on calculated stereoselectivity. Epoxide ring-opening transition structures optimized at the B3LYP/6-31G(d) level of theory are presented along with the difference in energy between the "Matched" and "Mismatched" transition structures. C–H bonds are omitted for clarity.

We conclude that stereoselectivity in the HKR of terminal epoxides arises primarily from the catalyst-catalyst interactions taking place in the different transition structures, and not from specific interactions with the epoxide enantiomers. If this model is correct, one could imagine that the chiral (salen)Co(III) catalysts should exert a form of stereoselectivity even with ethylene oxide, which is achiral and bears no epoxide substituent at all. In that case, stereoselectivity would be manifested as a preference for addition to one electrophilic position over the other. While this prediction would be extremely difficult to test experimentally—the product in each case is simply ethylene glycol—it can be addressed quite readily using computational tools.

We replaced the epoxide methyl substituent in **TS-1**•H_2O and **TS-2**•H_2O with a hydrogen atom and fully optimized the resulting structure to a transition structure (Figure 2.21). These

structures overlay nearly perfectly with **TS-1**•H_2O and **TS-2**•H_2O and there is a significant preference for addition by the same trajectory the leads to hydrolysis of the matched enantiomer of epoxide, with a selectivity that is nearly identical to the observed stereoselecitivty in the HKR of terminal epoxides. This provides a most compelling, final piece of evidence that stereoselectivity arises from the relative orientation of the two (salen)Co(III) catalysts and not from specific interactions of the chiral epoxide enantiomers with the chiral catalysts.

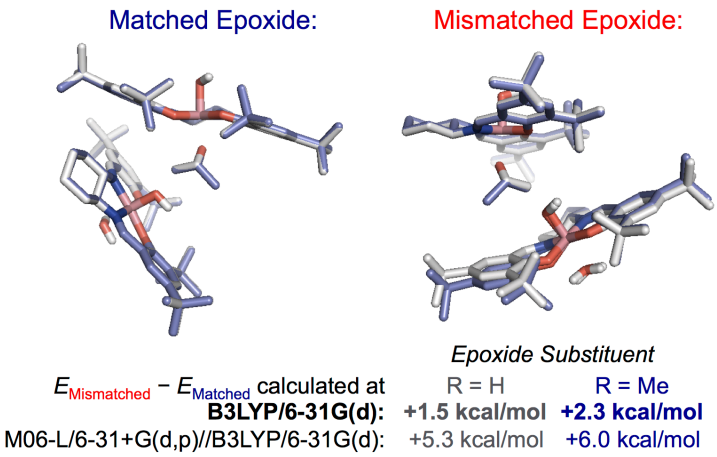

Figure 2.21. Computed selectivity for the hypothetical epoxide ring-opening reaction of ethylene oxide. The epoxide methyl substituent in **TS-1**•H_2O and **TS-2**•H_2O was replaced with a hydrogen atom and the resulting structure was optimized to a transition structure at the B3LYP/6-31G(d) level. The resulting structures were overlaid with their parent structures by minimizing the RMSD between the six atoms in the Lewis acidic Co(III) center's coordination sphere. C–H bonds are not shown for clarity.

2.10 Conclusions. A range of experimental and computational data support the proposal that the asymmetric induction in the epoxide ring-opening step of the HKR is controlled by interactions between two (salen)Co(III) complexes and that these interactions are mediated by the chiral, stepped conformations of the salen ligand. Furthermore, and perhaps more significantly, this model does not require a steric clash with the epoxide substituent to achieve stereoselectivity, providing an explanation for the extraordinary breadth of the HKR's substrate scope. Key findings include:

(1) Kinetic analyses using mixtures of (*R*,*R*)-, (*S*,*S*)-, and/or *meso*-(salen)Co(III) complexes establish that the absolute stereochemistry of Lewis acidic and nucleophilic catalysts must be matched to the chiral epoxide in order for any measurable hydrolysis to occur, and that the chiral, stepped conformation of the salen ligand mediates this stereochemical match.

(2) Computational studies show that epoxides bind to the cobalt center in almost identical geometries, that this geometry is insensitive to epoxide substituent and stereochemistry, and that there is a significant energetic penalty for accessing other binding orientations. DFT calculations also support the conclusion drawn from previous kinetic studies that the hexacoordinate singlet ^{1}**1b**•H_2O is a competent nucleophile in epoxide-opening chemistry.

(3) A computational analysis of bimetallic ring opening transition structures with the full catalyst structure reproduces that the matched stereochemical relationship between the catalysts and the epoxide that is observed experimentally. These transition structures led to the identification of a catalyst-catalyst interaction that may be important for selectivity and this proposal was validated by demonstrating experimentally that stereoselectivity is highly sensitive to the steric demands of substituents on the salen aromatic ring that are distant from the cobalt center.

(4) Computational investigations of hypothetical monometallic epoxide ring-opening reactions show that neither the Lewis acidic or the nucleophile-delivering (salen)Co(III) complex is able to achieve stereoselectivity on its own, and selectivity is only achieved in the bimetallic assembly. This supports the conclusion that stereochemical communication between catalysts is key to selectivity.

(5) Finally, inspection of the calculated transition structures led us to the observation that the epoxide substituent—which can be changed to nearly any organic fragment without the

selectivity factor dropping below 50—projects into open space. Indeed, the spatial relationship between the two (salen)Co(III) catalysts in the epoxide ring-opening transition structure changed very little when we replaced our model epoxide, propylene oxide, with other epoxides with larger substituents or with no substituent at all (ethylene oxide), indicating that a steric interaction between the epoxide substituent and the catalyst is not required for high stereoselectivity. We conclude that the role of the epoxide substituent is simply to position the epoxide's less-substituted electrophilic reactive site with respect to the catalyst. This serves to explain how enantiomeric epoxides can be resolved efficiently without relying on a specific interaction with the epoxide substituent.

More broadly, the mechanistic model for the HKR developed here provides a rationalization for how the HKR can be both so highly stereoselective and broad in scope with respect to terminal epoxide substrates. All terminal epoxides bind in essentially the same geometry and are subject to the same interactions with the catalyst in the ground state and the transition state. Binding of the epoxide ring in a specific orientation reduces the problem of selectively opening one enantiomer of a broad range of epoxides to the more straightforward proposition of discriminating between two trajectories along which two chiral (salen)Co(III) complexes can react. Hence, selectivity is primarily controlled by interactions between the aromatic groups of the two salen ligands, which are expected to be quite similar with different nucleophile–electrophile combinations.

This work joins a growing body of research that has been directed toward elucidating the mechanisms of so-called "privileged" chiral catalysts.[56] While the immediate practical goal of such mechanistic investigation may be to improve and expand these particular catalyst systems, a

[56] *Privileged Chiral Ligands and Catalysts*; Zhou, Q.-L., Ed.; Wiley-VCH: Weinheim, Germany, 2011.

broader, more fundamental objective is to understand how small-molecule chiral catalysts such as metal salen complexes can be so effective in catalyzing a wide variety of enantioselective transformations with broad substrate scope. It is hoped that detailed mechanistic investigations such as the one described here may help guide the discovery of new classes of broadly useful asymmetric catalysis methods in the future.

2.11 Computational Details

2.11.1. Methods: Calculations were performed using the Gaussian 09 program[57] on the Odyssey cluster supported by Harvard University's FAS Science Division Research Computing Group. Default geometric and SCF convergence criteria were used, but increased two-electron integral accuracy was used with basis sets containing diffuse functions (keyword Int=Acc2E=11). In cases where SCF convergence was difficult to achieve, a quadratic convergence (QC) algorithm was employed using the keyword SCF=(XQC,maxconventionalcycles=25) where QC only begins after 25 cycles of the default algorithm have failed to converge on an SCF. Spin density map generation and population analysis were performed using the electron density after the annihilation of the first spin contaminant using the keyword IOp(5/14=2). In calculations with pure DFT functionals (including M06-L), we employed the density fitting approximation using the /auto option in the basis set specification (automatic generation of the density fitting basis set). Stationary points were characterized by the presence of all positive eigenvalues of the Hessian for minima or a single negative eigenvalue of the Hessian for transition states. Spin density and MO surfaces were rendered in GaussView 5. All other molecular structures were rendered in CYLView.[58] All DFT methods were used as their default implementations in Gaussian 09. Methods not discussed explicitly in the body of the chapter include the OPTX

[57] Gaussian 09, Revision A.02, M. J. Frisch, G. W. Trucks, H. B. Schlegel, G. E. Scuseria, M. A. Robb, J. R. Cheeseman, G. Scalmani, V. Barone, B. Mennucci, G. A. Petersson, H. Nakatsuji, M. Caricato, X. Li, H. P. Hratchian, A. F. Izmaylov, J. Bloino, G. Zheng, J. L. Sonnenberg, M. Hada, M. Ehara, K. Toyota, R. Fukuda, J. Hasegawa, M. Ishida, T. Nakajima, Y. Honda, O. Kitao, H. Nakai, T. Vreven, J. A. Montgomery, Jr., J. E. Peralta, F. Ogliaro, M. Bearpark, J. J. Heyd, E. Brothers, K. N. Kudin, V. N. Staroverov, R. Kobayashi, J. Normand, K. Raghavachari, A. Rendell, J. C. Burant, S. S. Iyengar, J. Tomasi, M. Cossi, N. Rega, J. M. Millam, M. Klene, J. E. Knox, J. B. Cross, V. Bakken, C. Adamo, J. Jaramillo, R. Gomperts, R. E. Stratmann, O. Yazyev, A. J. Austin, R. Cammi, C. Pomelli, J. W. Ochterski, R. L. Martin, K. Morokuma, V. G. Zakrzewski, G. A. Voth, P. Salvador, J. J. Dannenberg, S. Dapprich, A. D. Daniels, O. Farkas, J. B. Foresman, J. V. Ortiz, J. Cioslowski, and D. J. Fox, Gaussian, Inc., Wallingford CT, 2009.

[58] CYLview, 1.0b; Legault, C. Y., Université de Sherbrooke, 2009 (http://www.cylview.org)

exchange functional,[59] the P86 exchange functional,[60] the PW91 exchange and correlation functionals,[61] and the TPSSh hybrid functional.[62] Due to the strong interactions between ligand- and metal-centered orbitals, we found restricted open shell DFT (RO-DFT) helpful to generate a representation of the singly occupied MOs. In RO-DFT calculations where the QC method is not available, Use=L506 was helpful for when SCF convergence was difficult.

[59] Hoe, W.-M.; Cohen, A.; Handy, N. C. *Chem. Phys. Lett.*, **2001**, *341*, 319–328.

[60] Perdew, J. P. *Phys. Rev. B.* **1986**, *33*, 8822–8824.

[61] Perdew, J. P.; Burke, K.; Wang, Y. *Phys. Rev. B.* **1996**, *54*, 16533–16539.

[62] J. M. Tao, J. P. Perdew, V. N. Staroverov, and G. E. Scuseria, *Phys. Rev. Lett.* **2003**, *91*, 146401.

2.11.2. Structures of (salen)Co(III) Complexes with Various Ligands

Optimized at B3LYP/6-31G(d), Cartesian coordinates in Å.

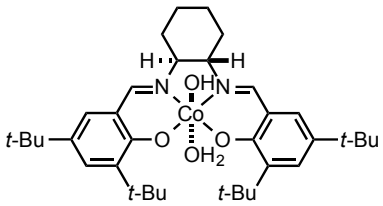

Charge: 0
Spin Multiplicity: 1
Solvation: gas phase
Electronic Energy (AU): -3198.13588842
Gibbs Free Energy at 298.150 K (AU): -3197.352337

N	-1.256807	2.077250	-0.184571
N	1.270881	2.071089	0.374911
C	2.551921	1.928355	0.293574
H	3.178047	2.820034	0.353024
C	-2.539356	1.936262	-0.229235
H	-3.156497	2.828236	-0.349924
C	3.260736	0.688716	0.152067
C	2.604064	-0.574199	0.265329
C	4.658921	0.775060	-0.041074
C	3.419634	-1.756240	0.195967
C	5.450147	-0.351799	-0.137503
H	5.094143	1.767346	-0.117208
C	4.785625	-1.594314	-0.006395
H	5.395252	-2.487493	-0.070389
C	-3.259754	0.696576	-0.148891
C	-2.597030	-0.571542	-0.163586
C	-4.672533	0.785701	-0.107681
C	-3.426054	-1.752381	-0.161988
C	-5.474208	-0.335683	-0.073073
H	-5.108580	1.780515	-0.102574
C	-4.803027	-1.583228	-0.107962
H	-5.418454	-2.474473	-0.096567
O	1.308071	-0.664551	0.481094
O	-1.289382	-0.686994	-0.177430
O	0.434827	0.763478	-1.727026
C	0.618408	3.376314	0.554629
C	-0.584957	3.365767	-0.409302
H	0.213554	3.384252	1.578277
H	-0.180808	3.308873	-1.429390
C	-1.435682	4.631965	-0.265207
H	-2.244110	4.637986	-1.005591
H	-1.905852	4.649171	0.728702
C	1.484777	4.625529	0.362193
H	2.300443	4.644305	1.094773
H	1.944248	4.601220	-0.635769
C	-0.565622	5.887148	-0.450465
C	0.630479	5.895961	0.509604
H	1.253204	6.780744	0.332133
H	0.267464	5.971718	1.544545
H	-1.178142	6.784475	-0.302614
H	-0.200912	5.924224	-1.486559
H	-0.002940	-0.013147	-2.112768
Co	0.009985	0.687457	0.044659
O	-0.340453	0.469352	2.092864
H	0.418450	-0.151963	2.141282
H	-1.122788	-0.109967	2.102544
C	-2.801519	-3.161269	-0.231886
C	-2.020234	-3.311872	-1.559533
C	-1.857579	-3.391022	0.973073
C	-3.863224	-4.279944	-0.196163
H	-2.697216	-3.210522	-2.416442
H	-1.236626	-2.558413	-1.646506
H	-1.552923	-4.302936	-1.614384
H	-2.410422	-3.304156	1.917618
H	-1.430012	-4.400339	0.930017
H	-1.037036	-2.673187	0.973565
H	-3.359556	-5.251609	-0.251299
H	-4.449495	-4.267793	0.730587
H	-4.556650	-4.224166	-1.043483
C	2.802208	-3.163055	0.337214
C	2.145801	-3.312809	1.731198
C	1.749523	-3.385731	-0.773407
C	3.853580	-4.284568	0.209858
H	2.890948	-3.186863	2.526442
H	1.354929	-2.575674	1.876804
H	1.705471	-4.312186	1.837463
H	2.217932	-3.329728	-1.763469
H	1.296381	-4.380058	-0.670757
H	0.960503	-2.635978	-0.720631
H	3.355784	-5.255282	0.314127
H	4.351121	-4.275759	-0.766955
H	4.622570	-4.225422	0.989354
C	-7.010101	-0.289701	-0.010865
C	-7.606371	-1.000169	-1.249409
C	-7.500114	-1.003636	1.271504
C	-7.544680	1.154741	0.013247
H	-7.288261	-0.505669	-2.174291
H	-7.295186	-2.048468	-1.308330
H	-8.702822	-0.981250	-1.212247
H	-7.106825	-0.510408	2.167900
H	-8.595841	-0.987119	1.326627
H	-7.182583	-2.051391	1.301385
H	-8.639541	1.144511	0.059916
H	-7.181875	1.708357	0.887111
H	-7.257998	1.710064	-0.887344
C	6.969581	-0.314353	-0.371353
C	7.308190	-1.047769	-1.691145
C	7.503867	1.126736	-0.474175

C	7.697679	-1.012876	0.801780
H	6.983158	-2.093469	-1.670063
H	6.817299	-0.564047	-2.543218
H	8.390782	-1.039169	-1.869829
H	7.320621	1.695480	0.445050
H	8.586943	1.110863	-0.641282
H	7.048790	1.670323	-1.310164
H	8.783139	-1.000980	0.641927
H	7.487505	-0.505096	1.750237
H	7.390062	-2.058527	0.908817

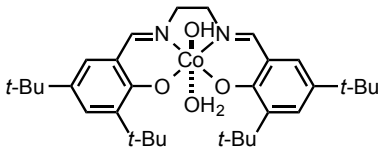

Charge: 0
Spin Multiplicity: 1
Solvation: gas phase
Electronic Energy (AU): -3042.08263933
Gibbs Free Energy at 298.150 K (AU): -3041.389563

N	1.257233	-2.569535	-0.094420
N	-1.271514	-2.563173	0.404132
C	-2.552307	-2.440907	0.292445
H	-3.155571	-3.354033	0.329591
C	2.540527	-2.444416	-0.158835
H	3.136866	-3.356109	-0.269082
C	-3.271230	-1.210238	0.146825
C	-2.622252	0.058404	0.265239
C	-4.667403	-1.305743	-0.059273
C	-3.445699	1.234798	0.189419
C	-5.464564	-0.183972	-0.159941
H	-5.095036	-2.300888	-0.139855
C	-4.808710	1.063165	-0.023155
H	-5.424067	1.952056	-0.091594
C	3.269259	-1.210411	-0.116811
C	2.609044	0.060572	-0.125730
C	4.682520	-1.303994	-0.112120
C	3.441136	1.238407	-0.152164
C	5.487293	-0.184696	-0.110465
H	5.115141	-2.300200	-0.109639
C	4.818519	1.064770	-0.135113
H	5.436734	1.954018	-0.146768
O	-1.329157	0.162511	0.489738
O	1.301645	0.183962	-0.105384
O	-0.393175	-1.276525	-1.684388
C	-0.640860	-3.868750	0.582845
C	0.609648	-3.864188	-0.296902
H	-0.351721	-3.982575	1.635690
H	0.315156	-3.930116	-1.350275
H	0.042606	-0.497398	-2.067429
Co	-0.010117	-1.180861	0.095457
O	0.299673	-0.943026	2.148042
H	-0.471612	-0.337660	2.189148
H	1.068613	-0.345457	2.152717
C	2.819159	2.649141	-0.215735
C	2.013453	2.796439	-1.529027
C	1.898157	2.890284	1.004978
C	3.885386	3.764133	-0.204804
H	2.673309	2.688948	-2.398401
H	1.225499	2.045483	-1.597588
H	1.548339	3.788754	-1.579331
H	2.464889	2.796325	1.940510
H	1.483505	3.905228	0.968406
H	1.067732	2.183907	1.019795
H	3.384117	4.737408	-0.252132
H	4.490585	3.752030	0.709679
H	4.560804	3.704166	-1.066218
C	-2.838500	2.645915	0.335796
C	-2.191971	2.800082	1.734015
C	-1.778999	2.877909	-0.766533
C	-3.897311	3.759642	0.201958
H	-2.939965	2.665351	2.525091
H	-1.393953	2.071173	1.882556
H	-1.762597	3.803791	1.843990
H	-2.237794	2.815306	-1.760643
H	-1.337668	3.877265	-0.661384
H	-0.982081	2.137138	-0.705418
H	-3.407806	4.733954	0.311282
H	-4.387393	3.748401	-0.778574
H	-4.671591	3.693499	0.975616
C	7.024228	-0.234695	-0.094663
C	7.583098	0.459373	-1.359709
C	7.556336	0.492470	1.163238
C	7.554939	-1.680552	-0.070369
H	7.234071	-0.044482	-2.268236
H	7.273792	1.508125	-1.420737
H	8.680057	0.436644	-1.357233
H	7.190250	0.011191	2.077448
H	8.653153	0.472428	1.183702
H	7.243844	1.541788	1.190836
H	8.650688	-1.673285	-0.056478
H	7.216750	-2.223293	0.820020
H	7.239934	-2.244802	-0.955789
C	-6.982121	-0.230376	-0.403834
C	-7.316372	0.501598	-1.725535
C	-7.506876	-1.674663	-0.510372
C	-7.721649	0.463455	0.764956
H	-6.997623	1.549198	-1.702151
H	-6.817543	0.020946	-2.574722
H	-8.397714	0.486839	-1.910905
H	-7.325946	-2.242426	0.409898
H	-8.588932	-1.665326	-0.684183
H	-7.043453	-2.215336	-1.343654
H	-8.805904	0.445196	0.598063
H	-7.514712	-0.043474	1.714566
H	-7.421055	1.510930	0.874379
H	-1.322356	-4.686265	0.317264
H	1.283651	-4.695270	-0.054965

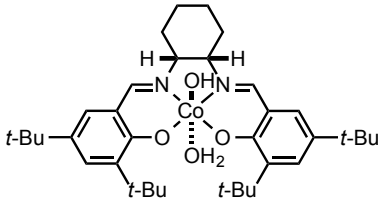

Charge: 0
Spin Multiplicity: 1
Solvation: gas phase
Electronic Energy (AU): -3198.13487421
Gibbs Free Energy at 298.150 K (AU): -3197.350465

Co	0.046166	0.726709	-0.134730
O	-1.191813	-0.716581	-0.211537
N	1.252437	2.179418	0.026643
O	1.414988	-0.524730	0.390129
C	3.309634	0.882009	-0.050107
C	2.538853	2.089262	-0.055501
H	3.106898	3.023019	-0.125903
C	-2.553253	1.837779	-0.503193
H	-3.210463	2.682100	-0.718933
C	0.594739	3.487819	0.020202
H	1.256362	4.229127	-0.450802
N	-1.280602	2.045912	-0.457108
C	-4.631701	0.605611	-0.290874
H	-5.117185	1.575332	-0.383221
C	-4.669291	-1.754496	-0.064769
H	-5.238940	-2.668087	0.030316
C	2.708013	-0.393284	0.181196
C	3.577459	-1.537691	0.234768
C	-2.505036	-0.658604	-0.208175
C	4.705798	1.014305	-0.234674
H	5.095530	2.013560	-0.405721
C	4.938085	-1.331511	0.038908
H	5.588182	-2.197235	0.071434
C	-0.664019	3.329852	-0.857778
H	-0.324176	3.159161	-1.886192
C	-3.281155	-1.864264	-0.094447
C	-3.220148	0.578425	-0.313426
C	-5.389746	-0.542967	-0.155983
C	5.548936	-0.077589	-0.203525
O	-0.283241	0.622759	1.936059
O	0.430804	0.666337	-1.916812
H	0.012834	-0.155875	-2.221899
C	-1.541997	4.590132	-0.804853
H	-0.978270	5.381179	-1.318372
H	-2.453729	4.454906	-1.398245
C	0.259697	3.953442	1.450017
H	1.196484	4.101470	2.001654
H	-0.286470	3.154164	1.962825
C	-1.864027	5.056398	0.623644
H	-2.430676	5.994691	0.584792
H	-2.507772	4.321487	1.125305
C	-0.576141	5.240835	1.439920
H	0.012862	6.063684	1.007947
H	-0.815501	5.535880	2.468592
C	-6.928752	-0.472731	-0.120581
C	-7.379419	0.402543	1.073118
C	-7.450414	0.154151	-1.435538
C	-7.578007	-1.861216	0.035505
H	-7.036081	-0.023843	2.022736
H	-6.982186	1.421073	1.002504
H	-8.473783	0.473754	1.108084
H	-7.153138	-0.448261	-2.301470
H	-8.545831	0.217568	-1.424473
H	-7.060764	1.166882	-1.585425
H	-8.668776	-1.757383	0.060541
H	-7.329773	-2.525461	-0.800159
H	-7.272051	-2.353116	0.965927
C	-2.596171	-3.245562	-0.021500
C	-1.805761	-3.495917	-1.328743
C	-1.643248	-3.310337	1.196864
C	-3.608414	-4.399302	0.131708
H	-2.485303	-3.519417	-2.189279
H	-1.061171	-2.716748	-1.496326
H	-1.288431	-4.462272	-1.281153
H	-2.197113	-3.141123	2.129603
H	-1.179369	-4.302323	1.261524
H	-0.848907	-2.568503	1.113512
H	-3.063367	-5.348824	0.177540
H	-4.198090	-4.315043	1.052424
H	-4.300126	-4.461406	-0.716326
C	3.020715	-2.952194	0.498197
C	2.351980	-3.004525	1.893178
C	1.994911	-3.323557	-0.597984
C	4.121265	-4.032924	0.483450
H	3.078342	-2.770527	2.681300
H	1.525353	-2.295853	1.961778
H	1.956830	-4.009641	2.086789
H	2.472929	-3.329181	-1.584982
H	1.591899	-4.327568	-0.413261
H	1.167427	-2.614794	-0.618895
H	3.663308	-5.011519	0.666682
H	4.633824	-4.088521	-0.484040
H	4.874815	-3.873720	1.264143
C	7.070337	0.008888	-0.410297
C	7.799247	-0.516651	0.849311
C	7.478759	-0.848988	-1.631645
C	7.537995	1.454133	-0.665143
H	7.542935	0.085144	1.728925
H	7.535271	-1.556657	1.069120
H	8.886900	-0.472367	0.711259
H	6.989437	-0.487601	-2.543238
H	8.564161	-0.805404	-1.786048
H	7.204322	-1.901229	-1.501619
H	8.624074	1.472943	-0.810845
H	7.076284	1.877923	-1.564421
H	7.307600	2.111788	0.181243
H	-1.012551	-0.022784	1.951567
H	0.521559	0.067071	2.021930

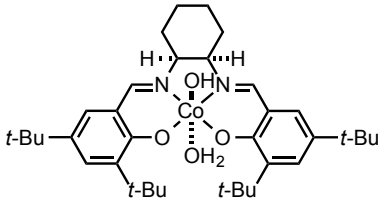

Charge: 0
Spin Multiplicity: 1
Solvation: gas phase
Electronic Energy (AU): -3198.13610791
Gibbs Free Energy at 298.150 K (AU): -3197.350961

Co	0.029588	0.724758	-0.274543
O	-1.233328	-0.692228	-0.576400
N	1.257336	2.163201	-0.217092
O	1.387275	-0.587698	-0.008355
C	3.309365	0.863950	-0.045971
C	2.543736	2.072072	-0.140811
H	3.117606	3.004974	-0.143760
C	-2.552896	1.869778	-0.532952
H	-3.213255	2.728718	-0.663500
C	0.612090	3.481657	-0.210993
H	1.268370	4.210626	-0.709644
N	-1.279963	2.049848	-0.654067
C	-4.608740	0.681608	-0.036966
H	-5.072426	1.663467	-0.011830
C	-4.663982	-1.688042	0.080303
H	-5.244219	-2.592654	0.216777
C	2.689232	-0.422924	0.044336
C	3.556404	-1.567401	0.182030
C	-2.523711	-0.624693	-0.322993
C	4.718444	1.004229	-0.022662
H	5.119505	2.010999	-0.093980
C	4.927763	-1.349497	0.189855
H	5.573629	-2.213701	0.286834
C	-0.674919	3.338356	-1.050584
H	-0.366962	3.204968	-2.096677
C	-3.300415	-1.823113	-0.155095
C	-3.214804	0.623872	-0.268605
C	-5.361664	-0.459008	0.155432
C	5.557514	-0.084103	0.086639
O	-0.351145	0.869726	1.503145
C	-1.551780	4.597760	-0.954554
H	-1.008506	5.393891	-1.482237
H	-2.484108	4.461883	-1.515489
C	0.333497	3.949689	1.230877
H	1.295980	4.105264	1.735025
H	-0.173328	3.135822	1.759701
C	-1.820445	5.053518	0.488243
H	-2.390945	5.990346	0.474036
H	-2.439599	4.314162	1.012143
C	-0.501834	5.236703	1.253233
H	0.067097	6.063914	0.801462
H	-0.702837	5.527370	2.291228
O	0.332585	0.376661	-2.313347
H	0.090206	0.103048	1.904376
C	2.978464	-2.989361	0.340972
C	2.161738	-3.061913	1.653606
C	2.082123	-3.351002	-0.868527
C	4.079650	-4.066645	0.424674
H	2.809620	-2.877094	2.518955
H	1.357248	-2.325342	1.660715
H	1.717058	-4.057841	1.771111
H	2.657335	-3.301908	-1.802308
H	1.705368	-4.375968	-0.763994
H	1.226932	-2.679203	-0.943039
H	3.609412	-5.050300	0.534175
H	4.698963	-4.097793	-0.479815
H	4.738166	-3.922893	1.289134
C	-2.644697	-3.218076	-0.229367
C	-2.019601	-3.435381	-1.628775
C	-1.557297	-3.342262	0.862857
C	-3.657961	-4.358696	-0.003499
H	-2.787556	-3.379110	-2.410176
H	-1.253940	-2.687277	-1.839535
H	-1.553694	-4.427151	-1.685702
H	-1.999986	-3.234963	1.860523
H	-1.079785	-4.329095	0.810631
H	-0.790099	-2.578324	0.740626
H	-3.134199	-5.319413	-0.063273
H	-4.128050	-4.303599	0.985249
H	-4.449364	-4.369010	-0.762341
C	7.091821	0.016351	0.110056
C	7.576794	1.473516	-0.007801
C	7.633113	-0.562810	1.439098
C	7.685254	-0.784572	-1.073368
H	7.250655	1.935814	-0.946721
H	7.214466	2.090721	0.822451
H	8.672132	1.503926	0.012053
H	7.353183	-1.613374	1.570828
H	8.728462	-0.505311	1.464662
H	7.242454	-0.003810	2.297088
H	8.781052	-0.728760	-1.064141
H	7.407156	-1.843031	-1.029648
H	7.332336	-0.386238	-2.031642
C	-6.874883	-0.449849	0.429630
C	-7.157891	-1.111655	1.799322
C	-7.448713	0.979354	0.461761
C	-7.612264	-1.237199	-0.679747
H	-6.800524	-2.146440	1.832840
H	-6.662825	-0.562113	2.607988
H	-8.235587	-1.125004	2.004957
H	-7.309532	1.496339	-0.495050
H	-8.525479	0.942853	0.662611
H	-6.986192	1.585604	1.249177
H	-8.693551	-1.242070	-0.493485
H	-7.437920	-0.783929	-1.662440
H	-7.280167	-2.279548	-0.730313
H	1.127072	-0.185640	-2.279187
H	-0.411436	-0.263550	-2.304934

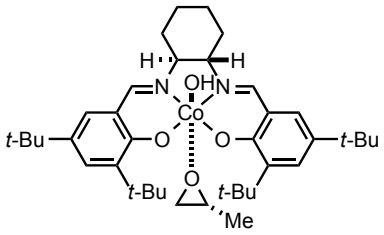

Charge: 0
Spin Multiplicity: 1
Solvation: gas phase
Electronic Energy (AU): -3314.82679462
Gibbs Free Energy at 298.150 K (AU): -3313.983778

Co	0.070704	0.692430	-0.117215
N	-1.183656	2.086369	-0.407785
N	1.331798	2.083319	0.190460
C	2.613782	1.925335	0.131051
H	3.248293	2.812400	0.171720
C	-2.466666	1.950869	-0.425441
H	-3.083438	2.842729	-0.552269
C	3.311408	0.678701	0.027158
C	2.636056	-0.581586	0.109011
C	4.717494	0.752742	-0.121065
C	3.451517	-1.770628	0.043584
C	5.502915	-0.377540	-0.201582
H	5.162222	1.742354	-0.176899
C	4.822689	-1.617131	-0.109825
H	5.426627	-2.514730	-0.167753
C	-3.187614	0.713215	-0.324179
C	-2.527037	-0.557032	-0.381305
C	-4.599164	0.805799	-0.259314
C	-3.366152	-1.732078	-0.453482
C	-5.405365	-0.312871	-0.251715
H	-5.030836	1.801828	-0.215706
C	-4.740807	-1.559461	-0.366508
H	-5.362276	-2.445857	-0.400761
O	1.342911	-0.670742	0.290433
O	-1.224735	-0.678647	-0.383784
O	0.528856	0.720951	-1.883987
O	-0.461169	0.793589	1.902252
C	0.444633	0.407095	2.971555
C	-0.743822	-0.405306	2.686269
H	0.435633	1.100219	3.810529
H	1.414779	0.067698	2.624801
H	-0.583826	-1.307913	2.105467
C	0.691764	3.402374	0.299534
C	-0.502969	3.359272	-0.675239
H	0.274759	3.470067	1.316721
H	-0.087513	3.259335	-1.687474
C	-1.343883	4.637259	-0.592761
H	-2.149475	4.614348	-1.336025
H	-1.818368	4.704483	0.397060
C	1.572323	4.632380	0.053745
H	2.383558	4.679972	0.790131
H	2.038605	4.554171	-0.938126
C	-0.461716	5.875072	-0.830934
C	0.730366	5.917000	0.133837
H	1.363220	6.785998	-0.082151
H	0.362431	6.046436	1.161868
H	-1.065869	6.784320	-0.727490
H	-0.091905	5.860964	-1.865771
H	0.137604	-0.092381	-2.242458
C	-1.996973	-0.349604	3.514533
H	-2.877939	-0.470690	2.875786
H	-1.993975	-1.163084	4.249555
H	-2.077937	0.603187	4.047345
C	2.819114	-3.174570	0.132343
C	2.115527	-3.346683	1.500123
C	1.804026	-3.362558	-1.019550
C	3.863017	-4.304011	0.014800
H	2.840919	-3.267226	2.319696
H	1.347234	-2.586273	1.642750
H	1.642702	-4.334880	1.564060
H	2.309816	-3.293729	-1.990251
H	1.335248	-4.352714	-0.953080
H	1.022901	-2.603666	-0.981670
H	3.352232	-5.271423	0.081589
H	4.392592	-4.279651	-0.944786
H	4.606648	-4.270250	0.820025
C	-2.758683	-3.136120	-0.660068
C	-1.999640	-3.168441	-2.009097
C	-1.793826	-3.493575	0.494533
C	-3.833199	-4.242044	-0.711868
H	-2.687267	-2.980320	-2.842406
H	-1.210121	-2.416016	-2.035465
H	-1.541917	-4.153458	-2.164100
H	-2.317201	-3.464055	1.459085
H	-1.402711	-4.509695	0.358894
H	-0.950461	-2.804516	0.525748
H	-3.342877	-5.209128	-0.870521
H	-4.401668	-4.313000	0.223358
H	-4.541869	-4.096699	-1.535532
C	-6.939514	-0.265756	-0.158399
C	-7.561981	-0.899129	-1.425749
C	-7.409178	-1.054029	1.087589
C	-7.467149	1.176278	-0.037567
H	-7.258821	-0.350488	-2.324787
H	-7.254766	-1.942515	-1.553619
H	-8.657587	-0.880137	-1.367429
H	-6.999544	-0.615147	2.004836
H	-8.503775	-1.040196	1.162971
H	-7.092857	-2.102005	1.049811
H	-8.560647	1.167828	0.036767
H	-7.078287	1.677114	0.856734
H	-7.201129	1.781350	-0.912044
C	7.029379	-0.350547	-0.384336
C	7.406378	-1.069003	-1.701933
C	7.579096	1.086919	-0.449845
C	7.713103	-1.070657	0.802389
H	7.072157	-2.112011	-1.706072

H	6.947662	-0.569611	-2.562825
H	8.494430	-1.067463	-1.844879
H	7.367855	1.646044	0.469325
H	8.667285	1.063577	-0.578858
H	7.158209	1.644663	-1.294351
H	8.803322	-1.067632	0.677678
H	7.477332	-0.572483	1.749989
H	7.392213	-2.114389	0.886276

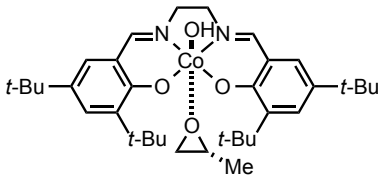

Charge: 0
Spin Multiplicity: 1
Solvation: gas phase
Electronic Energy (AU): -3158.77376397
Gibbs Free Energy at 298.150 K (AU): -3158.021577

Co	-0.072451	-1.142397	-0.212503
N	1.184950	-2.508028	-0.579693
N	-1.324359	-2.555762	-0.015594
C	-2.608265	-2.417646	-0.077369
H	-3.216189	-3.327761	-0.119055
C	2.468689	-2.382422	-0.595910
H	3.068583	-3.280316	-0.779341
C	-3.322227	-1.178535	-0.086367
C	-2.657712	0.081392	0.080672
C	-4.728236	-1.257065	-0.236743
C	-3.485478	1.263708	0.091478
C	-5.524527	-0.132064	-0.236655
H	-5.162723	-2.245260	-0.358701
C	-4.855325	1.105730	-0.067091
H	-5.468296	1.998784	-0.066090
C	3.193111	-1.156865	-0.426589
C	2.530045	0.114768	-0.392624
C	4.605245	-1.252579	-0.379701
C	3.368665	1.292165	-0.394140
C	5.410456	-0.136188	-0.303862
H	5.037010	-2.248995	-0.406643
C	4.743959	1.114863	-0.329388
H	5.364449	2.002410	-0.308961
O	-1.365683	0.175698	0.267625
O	1.227875	0.239063	-0.373284
O	-0.510629	-1.059211	-1.982331
O	0.442595	-1.373749	1.799116
C	-0.473415	-1.076908	2.888029
C	0.701091	-0.225812	2.663699
H	-0.454225	-1.825185	3.677978
H	-1.449338	-0.732638	2.562766
H	0.527343	0.711128	2.144300
C	-0.699168	-3.876513	-0.018304
C	0.531105	-3.766846	-0.921405
H	-0.383294	-4.128379	1.003084
H	0.209814	-3.704741	-1.967136
H	-0.127231	-0.218782	-2.282117
C	1.951835	-0.314866	3.492670
H	2.833018	-0.133300	2.868681
H	1.930289	0.445833	4.281881
H	2.049032	-1.300406	3.959007
C	-2.866744	2.665967	0.264802
C	-2.163194	2.763414	1.639775
C	-1.854321	2.934940	-0.873529
C	-3.922247	3.789902	0.215138
H	-2.885776	2.627365	2.454315
H	-1.386680	2.003941	1.735368
H	-1.700602	3.750990	1.761499
H	-2.358402	2.913256	-1.847264
H	-1.402093	3.927320	-0.750188
H	-1.060205	2.188530	-0.878598
H	-3.420835	4.756759	0.337403
H	-4.453737	3.816624	-0.743357
H	-4.664178	3.702801	1.018074
C	2.759567	2.706454	-0.507144
C	1.990708	2.823225	-1.846014
C	1.802060	2.993248	0.673042
C	3.834328	3.813405	-0.498575
H	2.670431	2.680461	-2.694614
H	1.195152	2.079487	-1.910787
H	1.538962	3.818789	-1.938635
H	2.329538	2.902083	1.631431
H	1.414170	4.017206	0.602662
H	0.956190	2.306455	0.664987
H	3.343204	4.788331	-0.594121
H	4.409334	3.827517	0.435276
H	4.537366	3.719268	-1.334423
C	6.945108	-0.189179	-0.222342
C	7.563005	0.543164	-1.437382
C	7.419382	0.497388	1.080725
C	7.473991	-1.635904	-0.219029
H	7.254685	0.070024	-2.376619
H	7.259148	1.594462	-1.478758
H	8.658785	0.516699	-1.385588
H	7.013961	-0.014159	1.961439
H	8.514349	0.478717	1.150212
H	7.101698	1.544498	1.128039
H	8.567946	-1.631488	-0.152763
H	7.093019	-2.206273	0.636132
H	7.201295	-2.170982	-1.136024
C	-7.052176	-0.161151	-0.408237
C	-7.450664	0.653698	-1.661990
C	-7.587301	-1.595060	-0.581352
C	-7.729818	0.456970	0.838024
H	-7.130326	1.698473	-1.588412
H	-6.995313	0.229026	-2.563831
H	-8.539981	0.648740	-1.793920
H	-7.363408	-2.220802	0.290610
H	-8.676612	-1.574083	-0.701140
H	-7.166552	-2.080784	-1.469311

H	-8.821167	0.454731	0.723905
H	-7.480746	-0.112561	1.740972
H	-7.415592	1.493490	1.001047
H	-1.393204	-4.650905	-0.367874
H	1.207502	-4.622349	-0.799078

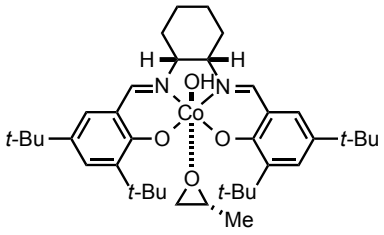

Charge: 0
Spin Multiplicity: 1
Solvation: gas phase
Electronic Energy (AU): -3314.82509051
Gibbs Free Energy at 298.150 K (AU): -3313.981949

Co	0.105161	0.703539	-0.323879
O	-1.127608	-0.741579	-0.447334
N	1.304231	2.169503	-0.192372
O	1.443693	-0.556233	0.192960
C	3.354879	0.859020	-0.155426
C	2.593447	2.067145	-0.226436
H	3.170784	2.993291	-0.321280
C	-2.483540	1.821875	-0.708279
H	-3.143468	2.663237	-0.929092
C	0.662735	3.481715	-0.322732
H	1.343058	4.170985	-0.843545
N	-1.209059	2.016623	-0.725585
C	-4.555227	0.607996	-0.367573
H	-5.035243	1.584262	-0.407177
C	-4.606565	-1.759170	-0.257321
H	-5.182668	-2.671465	-0.195607
C	2.735136	-0.419235	0.035984
C	3.606695	-1.568466	0.102547
C	-2.434515	-0.674656	-0.421333
C	4.760746	0.987874	-0.269137
H	5.159732	1.987971	-0.413226
C	4.973629	-1.361481	-0.018524
H	5.620231	-2.229265	0.028581
C	-0.581811	3.262536	-1.209422
H	-0.222914	3.009011	-2.213820
C	-3.223874	-1.879947	-0.370461
C	-3.146979	0.570770	-0.460903
C	-5.317231	-0.538064	-0.234257
C	5.599822	-0.103697	-0.205867
O	0.538696	0.581236	-2.093575
H	0.154148	-0.267398	-2.367810
C	-1.454359	4.525833	-1.280174
H	-0.884305	5.263598	-1.861504
H	-2.362121	4.335640	-1.864873
C	0.305584	4.082770	1.050114
H	1.232241	4.265491	1.609104
H	-0.274247	3.346039	1.616664
C	-1.787293	5.130459	0.092924
H	-2.341123	6.067453	-0.043175
H	-2.446274	4.455763	0.655907
C	-0.506908	5.377088	0.904031
H	0.101021	6.144242	0.401637
H	-0.753579	5.775789	1.895608
C	-6.851028	-0.457278	-0.110431
C	-7.228202	0.393073	1.125948
C	-7.440241	0.204133	-1.379157
C	-7.502553	-1.844176	0.050998
H	-6.836571	-0.057562	2.045326
H	-6.827339	1.410239	1.056843
H	-8.318462	0.470868	1.223137
H	-7.195453	-0.379748	-2.273720
H	-8.533009	0.275004	-1.306649
H	-7.050068	1.217125	-1.526220
H	-8.588400	-1.732910	0.151249
H	-7.317047	-2.487479	-0.816625
H	-7.139241	-2.363679	0.945176
C	-2.564333	-3.272515	-0.478739
C	-1.829136	-3.384255	-1.836915
C	-1.561812	-3.500655	0.676064
C	-3.595072	-4.419313	-0.420772
H	-2.536792	-3.281058	-2.668267
H	-1.063644	-2.613179	-1.935542
H	-1.343603	-4.364185	-1.926281
H	-2.063581	-3.415286	1.648719
H	-1.132950	-4.508451	0.609988
H	-0.746895	-2.779024	0.629627
H	-3.069887	-5.376475	-0.515512
H	-4.141920	-4.439198	0.529692
H	-4.325201	-4.365309	-1.236620
C	3.036795	-2.988499	0.296074
C	2.309228	-3.079824	1.658713
C	2.059890	-3.321770	-0.856475
C	4.133268	-4.073431	0.293749
H	3.010158	-2.900396	2.483748
H	1.505510	-2.345671	1.721534
H	1.877949	-4.079606	1.794616
H	2.583833	-3.300745	-1.819697
H	1.645140	-4.328788	-0.720532
H	1.236805	-2.608480	-0.896074
H	3.664542	-5.055317	0.425487
H	4.686997	-4.100073	-0.652070
H	4.853079	-3.943214	1.110860
C	7.130321	-0.018434	-0.326792
C	7.786116	-0.565399	0.963582
C	7.605786	-0.858415	-1.536282
C	7.613964	1.429386	-0.532073
H	7.483080	0.025216	1.835968
H	7.505318	-1.607007	1.153278
H	8.880033	-0.524661	0.887622
H	7.167518	-0.482972	-2.467948

H	8.698148	-0.814186	-1.630274
H	7.324064	-1.912167	-1.437562
H	8.706813	1.449151	-0.613639
H	7.206118	1.867423	-1.450387
H	7.334209	2.074383	0.309190
C	-0.660404	-0.210002	2.570748
C	0.489313	0.674923	2.791100
O	-0.425533	0.931981	1.691195
H	-0.459297	-1.149252	2.066209
H	1.476658	0.352240	2.478901
H	0.444834	1.434767	3.568983
C	-1.919187	-0.141289	3.389738
H	-2.790674	-0.358819	2.763776
H	-1.881354	-0.886786	4.192758
H	-2.046730	0.849221	3.838005

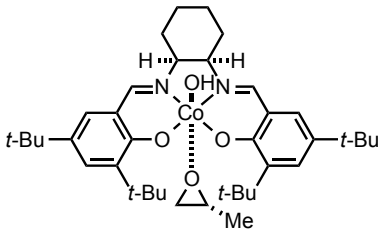

Charge: 0
Spin Multiplicity: 1
Solvation: gas phase
Electronic Energy (AU): -3314.82680605
Gibbs Free Energy at 298.150 K (AU): -3313.983628

Co	0.030670	0.743413	0.088058
O	1.263616	-0.682052	0.373527
N	-1.186086	2.192729	-0.035530
O	-1.316608	-0.562066	-0.253895
C	-3.236488	0.888805	-0.156881
C	-2.472868	2.099571	-0.081811
H	-3.049111	3.031467	-0.080519
C	2.610700	1.879561	0.372480
H	3.277227	2.735581	0.492239
C	-0.534868	3.505335	-0.075843
H	-1.195254	4.256061	0.384486
N	1.336092	2.075191	0.463063
C	4.667912	0.667672	-0.037287
H	5.141764	1.645210	-0.039094
C	4.701358	-1.700313	-0.180614
H	5.276373	-2.609431	-0.310082
C	-2.613114	-0.393920	-0.302160
C	-3.485062	-1.527840	-0.512601
C	2.553947	-0.618186	0.162593
C	-4.646079	1.025849	-0.146152
H	-5.047502	2.028297	-0.027764
C	-4.856161	-1.313548	-0.477368
H	-5.503805	-2.170360	-0.618776
C	0.737113	3.384887	0.792304
H	0.406072	3.304337	1.837231
C	3.330554	-1.823837	0.001145
C	3.264518	0.624987	0.145076
C	5.415816	-0.477129	-0.213737
C	-5.486013	-0.058534	-0.283751
O	0.460690	0.847649	-1.683205
C	1.628379	4.631479	0.661094
H	1.084268	5.453206	1.147364
H	2.550309	4.509759	1.242268
C	-0.228421	3.920632	-1.528295
H	-1.181732	4.065993	-2.052423
H	0.279080	3.083828	-2.019010
C	1.924842	5.028235	-0.793452
H	2.507320	5.957811	-0.805835
H	2.541607	4.261471	-1.279165
C	0.619782	5.198008	-1.584045
H	0.053484	6.046855	-1.170407
H	0.839198	5.449412	-2.628599
H	0.053784	0.054460	-2.068269
C	-2.913513	-2.931044	-0.809939
C	-2.100788	-2.877665	-2.126646
C	-2.010706	-3.415314	0.348760
C	-4.019686	-3.990258	-0.997512
H	-2.749974	-2.608724	-2.968553
H	-1.295436	-2.144711	-2.063155
H	-1.657215	-3.857988	-2.341098
H	-2.573230	-3.445286	1.290907
H	-1.647268	-4.430335	0.144972
H	-1.148414	-2.760602	0.469984
H	-3.554239	-4.957853	-1.216440
H	-4.630582	-4.116097	-0.095526
H	-4.685608	-3.751881	-1.834785
C	2.657937	-3.212213	0.017014
C	1.972153	-3.451699	1.383723
C	1.617171	-3.298121	-1.123794
C	3.665411	-4.360983	-0.192543
H	2.711585	-3.440228	2.194497
H	1.223936	-2.684494	1.585418
H	1.476945	-4.430929	1.394447
H	2.105624	-3.177943	-2.098367
H	1.123269	-4.278256	-1.113067
H	0.856627	-2.524815	-1.020173
H	3.127688	-5.315811	-0.175013
H	4.176350	-4.291298	-1.159878
H	4.425104	-4.398382	0.597309
C	-7.020623	0.036212	-0.261728
C	-7.507280	1.481604	-0.045728
C	-7.596407	-0.467432	-1.606902
C	-7.579148	-0.834847	0.888780
H	-7.153003	1.892066	0.907100
H	-7.173652	2.147053	-0.850389
H	-8.602898	1.507644	-0.029556
H	-7.315273	-1.506814	-1.807529
H	-8.692369	-0.415329	-1.599810
H	-7.231345	0.142919	-2.440797
H	-8.675363	-0.790495	0.908696

H	-7.291557	-1.886127	0.780506
H	-7.206985	-0.485854	1.859055
C	6.937269	-0.481600	-0.436725
C	7.259658	-1.132324	-1.803081
C	7.526775	0.941514	-0.435718
C	7.629865	-1.287593	0.687961
H	6.893520	-2.163032	-1.859644
H	6.796431	-0.569583	-2.621465
H	8.343442	-1.154418	-1.973674
H	7.359213	1.451713	0.520197
H	8.609510	0.895292	-0.599235
H	7.098008	1.559163	-1.233260
H	8.716284	-1.306620	0.534833
H	7.431975	-0.839420	1.668625
H	7.281595	-2.325399	0.720048
C	-0.806143	-0.530164	2.807130
C	0.432970	0.180462	3.143894
O	-0.457871	0.713549	2.125752
H	-0.708424	-1.386448	2.147509
H	1.376379	-0.185818	2.753333
H	0.475095	0.797441	4.039410
C	-2.046509	-0.470456	3.654121
H	-2.938116	-0.478829	3.018431
H	-2.090089	-1.344757	4.314149
H	-2.062890	0.434316	4.270058

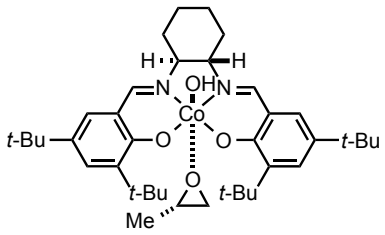

Charge: 0
Spin Multiplicity: 1
Solvation: gas phase
Electronic Energy (AU): -3314.82595867
Gibbs Free Energy at 298.150 K (AU): -3313.983644

Co	0.007830	0.648534	-0.155594
N	-1.250763	2.032863	-0.467925
N	1.275076	2.049065	0.083093
C	2.556104	1.887061	0.010857
H	3.191885	2.774221	0.010303
C	-2.534152	1.897533	-0.456916
H	-3.152796	2.785297	-0.601992
C	3.251912	0.637072	-0.058693
C	2.577405	-0.620145	0.068761
C	4.656780	0.705920	-0.222551
C	3.392119	-1.811015	0.028646
C	5.441411	-0.426409	-0.275124
H	5.101217	1.693183	-0.312773
C	4.761729	-1.662506	-0.141416
H	5.365029	-2.561523	-0.178931
C	-3.253011	0.664714	-0.303511
C	-2.593593	-0.606716	-0.332254
C	-4.662984	0.760084	-0.215586
C	-3.433352	-1.782572	-0.358268
C	-5.468554	-0.357444	-0.159969
H	-5.093835	1.757185	-0.193868
C	-4.806036	-1.607006	-0.251338
H	-5.427919	-2.493781	-0.248572
O	1.286824	-0.704135	0.268645
O	-1.291035	-0.729005	-0.352089
O	0.433670	0.620306	-1.930307
O	-0.483353	0.814625	1.873779
C	0.442241	0.455449	2.945606
C	-0.751856	-0.357314	2.688206
H	1.378618	0.068763	2.553760
H	-0.659404	-1.294047	2.151392
C	0.638967	3.373105	0.151422
C	-0.575545	3.293942	-0.796229
H	0.242025	3.483388	1.173003
H	-0.180816	3.156032	-1.812328
C	-1.413881	4.575209	-0.744079
H	-2.236462	4.524184	-1.467119
H	-1.865734	4.681296	0.252936
C	1.515422	4.590507	-0.162294
H	2.342430	4.666719	0.553969
H	1.960570	4.471249	-1.159727
C	-0.536941	5.801330	-1.050717
C	0.677147	5.879287	-0.115769
H	1.306411	6.737232	-0.381013
H	0.332901	6.051428	0.914276
H	-1.137803	6.715003	-0.969405
H	-0.190939	5.745775	-2.092352
H	0.035158	-0.203654	-2.254928
C	2.760246	-3.211622	0.161948
C	2.070716	-3.346724	1.540955
C	1.733342	-3.430039	-0.974024
C	3.802647	-4.344412	0.063998
H	2.804543	-3.246301	2.350699
H	1.304312	-2.582220	1.671088
H	1.597930	-4.332426	1.635751
H	2.229219	-3.387339	-1.951308
H	1.265274	-4.417901	-0.876268
H	0.952511	-2.670270	-0.948661
H	3.292160	-5.309461	0.160453
H	4.323437	-4.345177	-0.900706
H	4.553806	-4.290520	0.861173
C	-2.829844	-3.192206	-0.536189
C	-2.091967	-3.262088	-1.895515
C	-1.846866	-3.519721	0.611892
C	-3.905641	-4.298098	-0.541788
H	-2.791609	-3.092588	-2.722799
H	-1.299954	-2.514024	-1.953411
H	-1.640268	-4.252625	-2.032219
H	-2.353296	-3.460329	1.583979
H	-1.461028	-4.540641	0.498657

H	-1.001040	-2.832904	0.608199
H	-3.418500	-5.269515	-0.682952
H	-4.459037	-4.344337	0.403982
H	-4.627732	-4.173823	-1.357270
C	-7.000321	-0.306975	-0.035425
C	-7.650834	-0.985703	-1.264587
C	-7.440745	-1.049464	1.248680
C	-7.526612	1.138458	0.044407
H	-7.368551	-0.470031	-2.189576
H	-7.346435	-2.033192	-1.361686
H	-8.744862	-0.964262	-1.181994
H	-7.009563	-0.577832	2.139328
H	-8.533369	-1.032932	1.349030
H	-7.124012	-2.097952	1.241123
H	-8.618441	1.132370	0.140451
H	-7.120956	1.671082	0.912486
H	-7.278371	1.712264	-0.856028
C	6.966762	-0.406092	-0.467418
C	7.338360	-1.175623	-1.757476
C	7.515272	1.027848	-0.592224
C	7.655906	-1.079140	0.743630
H	7.006883	-2.218800	-1.719103
H	6.874534	-0.711616	-2.635275
H	8.425687	-1.177416	-1.905486
H	7.310233	1.621753	0.306274
H	8.602575	1.000160	-0.727973
H	7.087805	1.552222	-1.454618
H	8.745529	-1.082631	0.613743
H	7.425302	-0.543176	1.671709
H	7.333760	-2.118195	0.870620
H	-1.629613	-0.244898	3.321191
C	0.527898	1.439230	4.079865
H	1.009801	0.968933	4.945176
H	1.128982	2.309568	3.793642
H	-0.466541	1.784490	4.379489

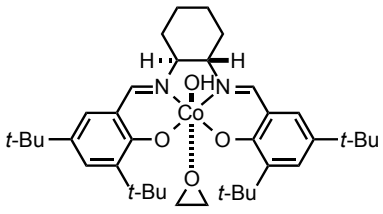

Charge: 0
Spin Multiplicity: 1
Solvation: gas phase
Electronic Energy (AU): -3275.50324285
Gibbs Free Energy at 298.150 K (AU): -3274.686605

Co	0.019534	0.685170	-0.039246
N	-1.240681	2.075238	-0.318143
N	1.282601	2.080192	0.243661
C	2.564052	1.923764	0.169318
H	3.197637	2.811992	0.197110
C	-2.523899	1.936721	-0.320419
H	-3.143580	2.826936	-0.444276
C	3.262234	0.677460	0.063941
C	2.590013	-0.583381	0.161362
C	4.666322	0.752747	-0.102023
C	3.406021	-1.771577	0.091357
C	5.452275	-0.376916	-0.186046
H	5.108987	1.742626	-0.168520
C	4.775005	-1.616924	-0.079964
H	5.379548	-2.513894	-0.141159
C	-3.241152	0.698721	-0.206595
C	-2.578853	-0.570291	-0.261317
C	-4.652107	0.789111	-0.128327
C	-3.415573	-1.746989	-0.321346
C	-5.455595	-0.331054	-0.107381
H	-5.085405	1.784461	-0.085375
C	-4.789532	-1.576679	-0.222677
H	-5.409548	-2.464396	-0.246531
O	1.299243	-0.673135	0.361435
O	-1.275622	-0.689280	-0.273944
O	0.451561	0.702669	-1.811385
O	-0.477671	0.796113	1.999016
C	0.453986	0.410364	3.043800
C	-0.739418	-0.398342	2.778874
H	0.467930	1.100958	3.883681
H	1.411594	0.064376	2.671053
H	-0.640515	-1.317808	2.214556
C	0.642229	3.399373	0.353461
C	-0.566501	3.347757	-0.603167
H	0.240130	3.473393	1.376235
H	-0.165600	3.242740	-1.620806
C	-1.408602	4.624709	-0.516259
H	-2.225303	4.595389	-1.247074
H	-1.868335	4.697447	0.480118
C	1.517066	4.629049	0.086682
H	2.338840	4.683159	0.810855
H	1.969126	4.544905	-0.911273
C	-0.532420	5.862385	-0.775903
C	0.673971	5.912812	0.170478
H	1.302094	6.781290	-0.060888
H	0.321346	6.048751	1.203028
H	-1.136530	6.771287	-0.669344
H	-0.178266	5.842037	-1.816097
H	0.052027	-0.111343	-2.159171
C	2.776805	-3.175962	0.194644
C	2.091333	-3.343072	1.572216
C	1.747184	-3.370174	-0.943198
C	3.820822	-4.304341	0.068529
H	2.827298	-3.260127	2.381967
H	1.324366	-2.582683	1.721919
H	1.619898	-4.331189	1.646195
H	2.240399	-3.305370	-1.920615
H	1.280191	-4.360376	-0.866171
H	0.965847	-2.611857	-0.898904
H	3.312490	-5.272221	0.145959
H	4.338052	-4.283165	-0.897833

H	4.574557	-4.265863	0.864083
C	-2.807437	-3.151083	-0.525474
C	-2.061038	-3.190062	-1.881322
C	-1.831326	-3.500441	0.622131
C	-3.880373	-4.259225	-0.560906
H	-2.756611	-3.007319	-2.709210
H	-1.272600	-2.436954	-1.919393
H	-1.603460	-4.175333	-2.035280
H	-2.344378	-3.461267	1.591794
H	-1.443286	-4.518353	0.491114
H	-0.986380	-2.812729	0.637990
H	-3.389824	-5.226360	-0.718630
H	-4.439950	-4.325800	0.379970
H	-4.597097	-4.120003	-1.378662
C	-6.988685	-0.287037	0.002564
C	-7.623829	-0.929045	-1.254066
C	-7.441844	-1.069366	1.258351
C	-7.518511	1.154374	0.121301
H	-7.332582	-0.384509	-2.159538
H	-7.315223	-1.972292	-1.379778
H	-8.718753	-0.912766	-1.183248
H	-7.021434	-0.624945	2.167954
H	-8.535485	-1.056993	1.346905
H	-7.124007	-2.116941	1.222310
H	-8.611119	1.143689	0.207628
H	-7.121175	1.660946	1.008606
H	-7.263635	1.755396	-0.759296
C	6.976438	-0.349032	-0.386833
C	7.338893	-1.073996	-1.704959
C	7.523526	1.088734	-0.466069
C	7.674531	-1.062318	0.795659
H	7.005758	-2.117348	-1.699807
H	6.869870	-0.579564	-2.563158
H	8.425209	-1.072122	-1.860328
H	7.322462	1.652170	0.452753
H	8.610141	1.066173	-0.607809
H	7.092034	1.641742	-1.308340
H	8.763242	-1.058455	0.658604
H	7.448831	-0.559739	1.743392
H	7.356053	-2.106060	0.888386
H	-1.612863	-0.308907	3.419865

2.11.3. Barrier for Rotation About the O(epoxide)–Co Bond

Starting from the optimal epoxide binding geometry, the indicated C–O–Co–O dihedral θ was iteratively varied in 15º increments while allowing all other degrees of freedom to relax (opt=modredundant). The minima were all set to ΔE = 0 kcal/mol. All calculations performed on singlet electronic states calculated using a restricted wavefunction. Energies are uncorrected electronic energies calculated at the B3LYP/6-31G(d) level of theory.

Table 2.6. Data used to create Figure 2.13.

θ **(º)**	**Δ*E* (*R*)-PO (kcal/mol)**	***θ*** **(º)**	**Δ*E* (*S*)-PO (kcal/mol)**	***θ*** **(º)**	**Δ*E* EO (kcal/mol)**
40.481	0	40.22	0	40.446	0
55.481	0.44153	55.22	0.41788	55.446	0.40227
70.481	1.5814	70.22	1.4653	70.446	1.4043
85.481	2.4966	85.22	2.2825	85.446	2.1931
100.48	3.3175	100.22	3.069	100.45	3.0925
115.48	4.3003	115.22	3.8156	115.45	4.0211
130.48	5.0652	130.22	4.2042	130.45	4.5712
145.48	5.2867	145.22	4.4147	145.45	4.9711
160.48	5.3576	160.22	4.6085	160.45	5.2635
175.48	5.6254	175.22	4.8634	175.45	5.5279
-169.52	6.1021	-169.78	5.2846	-169.55	5.9488
-154.52	6.378	-154.78	5.7158	-154.55	6.1913
-139.52	6.25	-139.78	5.7648	-139.55	6.0139
-124.52	5.859	-124.78	5.2549	-124.55	5.5676
-109.52	5.3614	-109.78	4.5701	-109.55	4.9638
-94.519	4.8742	-94.78	3.9902	-94.554	4.3723
-79.519	4.1801	-79.78	3.3702	-79.554	3.6643
-64.519	3.2254	-64.78	2.4674	-64.554	2.7342
-49.519	2.3433	-49.78	1.5815	-49.554	1.8794
-34.519	1.8532	-34.78	1.0243	-34.554	1.4066
-19.519	1.7788	-19.78	0.98986	-19.554	1.3735
-4.5191	1.371	-4.7804	0.86686	-4.5545	1.0816
10.481	0.69583	10.22	0.48056	10.446	0.55786
25.481	0.21646	25.22	0.14334	25.446	0.17114

2.11.4. Identity of the Nucleophilic Catalyst

All calculations performed at the B3LYP/6-31G(d) level of theory with the full ligand as in (*S,S*)-(salen)Co–X (**1**). Calculations of the singlet state were performed using restricted wavefunctions. Calculations of the triplet state were performed with unrestricted wavefuncitons. Cartesian coordinates in Å.

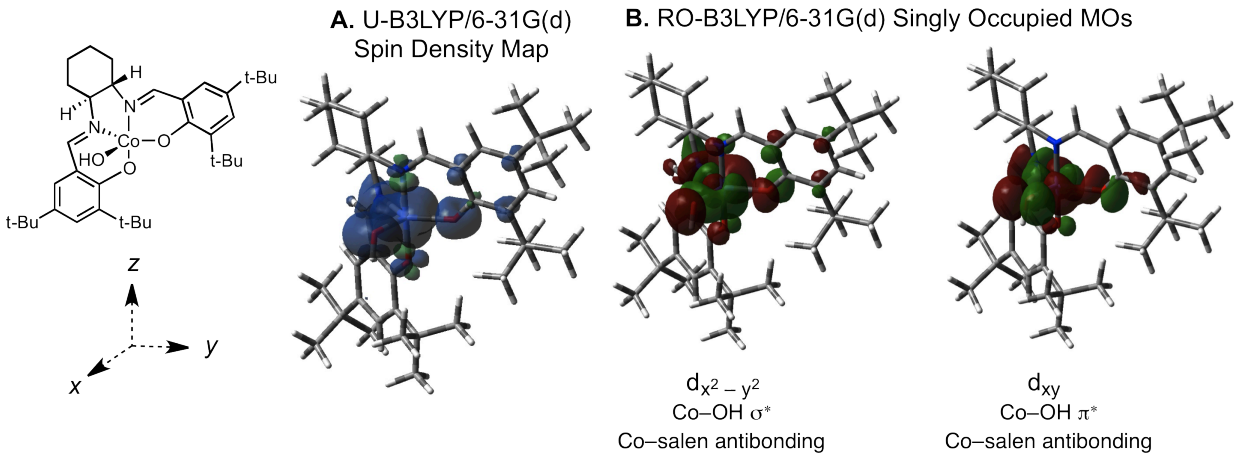

Figure 2.22. Distribution of unpaired spin density in ^{3}**1b** from the Unrestricted DFT wavefunction and singly occupied MO's calculated with Restricted Open Shell DFT. Note the small amount of unpaired electron density on the salen ligand.

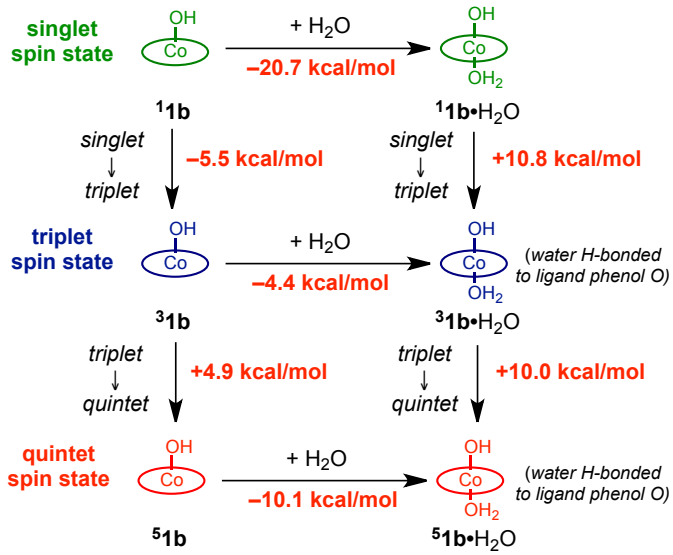

Figure 2.23. Interplay between coordination number and spin state preference for (salen)Co(III) hydroxo compounds calculated at the B3LYP/6-31G(d) level of theory in the gas phase. The triplet spin state is preferred for the 5-coordinate hydroxo complex, whereas the singlet is preferred for the six-coordinate complex. The quintet state is higher in energy for both stoichiometries.

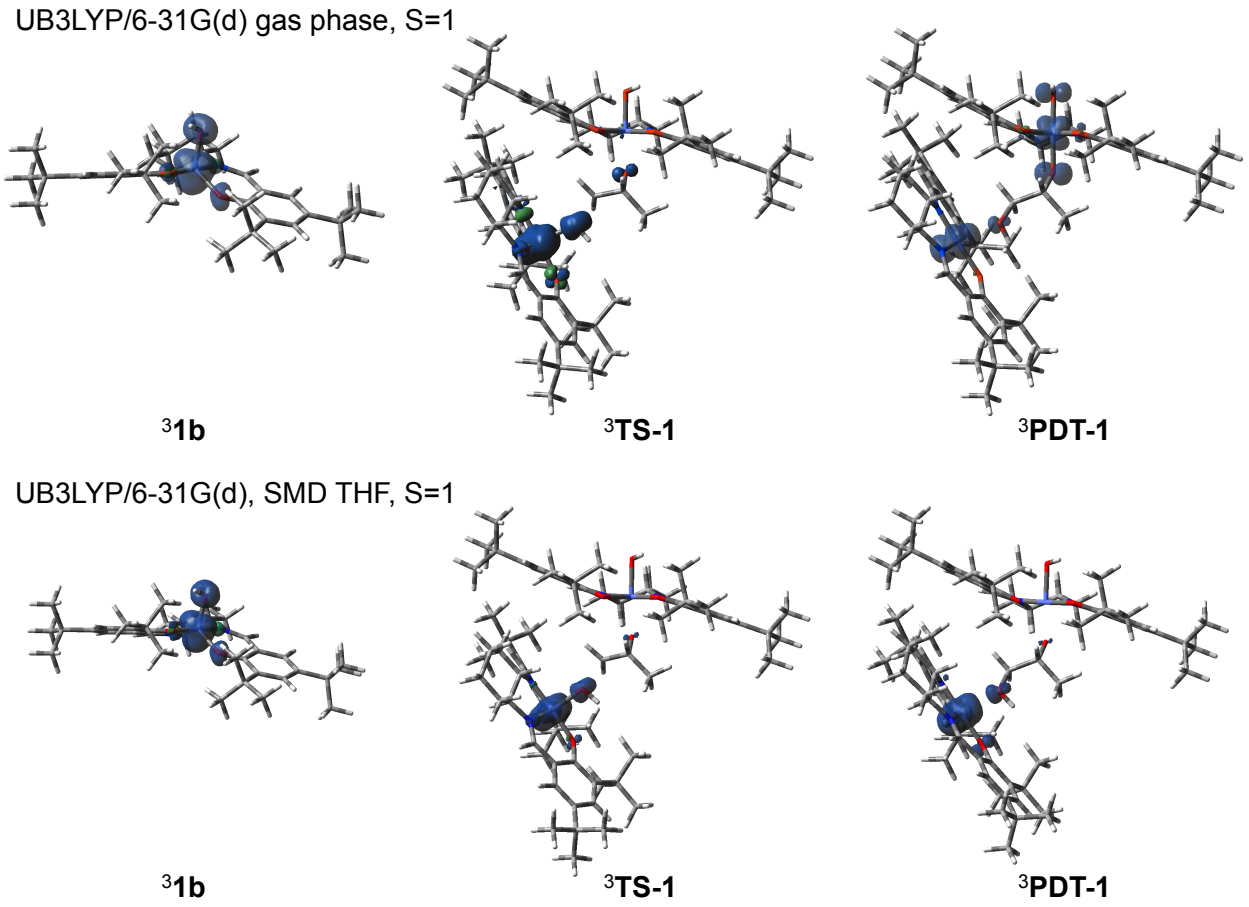

Figure 2.24. Spin density maps along the reaction coordinate to epoxide ring-opening in the triplet manifold at the UB3LYP/6-31G(d) level of theory. Note that unpaired spin density resides primarily on the nucleophile-delivering catalyst in ^{3}**TS-1**, but that there is significant unpaired spin density on both Co centers in ^{3}**PDT-1** in the gas phase. We attribute this to the calculation converging to a disproportionated Co(II)/Co(IV) configuration to minimize costly charge separation in the gas phase. Consistent with this notion, unpaired spin density remains on the nucleophile-delivering Co center in the product when the structure is optimized using Truhlar and Cramer's SMD model for THF. See Section 5-J for calculated energies using the SMD solvent model.

In addition to B3LYP/6-31G(d), we considered several other DFT methods and basis sets to test whether our results were robust to variation of the computational method. Optimizations at other levels of theory were initiated from the B3LYP/6-31G(d) geometry.

Table 2.7. Summary of how different DFT methods treat the interplay between coordination number and spin state for (salen)Co(III) complexes.

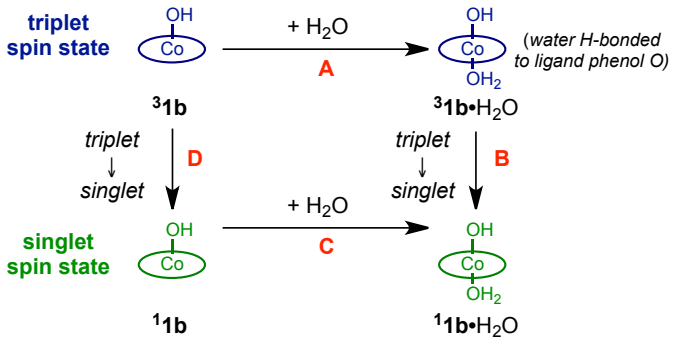

Entry	Level of Theory	Δ*E*(A) (kcal/mol)	Δ*E*(B) (kcal/mol)	Δ*E*(C) (kcal/mol)	Δ*E*(D) (kcal/mol)
1	B3LYP/6-31G(d)	–4.4	–10.8	–20.7	+5.5
2	BLYP/6-31G(d)	–8.9	–6.5	–18.8	+3.4
3	BLYP/6-311+G(d,p)	–2.9	–5.7	–9.1	+0.4
4	OLYP/6-31G(d)	–6.3	+0.4	–12.1	+6.2
5	OLYP/6-311+G(d,p)	–2.9	+2.6	–3.8	+3.5
6	PW91/6-31G(d)	–11.1	–9.2	–23.4	+3.0
7	BP86/6-31G(d)	–8.2	–8.8	–20.2	+3.2
8	TPSSh/6-31+G(d,p)	–5.7	–9.3	–15.8	+0.8

Conclusions: All of these methods, with the exception of Handy's OPTX functional, generally reproduce the trends observed in Entry 1. The OLYP methods predict that pentacoordinate **1b** would be more stable in the singlet electronic state, which is inconsistent with experimental NMR spectroscopy and magnetic susceptibility data. Water association energies (Δ*E*(A) and Δ*E*(C)) were considerably smaller with larger basis sets consistent with some amount of basis set superposition error. For triplet spin states we examined spin density maps, and they were similar to those observed for B3LYP/6-31G(d). We conclude that B3LYP/6-31G(d) does an adequate job of qualitatively capturing the interplay between coordination number and spin state for (salen)Co(III) complexes.

Table 2.8. Summary of how different DFT methods treat the relative nucleophilicity of the two potential nucleophile-delivering catalysts in the HKR.

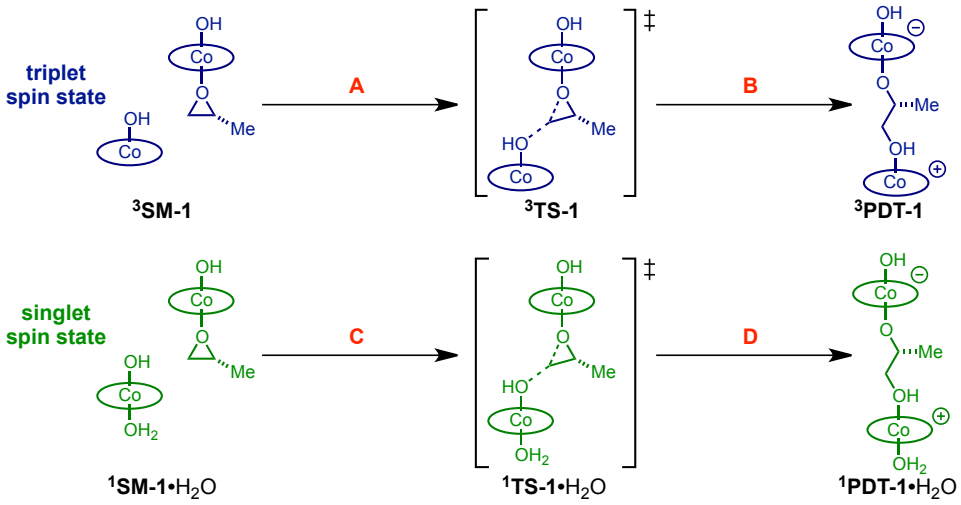

Entry	Single Point Energy	Geometry	Δ*E*(A) (kcal/mol)	Δ*E*(B) (kcal/mol)	Δ*E*(C) (kcal/mol)	Δ*E*(D) (kcal/mol)
1	B3LYP/6-31G(d)	B3LYP/6-31G(d)	+17.4	–22.5	+16.0	–10.4
2[a]	B3LYP/6-31G(d)	B3LYP/6-31G(d)	+14.7	–17.9	+12.7	N.D.
3	OLYP/6-31G(d)	OLYP/6-31G(d)	+17.4	N.D.	+18.9	–17.1
4	OLYP/6-31G(d)	B3LYP/6-31G(d)	+17.1	–26.2	+18.9	–12.3
5	TPSSh/6-31G(d)	B3LYP/6-31G(d)	+15.7	–24.6	+14.2	–9.3
6	TPSSh/cc-pVDZ	B3LYP/6-31G(d)	+16.0	–27.2	+15.0	–9.0
7	TPSSh/cc-pVTZ	B3LYP/6-31G(d)	+17.3	–26.8	+16.7	–9.0
8	BP86/6-311G(d,p)	B3LYP/6-31G(d)	+8.4	–28.3	+11.2	–13.4
9	M06L/6-311G(d,p)	B3LYP/6-31G(d)	+13.4	–31.8	+11.2	–12.7

[a]Calculated in THF using the SMD model.[63]

Conclusions: Of the methods presented above, B3LYP, TPSSh, and M06L predict that the singlet nucleophile is more reactive by 0.6–2.2 kcal/mol. OLYP and BP86 predict a more reactive triplet, by 1.5–2.8 kcal/mol. While these data are not in perfect agreement with one another, we can say that the **^{1}1b**•OH_2 is of comparable reactivity, and perhaps more reactive. Combined with the HKR's first-order kinetic dependence on the concentration of water[7] and the analysis of Co–OH bond lengths en route to the epoxide ring-opening transition state (see the

[63] Marenich, A. V.; Cramer, C. J.; Truhlar, D. G. *J. Phys. Chem. B.* **2009**, *113*, 6378–6396.

body of the chapter) we feel that the most probable assignment of the nucleophile is the six-coordinate $S = 0$ species and we used that species of the remainder of our analysis in the text.

During the course of our computational study, we also considered what selectivity we would predict with a nucleophile in the triplet spin state. Calculations were performed at the B3LYP/6-31G(d) level.

Table 2.9. Diastereomeric Transition States

	ΔE (kcal/mol)			
Lewis Acid/Epoxide/Nucleophile	(*S,S*)/(*R*)/(*S,S*)	(*S,S*)/(***S***)/(*S,S*)	(***R,R***)/(*R*)/(*S,S*)	(*S,S*)/(*R*)/(***R,R***)
S = 0	0 (defined)	+2.3	+3.1	+1.1
S = 1 ($-H_2O$)	0 (defined)	+3.2	+1.2	+1.6

Table 2.10. Selectivity in Epoxide Opening with An Achiral Lewis Acid (BH_3) and an (*S,S*)-(salen)Co–OH Nucleophile

	ΔE (kcal/mol)	
	(*R*)-1,2-epoxypropane (matched)	(*S*)-1,2-epoxypropane (mismatched)
S = 0	0 (defined)	–0.37
S = 1 ($-H_2O$)	0 (defined)	+0.02

Conclusion: Because kinetics data suggest that an aquo ligand is required to bind prior to the rate-determining step of the HKR and our calculations indicate that the hexacoordinate aquo complex ^{1}**1b**•H_2O is more nucleophilic than the pentacoordinate ^{3}**1b**, we based our analysis around the $S = 0$ spin state. Nevertheless, these calculations show that ^{3}**1b** should also be able to stereoselectively react with electrophilic ^{1}**1b**•(epoxide) complexes. Furthermore, this calculated selectivity appears to arise from catalyst-catalyst interactions because no selectivity is observed when opening an epoxide activated by an achiral Lewis acid (BH_3).

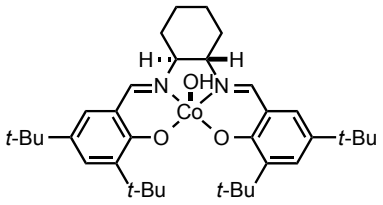

Charge: 0
Spin Multiplicity: 1
Solvation: gas phase
Electronic Energy (AU): -3121.69397466
Gibbs Free Energy at 298.150 K (AU): -3120.934322

N	1.279919	2.080921	0.123712
N	-1.248361	2.053870	-0.371098
C	-2.535132	1.902230	-0.428848
H	-3.150153	2.776233	-0.648356
C	2.566861	1.937124	0.201440
H	3.179173	2.830375	0.332921
C	-3.252423	0.681924	-0.238271
C	-2.580615	-0.567026	-0.049636
C	-4.667622	0.758383	-0.263514
C	-3.396681	-1.742895	0.131779
H	-5.113283	1.736939	-0.416971
C	-4.774519	-1.586549	0.100045
H	-5.385077	-2.470590	0.238853
C	3.284054	0.705940	0.109210
C	2.610007	-0.542149	-0.072987
C	4.698288	0.775285	0.169345
C	3.422154	-1.721058	-0.247037
H	5.146192	1.752940	0.321854
C	4.799523	-1.573548	-0.178494
H	5.407786	-2.462042	-0.297438
O	-1.276022	-0.668954	-0.073539
O	1.305026	-0.629027	-0.112139
O	-0.257922	0.883113	1.865189
C	-0.605326	3.365540	-0.592968
C	0.617225	3.377774	0.339950
H	-0.224020	3.365109	-1.627143
H	0.239419	3.345514	1.372048
C	1.461379	4.642118	0.150267
H	2.289482	4.663782	0.867819
H	1.904414	4.644368	-0.856190
C	-1.475972	4.612538	-0.399242
H	-2.304996	4.623958	-1.116133
H	-1.916739	4.593167	0.607057
C	0.591223	5.896364	0.342477
C	-0.632432	5.886349	-0.581614
H	-1.256112	6.768698	-0.395832
H	-0.300108	5.953879	-1.627442
H	1.194437	6.794254	0.163585
H	0.257373	5.946624	1.388316
H	-0.717118	0.065741	2.121539
Co	-0.001436	0.698904	0.080240
C	2.777963	-3.096614	-0.509455
C	1.865935	-3.484965	0.678248
C	1.956414	-3.040613	-1.820909
C	3.826543	-4.215702	-0.671624
H	2.450269	-3.562778	1.603356
H	1.077712	-2.747500	0.826841
H	1.400012	-4.460743	0.491100
H	2.609448	-2.822097	-2.675076
H	1.473963	-4.008483	-2.005543
H	1.182250	-2.273750	-1.771036
H	3.310704	-5.163466	-0.862202
H	4.500585	-4.034065	-1.517238
H	4.433459	-4.349331	0.231742
C	-2.757177	-3.125867	0.369902
C	-1.871730	-3.513858	-0.838274
C	-1.909978	-3.089493	1.665320
C	-3.811185	-4.238314	0.544360
H	-2.475028	-3.577993	-1.752353
H	-1.077238	-2.784810	-0.996479
H	-1.414107	-4.496663	-0.668389
H	-2.541292	-2.860425	2.532764
H	-1.441292	-4.065922	1.839043
H	-1.119322	-2.340912	1.600606
H	-3.299041	-5.192304	0.712210
H	-4.463890	-4.061015	1.407374
H	-4.439912	-4.356455	-0.346108
C	-5.457017	-0.358330	-0.098017
C	5.483730	-0.348870	0.036480
C	7.019913	-0.332510	0.099913
C	7.501637	-1.238993	1.257851
C	7.602183	-0.856169	-1.234782
C	7.574185	1.084408	0.340451
H	7.118139	-0.880520	2.219893
H	7.168340	-2.274510	1.131670
H	8.597572	-1.246557	1.308794
H	7.288525	-0.223602	-2.073152
H	8.698767	-0.857882	-1.200448
H	7.275468	-1.879256	-1.449266
H	8.668802	1.052898	0.384460
H	7.296527	1.772431	-0.466646
H	7.217898	1.505352	1.287830
C	-6.994224	-0.331472	-0.115502
C	-7.540269	-0.846659	1.237691
C	-7.545415	1.088623	-0.344120
C	-7.517058	-1.238443	-1.255090
H	-7.213769	-1.871057	1.446134
H	-7.198359	-0.213304	2.064236
H	-8.637375	-0.841727	1.235155
H	-7.217650	1.502579	-1.304868
H	-8.641098	1.065625	-0.351827
H	-7.235581	1.777865	0.450003
H	-8.614086	-1.239811	-1.272193
H	-7.161473	-0.885204	-2.229817
H	-7.186042	-2.275569	-1.135987

Water
Charge: 0
Spin Multiplicity: 1
Solvation: gas phase
Electronic Energy (AU): -76.4089533236
Gibbs Free Energy at 298.150 K (AU): -76.405452

O	0.000000	0.000000	0.119720
H	0.000000	0.761560	-0.478879
H	0.000000	-0.761560	-0.478879

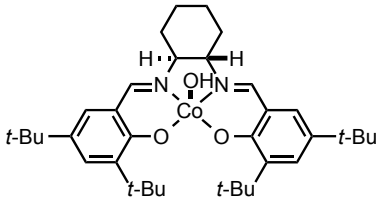

Charge: 0
Spin Multiplicity: 3
Solvation: gas phase
Electronic Energy (AU): -3121.70278977
Gibbs Free Energy at 298.150 K (AU): -3120.945148

N	1.338336	2.037468	0.498600
N	-1.095048	2.012750	-0.335147
C	-2.359120	1.853159	-0.588755
H	-2.915596	2.695236	-1.006804
C	2.613784	1.882611	0.351035
H	3.246198	2.771525	0.376430
C	-3.134027	0.676144	-0.356240
C	-2.582195	-0.515344	0.222167
C	-4.510779	0.752357	-0.696314
C	-3.478408	-1.626078	0.445326
H	-4.865936	1.683487	-1.128126
C	-4.807850	-1.468837	0.087103
H	-5.477120	-2.303017	0.258336
C	3.289753	0.642651	0.116768
C	2.564390	-0.561587	-0.139843
C	4.703984	0.675107	0.066061
C	3.324267	-1.742599	-0.456636
H	5.191366	1.624827	0.266540
C	4.708544	-1.636864	-0.479916
H	5.277239	-2.529614	-0.710460
O	-1.319951	-0.637131	0.533748
O	1.254114	-0.608521	-0.114936
O	-0.098736	0.883615	2.369359
C	-0.411989	3.308895	-0.515021
C	0.679532	3.345238	0.581454
H	0.106347	3.276535	-1.486664
H	0.169143	3.360801	1.553600
C	1.558561	4.591749	0.458045
H	2.303784	4.610911	1.262229
H	2.107469	4.573026	-0.494434
C	-1.285104	4.568998	-0.459718
H	-2.013700	4.574691	-1.278626
H	-1.854790	4.569192	0.479997
C	0.684801	5.855804	0.521284
C	-0.415019	5.835188	-0.549786
H	-1.051148	6.723433	-0.457805
H	0.047747	5.885378	-1.545860
H	1.313082	6.746183	0.401136
H	0.224979	5.928355	1.516656
H	-0.719959	0.209547	2.692848
Co	0.023771	0.673002	0.564094
C	2.619080	-3.087422	-0.722079
C	1.851864	-3.517864	0.551662
C	1.645361	-2.956977	-1.918763
C	3.614621	-4.214607	-1.065042
H	2.547683	-3.666399	1.386501
H	1.116729	-2.766940	0.844051
H	1.329154	-4.466333	0.375725
H	2.191078	-2.688173	-2.831914
H	1.143227	-3.915881	-2.098453
H	0.885639	-2.196866	-1.733223
H	3.057330	-5.140247	-1.247962
H	4.193468	-3.995771	-1.970502
H	4.316563	-4.413980	-0.246620
C	-2.966332	-2.953537	1.043081
C	-1.931734	-3.582893	0.079972
C	-2.323197	-2.714389	2.431268
C	-4.099874	-3.981330	1.241183
H	-2.399158	-3.824804	-0.882476
H	-1.096389	-2.905915	-0.100851
H	-1.537094	-4.513984	0.505990
H	-3.049426	-2.272397	3.124674
H	-1.990104	-3.668495	2.858086
H	-1.459276	-2.053001	2.360879
H	-3.679671	-4.897540	1.670543
H	-4.872281	-3.619659	1.930537
H	-4.581213	-4.256401	0.295449
C	-5.372464	-0.299727	-0.487865
C	5.443814	-0.452127	-0.223960
C	6.980398	-0.475649	-0.279510
C	7.523341	-1.485408	0.759902
C	7.445403	-0.899492	-1.693062
C	7.591341	0.903779	0.031752
H	7.217375	-1.204726	1.774148
H	7.159350	-2.500990	0.571275
H	8.619754	-1.514772	0.729743
H	7.090921	-0.190821	-2.450396
H	8.540953	-0.932156	-1.742879
H	7.071108	-1.892281	-1.964516
H	8.684719	0.845332	-0.016179
H	7.270131	1.663874	-0.690050
H	7.322984	1.250152	1.036572
C	-6.870101	-0.263919	-0.834009
C	-7.706165	-0.489320	0.448384
C	-7.289665	1.085314	-1.446934
C	-7.194547	-1.377737	-1.857957

H	-7.481675	-1.452670	0.918809
H	-7.508316	0.296012	1.186873
H	-8.777981	-0.476065	0.214608
H	-6.752887	1.293391	-2.379905
H	-8.360543	1.070923	-1.679330
H	-7.113296	1.918332	-0.756467
H	-8.262989	-1.370983	-2.107045
H	-6.627713	-1.233711	-2.784896
H	-6.951122	-2.372559	-1.470076

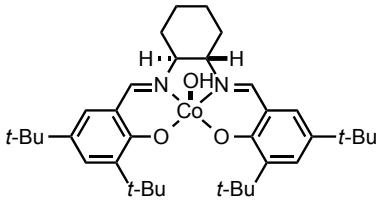

Charge: 0
Spin Multiplicity: 5
Solvation: gas phase
Electronic Energy (AU): -3121.69493345
Gibbs Free Energy at 298.150 K (AU): -3120.942207

N	1.368703	2.074899	0.381289
N	-1.172234	2.024957	-0.220738
C	-2.436105	1.874417	-0.477451
H	-2.998243	2.734279	-0.852090
C	2.647169	1.936682	0.234448
H	3.282696	2.827430	0.232811
C	-3.221296	0.686410	-0.316240
C	-2.647407	-0.569942	0.061290
C	-4.613245	0.807232	-0.553961
C	-3.534097	-1.694819	0.222865
H	-4.987064	1.782842	-0.850609
C	-4.886255	-1.492214	-0.012111
H	-5.552719	-2.337311	0.112358
C	3.340435	0.694308	0.056234
C	2.647530	-0.553533	-0.067840
C	4.752325	0.755642	-0.030718
C	3.435296	-1.737129	-0.303991
H	5.217699	1.731657	0.072598
C	4.814287	-1.597141	-0.369537
H	5.404901	-2.489599	-0.539676
O	-1.360267	-0.709345	0.224119
O	1.344918	-0.637275	-0.002676
O	-0.129788	0.643369	2.477324
C	-0.497204	3.315834	-0.466925
C	0.705622	3.372609	0.504896
H	-0.080004	3.270994	-1.485752
H	0.293899	3.409800	1.525230
C	1.553604	4.628791	0.278556
H	2.375374	4.666232	1.003778
H	2.008179	4.593760	-0.722237
C	-1.360685	4.581083	-0.343255
H	-2.170082	4.575269	-1.081790
H	-1.831636	4.595525	0.649758
C	0.687654	5.891583	0.409214
C	-0.512332	5.848391	-0.544438
H	-1.141399	6.735750	-0.405590
H	-0.152530	5.881211	-1.582915
H	1.296888	6.781906	0.213051
H	0.328838	5.979457	1.444339
H	-0.589888	-0.109872	2.881023
Co	0.006444	0.581521	0.678111
C	2.757293	-3.110335	-0.486509
C	1.947358	-3.476086	0.781234
C	1.820666	-3.067580	-1.719330
C	3.779310	-4.240665	-0.722353
H	2.603979	-3.526875	1.658521
H	1.163948	-2.742712	0.974136
H	1.478312	-4.460026	0.654629
H	2.393525	-2.860949	-2.631918
H	1.323377	-4.037280	-1.847496
H	1.055299	-2.298129	-1.607956
H	3.242842	-5.187805	-0.847970
H	4.374818	-4.079432	-1.628828
H	4.465544	-4.362822	0.124257
C	-2.987035	-3.074536	0.642881
C	-1.992806	-3.589721	-0.425546
C	-2.278195	-2.967359	2.015403
C	-4.103470	-4.128894	0.786334
H	-2.496056	-3.714679	-1.392173
H	-1.159682	-2.898342	-0.555025
H	-1.592434	-4.566706	-0.126215
H	-2.979329	-2.631377	2.789390
H	-1.889412	-3.947896	2.316539
H	-1.441491	-2.268252	1.971907
H	-3.657943	-5.083146	1.089221
H	-4.839466	-3.853243	1.551059
H	-4.633769	-4.300878	-0.157624
C	-5.471748	-0.261962	-0.409122
C	5.518465	-0.373027	-0.234366
C	7.053920	-0.359565	-0.317827
C	7.641141	-1.237593	0.813058
C	7.509295	-0.919303	-1.686823
C	7.629723	1.061254	-0.168451
H	7.353037	-0.850733	1.797200
H	7.291643	-2.273465	0.747558
H	8.736969	-1.251910	0.759241
H	7.116877	-0.309972	-2.509103
H	8.604344	-0.919698	-1.755290
H	7.167696	-1.947987	-1.842420
H	8.723161	1.027390	-0.233659
H	7.272286	1.730157	-0.960008
H	7.370086	1.505393	0.799374
C	-6.988971	-0.178583	-0.645736
C	-7.738673	-0.533588	0.660772
C	-7.430763	1.231058	-1.082079
C	-7.399431	-1.174542	-1.756619
H	-7.497826	-1.543995	1.007620

H	-7.477117	0.165587	1.463305
H	-8.823844	-0.485190	0.506262
H	-6.950978	1.534997	-2.019604
H	-8.514263	1.245990	-1.245526
H	-7.201979	1.984374	-0.319296
H	-8.481496	-1.128690	-1.932023
H	-6.891374	-0.940455	-2.699126
H	-7.150645	-2.207701	-1.491983

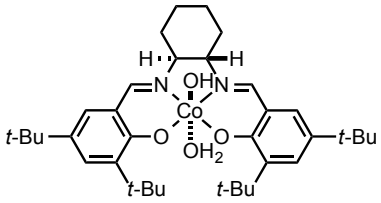

Charge: 0
Spin Multiplicity: 3
Solvation: gas phase
Electronic Energy (AU): -3198.11875253
Gibbs Free Energy at 298.150 K (AU): -3197.341256

N	-1.278777	2.118042	-0.193080
N	1.281255	2.110728	0.126534
C	2.563198	1.954227	0.154969
H	3.189143	2.834474	0.308827
C	-2.562551	1.953856	-0.134777
H	-3.195271	2.842591	-0.108556
C	3.263209	0.707381	0.055393
C	2.580551	-0.535301	0.209335
C	4.670065	0.765342	-0.071936
C	3.375795	-1.730546	0.260858
C	5.443221	-0.377602	-0.070246
H	5.124787	1.745719	-0.178143
C	4.751608	-1.599499	0.105873
H	5.346943	-2.503830	0.121454
C	-3.258149	0.706530	-0.115943
C	-2.577016	-0.545078	-0.255150
C	-4.668968	0.766146	0.018742
C	-3.384146	-1.742121	-0.259894
C	-5.446616	-0.369844	0.026242
H	-5.119367	1.749348	0.117918
C	-4.756821	-1.600812	-0.119659
H	-5.356962	-2.502200	-0.124259
O	1.266435	-0.593024	0.341699
O	-1.274596	-0.635232	-0.368517
O	0.422522	0.855380	-2.118930
C	0.637088	3.396850	0.450372
C	-0.652818	3.437243	-0.380374
H	0.339525	3.331686	1.508302
H	-0.359106	3.474300	-1.439619
C	-1.497129	4.672351	-0.049759
H	-2.384344	4.716332	-0.692128
H	-1.850188	4.610897	0.989575
C	1.476138	4.664487	0.249910
H	2.360725	4.651731	0.896852
H	1.832616	4.702820	-0.788801
C	-0.663033	5.950777	-0.246101
C	0.636123	5.913359	0.568315
H	1.230711	6.814139	0.375681
H	0.394331	5.922101	1.640601
H	-1.260971	6.826431	0.032868
H	-0.422104	6.063219	-1.312489
H	0.069092	0.075402	-2.578644
Co	0.034243	0.724007	-0.301787
O	-0.325299	0.139574	2.548998
H	0.415101	-0.260707	2.054823
H	-1.079130	-0.409718	2.284409
C	-2.741797	-3.135393	-0.413137
C	-1.989791	-3.223098	-1.763238
C	-1.771289	-3.391491	0.764293
C	-3.786078	-4.270896	-0.399067
H	-2.686136	-3.087806	-2.599805
H	-1.210605	-2.463772	-1.835938
H	-1.522062	-4.209483	-1.870847
H	-2.312188	-3.373113	1.719018
H	-1.305626	-4.379454	0.663637
H	-0.979040	-2.643267	0.793567
H	-3.269894	-5.230882	-0.511356
H	-4.345768	-4.310007	0.543001
H	-4.503696	-4.187588	-1.223923
C	2.731149	-3.117231	0.459459
C	2.003528	-3.169860	1.824630
C	1.741713	-3.400924	-0.694879
C	3.771998	-4.256517	0.460283
H	2.712709	-3.012965	2.646440
H	1.223058	-2.411796	1.898603
H	1.537282	-4.152802	1.965797
H	2.268413	-3.409358	-1.656941
H	1.274872	-4.384486	-0.558562
H	0.955911	-2.647198	-0.737826
H	3.254408	-5.211731	0.603204
H	4.317649	-4.320219	-0.488439
H	4.501813	-4.155751	1.272514
C	-6.976748	-0.362165	0.176054
C	-7.625915	-1.001604	-1.074591
C	-7.379660	-1.172410	1.431422
C	-7.535115	1.065123	0.328900
H	-7.369697	-0.438450	-1.979268
H	-7.297271	-2.035931	-1.221807
H	-8.718598	-1.011270	-0.976804
H	-6.945070	-0.732929	2.336553
H	-8.470502	-1.182781	1.547269
H	-7.043321	-2.213066	1.371853
H	-8.625122	1.028159	0.436091
H	-7.132978	1.565663	1.217396
H	-7.311129	1.685975	-0.546383
C	6.972031	-0.377607	-0.235849
C	7.357711	-1.206783	-1.484199
C	7.533908	1.045287	-0.415365

C	7.632896	-1.001744	1.016299
H	7.019216	-2.245386	-1.405189
H	6.912725	-0.779373	-2.389920
H	8.447147	-1.221415	-1.612905
H	7.323482	1.679123	0.454050

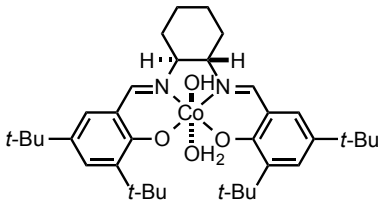

Charge: 0
Spin Multiplicity: 5
Solvation: gas phase
Electronic Energy (AU): -3198.11994305
Gibbs Free Energy at 298.150 K (AU): -3197.345239

N	-1.325780	2.092551	-0.330495
N	1.233759	2.038534	0.213160
C	2.514710	1.903123	0.348954
H	3.107979	2.777699	0.628148
C	-2.610055	1.963945	-0.247422
H	-3.235999	2.860096	-0.281821
C	3.281242	0.700212	0.172359
C	2.669091	-0.578783	-0.004731
C	4.689631	0.829935	0.220658
C	3.523609	-1.725067	-0.149997
C	5.525032	-0.259452	0.076747
H	5.096920	1.825385	0.370796
C	4.896615	-1.515477	-0.109176
H	5.542912	-2.377176	-0.223764
C	-3.333278	0.729344	-0.117547
C	-2.677527	-0.528376	0.064091
C	-4.745113	0.815057	-0.155694
C	-3.495227	-1.703824	0.195089
C	-5.544058	-0.303698	-0.035080
H	-5.184234	1.799365	-0.289278
C	-4.874023	-1.539669	0.136696
H	-5.491688	-2.424153	0.231304
O	1.360840	-0.714163	0.009630
O	-1.367114	-0.617301	0.148975
O	0.145008	0.496192	-2.356419
C	0.559471	3.316741	0.505524
C	-0.658076	3.392130	-0.445221
H	0.161292	3.227355	1.527911
H	-0.263775	3.445542	-1.472055
C	-1.503820	4.643013	-0.180988
H	-2.328001	4.703855	-0.901727
H	-1.954215	4.576355	0.819869
C	1.415426	4.588703	0.417214
H	2.229366	4.557509	1.150436
H	1.879058	4.643328	-0.578141
H	8.622401	1.002370	-0.535502
H	7.122365	1.535100	-1.305403
H	8.724467	-1.015750	0.906998
H	7.388070	-0.425792	1.916157
H	7.303041	-2.033055	1.180943
C	-0.641448	5.911114	-0.278007
C	0.562638	5.843453	0.668578
H	1.186109	6.738505	0.557108
H	0.208310	5.837659	1.709178
H	-1.253580	6.792494	-0.052901
H	-0.287501	6.031482	-1.311666
H	0.505519	-0.322415	-2.733530
Co	0.013353	0.562845	-0.561390
O	0.020197	-0.181711	2.664590
H	0.747026	-0.499574	2.103262
H	-0.738827	-0.337430	2.076720
C	-2.867269	-3.098759	0.403676
C	-1.878841	-3.421798	-0.742484
C	-2.134559	-3.149974	1.766686
C	-3.928953	-4.218934	0.414722
H	-2.387990	-3.392539	-1.713765
H	-1.049895	-2.714722	-0.762066
H	-1.469970	-4.431011	-0.607909
H	-2.838138	-2.980424	2.590747
H	-1.682192	-4.139164	1.911131
H	-1.341662	-2.404468	1.839855
H	-3.427557	-5.184508	0.543841
H	-4.642562	-4.111831	1.240214
H	-4.492307	-4.264484	-0.525013
C	2.932368	-3.135369	-0.355994
C	2.042421	-3.521848	0.850388
C	2.099412	-3.166995	-1.660586
C	4.026798	-4.214716	-0.485073
H	2.629507	-3.530602	1.776735
H	1.211899	-2.826032	0.973151
H	1.630724	-4.528427	0.704952
H	2.727388	-2.926929	-2.527425
H	1.678359	-4.167729	-1.816666
H	1.272998	-2.455546	-1.617739
H	3.551555	-5.191406	-0.628751
H	4.683122	-4.040417	-1.345934
H	4.648457	-4.282652	0.415360
C	-7.080857	-0.265743	-0.078866
C	-7.588084	-1.127302	-1.259990
C	-7.653255	-0.826148	1.245181
C	-7.619227	1.165413	-0.264674
H	-7.211807	-0.742323	-2.214679
H	-7.267132	-2.170702	-1.171856
H	-8.684496	-1.119264	-1.297411
H	-7.321108	-0.226433	2.100318
H	-8.749991	-0.812162	1.224196
H	-7.338282	-1.860112	1.421389
H	-8.714702	1.149829	-0.289827
H	-7.317692	1.823358	0.558686
H	-7.274308	1.611227	-1.204827
C	7.060074	-0.168710	0.108282

C	7.637690	-0.675439	-1.234933
C	7.549977	1.275439	0.325261
C	7.609700	-1.040772	1.262346
H	7.353064	-1.713797	-1.436015
H	7.279389	-0.063680	-2.070799
H	8.733579	-0.627957	-1.222824
H	7.199128	1.685683	1.279361
H	8.645501	1.297723	0.340460
H	7.218006	1.942801	-0.478569
H	8.705376	-0.993379	1.289855
H	7.229317	-0.694203	2.229989
H	7.326515	-2.092773	1.150722

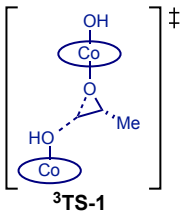

^{3}TS-1

Transition State
Charge: 0
Spin Multiplicity: 3
Solvation: gas phase
Electronic Energy (AU): -6436.51238387
Gibbs Free Energy at 298.150 K (AU): -6434.888783

Co	-3.563944	-0.003446	-0.088653
N	-4.468314	0.465110	-1.688645
N	-3.076452	-1.607688	-0.994177
C	-2.683895	-2.689461	-0.415212
H	-2.542948	-3.586070	-1.022753
C	-4.863415	1.650193	-2.002236
H	-5.303675	1.810847	-2.988438
C	-2.413059	-2.849153	0.988522
C	-2.423001	-1.738830	1.896927
C	-2.146280	-4.163982	1.435480
C	-2.174347	-2.034284	3.292580
H	-2.167379	-4.957304	0.692359
C	-1.934025	-3.352813	3.657591
H	-1.774266	-3.564847	4.708700
C	-4.813687	2.809538	-1.154732
C	-4.479858	2.719159	0.236017
C	-5.201221	4.037191	-1.740309
C	-4.628701	3.923937	1.023802
H	-5.439414	4.029007	-2.800429
C	-4.996393	5.093966	0.373265
H	-5.085623	5.995158	0.968570
O	-2.604723	-0.513309	1.502764
O	-4.086342	1.609004	0.798195
O	-5.077338	-0.883383	0.501798
O	-1.991646	0.884671	-0.888010
C	-0.196503	0.491113	-0.391426
C	-1.079310	1.638668	-0.124687
H	0.173406	0.370621	-1.399992
H	-0.357833	-0.394079	0.203926
H	-1.365769	1.726488	0.926223
C	-3.348840	-1.519556	-2.433968
C	-4.655649	-0.703903	-2.550897
H	-2.544341	-0.904374	-2.863041
H	-5.447150	-1.297136	-2.072595
C	-5.025642	-0.440173	-4.013878
H	-5.985946	0.085350	-4.076144
H	-4.269457	0.212399	-4.473697
C	-3.439772	-2.836568	-3.211690
H	-2.483956	-3.373053	-3.167170
H	-4.197437	-3.483140	-2.747218
C	-5.113177	-1.761776	-4.793801
C	-3.814749	-2.571943	-4.679556
H	-3.912361	-3.525144	-5.213536
H	-2.998490	-2.021188	-5.168795
H	-5.341403	-1.556689	-5.846858
H	-5.949132	-2.358416	-4.402120
H	-5.487309	-0.257098	1.119433
C	-0.734738	2.987295	-0.731030
H	-1.615976	3.636257	-0.707008
H	0.067645	3.481033	-0.166846
H	-0.420112	2.875910	-1.775222
N	2.318646	-1.722459	0.970963
N	4.258729	-0.203032	1.685405
C	5.157486	0.708312	1.930129
H	5.678159	0.664018	2.887634
C	1.781262	-2.757335	0.408203
H	1.278648	-3.484151	1.046577
C	5.534450	1.789125	1.084232
C	4.941115	1.993519	-0.203292
C	6.515601	2.684743	1.588416
C	5.368806	3.138893	-0.968042
H	6.925682	2.474194	2.571302
C	6.326889	3.966333	-0.402896
H	6.646110	4.828125	-0.976018
C	1.828063	-3.072965	-0.988953
C	2.594771	-2.288606	-1.900241
C	1.190170	-4.266202	-1.404321
C	2.724535	-2.758093	-3.250882
H	0.620340	-4.814219	-0.660523
C	2.077511	-3.942259	-3.585512
H	2.178555	-4.297589	-4.603585
O	4.044892	1.180280	-0.699754
O	3.188662	-1.170324	-1.532754
O	1.597328	0.803185	0.341405
C	3.916551	-1.251150	2.672956
C	2.425110	-1.560882	2.432282
H	4.484559	-2.152966	2.395071
H	1.849323	-0.660592	2.684659
C	1.946891	-2.724645	3.302066
H	0.875516	-2.896894	3.154636
H	2.474963	-3.644896	3.013091
C	4.188529	-0.933427	4.147950
H	5.258987	-0.772911	4.321723

H	3.671591	-0.002544	4.419392
C	2.223736	-2.421972	4.785220
C	3.700107	-2.090319	5.037914
H	3.857068	-1.830331	6.091164
H	4.315055	-2.980242	4.841182
H	1.919707	-3.282135	5.392637
H	1.598796	-1.577844	5.105599
H	1.807804	1.672401	-0.040250
Co	3.161546	-0.261754	0.103663
C	-4.423434	3.903068	2.553431
C	-5.465858	2.951662	3.189902
C	-2.993929	3.430864	2.906405
C	-4.617387	5.291732	3.196579
H	-6.483334	3.316939	3.004295
H	-5.379299	1.944559	2.780101
H	-5.319631	2.896511	4.276316
H	-2.246223	4.104500	2.468375
H	-2.851771	3.435716	3.995006
H	-2.817110	2.421487	2.537088
H	-4.464043	5.208415	4.278750
H	-3.897656	6.028059	2.818669
H	-5.628110	5.686043	3.039026
C	-2.231574	-0.915871	4.352746
C	-1.148612	0.150802	4.063879
C	-3.632819	-0.259176	4.332783
C	-1.991217	-1.439435	5.783501
H	-0.144322	-0.282242	4.164441
H	-1.253336	0.552176	3.055870
H	-1.227397	0.978174	4.780229
H	-4.405650	-0.998169	4.576107
H	-3.683873	0.543014	5.080227
H	-3.853132	0.162325	3.352577
H	-2.043745	-0.599796	6.486098
H	-2.749811	-2.169386	6.089176
H	-1.003411	-1.902969	5.900559
C	3.538844	-1.968380	-4.295859
C	2.888078	-0.580326	-4.510500
C	5.004732	-1.808990	-3.823283
C	3.576013	-2.677085	-5.665675
H	1.866537	-0.689340	-4.894787
H	2.849353	-0.010026	-3.581304
H	3.463579	-0.003735	-5.245028
H	5.479389	-2.790506	-3.702001
H	5.579519	-1.249275	-4.571311
H	5.063537	-1.276316	-2.873377
H	4.172161	-2.076832	-6.361871
H	4.041046	-3.668392	-5.606882
H	2.577786	-2.788968	-6.104759
C	4.795944	3.421666	-2.372687
C	5.171289	2.259234	-3.322152
C	3.257112	3.581586	-2.311951
C	5.361275	4.720948	-2.982117
H	6.260637	2.176140	-3.418167
H	4.782495	1.307662	-2.958222
H	4.758265	2.441832	-4.321957
H	2.976010	4.397696	-1.635360
H	2.867058	3.824163	-3.307789
H	2.772853	2.664386	-1.974636
H	4.920229	4.871668	-3.973476
H	5.117935	5.602819	-2.377669
H	6.448848	4.680459	-3.113391
C	-5.279434	5.205571	-1.010439
C	-1.906638	-4.454687	2.765504
C	6.930768	3.781548	0.870363
C	1.297476	-4.727299	-2.701360
C	-5.671204	6.566605	-1.609119
C	-6.958129	7.090196	-0.927528
C	-4.527811	7.584541	-1.383388
C	-5.937195	6.477803	-3.123646
H	-7.792087	6.396537	-1.084704
H	-6.825857	7.210807	0.152917
H	-7.243896	8.066803	-1.339098
H	-3.605580	7.250238	-1.872622
H	-4.796661	8.565698	-1.795674
H	-4.309183	7.719935	-0.318740
H	-6.201798	7.467271	-3.514576
H	-5.053258	6.130336	-3.670912
H	-6.767822	5.799640	-3.350975
C	-1.684703	-5.877951	3.306250
C	-2.822111	-6.238564	4.292697
C	-1.679489	-6.932016	2.183383
C	-0.329935	-5.966860	4.047991
H	-2.856185	-5.548891	5.142803
H	-3.796265	-6.196913	3.793149
H	-2.683457	-7.252270	4.690274
H	-0.884872	-6.743560	1.451157
H	-1.509307	-7.928619	2.606967
H	-2.635099	-6.959687	1.648017
H	-0.181072	-6.971891	4.462804
H	0.503847	-5.757171	3.366607
H	-0.272068	-5.254660	4.878586
C	7.982269	4.784630	1.372451
C	7.354856	6.196672	1.456396
C	8.513224	4.412733	2.769733
C	9.181032	4.814269	0.394485
H	6.987242	6.540240	0.483665
H	6.511284	6.209842	2.155858
H	8.097758	6.924318	1.805142
H	8.997658	3.429298	2.773439
H	9.259198	5.148405	3.090183
H	7.714427	4.405615	3.520443
H	9.933572	5.536033	0.734636
H	9.658450	3.829802	0.329910
H	8.877805	5.104823	-0.616910
C	0.659991	-6.037204	-3.196433
C	-0.247835	-5.758507	-4.417214
C	1.778649	-7.023578	-3.610888
C	-0.195917	-6.711461	-2.107956
H	-1.060142	-5.070841	-4.155098
H	0.308003	-5.315940	-5.250460
H	-0.697205	-6.691433	-4.778508
H	2.432094	-7.253177	-2.761519

H	1.346190	-7.964676	-3.972129
H	2.403914	-6.615178	-4.412175
H	-0.641080	-7.631454	-2.502641
H	0.400021	-6.986542	-1.230116
H	-1.015912	-6.064167	-1.775151

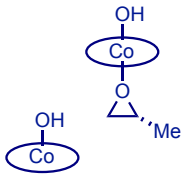

^{3}SM-1

Charge: 0
Spin Multiplicity: 3
Solvation: gas phase
Electronic Energy (AU): -6436.54008708
Gibbs Free Energy at 298.150 K (AU): -6434.921731

Co	3.690838	0.252642	-0.503949
N	3.882772	-0.357801	-2.290084
N	2.347838	1.410129	-1.191144
C	1.918916	2.467534	-0.588835
H	1.248747	3.136969	-1.130728
C	4.484520	-1.439303	-2.652160
H	4.474667	-1.711933	-3.709188
C	2.224784	2.858266	0.759042
C	2.958936	2.009026	1.649399
C	1.736991	4.118858	1.180464
C	3.156481	2.485503	2.999806
H	1.210762	4.720810	0.444306
C	2.647702	3.732272	3.338324
H	2.815048	4.086939	4.348329
C	5.210998	-2.331853	-1.791946
C	5.500380	-2.004226	-0.428001
C	5.707362	-3.518476	-2.383392
C	6.383090	-2.895587	0.289755
H	5.445664	-3.703890	-3.421303
C	6.816651	-4.046517	-0.354067
H	7.462833	-4.718450	0.197878
O	3.396891	0.832500	1.293340
O	5.013802	-0.944284	0.164351
O	4.921733	1.569356	-0.807659
O	2.218136	-1.192623	-0.309594
C	1.179254	-1.147303	0.717089
C	2.186319	-2.216407	0.728288
H	0.173674	-1.320728	0.334512
H	1.307893	-0.319175	1.407008
H	3.012574	-2.107189	1.425027
C	1.971763	1.065083	-2.570801
C	3.276893	0.585067	-3.238697
H	1.301760	0.195053	-2.503018
H	3.958700	1.446260	-3.269099
C	3.027544	0.082054	-4.664188
H	3.973958	-0.194897	-5.143690
H	2.402620	-0.822065	-4.633558
C	1.280803	2.151265	-3.401361
H	0.326489	2.437939	-2.944937
H	1.915459	3.048661	-3.427178
C	2.328815	1.168144	-5.499736
C	1.032903	1.650150	-4.834409
H	0.575311	2.450166	-5.428735
H	0.305406	0.826580	-4.809324
H	2.120274	0.782768	-6.505054
H	3.011346	2.020390	-5.625792
H	5.719275	1.255775	-0.351129
C	1.904551	-3.610318	0.239065
H	2.786399	-4.024322	-0.261484
H	1.656737	-4.260175	1.086819
H	1.064123	-3.616492	-0.461755
N	-2.369903	1.192629	0.998459
N	-4.088695	-0.328636	2.148301
C	-4.934111	-1.221250	2.570782
H	-5.160262	-1.253262	3.638771
C	-2.038545	2.299322	0.415829
H	-1.374817	2.980348	0.950317
C	-5.602419	-2.205597	1.783078
C	-5.395562	-2.336571	0.370053
C	-6.469350	-3.089133	2.479531
C	-6.087139	-3.406160	-0.310231
H	-6.581796	-2.935416	3.548560
C	-6.914384	-4.224473	0.442895
H	-7.432263	-5.024856	-0.071184
C	-2.491124	2.742088	-0.870232
C	-3.499639	2.030036	-1.588612
C	-1.970731	3.966982	-1.355808
C	-3.959117	2.591532	-2.832112
H	-1.225330	4.471007	-0.747633
C	-3.394613	3.789092	-3.250847
H	-3.740285	4.208434	-4.188205
O	-4.628482	-1.529457	-0.313217
O	-4.019682	0.912028	-1.141527
O	-1.994140	-1.248619	0.016598
C	-3.383507	0.584845	3.071533
C	-2.026155	0.878745	2.392334
H	-3.946940	1.531156	3.093453
H	-1.466503	-0.065290	2.357616
C	-1.214411	1.911083	3.176802
H	-0.245122	2.086044	2.696815
H	-1.746852	2.873068	3.194644
C	-3.181039	0.095347	4.511156
H	-4.144667	-0.048299	5.013666
H	-2.678931	-0.882057	4.489835
C	-1.005379	1.419255	4.619128
C	-2.339244	1.106063	5.310569
H	-2.162837	0.716128	6.319914
H	-2.912830	2.036261	5.431668
H	-0.451318	2.176327	5.185179
H	-0.377107	0.517783	4.607208

H	-2.319836	-2.061495	-0.404727
Co	-3.466968	-0.188554	0.300919
C	6.859539	-2.562563	1.719798
C	7.656407	-1.235412	1.694851
C	5.655434	-2.435315	2.682338
C	7.792265	-3.646161	2.299130
H	8.552760	-1.336813	1.071079
H	7.050221	-0.419073	1.299654
H	7.978953	-0.966240	2.708579
H	5.077555	-3.368529	2.703908
H	6.006802	-2.238269	3.703207
H	5.000499	-1.618002	2.381469
H	8.102154	-3.348675	3.307339
H	7.295515	-4.620350	2.382861
H	8.702689	-3.773983	1.702040
C	3.940718	1.644577	4.028113
C	3.229868	0.289627	4.260991
C	5.379362	1.406142	3.510830
C	4.053366	2.340659	5.399941
H	2.225497	0.446169	4.675861
H	3.139238	-0.270405	3.329779
H	3.796393	-0.318082	4.977731
H	5.904494	2.360540	3.384313
H	5.944884	0.802436	4.232029
H	5.370903	0.886613	2.552837
H	4.616747	1.695422	6.083718
H	4.587914	3.295684	5.337469
H	3.072876	2.524462	5.856128
C	-5.024850	1.867755	-3.678829
C	-4.473352	0.489718	-4.119197
C	-6.328679	1.691566	-2.862420
C	-5.389422	2.649035	-4.957435
H	-3.584982	0.616944	-4.750308
H	-4.202068	-0.122645	-3.258316
H	-5.227542	-0.049628	-4.705488
H	-6.741336	2.668530	-2.581320
H	-7.081713	1.171717	-3.467749
H	-6.155019	1.114157	-1.953991
H	-6.149616	2.089409	-5.513868
H	-5.808710	3.637266	-4.733620
H	-4.529123	2.781442	-5.624209
C	-5.928334	-3.617752	-1.830805
C	-6.468240	-2.377165	-2.580858
C	-4.441894	-3.852813	-2.195497
C	-6.715629	-4.844532	-2.335840
H	-7.538352	-2.242154	-2.381586
H	-5.943128	-1.471648	-2.276407
H	-6.340982	-2.505242	-3.663242
H	-4.045646	-4.728587	-1.666904
H	-4.346767	-4.039883	-3.272175
H	-3.828213	-2.986142	-1.946994
H	-6.559747	-4.949053	-3.415291
H	-6.380380	-5.775981	-1.864032
H	-7.794770	-4.742954	-2.172107
C	6.493410	-4.411073	-1.684792
C	1.937716	4.591030	2.462333
C	-7.141411	-4.104633	1.839673
C	-2.401293	4.515948	-2.546975
C	7.036941	-5.721431	-2.278418
C	8.584069	-5.692772	-2.280661
C	6.551743	-6.920092	-1.428602
C	6.560988	-5.941024	-3.726849
H	8.957749	-4.861638	-2.889569
H	8.990059	-5.573145	-1.270607
H	8.987030	-6.626518	-2.692938
H	5.457056	-6.977483	-1.423361
H	6.940346	-7.862740	-1.834411
H	6.886077	-6.844364	-0.388342
H	6.956715	-6.888860	-4.109544
H	5.467686	-5.987994	-3.792343
H	6.909616	-5.144960	-4.394958
C	1.460798	5.967558	2.955368
C	2.680977	6.811681	3.396388
C	0.712860	6.750571	1.859930
C	0.502831	5.796002	4.158542
H	3.238175	6.328613	4.205888
H	3.372581	6.961551	2.559850
H	2.358921	7.797402	3.755466
H	-0.184359	6.219244	1.519887
H	0.390752	7.722407	2.251090
H	1.349139	6.939055	0.987928
H	0.169533	6.773372	4.529730
H	-0.387074	5.222332	3.871716
H	0.984034	5.272057	4.991227
C	-8.091047	-5.084181	2.548629
C	-7.569512	-6.531078	2.378280
C	-8.203256	-4.790651	4.056450
C	-9.505610	-4.975490	1.930861
H	-7.499352	-6.818911	1.323888
H	-6.573450	-6.643172	2.821637
H	-8.243908	-7.241900	2.871571
H	-8.596503	-3.785357	4.247712
H	-8.888003	-5.506903	4.524275
H	-7.234997	-4.881986	4.562424
H	-10.193439	-5.674024	2.423135
H	-9.906894	-3.962392	2.047988
H	-9.503390	-5.211452	0.861357
C	-1.882799	5.849110	-3.112217
C	-1.266195	5.622393	-4.513251
C	-3.056388	6.851435	-3.229844
C	-0.803934	6.480618	-2.212400
H	-0.415197	4.933203	-4.460120
H	-1.992631	5.202546	-5.217016
H	-0.908809	6.571096	-4.932285
H	-3.502551	7.047353	-2.248148
H	-2.706034	7.806005	-3.641719
H	-3.848125	6.476566	-3.887025
H	-0.461593	7.425240	-2.649566
H	-1.186281	6.702176	-1.209333
H	0.072652	5.830054	-2.109184

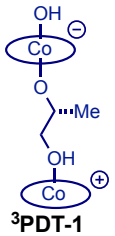

^{3}PDT-1

Product (catalyst-bound)
Charge: 0
Spin Multiplicity: 3
Solvation: gas phase
Electronic Energy (AU): -6436.54818827

Co	-3.309539	-0.169682	-0.083764
N	-4.176941	0.226958	-1.736677
N	-2.595162	-1.680489	-1.011794
C	-2.146430	-2.740431	-0.433892
H	-1.830374	-3.573615	-1.062588
C	-4.684811	1.377172	-2.014310
H	-5.075933	1.533846	-3.020720
C	-2.013443	-2.940900	0.980909
C	-2.172050	-1.872591	1.919365
C	-1.704152	-4.255101	1.404351
C	-1.973175	-2.184251	3.315096
H	-1.609885	-5.017689	0.637008
C	-1.685652	-3.500695	3.654071
H	-1.563957	-3.732885	4.704983
C	-4.809353	2.494423	-1.124951
C	-4.512002	2.403714	0.272676
C	-5.309283	3.691290	-1.692705
C	-4.797973	3.562471	1.086835
H	-5.511177	3.690624	-2.759618
C	-5.271771	4.702132	0.452206
H	-5.467282	5.573008	1.065365
O	-2.443283	-0.642649	1.551554
O	-4.030740	1.321435	0.831478
O	-4.731424	-1.194215	0.376153
O	-1.920850	0.821115	-0.740508
C	0.326931	0.498839	-0.138411
C	-0.909184	1.397905	0.047080
H	0.535421	0.384039	-1.208065
H	0.114096	-0.486723	0.279007
H	-1.183004	1.406370	1.108574
C	-2.711991	-1.515688	-2.463479
C	-4.108851	-0.896262	-2.677831
H	-1.971020	-0.753922	-2.740127
H	-4.850841	-1.630723	-2.334070
C	-4.358938	-0.574274	-4.155071
H	-5.379055	-0.198423	-4.297713
H	-3.670092	0.218982	-4.477623
C	-2.498931	-2.765222	-3.320873
H	-1.477402	-3.141788	-3.196065
H	-3.187212	-3.558613	-2.995766
C	-4.144941	-1.830100	-5.018278
C	-2.752764	-2.438141	-4.802130
H	-2.638448	-3.348397	-5.402133
H	-1.986387	-1.733369	-5.154050
H	-4.289395	-1.575726	-6.074913
H	-4.912011	-2.576710	-4.768305
H	-4.896856	-1.000656	1.314633
C	-0.667012	2.835940	-0.421812
H	-1.583070	3.423445	-0.310494
H	0.120252	3.313510	0.174118
H	-0.373176	2.854649	-1.478220
N	2.719733	-1.841452	0.990892
N	4.213072	0.124051	1.730246
C	4.875485	1.211503	1.985149
H	5.338455	1.323230	2.966906
C	2.216946	-2.912305	0.453184
H	1.862144	-3.709346	1.107360
C	5.078692	2.311403	1.088371
C	4.590947	2.302711	-0.258491
C	5.802712	3.418269	1.596872
C	4.869415	3.462595	-1.072351
H	6.144955	3.358471	2.626188
C	5.578306	4.509027	-0.499698
H	5.780242	5.377948	-1.114416
C	2.085049	-3.159177	-0.952509
C	2.462762	-2.182636	-1.932252
C	1.599813	-4.434494	-1.336947
C	2.326370	-2.554438	-3.323409
H	1.345772	-5.129519	-0.541420
C	1.844910	-3.821115	-3.620011
H	1.756105	-4.095304	-4.664721
O	3.913503	1.295455	-0.751016
O	2.910476	-1.001961	-1.606177
O	1.499730	0.974111	0.544688
C	4.129368	-0.968940	2.720999
C	2.779786	-1.658463	2.453058
H	4.918054	-1.695166	2.464284
H	1.994203	-0.929556	2.702348
C	2.587060	-2.897661	3.331991
H	1.591914	-3.327490	3.173335
H	3.324084	-3.665796	3.056028
C	4.281319	-0.595128	4.200645
H	5.270650	-0.165418	4.394174
H	3.539523	0.173422	4.458855
C	2.748969	-2.530582	4.816820
C	4.088541	-1.835895	5.090055
H	4.158821	-1.546250	6.145386
H	4.909780	-2.543446	4.905611
H	2.656782	-3.434088	5.431467
H	1.927047	-1.864628	5.115546
H	1.891196	1.693656	0.019829
Co	3.356016	-0.316616	0.102907
C	-4.619935	3.529790	2.619176
C	-5.579324	2.470474	3.214969
C	-3.155010	3.202880	2.991303
C	-4.965514	4.879794	3.282060
H	-6.623083	2.745880	3.021081

H	-5.399834	1.484001	2.785752
H	-5.444395	2.404098	4.301748
H	-2.476582	3.965990	2.590454
H	-3.039147	3.192144	4.082401
H	-2.853260	2.231814	2.601172
H	-4.824596	4.790447	4.365145
H	-4.315694	5.691409	2.933705
H	-6.007875	5.173893	3.112402
C	-2.102021	-1.101021	4.405997
C	-1.050203	0.010085	4.176582
C	-3.526032	-0.497686	4.377713
C	-1.872262	-1.661239	5.825140
H	-0.034511	-0.397360	4.259087
H	-1.157720	0.465298	3.191987
H	-1.157561	0.795635	4.934742
H	-4.278194	-1.274893	4.561743
H	-3.629866	0.261606	5.162602
H	-3.734309	-0.025405	3.418183
H	-1.970039	-0.845582	6.550113
H	-2.609182	-2.427060	6.094283
H	-0.869953	-2.089268	5.948104
C	2.745727	-1.580999	-4.443997
C	1.950283	-0.258017	-4.336373
C	4.263380	-1.297920	-4.329642
C	2.487715	-2.154614	-5.852184
H	0.872752	-0.445365	-4.435549
H	2.133059	0.233655	-3.380981
H	2.245462	0.425570	-5.142470
H	4.837503	-2.222424	-4.467578
H	4.577231	-0.587037	-5.104240
H	4.511622	-0.877284	-3.354386
H	2.797433	-1.417301	-6.601491
H	3.059596	-3.070675	-6.041212
H	1.425870	-2.370410	-6.023345
C	4.401724	3.532004	-2.541688
C	5.055199	2.383974	-3.346149
C	2.860067	3.418262	-2.620912
C	4.794850	4.858123	-3.224646
H	6.147227	2.487568	-3.347016
H	4.797152	1.414333	-2.920430
H	4.713671	2.409363	-4.389036
H	2.380413	4.229517	-2.059047
H	2.528781	3.491458	-3.664411
H	2.517621	2.462321	-2.222609
H	4.441913	4.844279	-4.262173
H	4.341928	5.728981	-2.735764
H	5.881035	5.004104	-3.251308
C	-5.532264	4.821088	-0.935315
C	-1.554811	-4.574428	2.738801
C	6.066756	4.533664	0.831075
C	1.474082	-4.800981	-2.661160
C	-6.048670	6.150370	-1.509451
C	-7.394823	6.520658	-0.842109
C	-5.016320	7.269488	-1.233035
C	-6.274775	6.073792	-3.031068
H	-8.150864	5.750466	-1.033150
H	-7.297000	6.629406	0.243281
H	-7.770631	7.472590	-1.237685
H	-4.055421	7.040625	-1.707909
H	-5.373450	8.227763	-1.630281
H	-4.834755	7.401759	-0.161103
H	-6.633916	7.040264	-3.402398
H	-5.349065	5.836876	-3.568181
H	-7.026594	5.320253	-3.293319
C	-1.303435	-6.001178	3.256602
C	-2.480196	-6.428410	4.167329
C	-1.193456	-7.022222	2.108729
C	0.010905	-6.052594	4.070376
H	-2.587908	-5.764213	5.031318
H	-3.426487	-6.412712	3.615044
H	-2.322652	-7.445719	4.546686
H	-0.361895	-6.788470	1.433544
H	-1.014287	-8.023309	2.516947
H	-2.113738	-7.068046	1.515424
H	0.174689	-7.060753	4.470487
H	0.871436	-5.796238	3.441330
H	-0.003663	-5.358697	4.917863
C	6.843580	5.759014	1.340825
C	5.953043	7.020511	1.242610
C	7.280939	5.598049	2.808802
C	8.114481	5.965238	0.482194
H	5.636828	7.217065	0.212695
H	5.049488	6.908750	1.852903
H	6.497316	7.904864	1.597490
H	7.944914	4.736248	2.943279
H	7.828113	6.490359	3.134000
H	6.421218	5.475403	3.477770
H	8.675341	6.842914	0.827867
H	8.774487	5.092416	0.545559
H	7.871191	6.121816	-0.574095
C	1.018225	-6.195103	-3.126543
C	-0.229689	-6.077955	-4.033260
C	2.159629	-6.868518	-3.927275
C	0.662298	-7.115346	-1.944245
H	-1.073937	-5.645817	-3.482874
H	-0.041491	-5.446153	-4.907861
H	-0.535856	-7.066472	-4.398233
H	3.055902	-6.982767	-3.307157
H	1.853385	-7.864366	-4.271911
H	2.438790	-6.282504	-4.809317
H	0.341076	-8.094447	-2.317465
H	1.521888	-7.279076	-1.284560
H	-0.157850	-6.706668	-1.341863

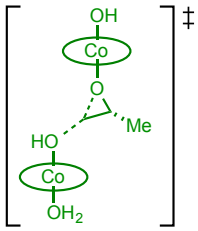

^{1}**TS-1**•H_2O

Transition State
Charge: 0
Spin Multiplicity: 1
Solvation: gas phase
Electronic Energy (AU): -6512.94792986
Gibbs Free Energy at 298.150 K (AU): -6511.296819

Co	-3.193038	-0.857561	-0.080213
N	-4.125801	-0.628293	-1.716589
N	-2.282617	-2.283160	-0.953062
C	-1.649803	-3.232611	-0.354946
H	-1.254482	-4.055729	-0.953625
C	-4.800598	0.416861	-2.050105
H	-5.232126	0.462538	-3.052161
C	-1.406881	-3.326833	1.060088
C	-1.726367	-2.256067	1.959442
C	-0.843868	-4.536790	1.526299
C	-1.462354	-2.483166	3.365249
H	-0.640820	-5.307687	0.787354
C	-0.919913	-3.702873	3.748900
H	-0.751681	-3.870151	4.806750
C	-5.075271	1.550309	-1.210489
C	-4.767358	1.551067	0.189250
C	-5.742915	2.639133	-1.817769
C	-5.228241	2.686288	0.959334
H	-5.942977	2.567503	-2.883375
C	-5.860298	3.724101	0.288108
H	-6.184574	4.578297	0.870940
O	-2.194001	-1.114401	1.549012
O	-4.128521	0.575070	0.774043
O	-4.458092	-2.089478	0.463212
O	-1.870714	0.403302	-0.833797
C	-0.043958	0.380037	-0.356450
C	-1.141575	1.304633	-0.032977
H	0.353945	0.394503	-1.359574
H	-0.005129	-0.546026	0.195157
H	-1.436661	1.282217	1.018789
C	-2.500773	-2.249644	-2.403626
C	-3.967464	-1.798898	-2.583406
H	-1.864527	-1.440019	-2.790475
H	-4.600634	-2.580947	-2.142088
C	-4.323427	-1.624503	-4.063539
H	-5.383826	-1.368039	-4.174008
H	-3.744016	-0.790548	-4.485351
C	-2.204317	-3.532821	-3.185895
H	-1.144022	-3.797078	-3.095639
H	-2.785842	-4.362679	-2.759839
C	-4.023689	-2.912571	-4.847689
C	-2.565685	-3.356080	-4.670086
H	-2.384260	-4.294371	-5.208649
H	-1.899724	-2.604410	-5.118394
H	-4.248054	-2.759756	-5.910498
H	-4.691465	-3.712888	-4.498590
H	-5.027545	-1.590391	1.070202
C	-1.099207	2.719472	-0.582080
H	-2.101043	3.158861	-0.540259
H	-0.423380	3.352734	0.008555
H	-0.767901	2.721191	-1.626947
N	2.826992	-1.247325	1.024505
N	3.925608	0.973229	1.787454
C	4.138603	2.211872	2.081998
H	4.364968	2.465915	3.118119
C	2.530565	-2.382466	0.480638
H	2.264405	-3.213276	1.134095
C	4.118330	3.316326	1.162535
C	4.038314	3.120552	-0.248523
C	4.233887	4.612083	1.717692
C	4.096382	4.281307	-1.091055
H	4.291434	4.691874	2.798993
C	4.198917	5.524058	-0.473175
H	4.229574	6.399698	-1.109428
C	2.526200	-2.673998	-0.925650
C	2.691431	-1.657710	-1.918043
C	2.362798	-4.034242	-1.286273
C	2.652875	-2.067016	-3.300271
H	2.242819	-4.751762	-0.480511
C	2.512225	-3.422247	-3.573842
H	2.508929	-3.727553	-4.613093
O	3.956333	1.908771	-0.777870
O	2.871945	-0.391245	-1.610392
O	1.634243	1.043936	0.438236
C	3.999047	-0.113366	2.778146
C	2.793341	-1.027786	2.482852
H	4.905732	-0.687017	2.533777
H	1.880586	-0.452050	2.686516
C	2.810763	-2.279621	3.365304
H	1.903249	-2.870542	3.204005
H	3.671535	-2.907011	3.090738
C	4.059116	0.287020	4.254861
H	4.948110	0.898228	4.452067
H	3.180020	0.895632	4.507903
C	2.903387	-1.895187	4.852273
C	4.094670	-0.971708	5.137705
H	4.103775	-0.677872	6.193763
H	5.033600	-1.514015	4.955711
H	2.975701	-2.806439	5.457156
H	1.973929	-1.394446	5.154051
H	1.644605	1.943256	0.069342
Co	3.321537	0.334521	0.099074
O	5.209397	-0.308067	-0.334846
H	5.464214	0.558673	-0.716623
H	5.080327	-0.885038	-1.109711

C	-5.058115	2.726679	2.492337
C	-5.845962	1.551441	3.120756
C	-3.564365	2.626249	2.879499
C	-5.603057	4.028904	3.113945
H	-6.918196	1.651668	2.912281
H	-5.504300	0.594330	2.724637
H	-5.712895	1.542583	4.210364
H	-2.998257	3.464165	2.452619
H	-3.453950	2.669168	3.971010
H	-3.132750	1.691936	2.522539
H	-5.457522	3.995409	4.199860
H	-5.079317	4.916816	2.739352
H	-6.676190	4.160400	2.932247
C	-1.831352	-1.413982	4.413960
C	-1.032290	-0.114421	4.156759
C	-3.348641	-1.119908	4.336734
C	-1.524394	-1.864151	5.856870
H	0.042662	-0.286727	4.302577
H	-1.191097	0.246854	3.140583
H	-1.341170	0.669897	4.859385
H	-3.926080	-2.027401	4.550092
H	-3.624120	-0.360409	5.079720
H	-3.625824	-0.757570	3.347398
H	-1.806193	-1.062969	6.549836
H	-2.092030	-2.757787	6.141475
H	-0.458296	-2.072291	6.013352
C	2.765440	-1.035085	-4.442367
C	1.582108	-0.041677	-4.360366
C	4.107098	-0.269309	-4.344404
C	2.716074	-1.692936	-5.836713
H	0.626865	-0.567812	-4.476947
H	1.572914	0.484538	-3.405196
H	1.655433	0.703257	-5.162349
H	4.954589	-0.964215	-4.409122
H	4.197669	0.442020	-5.174363
H	4.172994	0.289549	-3.410372
H	2.787912	-0.912848	-6.602661
H	3.547625	-2.388956	-5.999310
H	1.776810	-2.231652	-6.007301
C	4.053175	4.162454	-2.629038
C	5.283968	3.365651	-3.124442
C	2.748417	3.459141	-3.071764
C	4.090644	5.538288	-3.325928
H	6.214129	3.876961	-2.848063
H	5.301759	2.359786	-2.701754
H	5.261662	3.275172	-4.217318
H	1.871729	4.034682	-2.750040
H	2.714239	3.384159	-4.165633
H	2.678763	2.453534	-2.657008
H	4.051817	5.389620	-4.410699
H	3.233816	6.164545	-3.051574
H	5.009923	6.093844	-3.105893
C	-6.130582	3.753568	-1.102212
C	-0.593189	-4.764349	2.866835
C	4.265651	5.740637	0.923254
C	2.373657	-4.445200	-2.603182
C	-6.838563	4.969236	-1.723084
C	-8.224949	5.164094	-1.063876
C	-5.985747	6.240595	-1.497522
C	-7.052483	4.802877	-3.239462
H	-8.857059	4.282315	-1.219415
H	-8.143412	5.327862	0.015928
H	-8.738736	6.033355	-1.494233
H	-5.004784	6.141841	-1.976767
H	-6.485003	7.121994	-1.920467
H	-5.817217	6.432765	-0.432464
H	-7.554884	5.689197	-3.644426
H	-6.101948	4.687695	-3.773188
H	-7.680297	3.933801	-3.467852
C	-0.066218	-6.098086	3.425567
C	-1.142033	-6.730583	4.341777
C	0.259142	-7.108562	2.309443
C	1.222977	-5.869261	4.249233
H	-1.393281	-6.075203	5.182492
H	-2.064468	-6.920193	3.781938
H	-0.788608	-7.684357	4.754609
H	1.025919	-6.727025	1.623940
H	0.640622	-8.038256	2.747315
H	-0.628603	-7.362368	1.719485
H	1.583010	-6.814374	4.675218
H	2.022196	-5.457758	3.620485
H	1.058411	-5.174751	5.080211
C	4.371423	7.171918	1.476190
C	3.134677	7.990935	1.035598
C	4.436336	7.193466	3.015107
C	5.652908	7.846875	0.931614
H	3.048194	8.047005	-0.054778
H	2.211131	7.544445	1.421176
H	3.200976	9.017591	1.415945
H	5.312466	6.654131	3.393906
H	4.509468	8.228266	3.367601
H	3.539668	6.754030	3.467137
H	5.737197	8.871511	1.313840
H	6.548134	7.294463	1.239680
H	5.653986	7.900715	-0.162267
C	2.273686	-5.916387	-3.042151
C	1.057596	-6.113731	-3.977031
C	3.564100	-6.312788	-3.799524
C	2.111950	-6.867502	-1.841240
H	0.122254	-5.871753	-3.459811
H	1.119534	-5.482768	-4.870286
H	0.998448	-7.156383	-4.312454
H	4.445059	-6.200424	-3.157174
H	3.511604	-7.358892	-4.125320
H	3.719078	-5.694649	-4.690446
H	2.039073	-7.902369	-2.193850
H	2.967739	-6.812798	-1.158304
H	1.202908	-6.650507	-1.268198

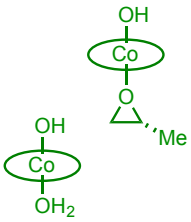

^{1}SM-1•H_2O

Starting Material (pre-complex)
Charge: 0
Spin Multiplicity: 1
Solvation: gas phase
Electronic Energy (AU): -6512.97337936
Gibbs Free Energy at 298.150 K (AU): -6511.326728

Co	3.402852	-0.447828	0.696474
N	3.424108	0.206012	2.477384
N	2.025960	-1.617867	1.289287
C	1.644657	-2.678402	0.660510
H	0.930851	-3.342390	1.150733
C	3.973685	1.305288	2.868044
H	3.868426	1.597441	3.914617
C	2.059151	-3.081422	-0.653811
C	2.878702	-2.249696	-1.483414
C	1.591738	-4.338779	-1.106805
C	3.195618	-2.745017	-2.804193
H	0.989402	-4.923668	-0.416625
C	2.701293	-3.987708	-3.176294
H	2.954620	-4.357189	-4.162964
C	4.757426	2.194194	2.055823
C	5.174434	1.841967	0.731662
C	5.178811	3.402109	2.662314
C	6.104692	2.733050	0.076532
H	4.821838	3.604782	3.668070
C	6.458239	3.905971	0.729441
H	7.139747	4.578183	0.222164
O	3.292462	-1.071820	-1.104412
O	4.758266	0.762441	0.121628
O	4.628152	-1.729152	1.139531
O	1.904978	0.954383	0.346218
C	1.062727	0.958396	-0.849037
C	1.985647	2.070930	-0.590948
H	-0.002464	1.052911	-0.631630
H	1.360669	0.204438	-1.570803
H	2.924973	2.068461	-1.136814
C	1.535748	-1.267673	2.631847
C	2.768283	-0.736692	3.391557
H	0.844139	-0.421807	2.501389
H	3.469595	-1.576458	3.494097
C	2.387936	-0.217160	4.781530
H	3.281329	0.105875	5.328872
H	1.733556	0.660665	4.680553
C	0.823325	-2.368623	3.424898
H	-0.083168	-2.697992	2.904707
H	1.488159	-3.239930	3.510990
C	1.666932	-1.314533	5.582601
C	0.448260	-1.861212	4.827430
H	-0.019884	-2.672899	5.397002
H	-0.308957	-1.069770	4.734308
H	1.363082	-0.918786	6.559255
H	2.370546	-2.135048	5.782504
H	5.450409	-1.419582	0.726183
C	1.529484	3.396477	-0.046622
H	2.275972	3.802666	0.644565
H	1.402190	4.110791	-0.868732
H	0.573028	3.297187	0.475287
N	-2.492818	-1.403584	-1.305797
N	-3.549544	0.634967	-2.496341
C	-3.828298	1.841277	-2.863420
H	-3.632297	2.126712	-3.898287
C	-2.220260	-2.483558	-0.653366
H	-1.569214	-3.222121	-1.123079
C	-4.404802	2.864726	-2.039071
C	-4.923326	2.582730	-0.739036
C	-4.502378	4.156710	-2.605015
C	-5.559284	3.658516	-0.029268
H	-4.093364	4.300303	-3.600889
C	-5.606644	4.905739	-0.642975
H	-6.076216	5.716989	-0.099928
C	-2.689930	-2.819320	0.663893
C	-3.413020	-1.891231	1.478173
C	-2.380647	-4.120059	1.132557
C	-3.788044	-2.322882	2.803240
H	-1.839239	-4.776542	0.457554
C	-3.457111	-3.616225	3.187081
H	-3.755469	-3.939228	4.177164
O	-4.876395	1.370384	-0.222112
O	-3.737365	-0.688342	1.062937
O	-2.141645	1.041671	-0.298750
C	-3.011305	-0.382787	-3.411984
C	-1.900008	-1.097544	-2.618399
H	-3.818572	-1.114297	-3.568422
H	-1.114073	-0.355135	-2.424979
C	-1.301759	-2.268659	-3.404678
H	-0.460877	-2.712275	-2.860559
H	-2.063030	-3.052934	-3.528786
C	-2.514352	0.093912	-4.780059
H	-3.335451	0.545874	-5.349395
H	-1.748262	0.870017	-4.643254
C	-0.814395	-1.794210	-4.784081
C	-1.923423	-1.085644	-5.571378
H	-1.538180	-0.725825	-6.532683
H	-2.723521	-1.803027	-5.803635
H	-0.432445	-2.651941	-5.349202
H	0.033771	-1.108734	-4.650359
H	-2.119394	1.030853	0.672444
Co	-3.602201	0.013527	-0.702919
O	-5.374863	-0.995455	-1.091224
H	-5.880289	-0.181640	-0.874886

H	-5.483780	-1.563809	-0.308471
C	6.714858	2.378100	-1.296710
C	7.523170	1.063521	-1.171014
C	5.605634	2.213847	-2.361730
C	7.684419	3.463424	-1.808836
H	8.351223	1.187369	-0.462642
H	6.891986	0.243378	-0.826178
H	7.949508	0.784959	-2.143109
H	5.032416	3.143920	-2.469482
H	6.050582	1.982431	-3.337886
H	4.925376	1.405539	-2.094067
H	8.092724	3.150344	-2.776484
H	7.185902	4.428502	-1.960282
H	8.531634	3.615941	-1.130185
C	4.083679	-1.926326	-3.763723
C	3.416624	-0.565865	-4.078514
C	5.471145	-1.698834	-3.117257
C	4.315184	-2.640194	-5.111248
H	2.456225	-0.715908	-4.589207
H	3.243832	0.005805	-3.166417
H	4.057934	0.027428	-4.742366
H	5.968425	-2.658309	-2.930599
H	6.110035	-1.112930	-3.790390
H	5.380935	-1.165766	-2.170983
H	4.950168	-2.010826	-5.745075
H	4.827098	-3.601728	-4.988803
H	3.379512	-2.814946	-5.656547
C	-4.534946	-1.376487	3.766497
C	-3.645952	-0.147854	4.074957
C	-5.875089	-0.920607	3.139865
C	-4.870441	-2.050348	5.112859
H	-2.728855	-0.459425	4.590313
H	-3.369736	0.380923	3.162076
H	-4.178270	0.551869	4.730957
H	-6.515503	-1.786770	2.928302
H	-6.416021	-0.271027	3.838899
H	-5.710172	-0.364703	2.216814
H	-5.394587	-1.330753	5.751661
H	-5.528361	-2.918700	4.988654
H	-3.972675	-2.372447	5.653224
C	-6.169189	3.443774	1.371537
C	-7.310802	2.401648	1.294911
C	-5.072508	2.962928	2.349899
C	-6.775141	4.736270	1.956263
H	-8.108736	2.750304	0.627828
H	-6.945671	1.442019	0.926501
H	-7.748035	2.243521	2.288804
H	-4.286083	3.721161	2.448889
H	-5.502212	2.792061	3.345176
H	-4.618222	2.034998	2.002960
H	-7.181297	4.522401	2.951386
H	-6.026690	5.528797	2.071894
H	-7.597837	5.124543	1.344215
C	6.009850	4.293684	2.016505
C	1.899364	-4.826317	-2.361564
C	-5.089394	5.205072	-1.925537
C	-2.761469	-4.555458	2.385813
C	6.469911	5.629587	2.623732
C	8.012656	5.650085	2.742197
C	6.013988	6.797259	1.716369
C	5.880930	5.859624	4.028131
H	8.365363	4.839486	3.390072
H	8.498657	5.532183	1.767808
H	8.353088	6.601567	3.170050
H	4.921397	6.820792	1.630480
H	6.343887	7.758699	2.130081
H	6.425743	6.711837	0.705024
H	6.223017	6.823514	4.422124
H	4.785032	5.879345	4.010708
H	6.197797	5.083345	4.734260
C	1.448492	-6.201203	-2.883377
C	2.690972	-7.071053	-3.191915
C	0.583305	-6.956207	-1.856723
C	0.616249	-6.030673	-4.176688
H	3.335959	-6.605200	-3.944367
H	3.292119	-7.224759	-2.288828
H	2.388818	-8.054423	-3.574119
H	-0.332953	-6.405161	-1.612063
H	0.283396	-7.928311	-2.264572
H	1.128585	-7.142728	-0.924652
H	0.307188	-7.007803	-4.569040
H	-0.288772	-5.441489	-3.984938
H	1.184858	-5.523144	-4.963268
C	-5.202612	6.632339	-2.486877
C	-4.445146	7.614201	-1.561508
C	-4.602298	6.747505	-3.900660
C	-6.691173	7.048315	-2.563089
H	-4.846502	7.604716	-0.542520
H	-3.382022	7.354366	-1.503100
H	-4.525627	8.640395	-1.941344
H	-5.116748	6.094797	-4.615671
H	-4.701112	7.776862	-4.263304
H	-3.535703	6.495008	-3.911671
H	-6.785196	8.069454	-2.953068
H	-7.250973	6.377959	-3.225474
H	-7.173589	7.024251	-1.580101
C	-2.486273	-5.970485	2.922659
C	-1.648016	-5.890158	4.220471
C	-3.829544	-6.676149	3.229187
C	-1.714451	-6.834829	1.908282
H	-0.679718	-5.412354	4.031678
H	-2.157949	-5.317256	5.002347
H	-1.458722	-6.895263	4.617116
H	-4.440711	-6.763905	2.323602
H	-3.652383	-7.686093	3.619170
H	-4.415981	-6.130249	3.976006
H	-1.541552	-7.832876	2.326146
H	-2.271535	-6.961349	0.972881
H	-0.734853	-6.405305	1.667765

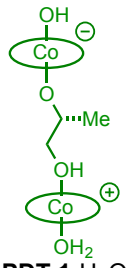

^{1}PDT-1•H_2O

Product (catalyst-bound)
Charge: 0
Spin Multiplicity: 1
Solvation: gas phase
Electronic Energy (AU): -6512.96456735
Gibbs Free Energy at 298.150 K (AU): -6511.309704

Co	-1.262900	-2.985177	-0.124698
N	-1.937422	-3.678393	-1.756171
N	0.461767	-3.164454	-0.913917
C	1.573102	-3.230105	-0.268473
H	2.491531	-3.442570	-0.821011
C	-3.156549	-3.575619	-2.155191
H	-3.412849	-3.932748	-3.155132
C	1.733704	-3.066179	1.154057
C	0.650719	-2.643569	1.997320
C	3.001753	-3.386921	1.687358
C	0.921003	-2.587672	3.421233
H	3.765105	-3.719805	0.988197
C	2.188679	-2.933019	3.872898
H	2.365220	-2.918927	4.942810
C	-4.252693	-3.042651	-1.392594
C	-4.128553	-2.730470	0.001167
C	-5.484794	-2.904628	-2.070399
C	-5.335037	-2.315781	0.685433
H	-5.502040	-3.161888	-3.126111
C	-6.503736	-2.186249	-0.052443
H	-7.396234	-1.858467	0.468486
O	-0.505311	-2.292634	1.525868
O	-3.006911	-2.843600	0.654031
O	-1.059203	-4.721529	0.515722
O	-1.459089	-1.254867	-0.975847
C	-0.013101	0.435864	-0.375759
C	-1.464296	-0.077451	-0.271122
H	0.278447	0.510027	-1.424440
H	0.653418	-0.229488	0.166549
H	-1.703022	-0.210939	0.796342
C	0.357237	-3.367324	-2.361353
C	-0.871600	-4.287275	-2.552870
H	0.092878	-2.387203	-2.783046
H	-0.638328	-5.241104	-2.060153
C	-1.163876	-4.532827	-4.037168
H	-1.995607	-5.238649	-4.149796
H	-1.473757	-3.590686	-4.511721
C	1.592956	-3.915720	-3.081102
H	2.431780	-3.215061	-2.984106
H	1.901675	-4.860192	-2.610733
C	0.080453	-5.083701	-4.752348
C	1.290127	-4.157686	-4.568826
H	2.173382	-4.580826	-5.063535
H	1.087212	-3.194493	-5.059157
H	-0.135178	-5.221113	-5.819227
H	0.320365	-6.078402	-4.350390
H	-1.855451	-4.868714	1.050124
C	-2.472043	0.911466	-0.879286
H	-3.467724	0.459742	-0.845288
H	-2.527722	1.868967	-0.333875
H	-2.229298	1.110952	-1.931019
N	2.761263	1.403065	1.056864
N	1.455031	3.466606	1.919629
C	0.499448	4.279522	2.227530
H	0.329602	4.500779	3.281622
C	3.516412	0.522169	0.480770
H	3.988827	-0.232665	1.108615
C	-0.369066	4.950694	1.300698
C	-0.116079	4.945659	-0.103571
C	-1.449191	5.681345	1.849550
C	-0.972953	5.730907	-0.944000
H	-1.586268	5.643539	2.925639
C	-2.022099	6.413100	-0.333969
H	-2.678320	6.993648	-0.969820
C	3.807369	0.432205	-0.919586
C	3.181918	1.273859	-1.889040
C	4.769523	-0.536860	-1.300157
C	3.553246	1.096436	-3.267840
H	5.201390	-1.146214	-0.512632
C	4.517458	0.138679	-3.559924
H	4.804211	0.018157	-4.597038
O	0.904511	4.271475	-0.623291
O	2.291219	2.191629	-1.560189
O	0.174561	1.776260	0.247924
C	2.363595	2.870270	2.914046
C	2.507281	1.391199	2.514034
H	3.341717	3.346182	2.748700
H	1.533741	0.903173	2.662008
C	3.553443	0.683364	3.381424
H	3.580237	-0.385698	3.150125
H	4.547233	1.102058	3.164409
C	1.992067	3.026914	4.390378
H	1.931972	4.088078	4.661039
H	1.003740	2.583514	4.573359
C	3.223856	0.857251	4.873878
C	3.048408	2.329702	5.265638
H	2.759478	2.410576	6.319797
H	4.007195	2.857890	5.162600
H	4.017663	0.397195	5.472901
H	2.303277	0.305291	5.101191
H	-0.519190	2.348931	-0.127355
Co	1.806166	2.789646	0.174967
O	3.389447	4.005498	-0.001232
H	2.858577	4.764839	-0.325377

H	3.826077	3.659657	-0.803196
C	-5.328580	-2.055682	2.205937
C	-4.965390	-3.368209	2.942352
C	-4.307345	-0.949943	2.561021
C	-6.702228	-1.597714	2.736743
H	-5.725075	-4.136752	2.753290
H	-3.998695	-3.747806	2.609825
H	-4.918549	-3.198932	4.026188
H	-4.576785	-0.006301	2.068895
H	-4.302215	-0.773580	3.645099
H	-3.303853	-1.234476	2.245952
H	-6.631218	-1.431587	3.818185
H	-7.029257	-0.655819	2.279708
H	-7.483350	-2.349174	2.571930
C	-0.207247	-2.237456	4.412997
C	-0.740731	-0.810147	4.143899
C	-1.357772	-3.260729	4.254148
C	0.251081	-2.289424	5.884787
H	0.036130	-0.060407	4.350966
H	-1.063811	-0.706027	3.107725
H	-1.593193	-0.590779	4.799239
H	-1.002770	-4.272118	4.485353
H	-2.175058	-3.020778	4.946497
H	-1.746353	-3.254094	3.236408
H	-0.595062	-2.032700	6.532778
H	0.593385	-3.289358	6.175389
H	1.057255	-1.576763	6.102388
C	2.893288	1.923428	-4.391929
C	1.381724	1.596925	-4.444693
C	3.105492	3.437967	-4.151363
C	3.481749	1.601324	-5.781326
H	1.224509	0.538861	-4.684781
H	0.894268	1.808147	-3.492210
H	0.890459	2.195135	-5.221912
H	4.176137	3.676752	-4.105191
H	2.673830	4.013390	-4.979194
H	2.626106	3.763877	-3.227752
H	2.976705	2.217573	-6.533216
H	4.553867	1.823987	-5.840970
H	3.329661	0.553764	-6.065053
C	-0.746408	5.825871	-2.467847
C	0.641314	6.449952	-2.751988
C	-0.836774	4.419812	-3.105163
C	-1.797362	6.715754	-3.163394
H	0.708373	7.459364	-2.328312
H	1.444025	5.841835	-2.331216
H	0.805657	6.527622	-3.833476
H	-1.823363	3.975010	-2.928169
H	-0.691922	4.489418	-4.190037
H	-0.074531	3.753107	-2.702362
H	-1.584834	6.743676	-4.237634
H	-2.814920	6.326623	-3.043055
H	-1.776257	7.749700	-2.799383
C	-6.627744	-2.459030	-1.436620
C	3.265692	-3.342100	3.045268
C	-2.305628	6.412875	1.052044
C	5.157522	-0.698669	-2.613316
C	-7.980764	-2.268552	-2.141855
C	-9.051723	-3.169218	-1.481293
C	-8.423341	-0.789860	-2.030039
C	-7.911216	-2.632370	-3.637081
H	-8.772817	-4.226346	-1.558979
H	-9.178883	-2.936994	-0.418602
H	-10.025795	-3.035791	-1.969872
H	-7.692885	-0.128284	-2.510132
H	-9.395457	-0.636595	-2.516830
H	-8.520626	-0.474277	-0.985660
H	-8.891649	-2.483137	-4.104903
H	-7.188771	-2.006182	-4.173342
H	-7.629912	-3.681302	-3.786471
C	4.594551	-3.801852	3.672632
C	4.338049	-5.050917	4.551065
C	5.640360	-4.178651	2.605977
C	5.202500	-2.687433	4.556104
H	3.631395	-4.836967	5.360110
H	3.917913	-5.866176	3.951946
H	5.272135	-5.404885	5.006608
H	5.869309	-3.334027	1.944120
H	6.575959	-4.482561	3.089922
H	5.303730	-5.015677	1.984486
H	6.124866	-3.036372	5.037641
H	5.452189	-1.803229	3.956747
H	4.514893	-2.373809	5.348979
C	-3.508704	7.204352	1.592359
C	-4.810806	6.661937	0.956203
C	-3.635977	7.086106	3.122715
C	-3.349165	8.701675	1.235782
H	-4.799619	6.747947	-0.135572
H	-4.959628	5.605578	1.206391
H	-5.677587	7.224134	1.324100
H	-2.754158	7.485336	3.637710
H	-4.504433	7.658338	3.466691
H	-3.779685	6.047095	3.440596
H	-4.205930	9.275200	1.609442
H	-2.439769	9.117810	1.684408
H	-3.291596	8.861509	0.153839
C	6.231468	-1.701111	-3.070244
C	5.635459	-2.680719	-4.108417
C	7.408616	-0.930609	-3.715986
C	6.785063	-2.527541	-1.894454
H	4.814837	-3.262001	-3.673200
H	5.246100	-2.159129	-4.989201
H	6.403293	-3.383792	-4.453121
H	7.864104	-0.237876	-2.998974
H	8.183910	-1.629083	-4.053654
H	7.086341	-0.347547	-4.585578
H	7.541726	-3.231239	-2.258554
H	7.263260	-1.893502	-1.138839
H	5.999921	-3.113819	-1.402984

2.11.5. Intrinsic Stereoselectivity of (salen)Co–OH as a Lewis Acid

In this section, we compare the barrier to opening an epoxide activated by (salen)Co–OH with a molecule of ammonia. All calculations restricted singlets at the B3LYP/6-31G(d) level. Cartesian coordinates in Å.

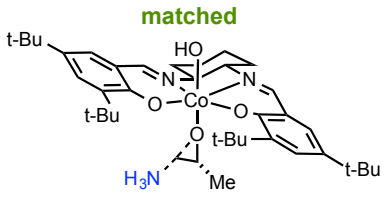

TS-2

Transition State
Charge: 0
Spin Multiplicity: 1
Solvation: gas phase
Electronic Energy (AU): -3371.35294617
Gibbs Free Energy at 298.150 K (AU): -3370.473863

Co	0.002213	0.738336	-0.183333
N	-1.255672	2.130419	-0.457080
N	1.269000	2.124696	0.122089
C	2.547256	1.981441	0.037948
H	3.177270	2.871437	0.096818
C	-2.535890	1.988069	-0.459025
H	-3.160987	2.878131	-0.555981
C	3.256383	0.740100	-0.116494
C	2.594394	-0.529988	-0.067518
C	4.657156	0.831870	-0.283278
C	3.425097	-1.706150	-0.192674
C	5.456829	-0.286156	-0.414803
H	5.090778	1.827747	-0.312308
C	4.793165	-1.535558	-0.359620
H	5.405560	-2.424057	-0.461783
C	-3.249385	0.742240	-0.380091
C	-2.583409	-0.522728	-0.481804
C	-4.658776	0.825142	-0.291839
C	-3.420827	-1.698559	-0.575922
C	-5.461679	-0.297200	-0.303139
H	-5.094440	1.817559	-0.213998
C	-4.794951	-1.536689	-0.463332
H	-5.413417	-2.424765	-0.513200
O	1.311040	-0.644359	0.141445
O	-1.283299	-0.637649	-0.515718
O	0.466052	0.813001	-1.968124
O	-0.517957	0.824747	1.737315
C	0.693405	0.038049	3.033122
C	-0.605404	-0.371237	2.464242
H	0.675925	0.831234	3.771940
H	1.540566	-0.009619	2.366189
H	-0.544041	-1.261795	1.832791
C	0.613920	3.426211	0.298009
C	-0.583842	3.415210	-0.676315
H	0.199392	3.426024	1.317156
H	-0.170140	3.358943	-1.692584
C	-1.434718	4.682016	-0.537798
H	-2.239717	4.685615	-1.282151
H	-1.910414	4.699450	0.453483
C	1.478943	4.677614	0.113011
H	2.290412	4.697749	0.850888
H	1.946313	4.654799	-0.881377
C	-0.564888	5.937672	-0.717363
C	0.622920	5.947519	0.253326
H	1.246064	6.833759	0.082566
H	0.249294	6.021819	1.284844
H	-1.178206	6.835879	-0.575975
H	-0.190168	5.973716	-1.750017
H	-0.003900	0.062660	-2.365588
C	-1.807371	-0.432321	3.393618
H	-2.723142	-0.461151	2.795143
H	-1.787572	-1.331537	4.025111
H	-1.847299	0.453966	4.037458
C	2.804475	-3.117911	-0.158620
C	2.114565	-3.358427	1.207846
C	1.769548	-3.261848	-1.299376
C	3.852026	-4.234963	-0.339058
H	2.859113	-3.319336	2.017574
H	1.343905	-2.604027	1.377015
H	1.645137	-4.349759	1.234538
H	2.259756	-3.142687	-2.272758
H	1.309382	-4.258124	-1.272446
H	0.985217	-2.510312	-1.213283
H	3.349291	-5.208543	-0.306968
H	4.365243	-4.163591	-1.304633
H	4.609803	-4.229349	0.453928
C	-2.809154	-3.091875	-0.835532
C	-2.072473	-3.077994	-2.197243
C	-1.820324	-3.476197	0.289777
C	-3.876645	-4.203610	-0.901735
H	-2.775793	-2.871794	-3.013060
H	-1.291775	-2.316101	-2.212807
H	-1.608144	-4.053684	-2.389737
H	-2.326872	-3.480638	1.263784
H	-1.421258	-4.483768	0.114520
H	-0.987113	-2.775243	0.327519
H	-3.383223	-5.162610	-1.097443

H	-4.429240	-4.304959	0.040271
H	-4.600255	-4.038463	-1.708474
C	-6.994371	-0.258792	-0.185113
C	-7.634729	-0.856910	-1.460637
C	-7.443037	-1.085121	1.043951
C	-7.525659	1.176691	-0.012943
H	-7.346716	-0.280993	-2.347552
H	-7.324693	-1.894651	-1.623625
H	-8.729672	-0.844576	-1.385916
H	-7.021075	-0.670968	1.967111
H	-8.536638	-1.078812	1.136099
H	-7.122174	-2.129878	0.971068
H	-8.617939	1.161911	0.079359
H	-7.122963	1.652487	0.888844
H	-7.276012	1.808195	-0.873437
C	6.979924	-0.232012	-0.620210
C	7.345542	-0.890225	-1.972053
C	7.511746	1.213593	-0.634705
C	7.693069	-0.991340	0.524050
H	7.023355	-1.936196	-2.014440
H	6.866401	-0.361436	-2.803659
H	8.431154	-0.868990	-2.132528
H	7.306807	1.732320	0.309313
H	8.598188	1.209351	-0.780295
H	7.071404	1.800001	-1.449165
H	8.781098	-0.970609	0.382114
H	7.468248	-0.534564	1.495188
H	7.385141	-2.041440	0.570282
N	1.436438	-1.367020	4.250714
H	0.740715	-1.680929	4.925278
H	2.275430	-1.081124	4.754382
H	1.676864	-2.149090	3.641255

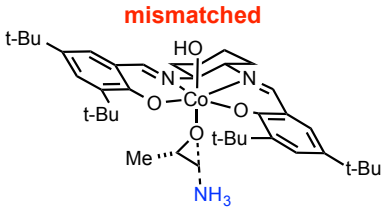

TS-3
+0.35 kcal/mol

Transition State
Charge: 0
Spin Multiplicity: 1
Solvation: gas phase
Electronic Energy (AU): -3371.35239302
Gibbs Free Energy at 298.150 K (AU): -3370.474068

Co	0.028679	0.739530	-0.181170
N	-1.220974	2.135075	-0.475688
N	1.303783	2.117306	0.104843
C	2.581593	1.957536	0.035579
H	3.220785	2.841153	0.088873
C	-2.501392	2.002535	-0.469188
H	-3.120605	2.896295	-0.571097
C	3.276227	0.707453	-0.099130
C	2.599836	-0.553859	-0.038316
C	4.678889	0.782076	-0.259002
C	3.418220	-1.739651	-0.147209
C	5.466774	-0.345640	-0.374266
H	5.123674	1.772725	-0.295377
C	4.788677	-1.586527	-0.309347
H	5.391368	-2.482990	-0.398061
C	-3.225589	0.761436	-0.381761
C	-2.572034	-0.509778	-0.482277
C	-4.632812	0.857436	-0.290211
C	-3.421987	-1.674924	-0.594130
C	-5.447885	-0.257098	-0.302949
H	-5.058725	1.853863	-0.209695
C	-4.794882	-1.501074	-0.476552
H	-5.423263	-2.381586	-0.536836
O	1.312696	-0.652409	0.158811
O	-1.272524	-0.638054	-0.500553
O	0.487838	0.778637	-1.966973
O	-0.490400	0.902910	1.745344
C	0.254325	0.264008	2.748867
C	-0.784029	-0.778582	2.643336
H	1.242249	-0.068534	2.413239
H	-0.787754	-1.360158	1.734542
C	0.661499	3.428763	0.256005
C	-0.538460	3.410932	-0.715234
H	0.248554	3.453872	1.275085
H	-0.127513	3.332987	-1.731225
C	-1.377690	4.687414	-0.598102
H	-2.185784	4.683874	-1.339223
H	-1.848921	4.728879	0.394603
C	1.538573	4.667066	0.042604
H	2.351841	4.694634	0.778066
H	2.003219	4.618752	-0.952151
C	-0.496472	5.930976	-0.805609
C	0.695566	5.948045	0.159839
H	1.326763	6.824352	-0.031258
H	0.326947	6.046902	1.191052
H	-1.100500	6.837682	-0.679175
H	-0.126103	5.943182	-1.840399
H	0.025160	0.014728	-2.346415
C	2.782652	-3.144096	-0.104023
C	2.064710	-3.352232	1.253460
C	1.770114	-3.292641	-1.263937
C	3.819975	-4.276033	-0.245010
H	2.787144	-3.301034	2.079396
H	1.309211	-2.576181	1.387936
H	1.581249	-4.337887	1.282259
H	2.282957	-3.201995	-2.228664
H	1.290286	-4.279620	-1.228237
H	0.999187	-2.523962	-1.210415
H	3.305339	-5.243281	-0.204797
H	4.351508	-4.228900	-1.202189

H	4.562891	-4.263858	0.561560
C	-2.828493	-3.070206	-0.888829
C	-2.093965	-3.031838	-2.251318
C	-1.837284	-3.500161	0.217888
C	-3.910033	-4.166587	-0.979425
H	-2.797122	-2.798294	-3.059526
H	-1.305877	-2.277363	-2.249641
H	-1.639761	-4.006963	-2.469194
H	-2.333574	-3.497107	1.198964
H	-1.475681	-4.519112	0.028968
H	-0.978300	-2.830520	0.245457
H	-3.430486	-5.125984	-1.205307
H	-4.460212	-4.286985	-0.038069
H	-4.634906	-3.968659	-1.777055
C	-6.979682	-0.203223	-0.178553
C	-7.632145	-0.783290	-1.456241
C	-7.432003	-1.035239	1.045325
C	-7.494636	1.236324	0.008573
H	-7.341864	-0.202681	-2.339298
H	-7.333904	-1.822832	-1.629849
H	-8.726551	-0.760109	-1.376682
H	-7.001676	-0.633192	1.970065
H	-8.525007	-1.018243	1.142579
H	-7.122648	-2.082770	0.961884
H	-8.586437	1.232481	0.107167
H	-7.081493	1.700616	0.911628
H	-7.243409	1.872063	-0.848273
C	6.991487	-0.310685	-0.570875
C	7.357661	-0.986848	-1.913676
C	7.539390	1.128774	-0.597011
C	7.689015	-1.065892	0.585617
H	7.023206	-2.029323	-1.947446
H	6.890207	-0.460926	-2.753784
H	8.444459	-0.980297	-2.067341
H	7.334637	1.659314	0.340383
H	8.626586	1.110932	-0.735953
H	7.110438	1.711539	-1.420191
H	8.778180	-1.057194	0.450819
H	7.461499	-0.598026	1.550618
H	7.370348	-2.112375	0.639754
H	-1.747367	-0.554693	3.086629
C	0.336323	1.056834	4.044115
H	0.809763	0.473900	4.846114
H	0.938870	1.957891	3.886887
H	-0.661696	1.368550	4.372291
N	-0.407854	-2.371667	3.795084
H	-0.297278	-2.140312	4.780866
H	0.464278	-2.770951	3.449086
H	-1.138495	-3.076273	3.700779

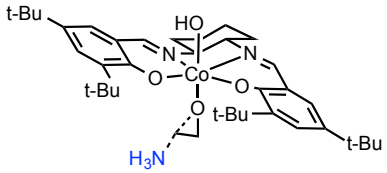

TS-4

Transition State
Charge: 0
Spin Multiplicity: 1
Solvation: gas phase
Electronic Energy (AU): -3332.03038649
Gibbs Free Energy at 298.150 K (AU): -3331.177610

Co	-0.045402	0.727634	-0.112191
N	-1.308264	2.114974	-0.383854
N	1.221966	2.119276	0.168459
C	2.499611	1.978044	0.073120
H	3.128400	2.869693	0.119056
C	-2.588313	1.969670	-0.370078
H	-3.216189	2.857735	-0.467315
C	3.209549	0.736670	-0.078786
C	2.550557	-0.534333	-0.014118
C	4.608378	0.829882	-0.260447
C	3.381832	-1.709613	-0.142875
C	5.408741	-0.287531	-0.393254
H	5.039930	1.826303	-0.300132
C	4.747836	-1.537672	-0.325030
H	5.360666	-2.425611	-0.429425
C	-3.298095	0.723476	-0.273988
C	-2.630636	-0.540805	-0.369456
C	-4.706443	0.804403	-0.170701
C	-3.466107	-1.718753	-0.446096
C	-5.506849	-0.319578	-0.163334
H	-5.143372	1.796558	-0.096595
C	-4.839160	-1.558873	-0.320290
H	-5.456190	-2.448619	-0.355730
O	1.269957	-0.649682	0.212019
O	-1.330239	-0.653479	-0.416057
O	0.398953	0.786006	-1.901809
O	-0.546090	0.828265	1.814408
C	0.695287	0.062307	3.093932
C	-0.602151	-0.363459	2.544301
H	0.686817	0.856751	3.830093
H	1.529631	0.018810	2.411020
H	-0.582128	-1.272304	1.939143
C	0.565843	3.420839	0.340807
C	-0.641807	3.399222	-0.620955
H	0.161683	3.427675	1.364097
H	-0.238350	3.335747	-1.640942
C	-1.494003	4.665380	-0.484026
H	-2.306606	4.660985	-1.220082
H	-1.959670	4.689812	0.511855
C	1.426167	4.672593	0.137530

H	2.244884	4.700436	0.867147
H	1.883805	4.643173	-0.861209
C	-0.628762	5.921431	-0.682366
C	0.568479	5.941542	0.276441
H	1.187804	6.827884	0.092782
H	0.204741	6.022900	1.310950
H	-1.242617	6.819438	-0.542051
H	-0.264385	5.950037	-1.718957
H	-0.080101	0.035059	-2.287135
C	2.763846	-3.122126	-0.096269
C	2.090737	-3.358562	1.279190
C	1.715743	-3.271509	-1.224230
C	3.810830	-4.238273	-0.285170
H	2.845503	-3.318738	2.079437
H	1.323094	-2.602754	1.455837
H	1.620332	-4.349119	1.314489
H	2.194577	-3.156061	-2.203693
H	1.256616	-4.267931	-1.187795
H	0.931947	-2.520111	-1.132393
H	3.310045	-5.212481	-0.243593
H	4.312330	-4.169447	-1.257050
H	4.577994	-4.228599	0.498703
C	-2.854439	-3.113140	-0.699618
C	-2.132553	-3.110407	-2.069286
C	-1.852744	-3.485375	0.418302
C	-3.920181	-4.227682	-0.744169
H	-2.844892	-2.912258	-2.879248
H	-1.353111	-2.347654	-2.100083
H	-1.668864	-4.087115	-2.258295
H	-2.347801	-3.478098	1.398127
H	-1.456063	-4.495057	0.249787
H	-1.019100	-2.784210	0.437851
H	-3.426821	-5.187486	-0.936206
H	-4.462541	-4.321446	0.204556
H	-4.652897	-4.071795	-1.544542
C	-7.037989	-0.283704	-0.026585
C	-7.693157	-0.895214	-1.288141
C	-7.468641	-1.099585	1.215826
C	-7.570731	1.152016	0.139006
H	-7.418582	-0.326458	-2.183915
H	-7.382130	-1.933474	-1.445873
H	-8.787086	-0.885458	-1.199176
H	-7.034460	-0.676512	2.129178
H	-8.560934	-1.094179	1.322731
H	-7.146893	-2.144409	1.147885
H	-8.661798	1.135484	0.244634
H	-7.158297	1.636823	1.031521
H	-7.333076	1.776336	-0.730095
C	6.929695	-0.232068	-0.613556
C	7.283315	-0.895832	-1.965879
C	7.459212	1.214232	-0.639303
C	7.654671	-0.985382	0.527261
H	6.961715	-1.942273	-2.000612
H	6.795960	-0.371152	-2.795306
H	8.367339	-0.874325	-2.136545
H	7.262208	1.736805	0.304299
H	8.544271	1.211029	-0.794883
H	7.010554	1.796477	-1.452214
H	8.741290	-0.963474	0.375180
H	7.438102	-0.524805	1.498488
H	7.348943	-2.035784	0.580836
H	-1.432292	-0.396471	3.263850
N	1.481493	-1.338875	4.306068
H	0.815931	-1.658427	5.007805
H	2.335258	-1.042810	4.777816
H	1.708314	-2.121066	3.691645

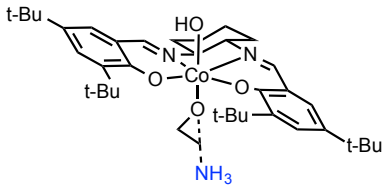

TS-5
–0.06 kcal/mol

Transition State
Charge: 0
Spin Multiplicity: 1
Solvation: gas phase
Electronic Energy (AU): -3332.03048564
Gibbs Free Energy at 298.150 K (AU): -3331.178574

Co	0.033941	0.766357	-0.072805
N	-1.217387	2.166036	-0.338771
N	1.306611	2.139116	0.244934
C	2.584641	1.983088	0.174193
H	3.222381	2.866159	0.249126
C	-2.497653	2.031468	-0.339480
H	-3.117838	2.926392	-0.423384
C	3.281066	0.737091	0.011766
C	2.606196	-0.525862	0.046756
C	4.683412	0.816748	-0.147191
C	3.425642	-1.708125	-0.088046
C	5.472574	-0.307499	-0.286383
H	5.126962	1.808456	-0.162933
C	4.795998	-1.550228	-0.247215
H	5.399603	-2.444086	-0.354744
C	-3.220408	0.787916	-0.281576
C	-2.564616	-0.480210	-0.403454
C	-4.628241	0.880381	-0.195596
C	-3.412376	-1.644423	-0.539043
C	-5.441758	-0.234649	-0.233943
H	-5.056014	1.874537	-0.098593
C	-4.786122	-1.474570	-0.425683
H	-5.412958	-2.354771	-0.504647
O	1.319148	-0.629413	0.243690
O	-1.264804	-0.606178	-0.420506
O	0.495234	0.842346	-1.856461
O	-0.485827	0.890241	1.856077

C	0.273458	0.235443	2.833701
C	-0.760170	-0.806972	2.728406
H	0.306127	0.773588	3.791665
H	1.276687	-0.065562	2.518852
H	-0.767876	-1.370457	1.808290
C	0.661558	3.445288	0.427611
C	-0.536516	3.448389	-0.546137
H	0.247303	3.444084	1.446499
H	-0.123468	3.395568	-1.562965
C	-1.378532	4.720046	-0.400544
H	-2.184794	4.732925	-1.143538
H	-1.852195	4.736864	0.591718
C	1.536487	4.690159	0.245860
H	2.348134	4.701336	0.983495
H	2.003136	4.666739	-0.748883
C	-0.499303	5.969720	-0.576483
C	0.690589	5.966379	0.391751
H	1.320427	6.848185	0.222727
H	0.319825	6.040081	1.424293
H	-1.105372	6.872055	-0.430123
H	-0.126518	6.007040	-1.609801
H	0.025929	0.091688	-2.253854
C	2.791359	-3.113720	-0.075491
C	2.074406	-3.352012	1.277439
C	1.777796	-3.236934	-1.237490
C	3.829171	-4.241499	-0.242650
H	2.797993	-3.322300	2.103542
H	1.321285	-2.576994	1.430075
H	1.587949	-4.336562	1.283766
H	2.289459	-3.122951	-2.200360
H	1.299709	-4.225328	-1.224395
H	1.005563	-2.471133	-1.165407
H	3.315138	-5.209716	-0.223408
H	4.359629	-4.172595	-1.199078
H	4.572807	-4.246706	0.563310
C	-2.815237	-3.033567	-0.854508
C	-2.076276	-2.971165	-2.213702
C	-1.826978	-3.479319	0.248609
C	-3.894368	-4.130253	-0.966879
H	-2.777697	-2.727428	-3.020423
H	-1.290995	-2.213975	-2.197350
H	-1.617853	-3.941081	-2.445600
H	-2.326690	-3.493334	1.227852
H	-1.462286	-4.494196	0.044257
H	-0.969886	-2.807968	0.289933
H	-3.412239	-5.084959	-1.206714
H	-4.447789	-4.266706	-0.029651
H	-4.616444	-3.920344	-1.763938
C	-6.974388	-0.184657	-0.118435
C	-7.617696	-0.743556	-1.410111
C	-7.433666	-1.037874	1.088125
C	-7.492432	1.250901	0.089845
H	-7.321630	-0.148198	-2.281343
H	-7.317682	-1.779938	-1.598938
H	-8.712634	-0.722183	-1.337764
H	-7.010598	-0.650579	2.022450
H	-8.527347	-1.024337	1.178003
H	-7.121794	-2.083299	0.989357
H	-8.584832	1.243970	0.181351
H	-7.085841	1.700454	1.003281
H	-7.236541	1.901421	-0.754449
C	6.997317	-0.266492	-0.481826
C	7.365631	-0.918476	-1.835943
C	7.542753	1.174114	-0.482969
C	7.695437	-1.040415	0.661852
H	7.033958	-1.961064	-1.888179
H	6.897347	-0.379158	-2.667056
H	8.452494	-0.906537	-1.988921
H	7.337577	1.687768	0.463670
H	8.629897	1.160393	-0.622693
H	7.112368	1.770447	-1.295613
H	8.784636	-1.028447	0.527540
H	7.467269	-0.589182	1.634594
H	7.377577	-2.087921	0.698114
H	-1.720103	-0.599934	3.184588
N	-0.361560	-2.426403	3.849205
H	-0.254970	-2.225118	4.841955
H	0.515054	-2.805854	3.492684
H	-1.083936	-3.136027	3.732707

Ammonia
Charge: 0
Spin Multiplicity: 1
Solvation: gas phase
Electronic Energy (AU): -56.5479476525
Gibbs Free Energy at 298.150 K (AU): -56.531456

N	0.000000	0.000000	0.119349
H	0.000000	0.938581	-0.278482
H	-0.812835	-0.469291	-0.278482
H	0.812835	-0.469291	-0.278482

2.11.6. Intrinsic Stereoselectivity of (salen)Co(OH)(OH_2) as a Nucleophile

In this section, we compare the barrier to opening an epoxide activated by BH_3 with a molecule of (salen)Co(OH)(OH_2). All calculations restricted singlets at the B3LYP/6-31G(d) level. Cartesian coordinates in Å.

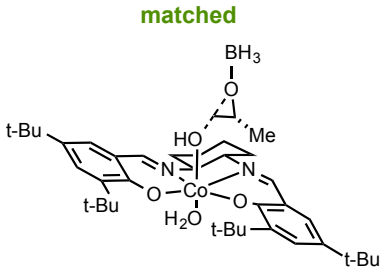

Transition State
Charge: 0
Spin Multiplicity: 1
Solvation: gas phase
Electronic Energy (AU): -3417.88148762
Gibbs Free Energy at 298.150 K (AU): -3416.989047

O	0.468319	3.209690	3.741780
C	0.404183	1.787007	2.575025
C	-0.635647	2.733122	2.979869
H	0.626424	0.961677	3.238756
H	1.171993	2.120004	1.899048
H	-0.946103	3.442266	2.207180
C	-1.795398	2.242643	3.818309
H	-2.297504	3.090118	4.296305
H	-2.517865	1.710378	3.189536
H	-1.443648	1.566083	4.604485
N	1.279095	1.724511	-0.682283
N	-1.256223	1.633886	-1.162898
C	-2.533886	1.531789	-1.004309
H	-3.153119	2.403256	-1.221673
C	2.560029	1.579327	-0.567317
H	3.182970	2.471463	-0.633596
C	-3.241910	0.350906	-0.598270
C	-2.603135	-0.923932	-0.538698
C	-4.627246	0.491021	-0.351570
C	-3.423165	-2.068537	-0.256884
H	-5.049611	1.489388	-0.414326
C	-4.776614	-1.852913	-0.015920
H	-5.390704	-2.716311	0.208665
C	3.268373	0.352203	-0.344294
C	2.602885	-0.898214	-0.151604
C	4.681892	0.444944	-0.296717
C	3.420088	-2.053674	0.115757
H	5.122995	1.425464	-0.447331
C	4.798725	-1.883407	0.138507
H	5.409914	-2.755950	0.334328
O	-1.312287	-1.067396	-0.788398
O	1.292970	-1.022392	-0.223877
O	-0.410715	0.573713	1.165901
C	-0.599310	2.842726	-1.689220
C	0.646851	3.053050	-0.813137
H	-0.252638	2.583180	-2.700856
H	0.304809	3.334827	0.191753
C	1.519922	4.196705	-1.337564
H	2.354558	4.377020	-0.652225
H	1.938736	3.928037	-2.318310
C	-1.440158	4.119895	-1.774798
H	-2.298603	3.972091	-2.441195
H	-1.836367	4.367162	-0.780181
C	0.683506	5.483702	-1.443282
C	-0.577597	5.283260	-2.295115
H	-1.175495	6.201947	-2.309915
H	-0.290551	5.080268	-3.336992
H	1.299950	6.286145	-1.864664
H	0.401460	5.802420	-0.431306
H	-0.341834	-0.319818	1.541834
Co	0.003106	0.314582	-0.629304
O	0.323710	-0.202391	-2.577324
H	-0.440265	-0.818298	-2.579362
H	1.099793	-0.786648	-2.491797
C	2.788769	-3.433477	0.398066
C	1.942325	-3.347179	1.691112
C	1.908883	-3.885209	-0.792844
C	3.849425	-4.531743	0.618911
H	2.579710	-3.109941	2.551223
H	1.172666	-2.578468	1.609724
H	1.449388	-4.306701	1.890168
H	2.508504	-3.955425	-1.709501
H	1.488865	-4.878866	-0.594012
H	1.083468	-3.193452	-0.961908
H	3.343051	-5.483142	0.815942
H	4.487077	-4.674778	-0.261514
H	4.492665	-4.320768	1.480753
C	-2.832063	-3.493826	-0.217877
C	-2.233928	-3.856920	-1.598438
C	-1.738981	-3.578299	0.872096
C	-3.893367	-4.563455	0.112352
H	-3.007035	-3.830032	-2.376023
H	-1.436069	-3.167049	-1.878208

H	-1.816041	-4.870893	-1.574457
H	-2.160699	-3.354629	1.859766
H	-1.318894	-4.591209	0.909187
H	-0.928020	-2.878882	0.670234
H	-3.414087	-5.548628	0.127592
H	-4.346969	-4.406120	1.097723
H	-4.694353	-4.600846	-0.635252
C	-5.421765	-0.594180	-0.040596
C	5.476911	-0.657121	-0.066644
B	1.159153	4.503945	3.174535
H	1.372848	4.326360	1.969021
H	2.193520	4.634454	3.792242
H	0.362697	5.414265	3.338575
C	7.013030	-0.609598	-0.015145
C	7.502208	-1.070314	1.378664
C	7.597110	-1.548443	-1.097613
C	7.555381	0.809775	-0.268649
H	7.115788	-0.413454	2.166040
H	7.179872	-2.091825	1.607713
H	8.597932	-1.050053	1.425072
H	7.279870	-1.236289	-2.099332
H	8.693481	-1.532376	-1.067448
H	7.277345	-2.586307	-0.954637
H	8.650364	0.801491	-0.227675
H	7.265705	1.186159	-1.256803
H	7.203472	1.521821	0.486589
C	-6.928021	-0.495325	0.253823
C	-7.216223	-1.039977	1.673209
C	-7.435865	0.957302	0.187603
C	-7.717535	-1.328536	-0.783793
H	-6.911334	-2.086542	1.779489
H	-6.680713	-0.458022	2.431905
H	-8.289073	-0.983188	1.894900
H	-7.295564	1.393461	-0.808364
H	-8.508320	0.985338	0.410420
H	-6.930147	1.599174	0.918193
H	-8.793671	-1.277681	-0.577144
H	-7.547894	-0.951476	-1.798912
H	-7.426506	-2.384264	-0.767311

mismatched

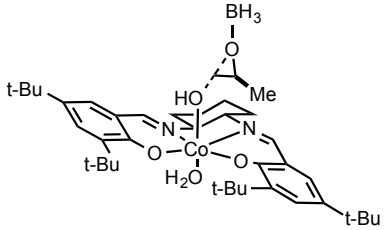

TS-7

Transition State
Charge: 0
Spin Multiplicity: 1
Solvation: gas phase

Electronic Energy (AU): -3417.88207624
Gibbs Free Energy at 298.150 K (AU): -3416.988487

O	-0.395033	3.461393	3.617114
C	0.551324	2.594895	3.002571
H	1.175025	3.113436	2.269302
C	-0.709611	2.056407	2.486983
H	-1.287847	1.398884	3.121129
H	-1.222375	2.597292	1.709830
C	1.363931	1.782590	3.987679
H	1.946701	1.013399	3.466499
H	2.058067	2.436360	4.525467
H	0.711747	1.298217	4.721904
N	1.239825	1.734924	-0.659981
N	-1.299600	1.629430	-1.120785
C	-2.577586	1.516218	-0.958525
H	-3.203058	2.385148	-1.167681
C	2.520864	1.595724	-0.553003
H	3.140867	2.489816	-0.628090
C	-3.271539	0.327700	-0.554402
C	-2.623090	-0.944129	-0.528457
C	-4.653516	0.455520	-0.281391
C	-3.430486	-2.097861	-0.247677
C	-5.434211	-0.639741	0.027736
H	-5.082950	1.452061	-0.319312
C	-4.780116	-1.894595	0.021740
H	-5.384589	-2.764910	0.245784
C	3.239344	0.371522	-0.340417
C	2.581249	-0.881429	-0.143165
C	4.652925	0.468592	-0.315896
C	3.406060	-2.037285	0.098940
C	5.455124	-0.632424	-0.104788
H	5.088922	1.450774	-0.472014
C	4.784382	-1.862689	0.101383
H	5.401494	-2.735143	0.278034
O	-1.339224	-1.072660	-0.812318
O	1.269944	-1.005654	-0.181856
O	-0.432309	0.527719	1.190631
C	-0.653890	2.837980	-1.662766
C	0.604294	3.061065	-0.805397
H	-0.319091	2.570716	-2.676510
H	0.266912	3.365185	0.193658
C	1.465384	4.194396	-1.374589
H	2.327261	4.386990	-0.725782
H	1.855161	3.904768	-2.361495
C	-1.499640	4.112527	-1.745161
H	-2.371832	3.954004	-2.390860
H	-1.867721	4.376113	-0.744760
C	0.627904	5.481579	-1.481070
C	-0.649617	5.267448	-2.304279
H	-1.247718	6.185746	-2.317442
H	-0.384904	5.049804	-3.349344
H	1.236624	6.276504	-1.927681
H	0.358998	5.812984	-0.470113
H	0.097228	-0.153086	1.638021
Co	-0.029573	0.315152	-0.608591

O	0.283055	-0.180749	-2.562236
H	-0.470262	-0.812110	-2.544453
H	1.075477	-0.746195	-2.520923
C	-2.828346	-3.518507	-0.239023
C	-2.253392	-3.858786	-1.635190
C	-1.715055	-3.605339	0.829932
C	-3.874641	-4.601086	0.096324
H	-3.041101	-3.828639	-2.397906
H	-1.467251	-3.158155	-1.921279
H	-1.826549	-4.869376	-1.632127
H	-2.124755	-3.412182	1.828851
H	-1.274327	-4.610299	0.836301
H	-0.924747	-2.881544	0.633154
H	-3.386958	-5.582306	0.090768
H	-4.311484	-4.459795	1.091609
H	-4.689000	-4.636204	-0.636957
C	2.783159	-3.423240	0.369330
C	1.952512	-3.362949	1.674039
C	1.889672	-3.856678	-0.818385
C	3.850789	-4.520879	0.557299
H	2.597651	-3.126823	2.528856
H	1.168976	-2.606775	1.611037
H	1.476667	-4.331905	1.868244
H	2.479261	-3.912771	-1.742555
H	1.471747	-4.853167	-0.630182
H	1.062108	-3.162812	-0.967078
H	3.350488	-5.477439	0.744254
H	4.477498	-4.646191	-0.333601
H	4.504316	-4.322364	1.414476
B	-0.519342	4.888527	2.964741
H	-0.654000	4.737309	1.744599
H	-1.500561	5.399896	3.457247
H	0.525156	5.468075	3.212969
C	6.991837	-0.581016	-0.080104
C	7.507495	-1.055869	1.299358
C	7.559249	-1.506062	-1.183153
C	7.526275	0.842429	-0.327395
H	7.135108	-0.408014	2.101027
H	7.190668	-2.080076	1.523686
H	8.603832	-1.034541	1.325750
H	7.224739	-1.182609	-2.175571
H	8.655955	-1.488638	-1.171159
H	7.243147	-2.545887	-1.047096
H	8.621775	0.837124	-0.304307
H	7.219667	1.228688	-1.306529
H	7.184692	1.545405	0.441180
C	-6.934746	-0.556129	0.354048
C	-7.187784	-1.114222	1.774909
C	-7.455822	0.892694	0.309913
C	-7.739146	-1.387928	-0.673202
H	-6.869341	-2.158221	1.867026
H	-6.643062	-0.531784	2.526547
H	-8.256387	-1.070702	2.018916
H	-7.338515	1.338359	-0.684888
H	-8.523995	0.909782	0.553481
H	-6.941670	1.532889	1.035910
H	-8.811122	-1.346291	-0.444072
H	-7.593209	-1.002301	-1.688809
H	-7.440664	-2.441740	-0.670503

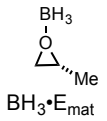

Charge: 0
Spin Multiplicity: 1
Solvation: gas phase
Electronic Energy (AU): -219.752104035
Gibbs Free Energy at 298.150 K (AU): -219.662518

O	0.537598	-0.046275	-0.481083
C	0.066585	1.228288	0.043503
C	-0.586545	-0.022002	0.461076
H	-0.392789	1.851579	-0.719369
H	0.778794	1.708006	0.707881
H	-0.289868	-0.419154	1.429084
C	-1.897592	-0.491510	-0.101989
H	-1.911274	-1.583294	-0.179863
H	-2.714557	-0.186647	0.562139
H	-2.076553	-0.067369	-1.094356
B	2.013964	-0.619301	0.057645
H	2.057785	-0.252161	1.214703
H	2.787572	-0.063768	-0.680730
H	1.895589	-1.809150	-0.094584

2.11.7. Diastereomeric Epoxide-Opening Transition States

In this section, we compare the barrier to opening an epoxide with two molecules of "matched" catalyst with the barrier to opening an epoxide with a mismatched nucleophilic catalyst, a mismatched Lewis acidic catalyst or with both catalysts mismatched (but matched with one another. All calculations restricted singlets at the B3LYP/6-31G(d) level. Cartesian coordinates in Å.

Table 2.11. Summary of results.

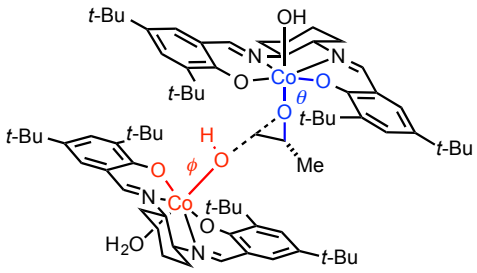

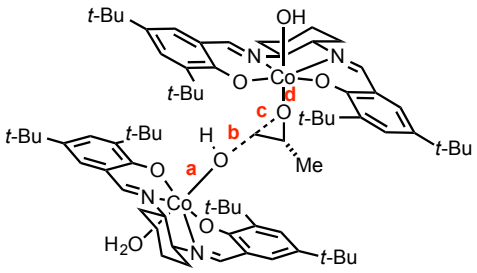

	TS-1•H_2O	**TS-8**•H_2O	**TS-9**•H_2O	**TS-10**•H_2O
Lewis Acid **Epoxide** **Nucleophile**	(*S*,*S*) (R) (S,S)	(*S*,*S*) **(*S*)** (*S*,*S*)	**(*R*,*R*)** (*R*) (*S*,*S*)	(*S*,*S*) (*R*) **(*R*,*R*)**
ΔE_{rel} (kcal/mol)	0 (defined)	+ 2.3	+ 3.1	+ 1.1
a (Å)	1.86	1.86	1.86	1.86
b (Å)	1.97	1.95	1.98	1.96
c (Å)	1.88	1.89	1.89	1.88
d (Å)	1.98	1.98	1.99	1.98
θ	54.4°	51.8°	8.3°	44.8°
ϕ	89.3°	0.6°	86.8°	97.3°

TS-2•H_2O (mismatched epoxide)

Transition State
Charge: 0
Spin Multiplicity: 1
Solvation: gas phase
Electronic Energy (AU): -6512.94426526
Gibbs Free Energy at 298.150 K (AU): -6511.294306

Co	3.227980	1.611041	-0.443513
N	4.855011	0.635474	-0.525540
N	3.464151	1.903904	-2.306932
C	2.875155	2.833140	-2.981800
H	3.178966	2.995387	-4.017977
C	5.290609	-0.173378	0.376014
H	6.208811	-0.731401	0.180018
C	1.827565	3.692868	-2.510132
C	1.222255	3.524671	-1.221931
C	1.387812	4.698044	-3.403022
C	0.145966	4.428146	-0.881568
C	0.367384	5.569534	-3.082419
H	1.890794	4.765411	-4.363724
C	-0.224273	5.393201	-1.807311
H	-1.027348	6.069768	-1.538505
C	4.707379	-0.388137	1.673954
C	3.644017	0.434361	2.171313
C	5.317310	-1.369782	2.486916
C	3.291244	0.271290	3.566479
C	4.937585	-1.582445	3.797649
H	6.118213	-1.953833	2.041991
C	3.926606	-0.724112	4.297902
H	3.649951	-0.841073	5.339807
O	1.573445	2.576929	-0.397876
O	3.029899	1.318706	1.441019
O	4.189481	3.158898	-0.145670
O	2.341385	-0.117175	-0.876118
C	1.083412	-0.167783	-1.512500
H	0.684483	0.820505	-1.758747
C	4.519353	1.049342	-2.865528
C	5.588508	0.940188	-1.757967
H	4.078613	0.048516	-2.984626
H	5.998293	1.948550	-1.607057
C	6.717192	-0.016637	-2.155149
H	7.495935	-0.030927	-1.383385
H	6.321969	-1.039762	-2.235108
C	5.139673	1.480003	-4.199524
H	4.379561	1.498156	-4.990052
H	5.533368	2.501740	-4.106124
C	7.335320	0.408184	-3.497806
C	6.273397	0.520883	-4.599532
H	6.731787	0.861829	-5.535844
H	5.852401	-0.474513	-4.802110
H	8.112973	-0.307628	-3.791142
H	7.834241	1.379684	-3.373831
H	4.018462	3.364600	0.786986
C	0.661502	-0.656708	-0.191439
H	0.929439	-1.672151	0.061032
H	0.579950	0.062210	0.609548
C	1.009472	-1.118875	-2.691890
H	-0.029025	-1.266219	-3.007411
H	1.577164	-0.710386	-3.535931
H	1.434345	-2.093685	-2.429168
N	-2.060356	-1.665759	2.283429
N	-1.358812	-3.604716	0.721106
C	-0.856048	-4.297283	-0.248940
H	-0.093261	-5.040148	-0.011207
C	-2.613588	-0.735320	2.992744
H	-2.233584	-0.565335	4.000092
C	-1.225618	-4.203803	-1.630523
C	-2.385205	-3.481895	-2.048433
C	-0.439381	-4.933916	-2.553054
C	-2.739811	-3.540617	-3.439896
C	-0.747997	-4.970053	-3.897237
H	0.424995	-5.465476	-2.166292
C	-1.910814	-4.264737	-4.290356
H	-2.172994	-4.296385	-5.340715
C	-3.695672	0.116532	2.596863
C	-4.256841	0.083690	1.283327
C	-4.178488	1.018051	3.578650
C	-5.333506	0.995114	0.994341
C	-5.212307	1.890982	3.318182
H	-3.700993	0.998134	4.553431
C	-5.757858	1.840248	2.011850
H	-6.568733	2.523021	1.791155
O	-3.143802	-2.832220	-1.186315
O	-3.828694	-0.745248	0.352153
O	-1.239251	-1.085064	-0.271818
C	-1.025300	-3.833320	2.136314
C	-0.900565	-2.436800	2.771657
H	-1.911482	-4.310695	2.580777
H	-0.004795	-1.958529	2.350645
C	-0.727043	-2.544996	4.291677
H	-0.585756	-1.555031	4.738011
H	-1.637541	-2.975532	4.732662
C	0.200231	-4.700210	2.442297
H	0.075693	-5.704889	2.021014
H	1.091511	-4.258470	1.975292
C	0.494169	-3.420354	4.622089
C	0.404890	-4.803106	3.964128
H	1.313193	-5.380034	4.172767
H	-0.431630	-5.365638	4.402731
H	0.584161	-3.525816	5.709561
H	1.404275	-2.908884	4.281457
H	-1.670792	-0.233963	-0.456888
Co	-2.555202	-2.143267	0.510268
O	-4.119196	-3.305928	1.120826
H	-4.257236	-3.637696	0.205895
H	-4.825299	-2.645647	1.245794
C	-0.565914	4.326188	0.482528
C	-1.241656	2.939912	0.618934
C	0.460840	4.534934	1.620444
C	-1.671282	5.387358	0.658152

H	-2.006774	2.808703	-0.157213
H	-0.502939	2.143517	0.521451
H	-1.735314	2.846323	1.594760
H	0.898231	5.538857	1.559829
H	-0.029552	4.438823	2.598144
H	1.265870	3.803036	1.558021
H	-2.134399	5.262885	1.644312
H	-1.275850	6.408644	0.608298
H	-2.465554	5.288762	-0.091627
C	2.284667	1.229780	4.237377
C	2.850451	2.670649	4.190450
C	0.917421	1.186495	3.517002
C	2.035436	0.884397	5.719749
H	3.792707	2.730891	4.748123
H	3.035396	2.984374	3.162221
H	2.141907	3.375035	4.644694
H	0.501267	0.170922	3.549443
H	0.204314	1.858483	4.011785
H	1.016205	1.489904	2.475419
H	1.312352	1.594064	6.138228
H	1.621270	-0.123956	5.848316
H	2.948629	0.956079	6.321579
C	-3.996780	-2.826425	-3.979603
C	-5.263074	-3.397023	-3.296278
C	-3.888127	-1.307471	-3.714585
C	-4.176686	-3.018994	-5.499415
H	-5.365522	-4.469908	-3.500566
H	-5.229980	-3.250587	-2.215685
H	-6.158744	-2.894236	-3.681384
H	-3.022085	-0.885441	-4.238648
H	-4.785673	-0.795056	-4.082903
H	-3.783792	-1.100494	-2.649952
H	-5.080271	-2.489637	-5.821667
H	-3.336643	-2.607336	-6.070728
H	-4.299188	-4.073265	-5.774520
C	-5.981726	1.054673	-0.404991
C	-4.926475	1.519647	-1.436706
C	-6.546890	-0.331001	-0.802007
C	-7.155638	2.054195	-0.467348
H	-4.572427	2.528882	-1.195768
H	-4.066605	0.848973	-1.457567
H	-5.363496	1.546529	-2.442468
H	-7.302688	-0.661530	-0.077547
H	-7.032676	-0.270864	-1.783516
H	-5.757163	-1.080406	-0.859310
H	-7.579055	2.043640	-1.477733
H	-7.961439	1.792190	0.228815
H	-6.839253	3.082584	-0.259258
C	5.587781	-2.631585	4.715721
C	6.263623	-1.928849	5.917952
C	4.513962	-3.611729	5.244386
C	6.661987	-3.457258	3.982513
H	7.040567	-1.235557	5.576496
H	5.543603	-1.353950	6.510112
H	6.731502	-2.664785	6.584468
H	4.028079	-4.140205	4.415068
H	4.965498	-4.361768	5.906551
H	3.735801	-3.092300	5.814126
H	7.094232	-4.198150	4.665291
H	6.243781	-3.998624	3.125770
H	7.481226	-2.826600	3.619019
C	-0.136086	6.681366	-4.017787
C	0.046438	8.059689	-3.338229
C	0.629409	6.704851	-5.354502
C	-1.636056	6.464179	-4.330388
H	-0.502521	8.122136	-2.392649
H	1.103794	8.250098	-3.121823
H	-0.319630	8.863607	-3.989932
H	0.516707	5.762633	-5.903537
H	0.241304	7.507787	-5.992204
H	1.699885	6.887926	-5.206083
H	-2.013717	7.259151	-4.986276
H	-1.794331	5.503196	-4.833513
H	-2.245192	6.467219	-3.420256
C	-5.771386	2.887875	4.346824
C	-5.598314	4.331214	3.816415
C	-7.274496	2.605839	4.581708
C	-5.047147	2.786105	5.702639
H	-4.540249	4.561951	3.648686
H	-6.126259	4.484963	2.869234
H	-5.995228	5.055113	4.538686
H	-7.427329	1.592884	4.971805
H	-7.688482	3.316068	5.307900
H	-7.856815	2.699399	3.658785
H	-5.474984	3.508964	6.406202
H	-5.153625	1.789943	6.148229
H	-3.977899	3.009123	5.611465
C	0.087100	-5.722848	-4.946383
C	0.614419	-4.721328	-6.001593
C	1.297242	-6.437699	-4.316412
C	-0.789026	-6.788971	-5.646256
H	-0.201909	-4.204094	-6.516999
H	1.248931	-3.959617	-5.534534
H	1.209600	-5.242654	-6.761391
H	0.988390	-7.186296	-3.577221
H	1.866893	-6.958840	-5.093872
H	1.977774	-5.731951	-3.826273
H	-0.205231	-7.328468	-6.402226
H	-1.168128	-7.520776	-4.923634
H	-1.651541	-6.342338	-6.152316

TS-3•H_2O (mismatched Lewis acidic catalyst)

Transition State
Charge: 0
Spin Multiplicity: 1
Solvation: gas phase
Electronic Energy (AU): -6512.94304256
Gibbs Free Energy at 298.150 K (AU): -6511.293757

Co	-3.337471	-0.952000	-0.129950
N	-3.019416	-2.702220	-0.803652
N	-4.047352	-0.561871	-1.848425
C	-4.793038	0.450970	-2.130380
H	-5.215085	0.521676	-3.134912
C	-2.338523	-3.625081	-0.219186
H	-2.211703	-4.582225	-0.729863
C	-5.123687	1.534993	-1.250661
C	-4.540792	1.666725	0.051926
C	-6.025152	2.500727	-1.755860
C	-4.926234	2.827010	0.826080
C	-6.398738	3.608957	-1.024535
H	-6.421489	2.335644	-2.754109
C	-5.820422	3.727058	0.263442
H	-6.105872	4.590446	0.852973
C	-1.761492	-3.557183	1.097491
C	-1.992839	-2.444138	1.972092
C	-1.067175	-4.706708	1.540422
C	-1.539929	-2.586694	3.342929
C	-0.589080	-4.831307	2.830754
H	-0.944655	-5.516171	0.825736
C	-0.857604	-3.742196	3.699176
H	-0.531193	-3.838987	4.728652
O	-3.674105	0.815349	0.525453
O	-2.590930	-1.355640	1.592341
O	-5.016992	-1.503916	0.396690
O	-1.574519	-0.460913	-0.921817
C	-0.953951	0.783595	-0.713672
H	-1.423421	1.370682	0.079318
C	-3.697117	-1.597057	-2.827705
C	-3.753345	-2.929862	-2.055333
H	-2.644480	-1.421109	-3.092305
H	-4.799302	-3.084587	-1.753712
C	-3.297686	-4.104463	-2.928385
H	-3.405493	-5.051985	-2.387575
H	-2.230972	-3.988705	-3.169926
C	-4.532143	-1.659944	-4.111477
H	-4.438809	-0.725375	-4.677502
H	-5.593730	-1.776065	-3.851712
C	-4.123353	-4.165805	-4.224189
C	-4.078145	-2.837107	-4.990459
H	-4.707579	-2.893919	-5.886982
H	-3.051888	-2.653170	-5.339927
H	-3.758059	-4.983408	-4.857841
H	-5.166931	-4.405166	-3.975287
H	-5.064603	-1.267555	1.336286
C	0.144015	-0.077808	-0.241385
H	0.687056	-0.642599	-0.983228
H	0.056464	-0.487177	0.753474
C	-0.759605	1.608847	-1.974546
H	-0.155069	2.505458	-1.779365
H	-1.735143	1.941369	-2.344972
H	-0.272743	1.017378	-2.758023
C	-4.374932	3.053102	2.249743
C	-2.834436	3.190932	2.213334
C	-4.773245	1.863519	3.153772
C	-4.929743	4.335328	2.903652
H	-2.535600	4.034838	1.578802
H	-2.371736	2.282552	1.827153
H	-2.445908	3.375107	3.223652
H	-5.864715	1.779169	3.221482
H	-4.382096	2.008998	4.169277
H	-4.375459	0.928908	2.759254
H	-4.508557	4.434902	3.910925
H	-6.020916	4.309781	3.006726
H	-4.658146	5.238613	2.344003
C	-1.886236	-1.513302	4.395785
C	-3.426403	-1.425248	4.531379
C	-1.312449	-0.136344	3.987180
C	-1.329796	-1.849874	5.794361
H	-3.833442	-2.378051	4.890603
H	-3.890638	-1.190991	3.573472
H	-3.702860	-0.644453	5.251059
H	-0.215612	-0.177709	3.930512
H	-1.577214	0.622808	4.734131
H	-1.699539	0.177862	3.018141
H	-1.604745	-1.050377	6.491962
H	-0.235750	-1.929566	5.800395
H	-1.740569	-2.785289	6.191894
N	3.037277	-1.089847	1.137333
N	3.815367	1.269539	1.873536
C	3.830236	2.537450	2.116349
H	3.895633	2.865199	3.154526
C	2.819342	-2.256937	0.621499
H	2.537896	-3.069204	1.292104
C	3.798965	3.584857	1.134877
C	3.944874	3.313995	-0.258224
C	3.696842	4.909729	1.618722
C	4.028370	4.434280	-1.152060
C	3.732563	5.996533	0.768602
H	3.585941	5.045318	2.690200
C	3.909082	5.708471	-0.605034
H	3.955732	6.551801	-1.282579
C	2.910986	-2.609448	-0.766201
C	3.176266	-1.644143	-1.787706
C	2.721623	-3.978253	-1.083016
C	3.258027	-2.115226	-3.146556
C	2.801943	-4.442454	-2.378525
H	2.508428	-4.655177	-0.261458
C	3.074442	-3.472817	-3.374172
H	3.139114	-3.823421	-4.396657
O	4.053128	2.076530	-0.719721
O	3.347251	-0.365434	-1.525408

O	1.706318	1.033810	0.237834
C	3.927581	0.243631	2.921712
C	2.862890	-0.814738	2.577685
H	4.910268	-0.230391	2.779541
H	1.878848	-0.336880	2.687503
C	2.942436	-2.018566	3.522676
H	2.118576	-2.712555	3.326669
H	3.882203	-2.560657	3.343503
C	3.821902	0.710620	4.375454
H	4.617535	1.429631	4.604969
H	2.862579	1.223183	4.531878
C	2.872068	-1.560811	4.990053
C	3.928172	-0.498706	5.319817
H	3.819408	-0.164791	6.358146
H	4.932686	-0.937163	5.234850
H	2.989904	-2.430758	5.646586
H	1.873635	-1.151234	5.191411
H	1.636621	1.714056	-0.453112
Co	3.484524	0.485982	0.174802
O	5.466797	0.029321	-0.000210
H	5.692021	0.918070	-0.347589
H	5.449983	-0.535022	-0.796096
C	4.247498	4.241600	-2.667885
C	5.596705	3.524459	-2.915576
C	3.088352	3.413674	-3.268963
C	4.298549	5.581911	-3.430247
H	6.430237	4.117787	-2.520289
H	5.614907	2.540978	-2.443315
H	5.760416	3.388878	-3.991664
H	2.130555	3.928924	-3.126408
H	3.238419	3.281076	-4.347620
H	3.028171	2.427263	-2.809283
H	4.455871	5.380426	-4.495667
H	3.362703	6.145247	-3.339443
H	5.122005	6.222640	-3.093549
C	3.516654	-1.144986	-4.318527
C	2.330759	-0.157525	-4.432360
C	4.837820	-0.367402	-4.102340
C	3.640788	-1.876675	-5.671221
H	1.404307	-0.696269	-4.664309
H	2.185343	0.394518	-3.502861
H	2.511794	0.565277	-5.237622
H	5.684484	-1.060187	-4.009926
H	5.035248	0.284206	-4.962202
H	4.787240	0.256199	-3.209372
H	3.831539	-1.140217	-6.459653
H	4.472245	-2.591566	-5.680950
H	2.723097	-2.411261	-5.941721
C	0.113425	-6.091813	3.366204
C	-0.730968	-6.712043	4.506304
C	0.294616	-7.164055	2.275458
C	1.513246	-5.734610	3.918537
H	-0.865014	-6.013370	5.338870
H	-1.726622	-6.990739	4.143833
H	-0.245760	-7.613638	4.902066
H	0.897577	-6.794577	1.437530
H	0.808003	-8.038222	2.692370
H	-0.667755	-7.504933	1.877711
H	2.007861	-6.624010	4.329463
H	2.155276	-5.330138	3.125951
H	1.456803	-4.988473	4.718752
C	-7.383010	4.677191	-1.528750
C	-7.888380	4.372362	-2.951480
C	-8.610628	4.742372	-0.588890
C	-6.690085	6.060636	-1.554365
H	-7.066107	4.341928	-3.675963
H	-8.418904	3.414343	-2.996941
H	-8.586373	5.153487	-3.274891
H	-8.322642	4.984521	0.439640
H	-9.316464	5.511987	-0.927256
H	-9.136697	3.781121	-0.568643
H	-7.386856	6.835413	-1.899615
H	-6.332195	6.354725	-0.561933
H	-5.826967	6.052346	-2.230143
C	2.611676	-5.915426	-2.776697
C	1.413673	-6.040740	-3.748097
C	3.891081	-6.435962	-3.474484
C	2.334833	-6.812241	-1.556155
H	0.487903	-5.696003	-3.273142
H	1.561939	-5.449365	-4.658050
H	1.273126	-7.085837	-4.050350
H	4.756422	-6.370478	-2.804921
H	3.766731	-7.485517	-3.768059
H	4.125991	-5.865483	-4.379646
H	2.209854	-7.851936	-1.878671
H	3.161567	-6.787508	-0.836684
H	1.417258	-6.516830	-1.034476
C	3.603504	7.454876	1.240032
C	2.370105	8.106804	0.570748
C	3.429499	7.554572	2.767230
C	4.875179	8.244713	0.848640
H	2.450701	8.106621	-0.521589
H	1.451334	7.572655	0.837789
H	2.264929	9.149231	0.895333
H	4.288396	7.134119	3.303509
H	3.340772	8.606060	3.062194
H	2.524634	7.039090	3.109102
H	4.790563	9.289378	1.172057
H	5.765386	7.813631	1.321105
H	5.039452	8.246534	-0.234228

TS-4•H_2O (mismatched nucleophile-delivering catalyst)

Charge: 0
Spin Multiplicity: 1
Solvation: gas phase
Electronic Energy (AU): -6512.94623029
Gibbs Free Energy at 298.150 K (AU): -6511.294794

Co	2.464274	-2.568034	0.229045
N	4.215679	-2.499361	0.955213
N	1.888418	-2.937351	2.006345
C	0.757181	-3.473199	2.314408
H	0.586166	-3.771890	3.351355
C	5.243771	-1.983005	0.374858
H	6.186424	-1.936681	0.924380
C	-0.338237	-3.724607	1.418611
C	-0.321191	-3.294010	0.049943
C	-1.449525	-4.414640	1.958938
C	-1.492644	-3.596268	-0.746588
C	-2.568404	-4.710659	1.204999
H	-1.383359	-4.726804	2.997993
C	-2.543059	-4.274141	-0.144572
H	-3.408274	-4.506891	-0.754495
C	5.290350	-1.480816	-0.970471
C	4.214724	-1.689262	-1.894599
C	6.493667	-0.854609	-1.372616
C	4.449020	-1.307589	-3.270308
C	6.695613	-0.417629	-2.665514
H	7.265068	-0.728680	-0.617717
C	5.647788	-0.681550	-3.582421
H	5.805145	-0.377771	-4.610578
O	0.667073	-2.620652	-0.460706
O	3.075789	-2.223043	-1.546499
O	2.643181	-4.391552	-0.005236
O	2.354208	-0.630090	0.643871
C	0.686664	0.241144	0.717906
C	1.785344	0.296997	-0.257941
H	0.835795	0.756626	1.654348
H	0.056778	-0.632894	0.689842
H	1.542186	-0.146791	-1.226568
C	2.956642	-2.699202	2.984422
C	4.262297	-3.125693	2.278802
H	3.010190	-1.608988	3.123692
H	4.188161	-4.206045	2.093082
C	5.490453	-2.837775	3.148736
H	6.400264	-3.203467	2.658360
H	5.606053	-1.751639	3.276125
C	2.814027	-3.371036	4.354297
H	1.911778	-3.014663	4.867317
H	2.700172	-4.455517	4.218180
C	5.345117	-3.508730	4.524504
C	4.047961	-3.085808	5.226735
H	3.949073	-3.604639	6.188098
H	4.091550	-2.010742	5.454307
H	6.212454	-3.264231	5.149770
H	5.348467	-4.600381	4.396867
H	2.843475	-4.488559	-0.949833
C	2.568876	1.586061	-0.404362
H	3.516918	1.383059	-0.913197
H	2.001076	2.319001	-0.988876
H	2.786637	2.019992	0.577959
C	-1.551205	-3.203720	-2.237346
C	-1.454878	-1.666172	-2.388008
C	-0.387142	-3.885741	-2.995071
C	-2.864468	-3.645424	-2.915574
H	-2.319562	-1.179212	-1.920095
H	-0.540776	-1.289894	-1.927268
H	-1.448826	-1.387839	-3.449482
H	-0.470086	-4.976954	-2.922674
H	-0.418598	-3.614086	-4.057967
H	0.576783	-3.584290	-2.585908
H	-2.841277	-3.342959	-3.968947
H	-2.998169	-4.733404	-2.890483
H	-3.745512	-3.176423	-2.459957
C	3.412186	-1.621854	-4.369769
C	3.223452	-3.155714	-4.465149
C	2.057430	-0.945439	-4.056636
C	3.858077	-1.127325	-5.761153
H	4.163372	-3.641665	-4.754264
H	2.897494	-3.571848	-3.510812
H	2.469365	-3.400216	-5.224257
H	2.175384	0.143519	-3.986811
H	1.337370	-1.153208	-4.858709
H	1.646623	-1.316380	-3.118384
H	3.087974	-1.387159	-6.496540
H	3.986904	-0.038676	-5.791966
H	4.793999	-1.594892	-6.088646
N	-2.945098	0.471735	1.520275
N	-1.495441	2.254727	2.707500
C	-0.525813	3.045253	3.038758
H	-0.073352	2.924055	4.024361
C	-3.850632	-0.215002	0.901233
H	-4.154677	-1.170211	1.329113
C	0.016336	4.096427	2.230063
C	-0.640279	4.543696	1.042698
C	1.193884	4.723215	2.702933
C	-0.070221	5.666255	0.350563
C	1.768394	5.782416	2.031735
H	1.637943	4.336136	3.615176
C	1.096364	6.220986	0.865328
H	1.531181	7.057674	0.332930
C	-4.513960	0.152111	-0.316089
C	-4.136639	1.302741	-1.075907
C	-5.557584	-0.704073	-0.750131
C	-4.844014	1.552534	-2.305340
C	-6.259563	-0.462534	-1.911856
H	-5.787840	-1.563607	-0.127881
C	-5.863244	0.676300	-2.655961
H	-6.399499	0.872468	-3.576300
O	-1.763154	3.991096	0.624963
O	-3.176102	2.119432	-0.693374

O	-0.739111	1.494510	0.221313
C	-2.065393	1.246517	3.616073
C	-2.295480	-0.009691	2.753356
H	-3.057012	1.624013	3.907542
H	-1.310001	-0.394778	2.460951
C	-3.020248	-1.105767	3.542427
H	-3.102944	-2.016692	2.940035
H	-4.038580	-0.771732	3.787921
C	-1.276721	0.920221	4.887456
H	-1.166336	1.814727	5.511849
H	-0.265459	0.583765	4.618603
C	-2.247427	-1.429914	4.832377
C	-1.996868	-0.180131	5.686343
H	-1.405150	-0.436764	6.572896
H	-2.956300	0.210683	6.053827
H	-2.800663	-2.179181	5.410661
H	-1.285793	-1.890256	4.565860
H	-0.984775	1.249988	-0.686941
Co	-2.291381	2.177903	0.982739
O	-3.936128	3.171113	1.677135
H	-3.513582	4.039913	1.495529
H	-4.586478	3.060522	0.960146
C	-4.474324	2.743805	-3.213482
C	-3.023263	2.570336	-3.723014
C	-4.615261	4.076412	-2.438332
C	-5.387367	2.843104	-4.452518
H	-2.932664	1.656154	-4.321327
H	-2.314441	2.512866	-2.896151
H	-2.740825	3.418666	-4.358510
H	-5.645525	4.208666	-2.082541
H	-4.381801	4.921331	-3.097567
H	-3.936418	4.113815	-1.586101
H	-5.079878	3.705490	-5.054346
H	-6.439704	2.991099	-4.182003
H	-5.316364	1.957410	-5.094199
C	-0.721023	6.236483	-0.926507
C	-2.145806	6.750573	-0.607894
C	-0.779298	5.139222	-2.014237
C	0.069164	7.426092	-1.510666
H	-2.111575	7.550756	0.141710
H	-2.781193	5.948459	-0.229689
H	-2.611946	7.157604	-1.513659
H	0.231499	4.810068	-2.283647
H	-1.257871	5.531231	-2.920421
H	-1.344115	4.273084	-1.670335
H	-0.437216	7.780136	-2.415520
H	1.089331	7.145356	-1.796847
H	0.125361	8.271949	-0.815104
C	7.973420	0.293505	-3.141206
C	8.655123	-0.537046	-4.254738
C	7.614101	1.691856	-3.697885
C	8.990002	0.482434	-1.999379
H	8.938749	-1.528332	-3.882981
H	7.994835	-0.681944	-5.116286
H	9.562621	-0.033357	-4.611721
H	7.149890	2.312295	-2.922498
H	8.513713	2.209038	-4.055788
H	6.911829	1.627045	-4.535702
H	9.880371	0.999699	-2.375538
H	8.576197	1.085451	-1.182811
H	9.316507	-0.477904	-1.583685
C	-3.773727	-5.506027	1.735223
C	-3.926539	-6.815764	0.924364
C	-3.613544	-5.883354	3.220034
C	-5.069858	-4.673185	1.592795
H	-4.087467	-6.616712	-0.140345
H	-3.026420	-7.433817	1.014150
H	-4.781552	-7.400012	1.288284
H	-3.513908	-4.996697	3.857922
H	-4.494706	-6.438875	3.561393
H	-2.737097	-6.520270	3.383967
H	-5.940021	-5.246385	1.937166
H	-5.014869	-3.756063	2.193268
H	-5.255264	-4.383557	0.552751
C	-7.411206	-1.346829	-2.418020
C	-8.706486	-0.505216	-2.510763
C	-7.063192	-1.906600	-3.817916
C	-7.679139	-2.538254	-1.479442
H	-8.988915	-0.111088	-1.527570
H	-8.592073	0.345390	-3.191243
H	-9.536547	-1.118258	-2.882748
H	-6.154171	-2.517175	-3.779733
H	-7.880859	-2.534326	-4.193022
H	-6.897552	-1.107938	-4.548780
H	-8.505943	-3.141000	-1.871520
H	-6.804794	-3.194057	-1.395584
H	-7.959511	-2.209551	-0.471890
C	3.059862	6.483937	2.484666
C	4.133968	6.353676	1.378404
C	2.775598	7.981708	2.749438
C	3.628353	5.869923	3.777693
H	4.363928	5.300942	1.178983
H	3.807302	6.807217	0.436584
H	5.061291	6.853699	1.684108
H	2.026380	8.104676	3.540095
H	3.691865	8.494901	3.066382
H	2.403561	8.492469	1.854943
H	4.545298	6.396289	4.065224
H	2.923693	5.955065	4.613363
H	3.882534	4.811616	3.647943

2.11.8. Transition States for Other Epoxides

In this section, we compare the predicted selectivity between opening (*R*)- and (*S*)-1,2-epoxypropane (2-methyloxirane) to the selectivity for 2-(*tert*-butyl)oxirane, 2-cyclohexyloxirane and 2-phenyloxirane. All calculations restricted singlets at the B3LYP/6-31G(d) level.

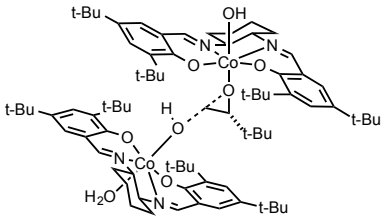

Transition State
Charge: 0
Spin Multiplicity: 1
Solvation: gas phase
Electronic Energy (AU): -6630.88331655
Gibbs Free Energy at 298.150 K (AU): -6629.149063

Co	-3.085324	-0.857237	-0.209701
N	-3.942083	-0.690387	-1.898041
N	-1.993168	-2.170963	-1.046624
C	-1.384952	-3.122121	-0.427224
H	-0.896815	-3.902289	-1.014384
C	-4.817657	0.202567	-2.209871
H	-5.222905	0.202102	-3.223825
C	-1.278715	-3.260180	1.001926
C	-1.693550	-2.217549	1.895574
C	-0.750424	-4.478723	1.484879
C	-1.520202	-2.465135	3.311606
H	-0.482774	-5.232106	0.748444
C	-1.007178	-3.692848	3.711257
H	-0.916617	-3.879397	4.775299
C	-5.354504	1.211694	-1.341168
C	-5.065082	1.245376	0.062146
C	-6.235020	2.148200	-1.933773
C	-5.769985	2.234114	0.851210
H	-6.404092	2.063056	-3.003711
C	-6.600607	3.129832	0.193318
H	-7.104581	3.880734	0.790004
O	-2.165016	-1.080814	1.471970
O	-4.221740	0.429695	0.630433
O	-4.257840	-2.216378	0.220440
O	-1.805901	0.532754	-0.873793
C	0.024596	0.478796	-0.314552
C	-1.082753	1.438127	-0.079031
H	0.431680	0.413630	-1.310645
H	-0.002515	-0.423091	0.276094
H	-1.421250	1.451916	0.963557
C	-2.076567	-2.075789	-2.506655
C	-3.560245	-1.777158	-2.808835
H	-1.505153	-1.178566	-2.783390
H	-4.137341	-2.655777	-2.486916
C	-3.785789	-1.538887	-4.307160
H	-4.852287	-1.400241	-4.519249
H	-3.273903	-0.614014	-4.609334
C	-1.561109	-3.266091	-3.319545
H	-0.494836	-3.428720	-3.123775
H	-2.093237	-4.178713	-3.014434
C	-3.255784	-2.723933	-5.131915
C	-1.783077	-3.021648	-4.821054
H	-1.442533	-3.893736	-5.392813
H	-1.163439	-2.173049	-5.146006
H	-3.384876	-2.516260	-6.201264
H	-3.859657	-3.615791	-4.911645
H	-4.878184	-1.802280	0.841163
C	-1.007339	2.885286	-0.633104
N	2.786761	-1.297176	1.167236
N	3.886144	0.903114	1.981232
C	4.087100	2.144400	2.272601
H	4.211482	2.416248	3.321391
C	2.506146	-2.431472	0.612788
H	2.176769	-3.249963	1.252306
C	4.198217	3.226726	1.333337
C	4.300822	2.994766	-0.071162
C	4.294564	4.531970	1.870167
C	4.581020	4.120723	-0.917485
H	4.201002	4.640285	2.946467
C	4.649611	5.375333	-0.319429
H	4.839108	6.227490	-0.960335
C	2.598103	-2.737204	-0.788203
C	2.861525	-1.735893	-1.774885
C	2.429748	-4.097194	-1.149025
C	2.921867	-2.158412	-3.152405
H	2.236146	-4.804055	-0.348293
C	2.764433	-3.511932	-3.424830
H	2.832230	-3.828112	-4.458560
O	4.188333	1.778763	-0.584442
O	3.046963	-0.471163	-1.466426
O	1.724217	1.056877	0.452535
C	3.865667	-0.169405	2.987202

C	2.669213	-1.069270	2.620969
H	4.777034	-0.761517	2.814536
H	1.751550	-0.484720	2.771070
C	2.628098	-2.318203	3.507502
H	1.730081	-2.907189	3.297187
H	3.501340	-2.948838	3.284510
C	3.831968	0.245974	4.460388
H	4.708897	0.856479	4.707721
H	2.940593	0.858988	4.652069
C	2.635298	-1.929830	4.996505
C	3.807997	-1.007047	5.352079
H	3.750336	-0.707142	6.404897
H	4.755718	-1.551366	5.233019
H	2.670459	-2.840279	5.605987
H	1.690322	-1.428209	5.242370
H	1.815014	1.916040	0.009241
Co	3.399780	0.252661	0.261062
O	5.283034	-0.481504	-0.000333
H	5.608002	0.362060	-0.381228
H	5.204384	-1.080842	-0.764707
C	-5.645410	2.261407	2.389408
C	-6.222319	0.939663	2.952377
C	-4.171994	2.431898	2.828644
C	-6.442796	3.416776	3.029906
H	-7.288754	0.854456	2.710787
H	-5.704630	0.074843	2.535780
H	-6.118945	0.909533	4.044518
H	-3.777160	3.395024	2.480041
H	-4.103158	2.422312	3.924310
H	-3.547720	1.632265	2.431393
H	-6.310413	3.382254	4.117665
H	-6.094833	4.398907	2.687420
H	-7.518203	3.343984	2.830163
C	-1.965528	-1.417270	4.352109
C	-1.207395	-0.085523	4.138032
C	-3.485869	-1.176711	4.208469
C	-1.704170	-1.868987	5.803417
H	-0.131406	-0.218170	4.314204
H	-1.350411	0.284563	3.122505
H	-1.567190	0.674777	4.842874
H	-4.041230	-2.104845	4.389501
H	-3.822682	-0.431519	4.940420
H	-3.726439	-0.816612	3.209070
H	-2.027405	-1.077293	6.489122
H	-2.265141	-2.774297	6.063161
H	-0.641031	-2.058836	5.998276
C	3.169182	-1.143583	-4.288033
C	2.031775	-0.094497	-4.309367
C	4.534495	-0.442443	-4.084992
C	3.202006	-1.811937	-5.677860
H	1.067458	-0.576229	-4.513084
H	1.959975	0.434176	-3.358180
H	2.211509	0.643570	-5.100728
H	5.349212	-1.178311	-4.081127
H	4.725139	0.259099	-4.906256
H	4.554226	0.118104	-3.149737
H	3.367585	-1.042844	-6.440382
H	4.013872	-2.543195	-5.769851
H	2.257261	-2.312863	-5.918978
C	4.820734	3.952337	-2.433384
C	6.054899	3.046502	-2.663961
C	3.575662	3.337119	-3.112217
C	5.109693	5.295865	-3.134976
H	6.951338	3.488679	-2.212654
H	5.905039	2.053370	-2.236711
H	6.241922	2.927559	-3.738229
H	2.706338	3.994322	-2.993673
H	3.756759	3.213730	-4.187241
H	3.334205	2.361600	-2.689893
H	5.274059	5.112566	-4.202543
H	4.270659	5.996123	-3.050001
H	6.009918	5.784886	-2.744720
C	-6.856390	3.136962	-1.200452
C	-0.616088	-4.738162	2.836924
C	4.496106	5.633404	1.063277
C	2.525797	-4.521014	-2.458720
C	-7.792686	4.195543	-1.806045
C	-9.195723	4.091341	-1.161610
C	-7.217509	5.607980	-1.543010
C	-7.954781	4.022625	-3.328084
H	-9.636359	3.104543	-1.344212
H	-9.158226	4.243141	-0.077703
H	-9.870024	4.849521	-1.580234
H	-6.231029	5.719732	-2.007638
H	-7.879868	6.379280	-1.956932
H	-7.103963	5.806506	-0.471886
H	-8.621010	4.798581	-3.722939
H	-6.995672	4.111546	-3.851423
H	-8.392941	3.050272	-3.581724
C	-0.146667	-6.087370	3.409921
C	-1.294235	-6.719279	4.235370
C	0.244439	-7.084872	2.303543
C	1.082270	-5.891221	4.328610
H	-1.596591	-6.075634	5.068315
H	-2.177077	-6.886059	3.608395
H	-0.983387	-7.684979	4.654562
H	1.067677	-6.706370	1.685313
H	0.576023	-8.028652	2.751852
H	-0.600593	-7.312074	1.644108
H	1.391085	-6.847366	4.769922
H	1.933995	-5.490959	3.764940
H	0.870753	-5.200821	5.152498
C	4.569458	7.076535	1.589461
C	3.448306	7.919168	0.935751
C	4.390136	7.144003	3.117903
C	5.944390	7.693513	1.239108
H	3.540882	7.945292	-0.155302
H	2.460701	7.510238	1.177094
H	3.486455	8.954019	1.297517
H	5.174931	6.589440	3.645676

H	4.443834	8.186478	3.450681
H	3.417936	6.747073	3.431879
H	6.003429	8.726464	1.603368
H	6.759053	7.123344	1.700273
H	6.121224	7.713937	0.158471
C	2.417824	-5.992793	-2.894183
C	1.265014	-6.165376	-3.911166
C	3.747335	-6.429781	-3.555641
C	2.147478	-6.929543	-1.701866
H	0.302826	-5.892369	-3.463341
H	1.407528	-5.544842	-4.802475
H	1.200762	-7.209220	-4.241762
H	4.583874	-6.333695	-2.853929
H	3.690070	-7.477674	-3.874822
H	3.982223	-5.826524	-4.439450
H	2.078080	-7.965651	-2.051446
H	2.952448	-6.886654	-0.959079
H	1.203832	-6.688861	-1.198584
C	-2.442180	3.405033	-0.826583
H	-2.424128	4.441963	-1.185589
H	-2.984769	2.796016	-1.553114
H	-3.006931	3.382327	0.110630
C	-0.293089	3.788803	0.391909
H	-0.236856	4.819035	0.019697
H	-0.837438	3.806597	1.343719
H	0.729951	3.462380	0.610460
C	-0.279992	2.934024	-1.988462
H	-0.332478	3.943768	-2.413385
H	0.782076	2.672799	-1.904401
H	-0.743267	2.242710	-2.700482

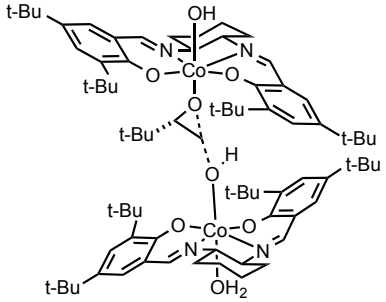

Transition State
Charge: 0
Spin Multiplicity: 1
Solvation: gas phase
Electronic Energy (AU): -6630.87700374
Gibbs Free Energy at 298.150 K (AU): -6629.144462

Co	3.572881	-0.341969	-0.417617
N	4.295942	-2.103785	-0.395313
N	4.203874	-0.253618	-2.204059
C	4.403521	0.842998	-2.852626
H	4.894228	0.789173	-3.826294
C	4.141648	-2.975052	0.539920
H	4.590926	-3.962418	0.411988
C	4.017731	2.160804	-2.436352
C	3.247886	2.394142	-1.250447
C	4.391663	3.224323	-3.290956
C	2.867181	3.762019	-0.975570
C	4.043573	4.533311	-3.029638
H	4.972434	2.971958	-4.173787
C	3.277244	4.751171	-1.858289
H	2.993244	5.773807	-1.639229
C	3.501164	-2.758972	1.809560
C	3.064114	-1.458019	2.223758
C	3.490416	-3.856137	2.700455
C	2.707122	-1.306008	3.619863
C	3.087037	-3.736190	4.015722
H	3.844064	-4.808816	2.315995
C	2.715504	-2.433144	4.432599
H	2.451191	-2.306327	5.476389
O	2.859709	1.431707	-0.461392
O	3.007956	-0.438698	1.417830
O	5.224443	0.296514	0.106205
O	1.868464	-1.158383	-1.123136
C	0.768537	-0.409917	-1.574596
H	0.949853	0.670336	-1.533074
C	4.588193	-1.572468	-2.717464
C	5.212704	-2.316337	-1.523808
H	3.651073	-2.095160	-2.956592
H	6.131376	-1.778270	-1.250309
C	5.559692	-3.765149	-1.884915
H	6.066236	-4.261036	-1.048754
H	4.634547	-4.326085	-2.081606
C	5.500617	-1.608737	-3.947760
H	5.012713	-1.123833	-4.801998
H	6.420966	-1.045829	-3.738595
C	6.470662	-3.807116	-3.123648
C	5.849346	-3.061243	-4.311805
H	6.533572	-3.074348	-5.168958
H	4.936537	-3.584053	-4.631891
H	6.678377	-4.849523	-3.394835
H	7.438451	-3.349450	-2.874516
H	5.072271	0.635860	1.001915
C	0.104950	-0.913820	-0.339914
H	-0.165123	-1.959250	-0.319561
H	0.447486	-0.474737	0.585958
C	0.221306	-0.782797	-2.977387
N	-2.575866	-0.198738	2.422940
N	-3.137593	-2.305897	1.026567
C	-3.176069	-3.225987	0.117471
H	-2.916669	-4.245531	0.406714
C	-2.459068	0.937070	3.033231
H	-1.997155	0.941190	4.020059
C	-3.587520	-3.051699	-1.244653
C	-4.242075	-1.857613	-1.678664
C	-3.443858	-4.166524	-2.105950
C	-4.819671	-1.854627	-2.995617

C	-3.927927	-4.149788	-3.397171
H	-2.934740	-5.041639	-1.713403
C	-4.622232	-2.979172	-3.788901
H	-5.039169	-2.966797	-4.788071
C	-2.872755	2.221153	2.550055
C	-3.445113	2.404863	1.254725
C	-2.665165	3.320045	3.421475
C	-3.799170	3.742948	0.861690
C	-3.009037	4.605857	3.063728
H	-2.218195	3.112771	4.388805
C	-3.572638	4.766055	1.773767
H	-3.841684	5.771964	1.476234
O	-4.373525	-0.813026	-0.885310
O	-3.664608	1.398621	0.431195
O	-1.712823	-0.321958	-0.191443
C	-2.914202	-2.586303	2.453076
C	-2.027004	-1.448873	2.986068
H	-3.898480	-2.475792	2.933125
H	-1.023860	-1.575487	2.553327
C	-1.921514	-1.530814	4.514480
H	-1.256370	-0.753404	4.903363
H	-2.914601	-1.361461	4.954858
C	-2.348152	-3.958675	2.828553
H	-3.006831	-4.758906	2.470830
H	-1.369918	-4.100412	2.348543
C	-1.373897	-2.906043	4.931799
C	-2.204957	-4.060495	4.357486
H	-1.747124	-5.021204	4.619679
H	-3.205717	-4.056015	4.812563
H	-1.345424	-2.971112	6.025834
H	-0.335962	-2.993969	4.586422
H	-1.657196	0.613861	-0.446042
Co	-3.354582	-0.449791	0.709872
O	-5.240903	-0.499037	1.479804
H	-5.618421	-0.756045	0.609243
H	-5.445593	0.451117	1.557286
C	2.043175	4.117363	0.279329
C	0.687626	3.369178	0.263020
C	2.844225	3.732121	1.544569
C	1.725439	5.623883	0.373904
H	0.103691	3.649185	-0.623442
H	0.842314	2.289514	0.251909
H	0.096439	3.631507	1.150038
H	3.779515	4.302689	1.594146
H	2.262217	3.957396	2.448108
H	3.086810	2.669647	1.541435
H	1.133783	5.808837	1.278573
H	2.631790	6.236380	0.445898
H	1.137056	5.978761	-0.480775
C	2.425022	0.092908	4.209016
C	3.710455	0.949884	4.102586
C	1.272292	0.792906	3.454368
C	2.034740	0.040246	5.700520
H	4.521482	0.501850	4.688775
H	4.038826	1.035105	3.065904
H	3.529686	1.960895	4.489274
H	0.359322	0.188039	3.512800
H	1.058492	1.770406	3.905762
H	1.521962	0.939855	2.404362
H	1.839699	1.058040	6.057894
H	1.126261	-0.551363	5.872370
H	2.833072	-0.376185	6.325244
C	-5.655212	-0.661277	-3.509635
C	-6.886206	-0.454613	-2.592967
C	-4.800231	0.625105	-3.540379
C	-6.191040	-0.892329	-4.938121
H	-7.510026	-1.356394	-2.565664
H	-6.585145	-0.209344	-1.572624
H	-7.503118	0.370446	-2.969660
H	-3.957960	0.512654	-4.232108
H	-5.408109	1.471242	-3.884880
H	-4.406155	0.861749	-2.552625
H	-6.777376	-0.019071	-5.244849
H	-5.382088	-1.013320	-5.667817
H	-6.848707	-1.767308	-5.002048
C	-4.393875	4.038321	-0.531319
C	-3.372773	3.641907	-1.624900
C	-5.718836	3.261317	-0.726086
C	-4.714119	5.534890	-0.726702
H	-2.453444	4.230649	-1.523353
H	-3.114009	2.584018	-1.565412
H	-3.789749	3.836118	-2.620684
H	-6.451169	3.548736	0.039317
H	-6.151656	3.496767	-1.705913
H	-5.559002	2.183745	-0.676586
H	-5.131121	5.682325	-1.729011
H	-5.456032	5.899025	-0.005971
H	-3.819969	6.164052	-0.650354
C	3.115191	-4.897229	5.025616
C	4.123321	-4.578797	6.156442
C	1.714566	-5.104198	5.647169
C	3.540600	-6.224994	4.370079
H	5.131715	-4.440968	5.750573
H	3.854695	-3.663615	6.695163
H	4.156977	-5.397775	6.886422
H	0.980360	-5.365155	4.875148
H	1.734857	-5.917693	6.383681
H	1.359324	-4.203658	6.159328
H	3.528775	-7.029040	5.115226
H	2.862045	-6.513322	3.558593
H	4.555979	-6.170008	3.961843
C	4.434535	5.720583	-3.925025
C	5.286900	6.727086	-3.115580
C	5.257103	5.276696	-5.149479
C	3.159524	6.431480	-4.438584
H	4.746849	7.104737	-2.240822
H	6.209909	6.256503	-2.758200
H	5.560931	7.589969	-3.736382
H	4.695509	4.582718	-5.785716
H	5.517234	6.149271	-5.760122

H	6.193052	4.788582	-4.854069
H	3.421955	7.289371	-5.071049
H	2.544008	5.745843	-5.032573
H	2.540986	6.803528	-3.614741
C	-2.807990	5.830273	3.972485
C	-1.874073	6.848295	3.275565
C	-4.175234	6.499295	4.250858
C	-2.176743	5.448342	5.324366
H	-0.893193	6.404236	3.071399
H	-2.286295	7.196528	2.322486
H	-1.724062	7.728203	3.913073
H	-4.853362	5.807244	4.763559
H	-4.045781	7.383129	4.887500
H	-4.666001	6.825128	3.327465
H	-2.054774	6.345026	5.942161
H	-2.805488	4.746001	5.884205
H	-1.185791	4.997609	5.197943
C	-3.771966	-5.318893	-4.383838
C	-3.003328	-4.837526	-5.637723
C	-2.991201	-6.494383	-3.766877
C	-5.167210	-5.836452	-4.807536
H	-3.525160	-4.021148	-6.148462
H	-2.003518	-4.477899	-5.369242
H	-2.889386	-5.658997	-6.355821
H	-3.504135	-6.910516	-2.891799
H	-2.891570	-7.299890	-4.502997
H	-1.980814	-6.196716	-3.463960
H	-5.067955	-6.666392	-5.517934
H	-5.731456	-6.197058	-3.939737
H	-5.763368	-5.056002	-5.292462
C	1.276803	-0.400397	-4.031930
H	2.181052	-1.003505	-3.929435
H	0.875878	-0.560519	-5.040672
H	1.562203	0.654694	-3.946211
C	-0.080683	-2.286617	-3.082305
H	-0.923565	-2.575182	-2.445611
H	-0.347197	-2.552435	-4.112998
H	0.794176	-2.876413	-2.788860
C	-1.050758	0.036564	-3.263447
H	-0.849691	1.114311	-3.195981
H	-1.408995	-0.165170	-4.280569
H	-1.853025	-0.209341	-2.565674

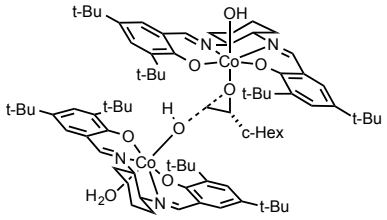

Transition State
Charge: 0
Spin Multiplicity: 1
Solvation: gas phase
Electronic Energy (AU): -6708.30851854
Gibbs Free Energy at 298.150 K (AU): -6706.537523

Co	-2.804248	-1.576983	-0.217203
N	-3.663974	-1.425036	-1.903334
N	-1.484193	-2.597238	-1.133826
C	-0.693483	-3.445515	-0.572145
H	-0.068469	-4.077980	-1.205510
C	-4.615840	-0.602839	-2.183113
H	-4.979354	-0.554183	-3.211806
C	-0.542698	-3.646103	0.845209
C	-1.159956	-2.775677	1.804084
C	0.241274	-4.750441	1.250493
C	-0.926956	-3.073209	3.201984
H	0.655501	-5.379829	0.467153
C	-0.153103	-4.181145	3.522600
H	-0.011606	-4.411200	4.572500
C	-5.300731	0.249546	-1.251385
C	-5.099571	0.144447	0.164185
C	-6.261331	1.136691	-1.793029
C	-6.001927	0.897471	1.009816
H	-6.351454	1.171026	-2.875391
C	-6.906569	1.757240	0.403608
H	-7.559132	2.336361	1.046192
O	-1.864862	-1.739567	1.456150
O	-4.171144	-0.601009	0.694140
O	-3.697395	-3.163408	0.088043
O	-1.828807	0.082048	-0.750447
C	-0.007825	0.317342	-0.269161
C	-1.241816	1.021782	0.119367
H	0.376012	0.453552	-1.267797
H	0.182640	-0.623921	0.221990
H	-1.511466	0.861952	1.169368
C	-1.599065	-2.438329	-2.587322
C	-3.116127	-2.380920	-2.870859
H	-1.192912	-1.443239	-2.818867
H	-3.533349	-3.357742	-2.588588
C	-3.399108	-2.114864	-4.353529
H	-4.477466	-2.145962	-4.548856
H	-3.051511	-1.106004	-4.618823
C	-0.896850	-3.479338	-3.463678
H	0.185037	-3.460278	-3.286786
H	-1.254334	-4.484289	-3.197238

C	-2.690124	-3.157228	-5.234298
C	-1.183143	-3.209660	-4.950089
H	-0.706611	-3.983349	-5.564643
H	-0.724581	-2.253020	-5.240456
H	-2.870496	-2.931587	-6.292484
H	-3.128285	-4.147560	-5.045984
H	-4.407285	-2.916298	0.701577
N	3.091418	-0.884071	1.148812
N	3.717093	1.456418	2.072730
C	3.665513	2.696784	2.426488
H	3.752725	2.937595	3.486718
C	3.052213	-2.024553	0.540237
H	2.911694	-2.924518	1.138774
C	3.526658	3.823679	1.545012
C	3.626744	3.686918	0.128023
C	3.367927	5.093062	2.149035
C	3.616839	4.884616	-0.664112
H	3.295070	5.128235	3.231799
C	3.446779	6.095884	-0.000934
H	3.422234	6.997325	-0.600663
C	3.183116	-2.234725	-0.875022
C	3.205370	-1.152332	-1.809862
C	3.297488	-3.579829	-1.306847
C	3.312960	-1.483883	-3.209230
H	3.277296	-4.351797	-0.543566
C	3.436487	-2.824381	-3.552838
H	3.538267	-3.066367	-4.603642
O	3.771586	2.502921	-0.447218
O	3.131363	0.106559	-1.437724
O	1.545128	1.197429	0.572732
C	3.923249	0.353148	3.025189
C	2.931540	-0.751350	2.609387
H	4.934652	-0.032509	2.826710
H	1.915349	-0.368245	2.774451
C	3.134727	-2.022310	3.439919
H	2.370736	-2.765695	3.191747
H	4.116018	-2.458958	3.202446
C	3.813384	0.681825	4.516449
H	4.555436	1.438400	4.798844
H	2.820271	1.100722	4.729820
C	3.058992	-1.705707	4.943544
C	4.031873	-0.592000	5.350574
H	3.916832	-0.356467	6.414995
H	5.066756	-0.938331	5.216995
H	3.264658	-2.617802	5.515636
H	2.034124	-1.404166	5.196692
H	1.420933	2.101880	0.239183
Co	3.349204	0.804721	0.323298
O	5.342771	0.509234	0.001680
H	5.467782	1.423552	-0.330961
H	5.369994	-0.046459	-0.798555
C	-5.991431	0.714281	2.542282
C	-6.326389	-0.761034	2.871802
C	-4.614505	1.094052	3.135511
C	-7.047129	1.588921	3.249911
H	-7.331183	-1.015286	2.512937
H	-5.611595	-1.440791	2.406768
H	-6.303011	-0.924481	3.956717
H	-4.410155	2.159893	2.974263
H	-4.607834	0.914146	4.218526
H	-3.814933	0.510500	2.679588
H	-6.997624	1.406494	4.329755
H	-6.871770	2.659663	3.090210
H	-8.067603	1.354782	2.924670
C	-1.585845	-2.220992	4.305856
C	-1.134367	-0.745410	4.193277
C	-3.123628	-2.308936	4.162685
C	-1.228254	-2.705378	5.725928
H	-0.054961	-0.654478	4.375933
H	-1.354818	-0.346772	3.202823
H	-1.650351	-0.131177	4.942083
H	-3.460020	-3.346150	4.279718
H	-3.610902	-1.704718	4.938633
H	-3.444599	-1.947120	3.186712
H	-1.715075	-2.053235	6.460253
H	-1.578228	-3.726895	5.914686
H	-0.148832	-2.671865	5.921419
C	3.303698	-0.384753	-4.292234
C	1.968668	0.395427	-4.231640
C	4.492289	0.584122	-4.078684
C	3.435286	-0.961378	-5.716642
H	1.121941	-0.272688	-4.431391
H	1.824118	0.855111	-3.253118
H	1.956918	1.187424	-4.990471
H	5.446447	0.043958	-4.133018
H	4.499875	1.350484	-4.863273
H	4.420586	1.087737	-3.114031
H	3.414654	-0.137979	-6.439015
H	4.379176	-1.500078	-5.861862
H	2.610076	-1.637601	-5.968519
C	3.806056	4.839565	-2.195218
C	5.194267	4.241166	-2.528157
C	2.689200	3.993058	-2.848885
C	3.753487	6.242135	-2.835405
H	5.994909	4.856294	-2.099771
H	5.292613	3.225362	-2.141547
H	5.340966	4.205925	-3.614562
H	1.705994	4.439837	-2.659082
H	2.833871	3.955269	-3.935801
H	2.688501	2.972162	-2.466589
H	3.891261	6.145080	-3.917887
H	2.788488	6.735814	-2.672501
H	4.546780	6.900634	-2.462529
C	-7.059609	1.929956	-0.995052
C	0.445996	-5.058401	2.583059
C	3.305744	6.249946	1.398636
C	3.445459	-3.907757	-2.639026
C	-8.090958	2.931686	-1.539292
C	-9.508604	2.548855	-1.051256
C	-7.748467	4.354481	-1.036253

C	-8.111158	2.964046	-3.079251
H	-9.785021	1.548785	-1.404398
H	-9.576413	2.545693	0.041774
H	-10.252489	3.262482	-1.428254
H	-6.755377	4.661840	-1.384469
H	-8.480996	5.083189	-1.406817
H	-7.748735	4.409450	0.057650
H	-8.848617	3.696880	-3.427202
H	-7.137434	3.252298	-3.492225
H	-8.387466	1.991529	-3.503112
C	1.203167	-6.307294	3.068881
C	0.227171	-7.226462	3.843746
C	1.793133	-7.120330	1.901306
C	2.367235	-5.908768	4.006249
H	-0.195353	-6.721113	4.718628
H	-0.606903	-7.534035	3.203439
H	0.741633	-8.130268	4.195036
H	2.507103	-6.530334	1.313614
H	2.327984	-7.995322	2.288618
H	1.012400	-7.483229	1.223702
H	2.883137	-6.801325	4.382331
H	3.104441	-5.293091	3.476580
H	2.016136	-5.340100	4.873964
C	3.110702	7.651234	2.002029
C	1.819795	8.284792	1.430834
C	2.984269	7.606934	3.536346
C	4.321854	8.545525	1.644603
H	1.857855	8.376681	0.340148
H	0.941479	7.680329	1.684061
H	1.671834	9.290128	1.843814
H	3.885651	7.198656	4.008374
H	2.839980	8.620920	3.925502
H	2.125399	7.006070	3.856793
H	4.190145	9.552002	2.060079
H	5.250292	8.128429	2.051474
H	4.448937	8.648795	0.561694
C	3.640040	-5.344979	-3.152608
C	2.523687	-5.707116	-4.160246
C	5.013817	-5.455109	-3.857445
C	3.605017	-6.376957	-2.010384
H	1.537373	-5.666813	-3.684342
H	2.509125	-5.027339	-5.019075
H	2.672015	-6.723235	-4.545690
H	5.829452	-5.219945	-3.164003
H	5.170688	-6.473253	-4.234362
H	5.091680	-4.770746	-4.709223
H	3.746072	-7.384907	-2.416022
H	4.401820	-6.202457	-1.278098
H	2.645425	-6.367367	-1.480681
C	-1.429513	2.498269	-0.262145
C	-1.180723	2.794438	-1.753272
C	-2.826234	2.992708	0.156536
H	-0.687428	3.062446	0.332252
C	-1.408234	4.276923	-2.091932
H	-1.859453	2.168804	-2.346229
H	-0.159973	2.509341	-2.042116
C	-3.049160	4.474155	-0.177121
H	-3.582611	2.387917	-0.357229
H	-2.969835	2.822081	1.230030
C	-2.804665	4.752415	-1.666831
H	-1.260122	4.440399	-3.167746
H	-0.650375	4.888225	-1.577527
H	-4.068114	4.769653	0.103916
H	-2.365356	5.094533	0.423041
H	-2.925642	5.821865	-1.884774
H	-3.563511	4.221466	-2.260200

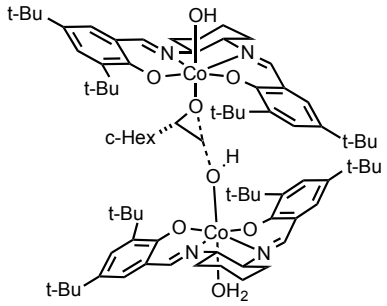

Transition State
Charge: 0
Spin Multiplicity: 1
Solvation: gas phase
Electronic Energy (AU): -6708.30373476
Gibbs Free Energy at 298.150 K (AU): -6706.534566

Co	3.622390	0.159863	-0.557740
N	4.674394	-1.403604	-0.307287
N	3.947131	-0.083238	-2.413505
C	3.812260	0.841316	-3.304067
H	4.154236	0.637148	-4.320462
C	4.761632	-2.086235	0.780615
H	5.357112	-3.001863	0.778121
C	3.235445	2.139270	-3.103864
C	2.628864	2.523243	-1.863927
C	3.259085	3.016469	-4.213491
C	2.048685	3.845817	-1.800700
C	2.711594	4.281692	-4.160204
H	3.733889	2.656376	-5.122111
C	2.115069	4.650373	-2.929122
H	1.682577	5.642439	-2.869400
C	4.197745	-1.727321	2.054571
C	3.598892	-0.444815	2.280921
C	4.394242	-2.642723	3.113178
C	3.293572	-0.100919	3.654295
C	4.039085	-2.351821	4.415718
H	4.858131	-3.593845	2.866277
C	3.503243	-1.058387	4.638471
H	3.266685	-0.791810	5.662505
O	2.549902	1.719582	-0.840056

O	3.358540	0.405517	1.326489
O	5.162413	1.177216	-0.505784
O	2.056859	-1.081009	-0.695095
C	0.823877	-0.724957	-1.274995
H	0.816800	0.302297	-1.657196
C	4.535393	-1.396145	-2.703608
C	5.457452	-1.711002	-1.509379
H	3.708837	-2.121023	-2.668064
H	6.266140	-0.966819	-1.521549
C	6.054842	-3.118025	-1.618170
H	6.757143	-3.302484	-0.796644
H	5.253219	-3.866021	-1.532424
C	5.271535	-1.556972	-4.038150
H	4.588187	-1.382972	-4.878264
H	6.069220	-0.804290	-4.109102
C	6.785784	-3.290300	-2.960339
C	5.873926	-2.967269	-4.151062
H	6.430996	-3.057222	-5.091585
H	5.060485	-3.705897	-4.198115
H	7.170524	-4.314217	-3.043090
H	7.660575	-2.625013	-2.982371
H	5.106969	1.641395	0.344356
C	0.342810	-0.810303	0.117327
H	0.236759	-1.794340	0.549201
H	0.605871	0.001892	0.779225
N	-2.322470	0.105090	2.689239
N	-2.770341	-2.283439	1.794172
C	-2.855415	-3.389212	1.127087
H	-2.536657	-4.309455	1.618473
C	-2.337856	1.336894	3.086427
H	-1.838926	1.578336	4.024701
C	-3.376026	-3.548304	-0.198421
C	-4.041294	-2.482991	-0.878614
C	-3.312618	-4.849513	-0.754433
C	-4.623315	-2.771248	-2.161576
C	-3.880472	-5.145137	-1.976572
H	-2.807088	-5.617265	-0.176427
C	-4.521096	-4.071842	-2.642732
H	-4.971259	-4.288906	-3.603611
C	-2.950068	2.446638	2.417402
C	-3.561170	2.324296	1.131520
C	-2.893485	3.694789	3.087342
C	-4.123143	3.512500	0.543286
C	-3.431020	4.838945	2.538714
H	-2.404186	3.719876	4.056136
C	-4.037466	4.695494	1.266440
H	-4.463205	5.586447	0.822234
O	-4.181062	-1.290439	-0.334063
O	-3.624717	1.176582	0.486723
O	-1.580940	-0.495759	0.106555
C	-2.404267	-2.241053	3.220672
C	-1.595706	-0.948606	3.422568
H	-3.350691	-2.115528	3.768654
H	-0.629698	-1.075008	2.913204
C	-1.337040	-0.706138	4.914691
H	-0.726166	0.189672	5.064212
H	-2.295515	-0.537900	5.426612
C	-1.667922	-3.454750	3.797953
H	-2.272337	-4.362724	3.688511
H	-0.733420	-3.616379	3.242945
C	-0.606694	-1.913912	5.525856
C	-1.364851	-3.226171	5.289402
H	-0.786803	-4.072043	5.678961
H	-2.311161	-3.209550	5.848736
H	-0.465329	-1.749643	6.600531
H	0.396953	-1.983626	5.086600
H	-1.643719	0.355326	-0.359355
Co	-3.152999	-0.551214	1.112394
O	-5.001782	-0.602621	1.981287
H	-5.389099	-1.015722	1.177836
H	-5.297093	0.325114	1.944093
C	1.390403	4.354776	-0.502735
C	0.203361	3.440296	-0.115065
C	2.440886	4.374821	0.632773
C	0.833124	5.786072	-0.640379
H	-0.561284	3.451446	-0.902154
H	0.540521	2.413230	0.029552
H	-0.264915	3.793158	0.812507
H	3.252854	5.071411	0.391057
H	1.979917	4.707160	1.572496
H	2.869853	3.384333	0.784579
H	0.383142	6.088266	0.312887
H	1.616560	6.515184	-0.877964
H	0.053211	5.856443	-1.408253
C	2.819124	1.321894	4.018427
C	3.935612	2.333919	3.661193
C	1.527528	1.685984	3.251316
C	2.523076	1.479621	5.523850
H	4.842022	2.128243	4.242967
H	4.185290	2.281576	2.600566
H	3.611576	3.357642	3.888229
H	0.732168	0.966068	3.482317
H	1.176554	2.683697	3.545360
H	1.698045	1.679422	2.175644
H	2.188958	2.505076	5.719791
H	1.729846	0.801893	5.865182
H	3.409753	1.302065	6.143115
C	-5.356371	-1.683415	-2.973599
C	-6.606525	-1.201812	-2.198334
C	-4.402230	-0.496078	-3.241801
C	-5.843729	-2.199414	-4.343295
H	-7.300833	-2.033381	-2.026115
H	-6.333657	-0.771218	-1.233793
H	-7.137385	-0.433894	-2.774367
H	-3.536576	-0.824402	-3.829977
H	-4.921082	0.282629	-3.814632
H	-4.042411	-0.059218	-2.310509
H	-6.331467	-1.378623	-4.880634
H	-5.016859	-2.554699	-4.969158
H	-6.578076	-3.008179	-4.248908

C	-4.787042	3.482088	-0.849615
C	-3.736316	3.090578	-1.916000
C	-5.961390	2.474298	-0.862556
C	-5.363908	4.854194	-1.256343
H	-2.933561	3.835854	-1.957917
H	-3.292658	2.117692	-1.700330
H	-4.202904	3.041216	-2.907612
H	-6.715970	2.750038	-0.114373
H	-6.450097	2.479432	-1.844390
H	-5.613990	1.460774	-0.661697
H	-5.825018	4.767172	-2.246376
H	-6.139188	5.200819	-0.562542
H	-4.590802	5.628008	-1.325153
C	4.258103	-3.313532	5.596521
C	5.241716	-2.681149	6.610700
C	2.914343	-3.595566	6.308819
C	4.845036	-4.663783	5.143226
H	6.208530	-2.476043	6.137559
H	4.861138	-1.735376	7.011255
H	5.412184	-3.357288	7.458421
H	2.203768	-4.074299	5.623976
H	3.063024	-4.265102	7.165802
H	2.452669	-2.675643	6.683303
H	4.967393	-5.326085	6.008190
H	4.189204	-5.171022	4.425932
H	5.829891	-4.543064	4.678194
C	2.724871	5.273354	-5.335424
C	3.481433	6.559465	-4.925156
C	3.420882	4.688675	-6.578801
C	1.273925	5.640863	-5.728141
H	3.013985	7.049599	-4.064474
H	4.518421	6.330956	-4.654183
H	3.494490	7.280892	-5.752419
H	2.914541	3.786006	-6.940077
H	3.409232	5.423109	-7.392672
H	4.467804	4.435394	-6.375942
H	1.268144	6.363120	-6.554692
H	0.719760	4.751060	-6.048817
H	0.727378	6.089140	-4.891467
C	-3.396061	6.215282	3.223680
C	-2.650059	7.227042	2.321341
C	-4.841327	6.713024	3.463405
C	-2.674824	6.165093	4.583840
H	-1.620560	6.900946	2.134897
H	-3.141214	7.349585	1.350224
H	-2.614236	8.212803	2.801083
H	-5.388912	6.025926	4.118981
H	-4.831722	7.701397	3.939137
H	-5.404047	6.801542	2.527750
H	-2.671770	7.162121	5.038235
H	-3.173246	5.485597	5.285183
H	-1.630980	5.847202	4.480234
C	-3.883384	-6.551365	-2.601063
C	-3.254996	-6.511888	-4.013955
C	-3.086222	-7.559950	-1.752634
C	-5.342616	-7.056246	-2.708970
H	-3.794682	-5.835755	-4.685517
H	-2.212413	-6.179045	-3.970957
H	-3.275882	-7.510907	-4.466535
H	-3.518176	-7.684482	-0.752756
H	-3.095545	-8.542209	-2.238099
H	-2.039274	-7.255694	-1.639498
H	-5.370439	-8.056247	-3.159222
H	-5.811078	-7.114454	-1.719739
H	-5.955995	-6.394535	-3.330121
C	0.240708	-1.689391	-2.320012
C	0.738644	-1.348983	-3.739003
C	0.499280	-3.171377	-1.994575
H	-0.847264	-1.520288	-2.302629
C	0.142449	-2.283325	-4.801912
H	1.833731	-1.425048	-3.766083
H	0.498217	-0.303988	-3.975216
C	-0.080756	-4.108131	-3.065729
H	1.581414	-3.329438	-1.904914
H	0.067888	-3.426722	-1.018153
C	0.424629	-3.755717	-4.472033
H	0.538339	-2.029825	-5.794220
H	-0.946089	-2.128616	-4.851392
H	0.167674	-5.150806	-2.823265
H	-1.177193	-4.037271	-3.050703
H	-0.038805	-4.412051	-5.220710
H	1.509041	-3.937223	-4.525992

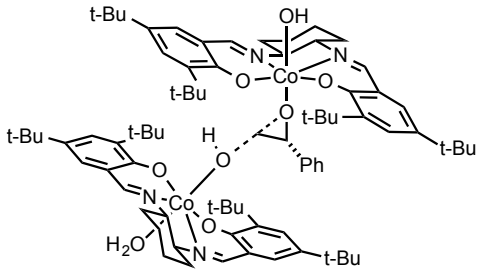

Transition State
Charge: 0
Spin Multiplicity: 1
Solvation: gas phase
Electronic Energy (AU): -6704.68500551
Gibbs Free Energy at 298.150 K (AU): -6702.985647

Co	0.222810	-3.327731	-0.005935
N	-0.273465	-4.189598	-1.621358
N	1.810880	-2.817292	-0.926492
C	2.906004	-2.445462	-0.358083
H	3.789237	-2.284178	-0.979369
C	-1.460511	-4.595855	-1.916703
H	-1.634750	-5.022243	-2.906764
C	3.093859	-2.219756	1.050019
C	1.999722	-2.243108	1.977316

C	4.419922	-1.984047	1.480571
C	2.321794	-2.031136	3.372848
H	5.198866	-1.993894	0.722375
C	3.649687	-1.818961	3.720950
H	3.881232	-1.688060	4.771912
C	-2.604207	-4.567468	-1.049652
C	-2.495650	-4.243313	0.341747
C	-3.840703	-4.947372	-1.622874
C	-3.690045	-4.393476	1.143486
H	-3.847190	-5.175883	-2.685183
C	-4.868690	-4.752460	0.505382
H	-5.763435	-4.838743	1.110600
O	0.765651	-2.405163	1.598201
O	-1.376689	-3.857428	0.893279
O	1.102510	-4.856941	0.531706
O	-0.683446	-1.720873	-0.750826
C	-0.173409	0.017083	-0.306808
C	-1.347393	-0.788830	0.067003
H	-0.122773	0.413695	-1.308412
H	0.742651	-0.172029	0.230164
H	-1.366934	-1.068648	1.123042
C	1.690802	-3.041404	-2.372084
C	0.878143	-4.347257	-2.513319
H	1.060970	-2.226579	-2.759059
H	1.484656	-5.152075	-2.075376
C	0.583651	-4.669688	-3.982119
H	0.063367	-5.631206	-4.065644
H	-0.084840	-3.903300	-4.400575
C	2.988771	-3.093578	-3.183018
H	3.515800	-2.134408	-3.118619
H	3.652646	-3.861396	-2.761158
C	1.886882	-4.720087	-4.795439
C	2.690959	-3.420368	-4.655935
H	3.631394	-3.491871	-5.215999
H	2.122896	-2.591516	-5.102968
H	1.657852	-4.914129	-5.850451
H	2.498604	-5.564411	-4.447265
H	0.481142	-5.277628	1.147365
N	2.161712	2.412018	0.960170
N	0.328266	4.039623	1.801371
C	-0.803348	4.556218	2.146974
H	-0.944640	4.841588	3.190097
C	3.159303	1.835889	0.372934
H	3.926773	1.374881	0.994793
C	-1.916935	4.814348	1.277148
C	-1.809428	4.691943	-0.140432
C	-3.115061	5.254305	1.887133
C	-2.948161	5.059517	-0.933540
H	-3.129954	5.324815	2.970547
C	-4.094958	5.473452	-0.263285
H	-4.957558	5.737141	-0.862132
C	3.372743	1.747216	-1.044491
C	2.386635	2.161972	-1.994061
C	4.627755	1.239472	-1.462733
C	2.708026	2.015649	-3.392400
H	5.329055	0.945064	-0.687911
C	3.966910	1.529765	-3.723430
H	4.211395	1.444274	-4.775183
O	-0.685818	4.297210	-0.719580
O	1.223233	2.659317	-1.635448
O	-0.377925	1.833027	0.492883
C	1.443874	3.842203	2.741701
C	2.008979	2.443348	2.426529
H	2.215002	4.573925	2.457326
H	1.229845	1.708849	2.670789
C	3.263151	2.145576	3.254059
H	3.595733	1.116554	3.082718
H	4.075698	2.816423	2.938437
C	1.141656	4.008601	4.233489
H	0.784751	5.024311	4.442386
H	0.342843	3.313702	4.527432
C	2.983871	2.339764	4.754373
C	2.407872	3.727971	5.060495
H	2.175115	3.816806	6.128018
H	3.161899	4.496914	4.839368
H	3.910218	2.179285	5.317906
H	2.277207	1.570101	5.091748
H	-1.258277	2.046358	0.137114
Co	0.712989	3.285165	0.096953
O	1.791131	4.950028	-0.395444
H	0.997234	5.409327	-0.743475
H	2.280789	4.677801	-1.192904
C	-3.651718	-4.188768	2.672489
C	-2.704301	-5.240191	3.299633
C	-3.163384	-2.762859	3.019002
C	-5.035941	-4.368495	3.329069
H	-3.082995	-6.254071	3.120977
H	-1.701284	-5.166015	2.877322
H	-2.633795	-5.092393	4.384989
H	-3.823610	-2.010293	2.569945
H	-3.171811	-2.614519	4.106901
H	-2.149936	-2.602075	2.653450
H	-4.940434	-4.216473	4.410444
H	-5.767626	-3.640659	2.958012
H	-5.442661	-5.374977	3.175569
C	1.221439	-2.097688	4.451510
C	0.166308	-0.992374	4.208853
C	0.542243	-3.487585	4.408603
C	1.772983	-1.900802	5.878352
H	0.613389	0.003080	4.333277
H	-0.249153	-1.063349	3.203528
H	-0.653235	-1.081564	4.932999
H	1.273644	-4.277961	4.615547
H	-0.245048	-3.546264	5.171154
H	0.097110	-3.674580	3.431978
H	0.944375	-1.956275	6.593690
H	2.494942	-2.678572	6.153324
H	2.255418	-0.924070	6.011417
C	1.689159	2.391418	-4.489342
C	0.426049	1.509081	-4.348416

C	1.306029	3.887017	-4.376767
C	2.246676	2.170243	-5.910392
H	0.679968	0.449592	-4.475856
H	-0.042237	1.638418	-3.372102
H	-0.309124	1.773587	-5.118367
H	2.193706	4.523165	-4.489906
H	0.601441	4.156740	-5.172910
H	0.831090	4.100874	-3.418812
H	1.480083	2.448102	-6.642200
H	3.130179	2.787579	-6.111853
H	2.508429	1.121858	-6.094531
C	-2.906728	5.007511	-2.475335
C	-1.838385	5.997820	-2.998879
C	-2.585927	3.572173	-2.954318
C	-4.252564	5.411663	-3.112221
H	-2.079730	7.025185	-2.699527
H	-0.846136	5.749580	-2.618034
H	-1.799118	5.966816	-4.094670
H	-3.349824	2.866158	-2.608818
H	-2.570733	3.540576	-4.051081
H	-1.614433	3.239394	-2.589124
H	-4.162972	5.351915	-4.202572
H	-5.067018	4.741282	-2.814497
H	-4.541668	6.440070	-2.864898
C	-4.999223	-5.025040	-0.878989
C	4.737456	-1.788132	2.811606
C	-4.230146	5.579166	1.141400
C	4.965169	1.138202	-2.796620
C	-6.372020	-5.392622	-1.465326
C	-6.912905	-6.671869	-0.783172
C	-7.364927	-4.229989	-1.226098
C	-6.302069	-5.655605	-2.981386
H	-6.237336	-7.518583	-0.950904
H	-7.019834	-6.541796	0.298953
H	-7.899177	-6.936982	-1.185430
H	-7.009789	-3.309789	-1.703996
H	-8.352533	-4.473304	-1.639196
H	-7.492910	-4.019967	-0.158840
H	-7.298934	-5.905774	-3.362968
H	-5.948532	-4.774779	-3.529783
H	-5.637124	-6.494412	-3.217829
C	6.175036	-1.616565	3.333336
C	6.523190	-2.793215	4.277501
C	7.208863	-1.603027	2.191873
C	6.313135	-0.288681	4.114644
H	5.848026	-2.835694	5.138745
H	6.447101	-3.750091	3.749369
H	7.547065	-2.692962	4.660259
H	7.025435	-0.783285	1.486509
H	8.216488	-1.467414	2.601563
H	7.204780	-2.543418	1.629563
H	7.326439	-0.183915	4.522711
H	6.123701	0.571578	3.461039
H	5.611392	-0.233481	4.954140
C	-5.562781	6.040892	1.754791
C	-6.687452	5.057804	1.351323
C	-5.502484	6.094310	3.292989
C	-5.912496	7.456726	1.237455
H	-6.808869	4.999957	0.264425
H	-6.474000	4.047237	1.718477
H	-7.646927	5.377448	1.776217
H	-4.745396	6.803702	3.647274
H	-6.470099	6.419689	3.690836
H	-5.281836	5.111904	3.726261
H	-6.863199	7.796903	1.666004
H	-5.136164	8.178293	1.516700
H	-6.013943	7.480523	0.147207
C	6.341092	0.667433	-3.299285
C	6.181790	-0.564071	-4.221360
C	7.012723	1.812315	-4.096170
C	7.278340	0.278246	-2.140897
H	5.748530	-1.409263	-3.674585
H	5.535084	-0.354252	-5.080063
H	7.157511	-0.878851	-4.611433
H	7.158535	2.696127	-3.464476
H	7.994313	1.494956	-4.469079
H	6.411807	2.115588	-4.960370
H	8.244058	-0.051419	-2.539822
H	7.470788	1.123907	-1.470657
H	6.869748	-0.546030	-1.544763
C	-2.703975	-0.333485	-0.417118
C	-3.485976	0.509567	0.385601
C	-3.186566	-0.718846	-1.671283
C	-4.724038	0.970484	-0.065098
H	-3.127842	0.793934	1.373135
C	-4.429862	-0.267408	-2.117545
H	-2.582997	-1.387589	-2.275131
C	-5.200125	0.581556	-1.319499
H	-5.319961	1.624686	0.566317
H	-4.800554	-0.582269	-3.089988
H	-6.169051	0.930161	-1.667897

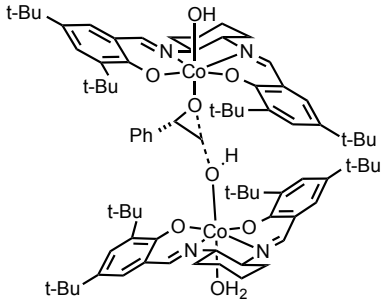

Transition State
Charge: 0
Spin Multiplicity: 1
Solvation: gas phase
Electronic Energy (AU): -6704.67826498
Gibbs Free Energy at 298.150 K (AU): -6702.981218

Co	3.528719	0.700381	-0.875905
N	4.762495	-0.743960	-0.887346
N	3.533554	0.542910	-2.770622
C	3.123916	1.459105	-3.581794
H	3.287000	1.315996	-4.651509
C	5.074338	-1.470553	0.128735
H	5.742954	-2.321270	-0.020550
C	2.449508	2.674075	-3.223490
C	2.045842	2.955987	-1.878120
C	2.165948	3.571718	-4.279429
C	1.340113	4.196770	-1.652545
C	1.497024	4.760512	-4.071951
H	2.501270	3.291502	-5.274216
C	1.101706	5.027615	-2.738169
H	0.575566	5.957529	-2.556656
C	4.663186	-1.242647	1.488980
C	3.990891	-0.039649	1.882457
C	5.063505	-2.203934	2.444453
C	3.823818	0.181949	3.303421
C	4.843217	-2.035148	3.797526
H	5.569762	-3.090752	2.072985
C	4.231297	-0.814725	4.180419
H	4.094952	-0.640771	5.241937
O	2.247382	2.123002	-0.893948
O	3.569693	0.848935	1.030937
O	4.928996	1.887641	-1.041509
O	2.108817	-0.713184	-0.806741
C	0.837625	-0.493601	-1.370318
H	0.674899	0.541352	-1.685208
C	4.203840	-0.683619	-3.222360
C	5.352108	-0.919768	-2.218929
H	3.480787	-1.501092	-3.089198
H	6.055730	-0.083199	-2.331636
C	6.079060	-2.239209	-2.497323
H	6.927324	-2.361554	-1.813171
H	5.395878	-3.082581	-2.319723
C	4.713272	-0.710710	-4.667598
H	3.879160	-0.599915	-5.370664
H	5.392530	0.137435	-4.832473
C	6.583711	-2.276530	-3.949795
C	5.447315	-2.031592	-4.951660
H	5.839658	-2.023542	-5.975919
H	4.728969	-2.862279	-4.898338
H	7.066329	-3.241142	-4.149609
H	7.356481	-1.506155	-4.082192
H	4.981843	2.308337	-0.168600
C	0.434207	-0.736176	0.028800
H	0.475883	-1.752625	0.388313
H	0.579564	0.072657	0.729234
N	-2.026597	-0.266334	2.812130
N	-2.159725	-2.693175	1.922897
C	-2.085194	-3.777214	1.219335
H	-1.533504	-4.621876	1.634545
C	-2.194587	0.948663	3.225971
H	-1.636272	1.272093	4.104665
C	-2.703288	-4.007373	-0.051573
C	-3.662199	-3.099299	-0.594815
C	-2.416934	-5.240473	-0.685237
C	-4.333705	-3.484179	-1.805440
C	-3.048540	-5.620218	-1.850445
H	-1.682441	-5.887274	-0.215050
C	-4.000437	-4.709968	-2.370177
H	-4.508899	-4.997420	-3.282218
C	-3.049326	1.942402	2.646358
C	-3.779085	1.717217	1.438276
C	-3.115034	3.187658	3.321089
C	-4.566835	2.806043	0.921013
C	-3.882906	4.230509	2.849947
H	-2.532092	3.294158	4.230773
C	-4.588325	3.991422	1.644825
H	-5.187517	4.805577	1.256439
O	-3.979885	-1.975361	0.018399
O	-3.755021	0.563465	0.802616
O	-1.528260	-0.746098	0.137049
C	-1.656996	-2.595954	3.302654
C	-1.061872	-1.184859	3.447893
H	-2.546773	-2.636665	3.949253
H	-0.145187	-1.146050	2.842513
C	-0.694788	-0.908533	4.911315
H	-0.235937	0.079104	5.019801
H	-1.609046	-0.913594	5.522069
C	-0.668287	-3.668185	3.772812
H	-1.119237	-4.665192	3.705023
H	0.216380	-3.665414	3.121028
C	0.293215	-1.974746	5.414842
C	-0.251110	-3.397031	5.229259
H	0.501089	-4.132272	5.537326
H	-1.121062	-3.545197	5.884855
H	0.518319	-1.793344	6.472387
H	1.241364	-1.869016	4.871042
H	-1.793061	0.068848	-0.321532
Co	-2.921994	-1.057403	1.331541

O	-4.609763	-1.423192	2.424160
H	-5.014972	-1.903596	1.668037
H	-5.059971	-0.559352	2.434547
C	0.876276	4.592118	-0.236324
C	-0.122699	3.540907	0.304615
C	2.104303	4.694340	0.699193
C	0.160891	5.958085	-0.205137
H	-1.020969	3.502239	-0.325020
H	0.333229	2.550135	0.323302
H	-0.440836	3.801838	1.321924
H	2.785394	5.479954	0.350178
H	1.786649	4.952078	1.718202
H	2.651120	3.752018	0.731194
H	-0.138193	6.182134	0.825982
H	0.812416	6.773430	-0.540656
H	-0.747758	5.968090	-0.819130
C	3.260736	1.521059	3.823557
C	4.216080	2.668078	3.410624
C	1.853254	1.785530	3.241420
C	3.139613	1.556802	5.360897
H	5.204320	2.528012	3.864795
H	4.334468	2.705955	2.326864
H	3.820975	3.634472	3.749069
H	1.165940	0.979075	3.527942
H	1.449472	2.728141	3.633353
H	1.885795	1.844130	2.154265
H	2.733895	2.528201	5.666675
H	2.463505	0.781656	5.743979
H	4.109249	1.437523	5.857853
C	-5.393377	-2.573951	-2.460486
C	-6.593319	-2.381200	-1.502106
C	-4.761997	-1.205707	-2.806801
C	-5.951510	-3.168703	-3.770013
H	-7.063829	-3.344159	-1.268383
H	-6.282071	-1.910620	-0.568041
H	-7.351555	-1.740552	-1.969103
H	-3.921582	-1.335654	-3.498736
H	-5.505110	-0.559079	-3.290445
H	-4.395520	-0.704033	-1.911665
H	-6.685308	-2.473627	-4.193032
H	-5.168924	-3.317092	-4.523039
H	-6.463149	-4.125223	-3.609767
C	-5.350067	2.671283	-0.402356
C	-4.359895	2.413866	-1.563647
C	-6.375113	1.515566	-0.305261
C	-6.139616	3.950256	-0.749885
H	-3.668400	3.257593	-1.674309
H	-3.776786	1.507614	-1.395205
H	-4.905018	2.298595	-2.508520
H	-7.088607	1.700319	0.508223
H	-6.947085	1.440694	-1.238191
H	-5.879925	0.559665	-0.133211
H	-6.672750	3.795004	-1.694347
H	-6.888455	4.195999	0.012495
H	-5.484761	4.818741	-0.884490
C	5.270374	-3.056154	4.866347
C	6.306700	-2.414852	5.820265
C	4.039877	-3.505911	5.689327
C	5.909392	-4.312523	4.245226
H	7.201397	-2.103702	5.269320
H	5.902390	-1.529995	6.323103
H	6.613626	-3.128254	6.595957
H	3.294166	-3.984696	5.042899
H	4.332738	-4.228071	6.462314
H	3.556638	-2.660576	6.191193
H	6.188465	-5.018735	5.035975
H	5.218005	-4.827473	3.567963
H	6.818718	-4.069863	3.683912
C	1.174296	5.769649	-5.186535
C	1.820723	7.136940	-4.858443
C	1.706351	5.309506	-6.556754
C	-0.358435	5.947419	-5.303296
H	1.456401	7.542647	-3.908588
H	2.910216	7.044813	-4.783638
H	1.592421	7.870402	-5.642541
H	1.259729	4.357602	-6.866792
H	1.460090	6.055141	-7.321771
H	2.795770	5.189664	-6.548771
H	-0.604918	6.679534	-6.083139
H	-0.841768	4.998109	-5.562179
H	-0.799469	6.299806	-4.364641
C	-3.994128	5.595711	3.548805
C	-3.514869	6.712350	2.590859
C	-5.467708	5.858123	3.941796
C	-3.137667	5.661406	4.827120
H	-2.472695	6.552423	2.292621
H	-4.119025	6.756118	1.678408
H	-3.583894	7.691557	3.080369
H	-5.831020	5.091496	4.636029
H	-5.564937	6.834503	4.432281
H	-6.129423	5.858865	3.068761
H	-3.243798	6.646803	5.294332
H	-3.447935	4.912313	5.565160
H	-2.073387	5.511545	4.612113
C	-2.789012	-6.956282	-2.566573
C	-2.334212	-6.693376	-4.021377
C	-1.693656	-7.782840	-1.866586
C	-4.089648	-7.794707	-2.582146
H	-3.092067	-6.149355	-4.595013
H	-1.414269	-6.099169	-4.039783
H	-2.143172	-7.641100	-4.539966
H	-1.973012	-8.043592	-0.839080
H	-1.531529	-8.720310	-2.410380
H	-0.737810	-7.247018	-1.836823
H	-3.927313	-8.746212	-3.103427
H	-4.423494	-8.018093	-1.562243
H	-4.904956	-7.270813	-3.092450
C	0.432533	-1.461463	-2.454869
C	0.945491	-2.764135	-2.481840
C	-0.432029	-1.052811	-3.476694

C	0.598580	-3.640154	-3.510973
H	1.638586	-3.069620	-1.703325
C	-0.786277	-1.929263	-4.503799
H	-0.818998	-0.036067	-3.474719
C	-0.268250	-3.225458	-4.525312
H	1.012579	-4.645740	-3.527609
H	-1.452587	-1.594300	-5.294746
H	-0.530549	-3.904993	-5.331975

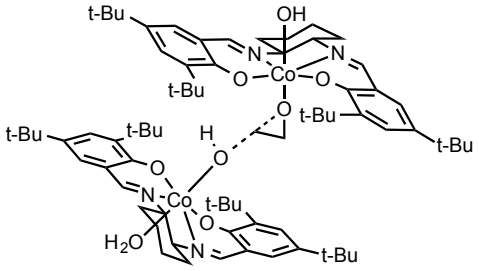

Transition state

Charge: 0
Spin Multiplicity: 1
Solvation: gas phase
Electronic Energy (AU): -6473.62509295
Gibbs Free Energy at 298.150 K (AU): -6472.000841

Co	-3.254765	-0.586276	-0.091844
N	-4.165953	-0.282665	-1.728522
N	-2.449665	-2.070428	-0.970366
C	-1.894612	-3.069173	-0.375199
H	-1.562711	-3.918142	-0.976259
C	-4.756512	0.813600	-2.058723
H	-5.178532	0.898161	-3.062369
C	-1.662098	-3.186788	1.039806
C	-1.894165	-2.095494	1.940994
C	-1.198184	-4.438961	1.503316
C	-1.643316	-2.343769	3.345547
H	-1.061976	-5.223407	0.763422
C	-1.196647	-3.602479	3.726401
H	-1.036437	-3.782959	4.783389
C	-4.947894	1.959359	-1.213252
C	-4.644700	1.930058	0.187003
C	-5.526682	3.100001	-1.816685
C	-5.023790	3.090706	0.962725
H	-5.725951	3.050411	-2.883706
C	-5.572226	4.177238	0.295824
H	-5.834180	5.049693	0.882692
O	-2.271767	-0.919999	1.532772
O	-4.083135	0.905426	0.768672
O	-4.605031	-1.725090	0.447248
O	-1.847610	0.585760	-0.835532
C	-0.026659	0.422929	-0.365751
C	-1.055690	1.409869	-0.017886
H	0.371316	0.424212	-1.367810
H	-0.056385	-0.511910	0.171167
H	-1.346771	1.433949	1.033244
C	-2.661289	-2.013211	-2.420953
C	-4.090994	-1.456678	-2.602161
H	-1.968072	-1.248690	-2.801895
H	-4.780873	-2.193358	-2.167797
C	-4.427758	-1.248211	-4.082385
H	-5.466567	-0.915798	-4.194741
H	-3.788119	-0.455549	-4.496761
C	-2.454390	-3.309663	-3.210110
H	-1.416686	-3.651198	-3.117104
H	-3.096839	-4.098092	-2.792930
C	-4.217290	-2.549804	-4.873877
C	-2.795345	-3.097372	-4.694200
H	-2.679369	-4.042454	-5.238859
H	-2.075639	-2.392060	-5.134783
H	-4.426309	-2.374783	-5.936380
H	-4.941551	-3.302714	-4.531986
H	-5.148080	-1.180484	1.039272
N	2.736628	-1.414870	1.033830
N	3.990603	0.728540	1.778241
C	4.286940	1.951704	2.065211
H	4.534748	2.195818	3.098842
C	2.354633	-2.527776	0.497172
H	2.034223	-3.334862	1.155958
C	4.336079	3.050289	1.139493
C	4.238075	2.852650	-0.270173
C	4.540893	4.338353	1.686642
C	4.372296	4.002093	-1.119618
H	4.607156	4.420082	2.767288
C	4.562430	5.238294	-0.509472
H	4.652175	6.105983	-1.151109
C	2.315891	-2.823389	-0.907569
C	2.547861	-1.826376	-1.906252
C	2.045281	-4.168674	-1.260958
C	2.464843	-2.236497	-3.286187
H	1.879178	-4.872124	-0.450988
C	2.217649	-3.577707	-3.552333
H	2.180922	-3.885072	-4.590153
O	4.072365	1.646022	-0.791904
O	2.828411	-0.576284	-1.606426
O	1.702044	0.950036	0.439793
C	3.996911	-0.356016	2.773957
C	2.729423	-1.186935	2.491343
H	4.860488	-0.991447	2.526350
H	1.860079	-0.548886	2.698952
C	2.667694	-2.433417	3.380008
H	1.719737	-2.960471	3.230284
H	3.479850	-3.120519	3.100516
C	4.095309	0.045726	4.248247
H	5.024536	0.597490	4.435343
H	3.260732	0.712393	4.505650
C	2.800385	-2.050716	4.864500
C	4.054124	-1.209618	5.135860

H	4.092778	-0.913757	6.190669
H	4.952620	-1.814421	4.947237
H	2.815866	-2.962769	5.472377
H	1.910123	-1.486773	5.172859
H	1.780871	1.849851	0.080689
Co	3.334639	0.124159	0.096975
O	5.170799	-0.648879	-0.345386
H	5.481670	0.197582	-0.731494
H	4.994455	-1.216239	-1.118162
C	-4.855651	3.109349	2.496314
C	-5.730343	1.992508	3.116216
C	-3.374095	2.897845	2.885809
C	-5.305217	4.444424	3.125054
H	-6.791425	2.174321	2.905762
H	-5.460576	1.014636	2.715515
H	-5.601740	1.967515	4.206090
H	-2.746312	3.689035	2.456045
H	-3.262238	2.936317	3.977366
H	-3.012575	1.932740	2.532794
H	-5.167606	4.392765	4.211379
H	-4.716026	5.294153	2.759314
H	-6.364981	4.656253	2.940353
C	-1.928321	-1.251693	4.396634
C	-1.034775	-0.014796	4.141856
C	-3.420088	-0.846878	4.322465
C	-1.653472	-1.725977	5.838322
H	0.023851	-0.264836	4.295256
H	-1.160030	0.355144	3.124148
H	-1.289643	0.791555	4.841115
H	-4.061330	-1.709502	4.539859
H	-3.637608	-0.067496	5.063999
H	-3.673203	-0.468273	3.332784
H	-1.872118	-0.906460	6.532701
H	-2.286950	-2.574093	6.123051
H	-0.605859	-2.014461	5.991944
C	2.645213	-1.221341	-4.434615
C	1.540870	-0.141345	-4.347352
C	4.041894	-0.558998	-4.352787
C	2.533885	-1.880516	-5.824941
H	0.547501	-0.595785	-4.445133
H	1.584679	0.392857	-3.397582
H	1.657430	0.589152	-5.157522
H	4.833831	-1.316242	-4.421380
H	4.178500	0.139755	-5.187115
H	4.159044	-0.002697	-3.422208
H	2.660959	-1.112481	-6.595833
H	3.307446	-2.640136	-5.989033
H	1.554220	-2.345204	-5.986063
C	4.312255	3.877827	-2.656623
C	5.481142	2.994122	-3.154514
C	2.958840	3.263397	-3.085882
C	4.439698	5.243418	-3.362274
H	6.446654	3.441902	-2.889386
H	5.432360	1.992895	-2.723519
H	5.443650	2.896875	-4.246404
H	2.126186	3.901111	-2.764294
H	2.912160	3.182169	-4.178874
H	2.822586	2.268218	-2.662464
H	4.382471	5.091862	-4.445780
H	3.630214	5.928699	-3.085369
H	5.396747	5.735152	-3.151747
C	-5.831131	4.236404	-1.095704
C	-0.962410	-4.686933	2.842811
C	4.647652	5.457611	0.885521
C	2.010846	-4.583681	-2.576194
C	-6.437350	5.507886	-1.712236
C	-7.812136	5.802677	-1.065733
C	-5.492417	6.708212	-1.465744
C	-6.646270	5.371668	-3.232245
H	-8.508366	4.973521	-1.236313
H	-7.730272	5.950096	0.016473
H	-8.253347	6.712799	-1.492427
H	-4.516700	6.538047	-1.935516
H	-5.918146	7.628793	-1.885556
H	-5.321181	6.878069	-0.397355
H	-7.070117	6.298985	-3.635263
H	-5.701916	5.183328	-3.756064
H	-7.339940	4.558371	-3.475288
C	-0.540803	-6.058278	3.399844
C	-1.645847	-6.590977	4.344391
C	-0.328733	-7.099532	2.284537
C	0.781749	-5.935216	4.192706
H	-1.820843	-5.911820	5.185295
H	-2.593797	-6.704236	3.806925
H	-1.365768	-7.569089	4.756465
H	0.457105	-6.792802	1.583438
H	-0.024654	-8.057584	2.722079
H	-1.246735	-7.273672	1.712408
H	1.067663	-6.903535	4.622999
H	1.598899	-5.602456	3.540843
H	0.697002	-5.219009	5.016943
C	4.852923	6.881451	1.430113
C	3.673540	7.780140	0.987611
C	4.923408	6.906656	2.968531
C	6.176043	7.463511	0.878037
H	3.586722	7.833975	-0.102852
H	2.723194	7.400453	1.379651
H	3.811320	8.802486	1.360031
H	5.762388	6.311630	3.348028
H	5.066681	7.935837	3.315867
H	4.000480	6.530709	3.424967
H	6.330538	8.483186	1.251491
H	7.032283	6.854083	1.189381
H	6.178395	7.507905	-0.216257
C	1.797667	-6.044501	-3.009303
C	0.565380	-6.154266	-3.937472
C	3.051038	-6.538230	-3.771931
C	1.572861	-6.977654	-1.804565
H	-0.347954	-5.846064	-3.416066
H	0.668052	-5.529789	-4.831449

H	0.430231	-7.190210	-4.271524
H	3.942111	-6.484824	-3.135976
H	2.921127	-7.580192	-4.089190
H	3.244653	-5.939834	-4.668931
H	1.422098	-8.005307	-2.153622
H	2.434264	-6.984241	-1.126645
H	0.685312	-6.693292	-1.227197
H	-0.925943	2.424130	-0.416955

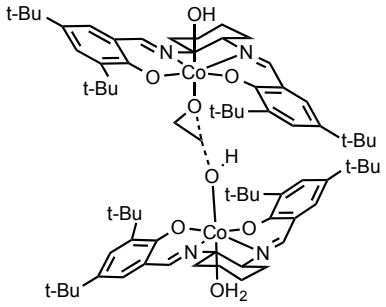

Transition State
Charge: 0
Spin Multiplicity: 1
Solvation: gas phase
Electronic Energy (AU): -6473.62268986
Gibbs Free Energy at 298.150 K (AU): -6472.000356

Co	-3.135237	1.509581	-0.937804
N	-4.829324	0.849428	-0.388902
N	-3.444136	2.933417	0.280455
C	-2.827797	4.066856	0.251179
H	-3.169984	4.862287	0.916125
C	-5.264850	-0.345961	-0.584881
H	-6.225113	-0.631673	-0.150016
C	-1.704757	4.402526	-0.575998
C	-1.043450	3.432505	-1.398156
C	-1.253725	5.741215	-0.509046
C	0.099597	3.889643	-2.156333
C	-0.169663	6.187328	-1.236329
H	-1.801135	6.419008	0.140109
C	0.475694	5.221154	-2.046506
H	1.329003	5.554803	-2.625597
C	-4.623729	-1.360562	-1.379438
C	-3.485100	-1.072422	-2.201512
C	-5.240415	-2.631863	-1.400042
C	-3.062348	-2.111198	-3.118177
C	-4.794414	-3.654689	-2.213799
H	-6.099189	-2.777379	-0.750468
C	-3.708762	-3.339625	-3.068883
H	-3.378242	-4.113773	-3.752210
O	-1.407687	2.180273	-1.436510
O	-2.862107	0.069947	-2.175119
O	-3.959665	2.528778	-2.236856
O	-2.405591	0.437656	0.568125
C	-1.197425	0.797189	1.198434
H	-0.783241	1.760580	0.893622
C	-4.581464	2.659586	1.166847
C	-5.600260	1.888360	0.300516
H	-4.218496	1.960312	1.934947
H	-5.931873	2.574705	-0.491050
C	-6.810477	1.435183	1.123787
H	-7.548712	0.942717	0.479592
H	-6.491387	0.696317	1.873276
C	-5.235401	3.860740	1.859005
H	-4.515790	4.366777	2.514115
H	-5.550940	4.590660	1.100483
C	-7.463276	2.637869	1.825959
C	-6.452238	3.409581	2.684153
H	-6.931456	4.282901	3.143214
H	-6.112559	2.769086	3.510967
H	-8.303401	2.295886	2.442754
H	-7.885034	3.312836	1.068025
H	-3.760570	2.061663	-3.063699
C	-0.707622	-0.369066	0.462940
H	-0.978232	-1.341936	0.842229
H	-0.552572	-0.261685	-0.599117
N	2.160263	-2.805029	-0.430762
N	1.088015	-3.134558	1.901378
C	0.395084	-2.941202	2.976781
H	-0.438301	-3.614930	3.181901
C	2.865712	-2.603042	-1.496909
H	2.594112	-3.147663	-2.401490
C	0.635770	-1.925154	3.959121
C	1.847966	-1.169093	3.968349
C	-0.336042	-1.772916	4.976643
C	2.066402	-0.274594	5.071511
C	-0.159313	-0.884423	6.017240
H	-1.233790	-2.380118	4.908426
C	1.061859	-0.167581	6.026987
H	1.221532	0.517849	6.850336
C	3.990964	-1.725969	-1.628380
C	4.434326	-0.882869	-0.563259
C	4.642166	-1.720970	-2.887886
C	5.569331	-0.032659	-0.813421
C	5.732181	-0.916403	-3.139319
H	4.249038	-2.379221	-3.656656
C	6.159023	-0.091836	-2.069470
H	7.012585	0.548475	-2.252812
O	2.767758	-1.326747	3.036269
O	3.849969	-0.869312	0.617752
O	1.183179	-0.630410	0.904453
C	0.864705	-4.262290	0.983178
C	0.968214	-3.675276	-0.436378
H	1.724307	-4.935822	1.117911
H	0.099685	-3.018784	-0.587337
C	0.925386	-4.787973	-1.490767
H	0.941106	-4.365866	-2.501292
H	1.817026	-5.422737	-1.387198

C	-0.421860	-5.074986	1.160515
H	-0.460304	-5.519594	2.162245
H	-1.294425	-4.413881	1.063140
C	-0.352809	-5.627845	-1.321761
C	-0.490337	-6.187435	0.100021
H	-1.436611	-6.731097	0.201071
H	0.311518	-6.915622	0.288380
H	-0.350639	-6.446652	-2.050689
H	-1.225651	-5.003315	-1.554766
H	1.663072	0.099295	0.478454
Co	2.432408	-1.960412	1.251701
O	3.893057	-3.265541	1.828183
H	3.897118	-2.892523	2.737615
H	4.680838	-2.875717	1.406487
C	0.878987	2.922752	-3.070433
C	1.497950	1.785227	-2.221771
C	-0.070972	2.335064	-4.140232
C	2.039040	3.612529	-3.816770
H	2.217187	2.193485	-1.499852
H	0.720881	1.248242	-1.676466
H	2.033564	1.073797	-2.863616
H	-0.460769	3.133001	-4.783729
H	0.469017	1.621569	-4.776583
H	-0.913907	1.822869	-3.676947
H	2.544097	2.875887	-4.452758
H	1.687224	4.421299	-4.467863
H	2.790652	4.023970	-3.132237
C	-1.964275	-1.833986	-4.167058
C	-2.439751	-0.700672	-5.109601
C	-0.641175	-1.419957	-3.483908
C	-1.659974	-3.063528	-5.047536
H	-3.348436	-1.002272	-5.644203
H	-2.653347	0.210193	-4.548856
H	-1.666916	-0.474727	-5.855352
H	-0.280988	-2.225388	-2.830017
H	0.133153	-1.227444	-4.237590
H	-0.777379	-0.518206	-2.888230
H	-0.877707	-2.802691	-5.769775
H	-1.294829	-3.915857	-4.460096
H	-2.534863	-3.393637	-5.619219
C	3.368155	0.543882	5.195346
C	4.583436	-0.409707	5.297904
C	3.520488	1.468666	3.966552
C	3.386185	1.437483	6.452345
H	4.497545	-1.057338	6.179081
H	4.667794	-1.039489	4.410881
H	5.510027	0.169386	5.394991
H	2.688387	2.180951	3.914830
H	4.451726	2.044264	4.040106
H	3.540531	0.892769	3.042091
H	4.331700	1.990279	6.483792
H	2.577071	2.176917	6.445359
H	3.315939	0.855891	7.379308
C	6.098159	0.938330	0.263189
C	5.009712	1.994365	0.570430
C	6.480872	0.168059	1.550607
C	7.359493	1.698193	-0.198184
H	4.787727	2.587310	-0.324656
H	4.085722	1.525434	0.911055
H	5.353946	2.681457	1.353267
H	7.254909	-0.580325	1.336096
H	6.887865	0.861768	2.296196
H	5.615270	-0.330486	1.987096
H	7.690831	2.361339	0.608559
H	8.190378	1.020608	-0.428635
H	7.170990	2.325867	-1.076601
C	-5.437943	-5.051068	-2.262788
C	-5.991051	-5.326598	-3.681631
C	-4.384421	-6.129258	-1.914123
C	-6.603260	-5.187973	-1.264438
H	-6.752603	-4.586443	-3.951870
H	-5.203224	-5.284580	-4.441212
H	-6.449305	-6.322712	-3.732292
H	-3.990683	-5.974735	-0.901982
H	-4.826922	-7.132804	-1.956741
H	-3.538559	-6.109811	-2.610009
H	-7.025608	-6.198098	-1.320041
H	-6.275350	-5.021130	-0.231683
H	-7.410834	-4.480380	-1.483979
C	0.344995	7.636091	-1.206129
C	0.260455	8.248811	-2.624640
C	-0.479189	8.523572	-0.254293
C	1.816471	7.661147	-0.728247
H	0.853479	7.679848	-3.348605
H	-0.775602	8.261750	-2.981778
H	0.635008	9.280559	-2.623721
H	-0.436283	8.159719	0.779013
H	-0.084135	9.546196	-0.262336
H	-1.531875	8.573048	-0.555502
H	2.200147	8.689444	-0.711785
H	1.905022	7.247977	0.283261
H	2.467863	7.074541	-1.384897
C	6.471420	-0.869612	-4.486981
C	6.398306	0.562446	-5.069049
C	7.953785	-1.263135	-4.282446
C	5.857261	-1.836467	-5.516835
H	5.358079	0.866391	-5.231613
H	6.859950	1.298976	-4.402776
H	6.922737	0.611314	-6.031256
H	8.037967	-2.283039	-3.889730
H	8.495763	-1.219232	-5.235096
H	8.462389	-0.592566	-3.581515
H	6.410539	-1.772914	-6.460450
H	5.904248	-2.877772	-5.176943
H	4.810735	-1.591715	-5.731814
C	-1.191310	-0.658762	7.134628
C	-1.625850	0.826304	7.146490
C	-2.450545	-1.524477	6.940901
C	-0.565644	-1.019209	8.503142
H	-0.777993	1.498673	7.315632

H	-2.088167	1.106157	6.193032
H	-2.355963	1.005486	7.945411
H	-2.216062	-2.595266	6.960797
H	-3.163123	-1.329067	7.750113
H	-2.956296	-1.301596	5.994276
H	-1.289250	-0.854945	9.311122
H	-0.260470	-2.071653	8.528679
H	0.318220	-0.410391	8.721722
H	-1.220716	0.696312	2.289600

Chapter 3

The Mechanism of α-Chloroether Activation by H-Bond Donor Catalysts: Cooperative Anion Abstraction[1]

3.1 Introduction

Hydrogen bond (H-bond) donors such as chiral urea and thiourea derivatives are an emerging class of catalysts that promote a range of highly enantioselective transformations.[2] These catalysts have many desirable properties compared to transition metal catalysts, including stability to air and moisture, comparatively low cost, and ease of synthesis from abundant building blocks. In spite of this, H-bond donor catalysis has been slow to make inroads into the set of exceptionally general and practical methods that comprise the toolkit of the synthetic chemist. A significant limitation that has hampered the application of these catalysts is that they often suffer from low catalytic activity. While there are some noteworthy examples that stand apart from this trend,[3] many H-bond donor-catalyzed reactions require high catalyst loadings

[1] The research presented in this chapter was performed in collaboration with Dr. Dan Lehnherr. This work is being prepared in article form: Ford, D. D.; Lehnherr, D.; Jacobsen, E. N. *Manuscript in preparation.*

[2] (a) Taylor, M. S.; Jacobsen, E. N. *Angew. Chem. Int. Ed.* **2006**, *45*, 1520–1543. (b) Doyle, A. G.; Jacobsen, E. N. *Chem. Rev.* **2007**, *107*, 5713–5743.

[3] Selected examples: (a) Zuend, S. J.; Coughlin, M. P.; Lalonde, M. P.; Jacobsen, E. N. *Nature* **2009**, *461*, 968–970. (b) Martin, C. L.; Rötheli, A. R.; Jacobsen, E. N. *Manuscript in preparation.*

(10–20 mol %) and long reaction times (several days). Furthermore, these catalysts are often most effective under dilute reaction conditions (less than 0.1 M in substrate), making it impractical to apply these reactions on large scale. For this reason, the development of highly active H-bond donor catalysts is an important challenge, whose solution could be transformative to the field. In spite of this, fundamental mechanistic details of H-bond donor catalysis have not been rigorously investigated. An understanding of how H-bond donors activate their substrates could yield new catalyst design principles that could lead to more active catalysts.

H-bond donor-catalyzed reactions can be broadly divided into categories according to the mode by which the catalyst engages its substrate.[4] Perhaps the most apparent way for an H-bond donor catalyst to activate an electrophilic compound is for it to bind in such a way that it can provide increased stabilization as negative charge builds concomitant with the nucleophile's attack (Scheme 3.1**A**). This mode of activation is analogous to the oxyanion hole formed by amide H-bond donors that is thought to stabilize tetrahedral intermediates in serine proteases and other classes of hydrolases.[5] This type of direct activation has been shown to be viable in the case of a thiourea-catalyzed ketone cyanosilation reaction[6] and a guanidinium-catalyzed Claisen rearrangement.[7]

The anion-binding mode of catalysis—wherein an H-bond donor stabilizes a reactive cationic intermediate by binding its counter-anion—is a conceptually distinct mechanism that

[4] Knowles, R. R.; Jacobsen, E. N. *Proc. Natl. Acad. Sci. U. S. A.* **2010**, *107*, 20678–20685.

[5] This elucidation of the mechanism of action of chymotrypsin and related proteases is one of the landmark achievements of mechanistic enzymology. As a starting point, we direct the reader to the first report of the concept of the oxyanion hole (a), and two reviews of the mechanism of serine proteases (b, c). (a) Henderson, R. *J. Mol. Biol.* **1970**, *54*, 341–354. (b) Warshel, A.; Naray-Szabo, G.; Sussman, F.; Hwang, J.-K. *Biochemistry* **1989**, *28*, 3629–3637. (c) Hedstrom, L. *Chem. Rev.* **2002**, *102*, 4501–4523.

[6] Zuend, S. J.; Jacobsen, E. N. *J. Am. Chem. Soc.* **2007**, *129*, 15872–15883.

[7] Uyeda, C.; Jacobsen, E. N. *J. Am. Chem. Soc.* **2011**, *133*, 5062–5075.

has become increasingly important in H-bond donor catalysis.[8,9] Anion binding catalysis can itself be subdivided according to the origin of the key ion pair intermediate. In one scenario, an H-bond donor catalyst abstracts an anionic leaving group from a neutral substrate to generate a reactive cationic intermediate (Scheme 3.1**B**).[10] An H-bond donor can also bind a neutral Brønsted acid, rendering it more acidic by stabilizing its conjugate base (Scheme 3.1**C**).[11] In the case of a recently developed, enantioselective Povarov reaction that is co-catalyzed by a urea and triflic acid, the H-bond donor binds an iminium•triflate ion pair, directing the reaction of the iminium ion with an electron-rich alkene (Scheme 3.1**D**).[12] Notably, the chiral sulfinamidourea actually *decelerates* the reaction relative to the reaction catalyzed by triflic acid alone: the H-bond donor's role is solely to bind the ion pair and induce selectivity.

[8] Zhuang, Z.; Schreiner, P. R. *Chem. Soc. Rev.* **2009**, *38*, 1187–1198.

[9] We note the parallels between this concept and the use of chiral counteranions to achieve selectivity with an achiral, cationic catalyst. While the mechanism of catalysis in these cases involves covalent catalyst-substrate binding, stereoinduction has been proposed to occur by non-covalent interactions. (a) Mayer, S.; List, B. *Angew. Chem. Int. Ed.* **2006**, *45*, 4193–4195. (b) Hamilton, G. L.; Kang, E. J.; Mba, M.; Toste, F. D. *Science* **2007**, *317*, 496–499.

[10] Raheem, I. T.; Thiara, P. S.; Peterson, E. A.; Jacobsen, E. N. *J. Am. Chem. Soc.* **2007**, *129*, 13404–13405.

[11] Klausen, R. S.; Jacobsen, E. N. *Org. Lett.* **2009**, *11*, 887–890.

[12] Xu, H.; Zuend, S. J.; Woll, M. G.; Tao, Y.; Jacobsen, E. N. *Science* **2010**, *327*, 986–990.

Scheme 3.1. Selected modes by which a dual H-bond donor can promote selective reactions of electrophilic functional groups.

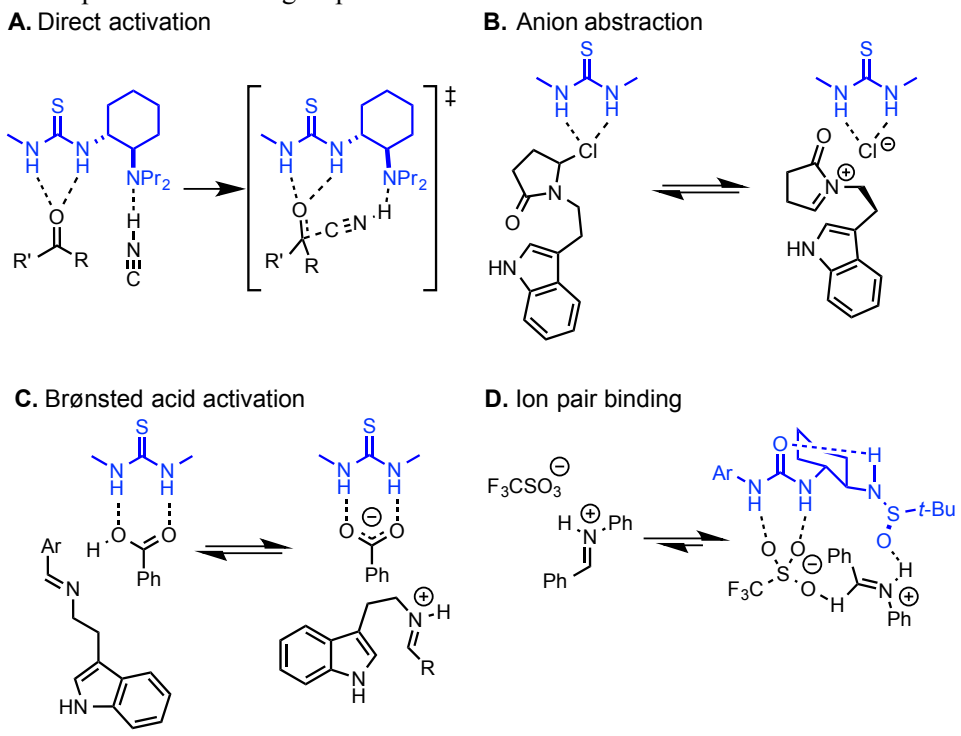

Anion abstraction (Scheme 3.1**B**) has been used in a predictive sense to discover several new urea- and thiourea-catalyzed reactions,[13,14] and while ion pair intermediates have been implicated in these reactions, no reaction proposed to proceed by this mechanism has been rigorously characterized. In this article, we describe our investigations into the mechanism of anion abstraction in the context of the enantioselective alkylation of α-chloroether electrophiles with silyl ketene acetals catalyzed by **1a** (Scheme 3.2).[13] We selected this reaction because the active chloroether electrophile can be isolated and distilled to purity, and that as an intermolecular reaction, it is possible to study catalyst-electrophile interactions without nucleophilic addition complicating the analysis. To gain additional insight into the mechanism of

[13] Reisman, S. E.; Doyle, A. G.; Jacobsen, E. N. *J. Am. Chem. Soc.* **2008**, *130*, 7198–7199.

[14] (a) Raheem, I. T.; Thiara, P. V.; Jacobsen, E. N. *Org. Lett.* **2008**, *10*, 1577–1580. (b) Peterson, E. A.; Jacobsen, E. N. *Angew. Chem., Int. Ed.* **2009**, *48*, 6446–6449. (c) De, C. K.; Klauber, E. G.; Seidel, D. *J. Am. Chem. Soc.* **2009**, *131*, 17060–17061. (d) Knowles, R. R.; Lin, S.; Jacobsen, E. N. *J. Am. Chem. Soc.* **2010**, *132*, 5030-5032. (e) Brown, A. R.; Kuo, W.-H.; Jacobsen, E. N. *J. Am. Chem. Soc.* **2010**, *132*, 9286–9288. (f) Burns, N. Z.; Witten, M. G.; Jacobsen, E. N. *J. Am. Chem. Soc.* **2011**, *133*, 14578–14581.

this reaction and into the differences between related urea and thiourea catalysts, we repeated many of our analyses using the urea analog (**1b**) of the optimal thiourea catalyst **1a**.[15]

Scheme 3.2. Thiourea-catalyzed asymmetric alkylation of chloroisochromans.

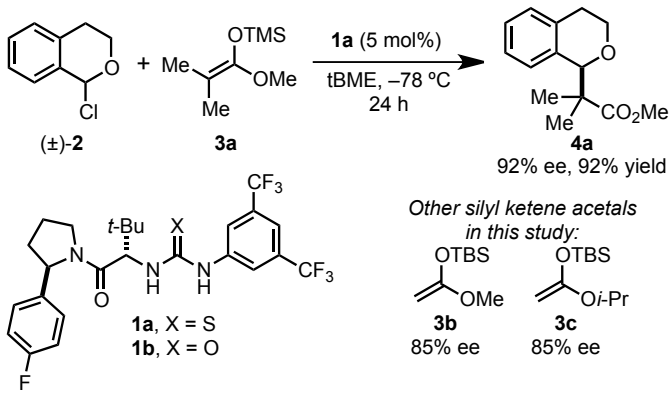

We initially observed that these reactions displayed a near-first-order kinetic dependence on the concentration of H-bond donor catalyst, but deviation from the first-order dependence at low catalyst loading led us to determine that the resting state of the catalyst is dimeric under typical reaction conditions. Hence, the observed first-order dependence indicates that both units of the dimer act cooperatively in the turnover-limiting transition state (Scheme 3.3). We discuss the implications of this discovery for the design of new H-bond donors of higher activity.

[15] **1b** is a competent, but less selective catalyst for the formation of **4a** (84 % ee), **4b** (67% ee), and **4c** (65% ee).

Scheme 3.3. Mechanism for chloroether alkylation established in this chapter.

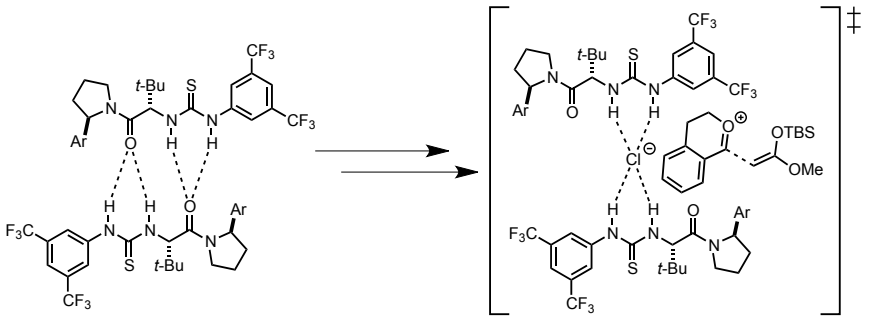

3.2 Kinetics of Chloroether Racemization

The alkylation reaction of **2** transforms a chiral, racemic substrate into enantioenriched products in high yield. There are two limiting mechanisms that could lead to this stereoconvergent behavior. In one, the thiourea acts by direct activation and makes chloride a better leaving group for a stereospecific, invertive S_N2 displacement reaction (Scheme 3.4, **A**). In this scenario, a separate racemization step would be necessary to achieve a yield greater than 50% by means of a dynamic kinetic resolution (DKR).[16] An alternative mechanism involves an S_N1-type ionization of **2** to form an oxocarbenium•chloride ion pair followed by rate-determinining C–C bond formation (Scheme 3.4, **B**). In this mechanism, racemization could occur by means of a reversible ionization step: the chloride ion could attack either π-face of the oxocarbenium ion to form either enantiomer of **2**. Because the S_N2-type mechanism requires background racemization of **2**, while the S_N1-type mechanism would lead to H-bond donor-catalyzed racemization, we reasoned that determining the dependence of the racemization rate on

[16] Theoretically, greater than 50% yield could be achieved without racemization by two stereospecific mechanisms: an invertive and retentive mechanism for transforming both enantiomers of **2** into a single enantiomer of product. This is has precedent in the context of S_N2' allylic substitution reactions: Ito, H.; Kunii, S.; Sawamura, M. *Nature Chem.* **2010**, *2*, 972–976.

the concentration of catalyst could allow us to state definitively whether the oxocarbenium•chloride ion pair invoked in an anion abstraction mechanism is accessible by H-bond donor catalysts.

Scheme 3.4. Two mechanisms that would lead to stereoconvergent chloroether alkylation.

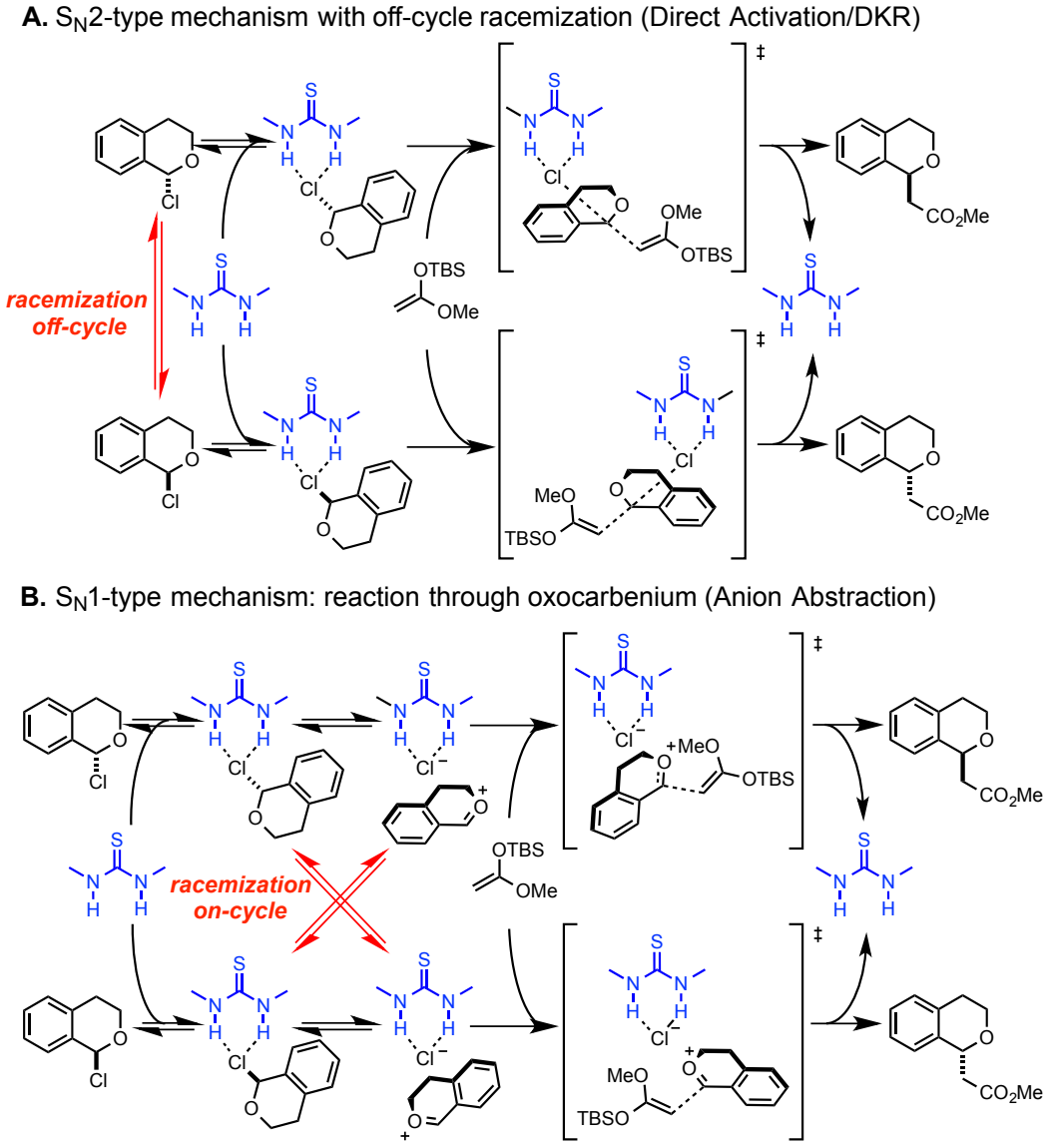

The most apparent way to perform such an experiment would be to isolate **2** in enantiomerically enriched form, then expose it to catalyst and monitor the e.e. of **2** over time. We considered this, but there are no known methods for the preparation of highly reactive chloroethers such as **2** in enantioenriched form. Examination of the ^{1}H NMR spectrum of **2**

suggested a second strategy to measure the rate of racemization. The protons in the diastereotopic pairs H_A/H_B and H_C/H_D are separated from one another by ca. 0.5 ppm according to their stereochemical relationship to the C1 stereogenic center (Figure 3.1). If racemization were fast compared to the difference in the Larmor frequencies, H_A and H_B should coalesce, as should H_C and H_D. While no broadening was observed even at elevated temperatures at a 500 MHz ^{1}H frequency, this only indicated that racemization was slower than the difference of the Larmor frequencies, i.e. that the first order rate constant for racemization is less than ca. 10^2 s^{-1} at that temperature.

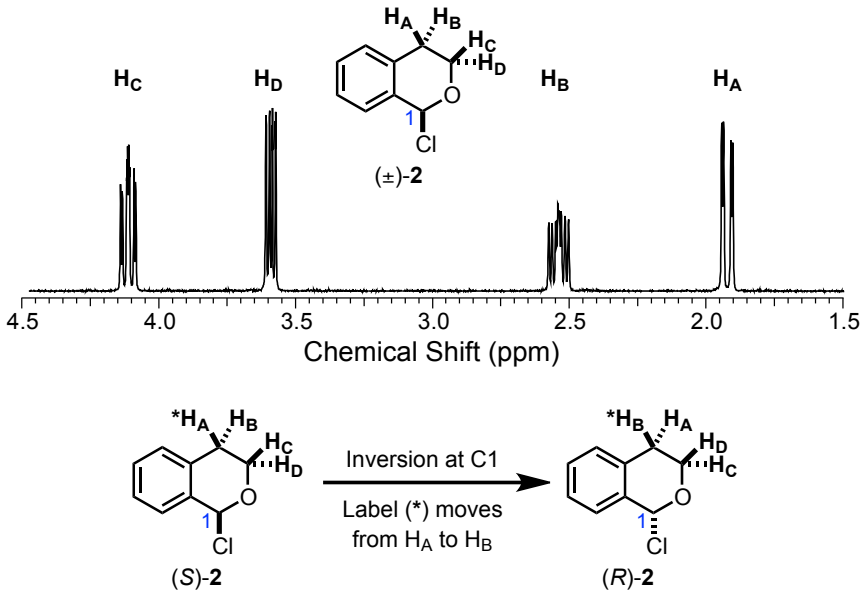

Figure 3.1. Top: Portion of the ^{1}H NMR spectrum of (±)-**2** (C_6D_6, 23 ºC). Bottom: Demonstration of how inversion at C1 (i.e. racemization) leads to chemical exchange between H_A and H_B.

While racemization is too slow to measure by 1D ^{1}H NMR line broadening, the selective inversion-recovery (SIR) experiment allows for measurement of chemical exchange on the considerably slower T_1 (spin-lattice relaxation) timescale.[17] The SIR experiment has proven a powerful technique for the measurement of equilibrium first-order rate constants ranging from

[17] Bain, A. D. *Prog. Nucl. Mag. Res. Sp.* **2003**, *43*, 63–103.

10^{-2}–10^{1} s^{-1}.[18] A challenge in applying the SIR experiment to measuring racemization of **2** is that the SIR pulse sequence detects both chemical exhange and nuclear Overhauser effect (nOe) relaxation pathways. To prevent competitive relaxation by an nOe pathway, we prepared the selectively deuterated analog **2**-d_3. This changes the problem from measuring an intramolecular chemical exchange process to one of measuring the rate of equilibration between two diastereomers found in a 1:1 ratio (Figure 3.2). In the absence of an H-bond donor catalyst, epimerization of **2**-d_3 was too slow to measure by SIR at –40 ºC in toluene-d_8. Upon addition of catalyst **1a** or **1b**, significant amounts of chemical exchange occurs demonstrating that epimerization was taking place. Fitting the data according to Bain's procedure allowed us to extract values of the first order rate constant k_{obs} as well as the spin-lattice relaxation constant T_1.[19]

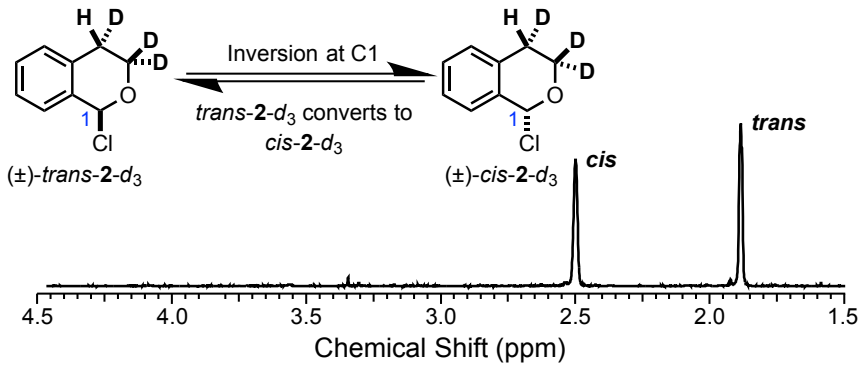

Figure 3.2. Top: Demonstration of how inversion at C1 (i.e. epimerization) leads to chemical exchange between H_{anti} and H_{syn}. Bottom: Portion of the ^{1}H NMR spectrum of (±)-**2**-d_3 (C_6D_6, 23 ºC).

The resulting data are summarized in Figure 3.3. The rate of chloroether epimerization obeys a strict first-order dependence on the amount of added **1a**. In contrast, while there is a

[18] Recent examples: (a) Bradley, C. A.; Lobkovsky, E.; Keresztes, I.; Chirik, P. J. *J. Am. Chem. Soc.* **2005**, *127*, 10291–10304. (b) Davis, A. V.; Fiedler, D.; Seeber, G.; Zahl, A.; van Eldik, R.; Raymond, K. N. *J. Am. Chem. Soc.* **2006**, *128*, 1324–1333. (c) Goodman, J.; Grushin, V. V.; Larichev, R. B.; Macgregor, S. A.; Marshall, W. J.; Roe, D. C. *J. Am. Chem. Soc.* **2009**, *131*, 4236–4238. (d) Conley, B. L.; Williams, T. J. *J. Am. Chem. Soc.* **2010**, *132*, 1764–1765.

[19] Bain, A. D.; Cramer, J. A. *J. Magn. Reson., Ser. A* **1996**, *118*, 21–27.

linear dependence of rate on $[\mathbf{1b}]_T$[20] at high catalyst loading, this breaks down for catalyst concentrations below ca. 2 mM: below this concentration, the rate of epimerization drops off sharply. While the deviation from an overall first-order dependence on **1b** was slight, we focused our attention on understanding its origin because we hoped that understanding non-ideal behavior at low catalyst loading might give us insight into why H-bond donor catalysts such as **1a** and **1b** are often ineffective at low loadings.

In our group's methodology development efforts, we had attributed slow reactions at low catalyst loading to poor catalyst activity, but these data suggested that the catalyst behaves in a fundamentally different fashion at low loading. Therefore, we hoped that a better understanding of the anomalously low activity at low loadings could lead to a solution to this problem. As we will demonstrate below, this behavior is more readily explained in the context of the two-catalyst mechanism described in the introduction.

[20] We use the convention of denoting total catalyst concentration with a subscript T. Thus, $[\mathbf{1b}]_T$ refers to the concentration of **1b** in total for all forms of the catalyst, including complexes with reagents and aggregates.

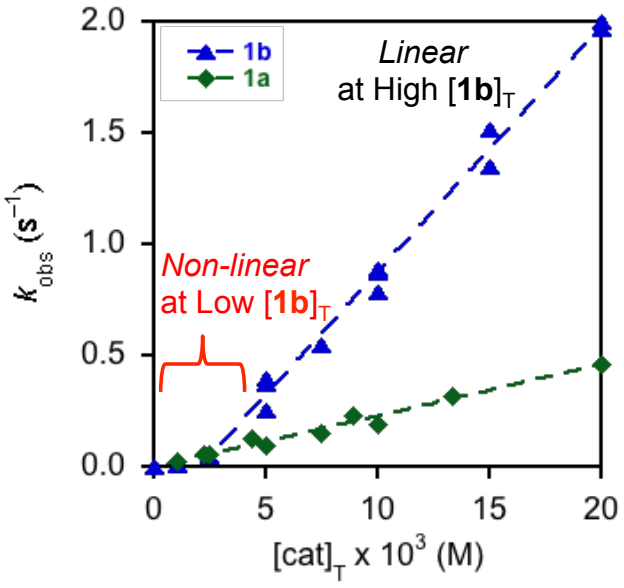

Figure 3.3. Dependence of the observed first-order rate constant k_{obs} for epimerization of **2**-d_3 on the total concentration of catalyst. The rate constant was measured using selective inversion-recovery NMR experiments with [**2**-d_3] = 0.1 M in toluene-d_8 at –40 ºC.

The fact that urea **1b** is a highly active epimerization catalyst demonstrates that the mechanism of epimerization does not rely on the nucleophilicity of the thiourea sulfur atom of **1a**, but the fact that **1b** is actually more reactive was unexpected, as thiourea derivatives are typically more acidic[21] and more active catalysts[14e] than their urea analogs. Hence, these chloroether epimerization experiments demonstrate that H-bond donor catalysts are capable of reversibly ionizing *a*-chloroether substrates to form a catalyst-bound chloride•oxocarbenium ion pair. The fact that these types of highly electrophilic intermediates are generated by catalysts such as **1a** and **1b** strongly suggests that they are the active electrophiles for the enantioselective alkylation reaction.

[21] Jakab, G.; Tancon, C.; Zhang, Z.; Lippert, K. M.; Schreiner, P. R. *Org. Lett.* **2012**, *14*, 1724–1727.

3.3 Kinetics of Chloroether Alkylation.

Our chloroether epimerization experiments established that catalyst-mediated ionization of **2** by anion abstraction is a viable mechanism. We sought to put those experiments back in the context of the enantioselective alkylation reaction of **2**. Both the silyl ketene acetals and the ester products of these reactions have well-resolved IR absorbances, making these reactions amenable to monitoring by *in situ* attenuated total reflectance Fourier-transform infrared (ATR FTIR) spectroscopy. For technical reasons, as well as for its higher reactivity, it was advantageous to use silyl ketene acetal **3b** in our studies. All of the kinetics experiments presented in this section were performed under near-preparative conditions using the *reaction progress kinetics analysis* strategy of analyzing kinetics data in *rate vs. conversion* form. This approach has been shown to be a powerful tool for elucidating nuances of catalytic mechanisms.[22]

To determine whether **1a** was slow to enter the catalytic cycle, suffering from product inhibition, undergoing decomposition, or otherwise changing in activity over the course of the reaction, we performed a *same excess* experiment. In these experiments, a series of reactions are performed with the same concentration of **1a**, but with different initial concentrations of **2** and **3b**. Critically, the concentrations are chosen such that there is a constant excess of **3b** over **2** (0.050 M in this case). All of the reaction rates are plotted as a function of the concentration of limiting reagent (Figure 3.4). The overlay of the curves shown in Figure 3.4 is evidence for the activity and composition of the catalyst remaining constant over the course of the reaction.[22] Having this information in hand greatly simplifies the task of determining the rate law for the catalytic reaction.

[22] Reviewed: Blackmond, D. G. *Angew. Chem. Int. Ed.* **2005**, *44*, 4302–4320.

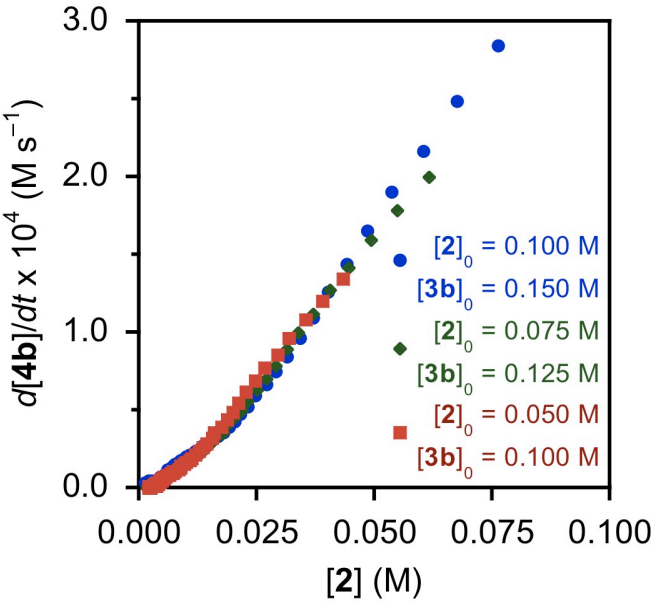

Figure 3.4. *Same excess* experiment demonstrating that the catalyst's activity remains constant for the full course of the reaction. This reaction was performed with total catalyst concentration $[\mathbf{1a}]_T$ = 0.01 M. The reaction was initiated by addition of neat **3b** to a solution of the other reactants in TBME at −78 ºC. The reaction was monitored by following the ester absorbance of product **4b** and [**2**] was inferred from $[\mathbf{2}]_0$ and the amount of **4b** formed (see Section 3.6.6).

The kinetic order in **2** was determined by performing kinetics experiments with different initial concentrations of **2** while holding the initial concentration of **3b** and **1a** constant. We then extracted the rate at the same extent of conversion of **3b** and plotted them as a function of [**2**]. The results show a simple first-order dependence in the concentration of **2** and the reaction was determined to be first order in **3b** in a similar fashion. In the case of **3b**, deleterious effects on the reaction rate are observed at high concentrations of **3b**, possibly due to an increase in the viscosity of the reaction medium: the reaction mixture is frozen solid at [**3b**] = 0.8 M.[23] The observation of a secondary kinetic isotope effect of k_H/k_D = 0.88 by competition between **3d** and **3d**-d_2 (eq 3.1),[24] combined with a lack of a strong rate dependence on the identity of the silyl

[23] These kinetics data are presented in Section 3.6.6.

[24] This experiment was performed twice, leading to observed KIEs of 0.880 and 0.888.

group on the silyl ketene acetal[25] suggests that the rate-determining step is C–C bond formation, which is then followed by rapid desilylation to furnish **4b**.

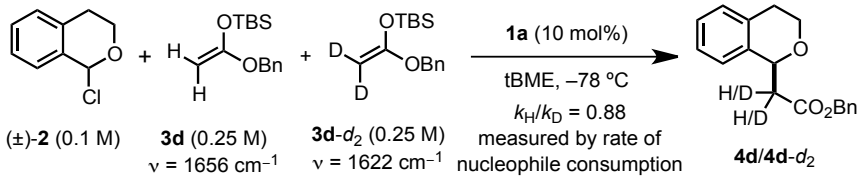

(±)-**2** (0.1 M) **3d** (0.25 M) ν = 1656 cm^{-1} **3d**-d_2 (0.25 M) ν = 1622 cm^{-1} **4d**/**4d**-d_2 (3.1)

We determined the kinetic order in catalyst by holding the initial concentration of **2** and **3b** constant while changing the total concentration of **1a** or **1b** added (Figure 3.5).[26] In contrast to the chloroether epimerization studies presented above, **1a** is a more active alkylation catalyst than **1b**, which is consistent with the fact that thioureas are typically more acidic and superior catalysts (*vide supra*). The fact that **1a** is a considerably more active alkylation catalyst than **1b**, while **1b** is the more active epimerization catalyst suggests that there is some difference between the mechanism of racemization and activation prior to alkylation. This subtlety is the focus of ongoing studies.

As in the chloroether epimerization studies discussed in the preceding section, we observed a sharp drop-off in catalyst activity at low catalyst loadings. In contrast to the epimerization studies, the effect is observed for both **1a** and **1b**, and is especially dramatic for **1b**: very little catalysis is observed below $[\mathbf{1b}]_T$ = 5 mM (5 mol % with respect to **2**). In the next section, we present and ultimately validate an alternative explanation: the catalyst is a resting state dimer at high concentrations, but a resting state monomer at low concentrations.

[25] Relative rates and enantioselectivity for analogs of **3a**: $SiMe_3$ (**3a** itself), $SiEt_3$, and $Si(i\text{-}Pr)_3$ are 1.0 (defined; 92% e.e.), 0.75 (94% e.e.), 2.0 (93% e.e.). For an example of a related reaction where a strong dependence on the identity of the silyl group was taken as evidence for rate-limiting desilylation of a silyl ketene acetal, see ref 14f.

[26] While the data shown in Figure 5 are at 30% conversion of **2**, similar relationships between rate and catalyst concentration were observed over the full course of the reaction. See the Supporting Information for these data.

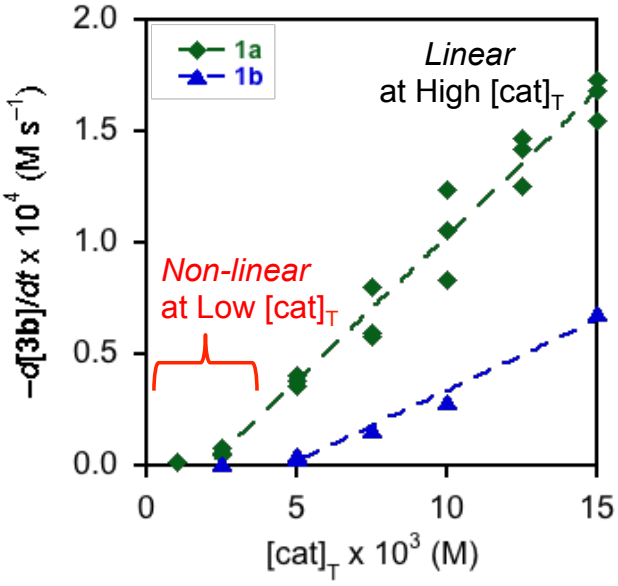

Figure 3.5. Dependence of alkylation rate on total concentration of dual H-bond donors $[cat]_T$ for **1a** (green diamonds) and **1b** (blue triangles) on the reaction between **2** and **3b**. These data were extracted from kinetics experiments performed at –78 ºC at 30% conversion with $[\mathbf{2}]_0$ = 0.1 M and $[\mathbf{3b}]_0$ = 0.15 M in TBME. The reaction was initiated by addition of the catalyst dissolved in THF (50 µL).

3.4 Cooperative Electrophile Activation.

In Sections A and B, we showed that the rates of both chloroether epimerization and alkylation appear to obey first-order kinetics in catalyst, but that this relationship breaks down at low catalyst loadings. We hypothesized that this was due to a small amount of catalyst poison, but as we were searching for a plausible poison to explain the rate behavior, we considered an alternative possibility. Because kinetic order indicates the difference in stoichiometry between the resting state and the rate-limiting transition state, first-order kinetics could be the result of a resting state dimer and a transition state containing two molecules of catalyst (Figure 3.6).[27]

[27] This kinetic scenario is similar to what has been observed in the (salen)Co(III)-catalyzed asymmetric epoxide fluorination reaction. In this case, a bimetallic dimer is the presumed resting state of the catalyst, which is required to dissociate for cooperative epoxide fluorination: Kalow, J. A.; Doyle, A. G. *J. Am. Chem. Soc.* **2011**, *133*, 16001–16012.

A. *Monomeric Catalyst Resting State, One Molecule of Catalyst in the Turnover-Limiting Step*

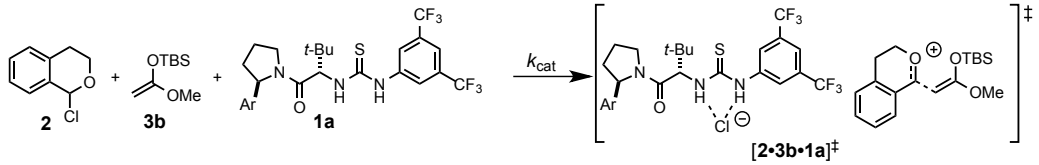

$$\frac{-d[\mathbf{3b}]}{dt} = k_{cat}[\mathbf{2}][\mathbf{3b}][\mathbf{1a}]$$

B. *Dimeric Catalyst Resting State, Two Molecules of Catalyst in the Turnover-Limiting Step*

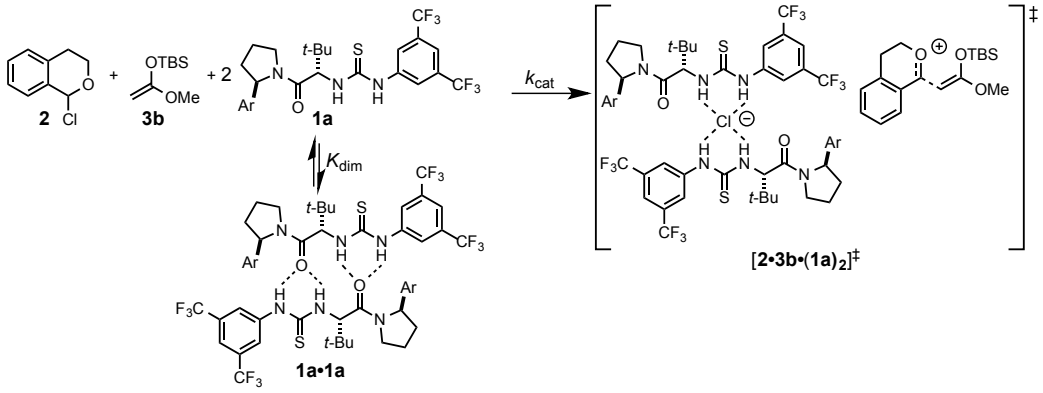

$$\frac{-d[\mathbf{3b}]}{dt} = \frac{4k_{cat}[\mathbf{2}][\mathbf{3b}][\mathbf{1a}]_T^2}{\left(1+\sqrt{1+8K_{dim}[\mathbf{1a}]_T}\right)^2}$$

for small $K_{dim}[\text{cat}]_T$ (resting state monomer):

$$\frac{-d[\mathbf{3b}]}{dt} = k_{cat}[\mathbf{2}][\mathbf{3b}][\mathbf{1a}]_T^2$$

for large $K_{dim}[\text{cat}]_T$ (resting state dimer):

$$\frac{-d[\mathbf{3b}]}{dt} = \frac{k_{cat}}{2K_{dim}}[\mathbf{2}][\mathbf{3b}][\mathbf{1a}]_T$$

Figure 3.6. Two scenarios that could lead to an observed first-order dependence on the concentration of catalyst **1a** (Ar = 4-F-Ph). Definitions used in these rate laws: $[\mathbf{1a}]_T = [\mathbf{1a}] + 2[\mathbf{1a}\bullet\mathbf{1a}]$, and $K_{dim} = [\mathbf{1a}\bullet\mathbf{1a}]/[\mathbf{1a}]^2$.

This might explain the deviation from linearity observed at low catalyst concentration in Figures 3.3 and 3.5: if the resting state of the catalyst is monomeric at low concentration, the rate would be second-order in catalyst at those concentrations, transitioning to first order as the catalyst resting state becomes predominantly dimeric. While this proposal is novel in thiourea catalysis, the aggregation behavior of these catalysts is well documented. In two detailed investigations of thiourea-catalyzed cyanation reactions, a less-than-first-order kinetic dependence on the catalyst was attributed to inactive aggregates that lie off of the catalytic

cycle.[6,28] Additionally, in the course of developing a thiourea-catalyzed acyl-Mannich reaction, the solid-state structure of the active catalyst was determined to be a head-to-tail dimer.[29]

A classic test for stereochemically dependent interactions between molecules of catalyst is to examine the relationship between the enantiomeric purity of the catalyst and the enantioselectivity of the reaction. A nonlinear relationship between catalyst e.e. and product e.e. is strong evidence of interactions between molecules of catalyst. This so-called "nonlinear effect experiment" was developed by Kagan and it has seen wide use in asymmetric catalysis.[30] A nonlinear effect can occur either by aggregation in the resting state (the reservoir effect) or by the presence of multiple catalyst molecules in the selectivity-determining transition state. In the case of the mechanism proposed above, we would expect both of these effects to be operative. Indeed, in the case of the reaction between **2** and **3b**, we observe a nonlinear realationship between the ee of catalyst **1a** and the ee of product **4b** (Figure 3.7).

[28] Zuend, S. J.; Jacobsen, E. N. *J. Am. Chem. Soc.* **2009**, *131*, 15358–15374.

[29] Taylor, M. S.; Tokunaga, N.; Jacobsen, E. N. *Angew. Chem. Int. Ed.* **2005**, *44*, 6700–6704.

[30] (a) Puchot, C.; Samuel, O.; Duñach, E.; Zhao, S.; Agami, C.; Kagan, H. B. *J. Am. Chem. Soc.* **1986**, *108*, 2353–2357. Guillaneux, D.; Zhao, S.; Samuel, O.; Rainford, D.; Kagan, H. B. *J. Am. Chem. Soc.* **1994**, *116*, 9430–9439. (c) Satyanarayana, T.; Abraham, S.; Kagan, H. B. *Angew. Chem. Int. Ed.* **2009**, *48*, 456–494.

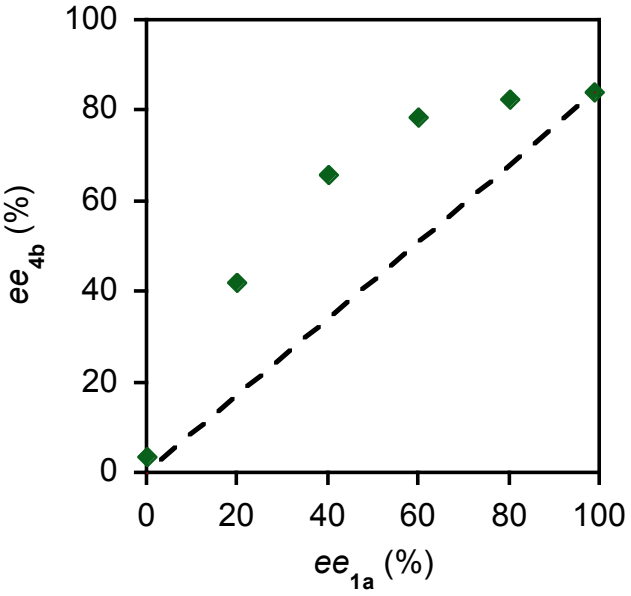

Figure 3.7. Relationship between catalyst enantiopurity and enantioselectivity for the reaction between **2** and **3b** catalyzed by **1a**. Non-enantiopure **1a** was prepared by mixing **1a** and *ent*-**1a**. The dashed line indicates the relationship expected if molecules of **1a** did not interact with one another under the reaction conditions. For details of the experiment, see Section 3.6.10.

To better understand the structure of the proposed resting state aggregates, we determined the solid-state structure of **1a** by single crystal X-ray diffraction.[31] This catalyst organizes into a head-to-tail dimer (Figure 3.8). We also isolated crystals from mixtures of **1a** and tetramethylammonium chloride (TMAC) and found that two molecules of **1a** bind the chloride ion together (Figure 3.9). While this demonstrated clearly that **1a** can form head-to-tail aggregates and that two molecules of **1a** can bind a chloride ion, we needed to evaluate whether these aggregation states were viable at relevant concentrations in solution.

[31] The crystal structures shown in Figures 3.8 and 3.9 were solved using the enantiomeric catalyst *ent*-**1a** instead of **1a**, but we present the mirror images of those structures below to avoid unnecessary confusion. See the Supporting Information for additional information.

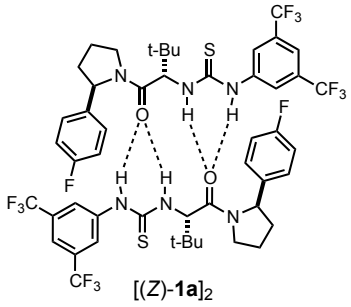

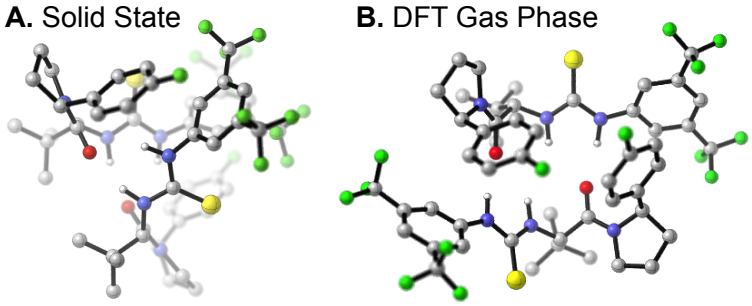

Figure 3.8. Geometries available for the homodimer [(*Z*)-**1a**]$_2$. **A.**: Dimeric form observed in solid state by X-ray crystallography. **B.**: Alternative conformation predicted to be comparable in energy by gas-phase DFT calculations. The geometry shown was optimized at the B3LYP/6-31G(d,p) level of theory.

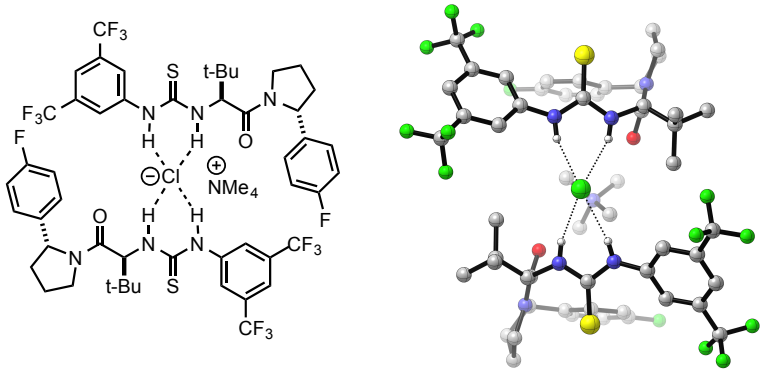

Figure 3.9. Solid-state structure of the 2:1 complex of **1a** to tetramethylammonium chloride determined by X-ray crystallography. Note that the tetramethylammonium cation is sandwiched between the two 4-fluorophenyl catalyst substituents.

To test whether the solution structures of **1a** and **1b** were the head-to-tail dimers analogous to what we had observed in the solid state, we performed 2D NOESY experiments on solutions of **1a** and **1b** at a total H-bond donor concentration of 10 mM. Analysis of those spectra led to the identification of intermolecular 2D ^{1}H-^{1}H NOESY cross-peaks[32] corresponding to

[32] Reviewed: Mo, H.; Pochapsky, T. C. *Prog. Nucl. Mag. Res. Sp.* **1997**, *30*, 1–38.

head-to-tail dimers of **1a** and **1b** (Figure 3.10). We note that these particular cross-peaks are more consistent with an alternate geometry of the dimer that we identified by DFT calculations (Figure 3.8). A more detailed discussion of this topic is presented in the Supporting Information.

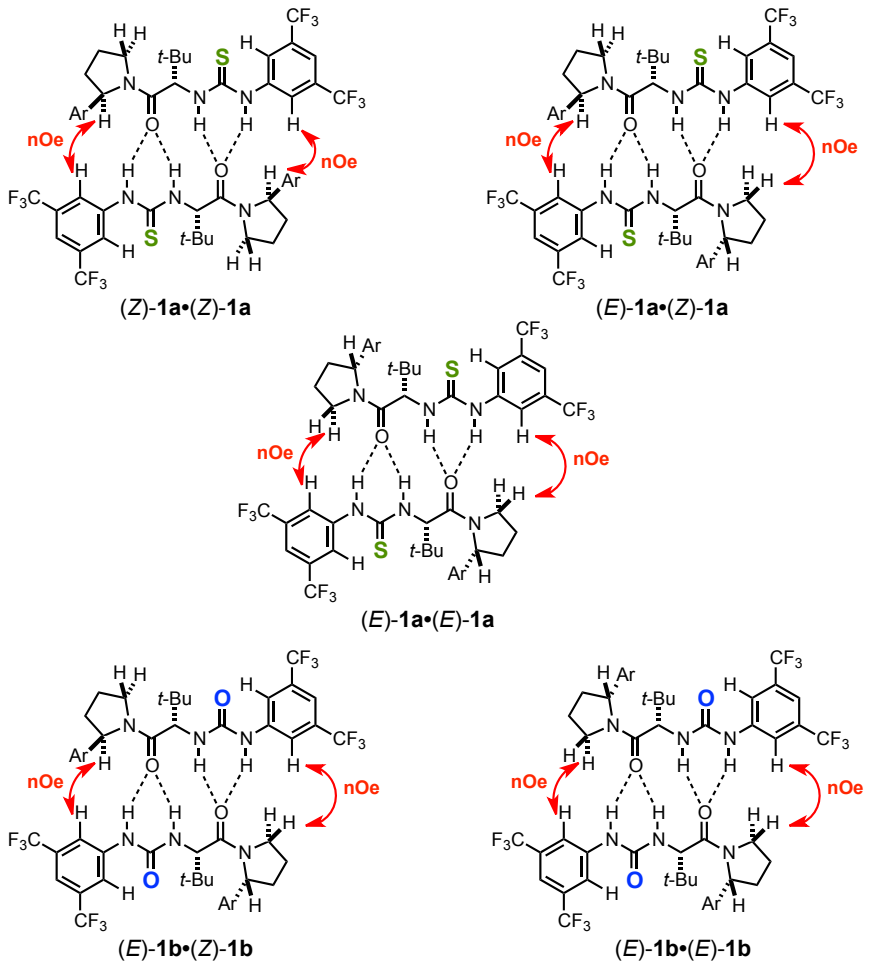

Figure 3.10. Head-to-tail dimers of **1a** and **1b** identified at 10 mM concentration by 2D NOESY NMR experiments (t_{mix} = 400 ms) in toluene-d_8 at 23 ºC. They key instances of nuclear Overhauser effect (nOe) that were used to assign these structures are labeled.

While these NOESY experiments demonstrated that these catalysts are aggregated to a significant extent, it was not possible to quantify the amount of dimer present in solution. The intensity of the nOe (or peak volume) depends on both the concentration of the relevant species

and the distance between the protons in question. Therefore, we needed a different technique to determine how much of the catalyst was dimerized in solution.

NMR dilution experiments proved a straightforward way to determine whether the catalyst was undergoing a change in aggregation state over a given concentration range. These experiments allow us to determine equilibrium constants for dimerization for each rotamer individually.[33] ^{1}H NMR spectra of **1a** and **1b** were acquired in toluene-d_8 over a wide range of concentrations (0.1–15 mM). At 25 ºC, the spectra of **1a** and **1b** are both concentration-dependent. Upon dilution, several peaks shift, but no new peaks are observed. We attribute the shift at lower concentration to an increasing fraction of catalyst monomer, and that monomer-dimer equilibria are sufficiently fast for monomer and dimer signals to coalesce (Scheme 3.5). While this makes it impossible to study these dimeric species individually, it simplifies the spectra considerably.

Scheme 3.5. Catalyst equilibria in solution.

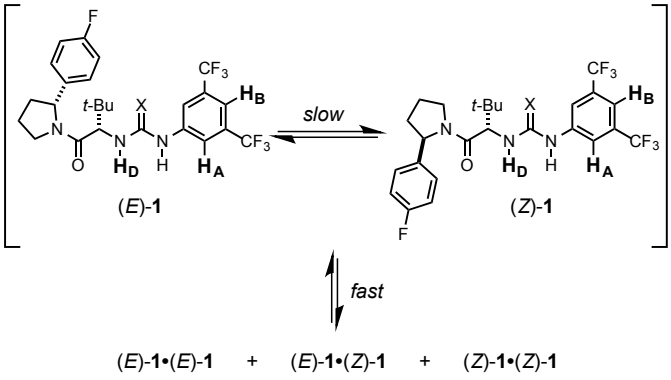

We plotted the chemical shift of each proton as a function of concentration (Figure 3.10) and fitted the resulting curves to a simple monomer-dimer equilibrium model where observed

[33] Amide rotation in catalysts such as **1a** and **1b** is generally quite slow. No EXSY cross peaks are observed between amide rotamers at room temperature, but strong EXSY is observed at 70 ºC (toluene-d_8, t_{mix} = 400 ms).

chemical shift is a weighted average of the chemical shifts of the monomeric and dimeric species (eq 3.2):

$$\begin{aligned}\delta_{obs} &= \chi_{monomer}\delta_{monomer} + \chi_{dimer}\delta_{dimer} \\ &= \chi_{monomer}\delta_{monomer} + (1-\chi_{monomer})\delta_{dimer} \\ &= \delta_{dimer} + \chi_{monomer}(\delta_{monomer} - \delta_{dimer})\end{aligned} \tag{3.2}$$

In eq 3.2, δ_{obs} is the observed chemical shift, and χ and δ refer to the mole fraction and chemical shift, respectively, of the monomeric and dimeric species in equilibrium. The mole fraction of dimer is a function of total concentration and the equilibrium constant for dimerization K_{dim} (eq 3.3):[34]

$$\chi_{monomer} = \frac{2}{1+\sqrt{1+8K_{dim}[\mathbf{1}]_T}} \tag{3.3}$$

The fitted parameters for the data in Figure 3.11 are presented in Table 3.1. The data show that for both **1a** and **1b**, the *E* amide rotamer is aggregated significantly more than the *Z* rotamer. We attribute this to steric crowding in dimers involving the *Z* rotamer, in which the aryl substituent on the pyrrolidine ring of one molecule projects toward the other molecule in the dimer.

[34] See the Section 3.6.4 for the full derivation.

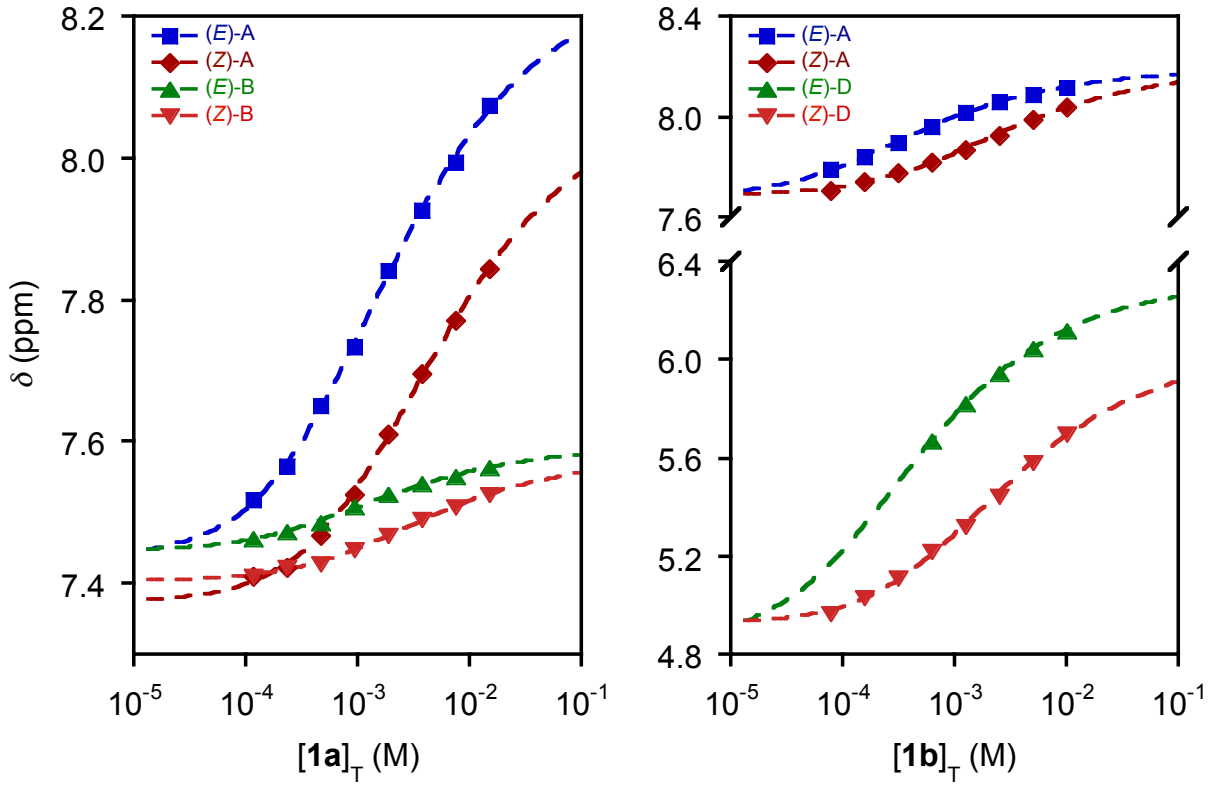

Figure 3.11. Dependence of key ^{1}H NMR chemical shifts of **1a** and **1b** on total catalyst concentration. Spectra were acquired in toluene-d_8 at 25 ºC. The dashed line represents a fit to a simple monomer-dimer model with the parameters in Table 3.1. See Section 3.6.8 for additional details.

Table 3.1. Fitted parameters for NMR dilution experiments with **1a** and **1b** at 25 ºC.

Catalyst	Peak[a]	δ_{dimer} (ppm)	$\delta_{monomer}$ (ppm)	$K_{dim,obs}$ x 10^2 (M^{-1})
1a	(*E*)-A	8.25 ± 0.01	7.44 ± 0.01	4.9 ± 0.5
	(*Z*)-A	8.09 ± 0.02	7.374 ± 0.006	1.9 ± 0.2
	(*E*)-B	7.595 ± 0.004	7.446 ± 0.004	6 ± 1
	(*Z*)-B	7.580 ± 0.005	7.403 ± 0.002	2.4 ± 0.3
1b	(*E*)-A	8.193 ± 0.003	7.68 ± 0.01	21 ± 2
	(*Z*)-A	8.19 ± 0.01	7.69 ± 0.01	3.7 ± 0.5
	(*E*)-D[b]	6.33 ± 0.01	4.9 ± 0.1	22 ± 6
	(*Z*)-D	6.03 ± 0.04	4.93 ± 0.02	3.6 ± 0.5

[a]See Scheme 4. [b]Fit based on a smaller set of data because the peak was not well resolved for some concentrations (see Section 3.6.8).

One surprising finding in these dilution experiments is that the urea **1b** dimerizes more tightly than the corresponding thiourea **1a**. Intuitively, we would expect the thiourea to dimerize more tightly because thioureas are typically better H-bond donors and the amide carbonyl H-bond acceptor should be nearly identical in **1a** and **1b**. Because these experiments were performed at room temperature, we wondered whether different behavior would be observed under the lower temperatures of our alkylation and epimerization experiments (Sections 3.2 and 3.3). At lower temperatures, the peaks begin to broaden, perhaps due to slowing of the monomer-dimer equilbrium on the NMR timescale.

We repeated the dilution experiments at –40 ºC, and observed that the ^{1}H NMR spectrum of **1a** changed very little upon dilution from 15 mM to 0.1 mM. Significant peak broadening precluded a definitive assignment of the spectrum at this temperature. We were able to identify one resonance that changed in a well-behaved manner across the concentration range examined (labeled P3 in Figure 3.12). The spectrum of **1b** changes significantly on dilution, but only the peaks corresponding to the *Z* rotamer change as a function of concentration, while the peaks corresponding to the *E* rotamer remain fairly constant. Because our room temperature data show that the *E* rotamer forms a more stable dimer than the *Z* rotamer, our interpretation of these data is that the *E* rotamer is fully dimerized over the full concentration range, while the *Z* rotamer undergoes a transition to monomer at lower concentrations. While these data do not allow for a clear comparison between **1a** and **1b**, it does appear that **1a** is aggregated to at least the same extent as **1b** at –40 ºC, perhaps slightly more so**.**

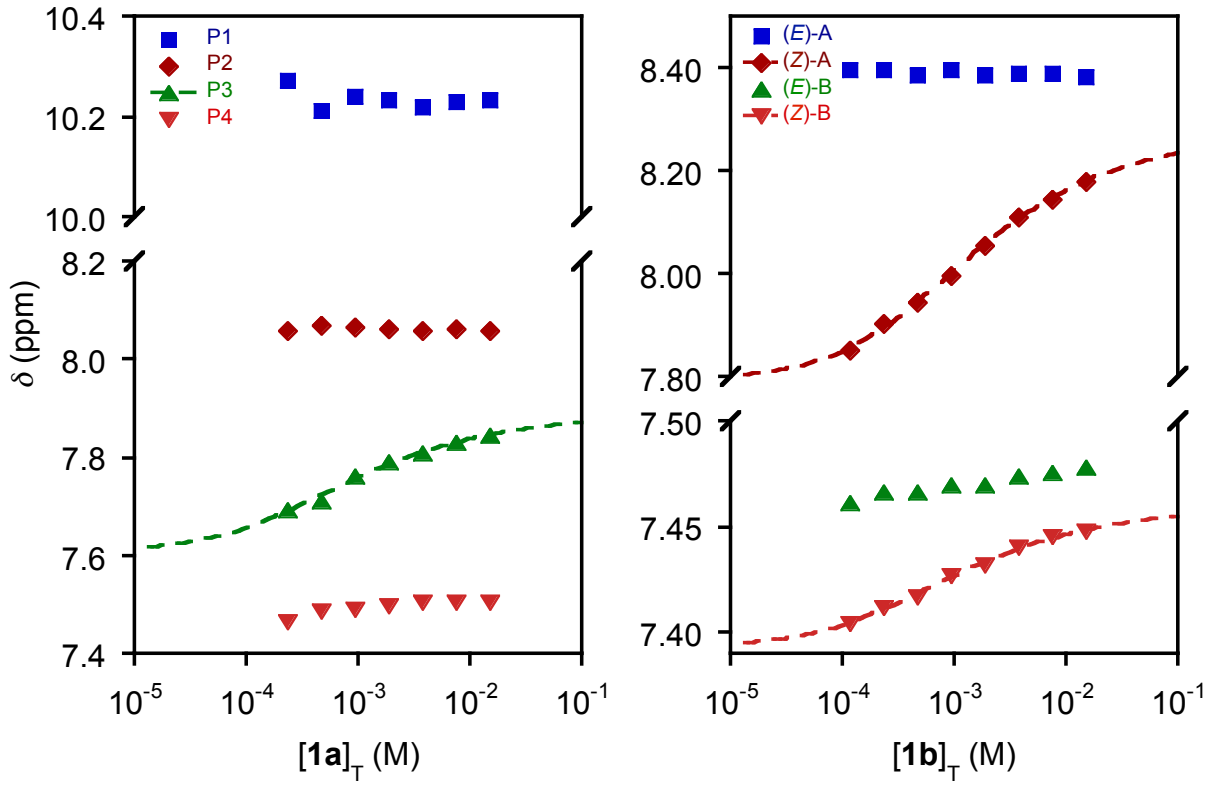

Figure 3.12. Dependence of key ^{1}H NMR chemical shifts of **1a** and **1b** on total catalyst concentration. Spectra were acquired in toluene-d_8 at –40 ºC. The dashed line represents a fit to a simple monomer-dimer model with the parameters in Table 3.2. See Section 3.6.8 for additional details.

Table 3.2. Fitted parameters for NMR dilution experiments with **1a** and **1b** at –40 ºC.

Catalyst	Proton	δ_{dimer} (ppm)	$\delta_{monomer}$ (ppm)	$K_{dim,obs}$ x 10^2 (M^{-1})
1a	P3	7.89 ± 0.01	7.61 ± 0.04	13 ± 8
1b	(*Z*)-A	8.272 ± 0.009	7.80 ± 0.01	7 ± 1
	(*Z*)-B	7.459 ± 0.001	7.393 ± 0.003	10 ± 2

These dilution experiments lead to two important conclusions about the structure of the catalyst in solution. First, the fact that the H-bond donor moieties of the catalysts are engaged in this mode of aggregation suggests that the hydrogen bonds between catalyst monomers must break before any productive H-bond donor catalysis can occur. Second, the catalyst is present in solution as a mixture of rotamers, some or all of which are active in catalysis. This raises the

question of whether both rotamers are required or whether one is active, while the other is not. Another possibility is that one rotamer catalyzes a highly selective pathway, but the other is less selective. These issues are the focus of ongoing studies.

Having characterized the dimeric solution structure of the catalyst, and the equilibrium for its formation, we returned to the kinetics data for chloroether alkylation and racemization presented above. The simplest rate law that satisfies the mechanism in Figure 3.6B is one where the only two resting states for catalyst are monomer and dimer and all species with substrates bound are present in vanishing concentrations. This model uses two fitted parameters, a rate constant k_{cat} and the equilibrium constant for catalyst dimerization, K_{dim}. The derivation of this rate law and the analogous rate law for chloroether racemization can be found in the Supporting Information. We denote the rate constant for chloroether racemization k'_{cat} to avoid confusion.

In Figure 3.13, the kinetics data presented in Sections 3.2 and 3.3 are reproduced with curves of best fit to the rate law in Figure 3.6B. In the case of chloroether epimerization catalyzed by **1a**, which obeys strict first-order kinetics in **1a**, we used the simplified form for $8K_{dim}[cat]_T >> 1$ (resting state dimer).[35] Given the differences in measurement conditions, the values of K_{dim} from the kinetics model are consistent with the values determined by studying the concentration dependence of the ^{1}H NMR spectrum of **1b**. On the basis of the fit to this rate law as well as our NMR studies that demonstrate that catalysts **1a** and **1b** are significantly aggregated at catalytically relevant concentrations in solution, we conclude that chloroether activation requires two molecules of catalyst working cooperatively.

[35] The complete form of the rate law also provides a very good fit to the experimental data, but there is no unique solution for the best fit because k_{cat} and K_{dim} are no longer independent at high values of K_{dim}. For this reason, we fit for the ratio, k_{cat}/K_{dim} instead, which does have a unique solution.

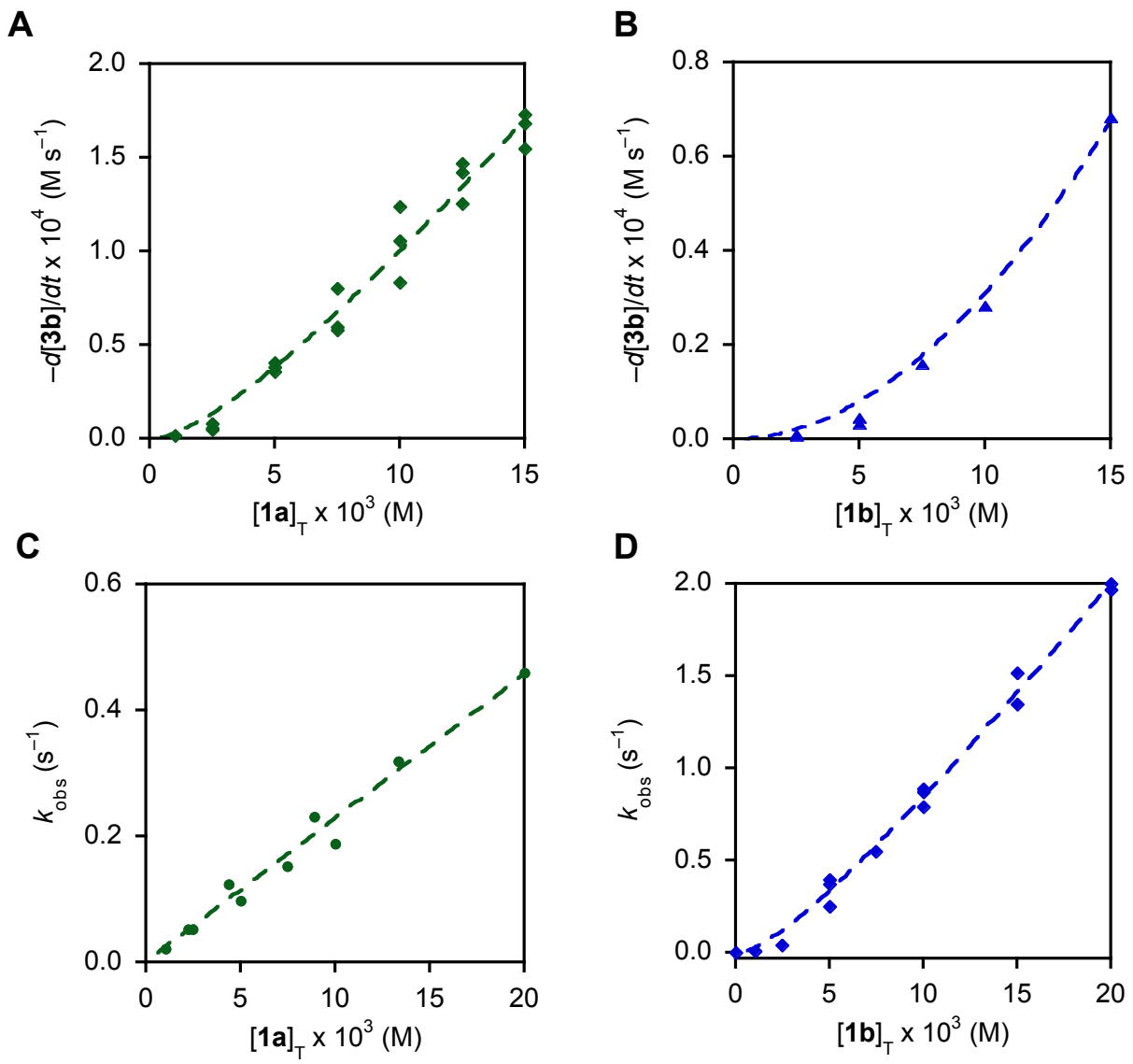

Figure 3.13. Fitting of the model shown in Figure 3.6B to the observed rate laws for chloroether alkylation and chloroether racemization. **A**, chloroether alkylation with **1a**. $k_{cat} = 4.6 \pm 1.9 \times 10^2$ M^{-3} s^{-1}, $K_{dim} = 94 \pm 56$ M^{-1}, $R^2 = 0.97$. **B**, chloroether alkylation with **1b**. $k_{cat} = 39 \pm 9$ M^{-3} s^{-1}, $K_{dim} = 1.6 \pm 4.5$ M^{-1}, $R^2 = 0.987$. **C**, chloroether racemization with **1a**. $k'_{cat}/K_{dim} = 46 \pm 1$ M^{-1} s^{-1}, $R^2 = 0.98$. **D**, chloroether racemization with **1b**. $k'_{cat} = 4 \pm 1 \times 10^4$ M^{-2} s^{-1}, $K_{dim} = 1.4 \pm 0.5 \times 10^2$ M^{-1}, $R^2 = 0.993$.

If the rate-determining step for alkylation involves two molecules of catalyst, then it might be possible to achieve higher reactivity by linking two molecules of catalyst covalently. Indeed, bis(thiourea) catalysts have been developed[36,14c] for several transformations.

[36] (a) Sohtome, Y.; Tanatani, A.; Hashimoto, Y.; Nagasawa, K. *Tetrahedron Lett.* **2004**, *45*, 5589–5592. (b) Sohtome, Y.; Takemura, N.; Takagi, R.; Hashimoto, Y.; Nagasawa, K. *Tetrahedron* **2008**, *64*, 9423–9429.

Nevertheless, instead of relying on existing diamine linker strategies or designing new bis(thiourea) catalysts *a priori*, we sought to take advantage of the optimized catalyst structure in **1a** by designing a linker that would hold two catalyst moieties in place while perturbing the properties of **1a** as little as possible.

The strategy of linking optimized monomeric catalysts has been employed successfully in several reactions that display a second-order kinetic dependence on the concentration of catalyst.[37] The ideal linker would prevent the two catalyst moieties from deactivating one another, but would not hinder the two catalysts from cooperatively catalyzing the chloroether alkylation reaction. While it is unclear how closely the solid-state structures (Figures 3.8 and 3.9) resemble their solution-state counterparts, the solid-state structures clearly show that the relative orientation of the two catalyst molecules changes significantly upon binding Me_4N•Cl, lending credence to the notion that the appropriate linker could favor one type of dimer over the other. On the basis of this information, and after trying several simpler designs, Drs. Dan Lehnherr, Naomi Rajapaksa, and Masayuki Wasa have succeeded in preparing linked catalysts that catalyze the reactions studied in this chapter, reaching full conversion in one hour at a 0.5 mol% loading, with selectivity comparable to the monomeric system. These results will be reported in due course, and this is an active area of research.

3.5 Conclusion.

The physical-organic study described above led to the unexpected conclusion that two molecules of the thiourea catalyst must work cooperatively to ionize an α-chloroether substrate for attack by a silyl ketene acetal nucleophile. While this mode of cooperative activation is

[37] Examples where the linker connects two (or more) identical catalytic moieties: (a) Konsler, R. G.; Karl, J.; Jacobsen, E. N. *J. Am. Chem. Soc.* **1998**, *120*, 10780–10781. (b) Denmark, S. E.; Fu, J. *J. Am. Chem. Soc.* **2000**, *122*, 12021–12022. (c) Ready, J. M.; Jacobsen, E. N. *J. Am. Chem. Soc.* **2001**, *123*, 2687–2688. Examples where the linked catalytic moieties are different: (d) Liu, X.; Henderson, J. A.; Sasaki, T.; Kishi, Y. *J. Am. Chem. Soc.* **2009**, *131*, 16678–16680.

certainly not operative in all thiourea- and urea-catalyzed reactions, we suspect that it is not unique either. In particular, we expect that cooperative catalysis with two thiourea catalysts may be occurring in reactions thought to occur by anion abstraction with leaving groups that support binding by multiple catalysts. The ubiquity of dimeric forms of the catalyst may also explain why some thiourea and urea catalysts are only effective at high dilution: at higher concentrations, the vast majority of the catalyst is off the catalytic cycle, tied up as an inactive dimer. It also brings up an important point for catalyst optimization: a catalyst that has perfectly tuned catalytic machinery might give little or no reactivity simply because it is highly aggregated.

Gaining insight into the cooperative mechanism of chloroether alkylation led to the discovery of a new class of linked bis(thiourea) catalysts that provide unprecedented levels of reactivity with comparable levels of enantioselectivity to monomeric catalysts. In certain cases, this linking strategy may be a key to addressing the reactivity problems that limit the application of H-bond donor catalysis to organic synthesis. The design of more reactive and enantioselective bis(thiourea) catalysts, as well as their application to other reactions thought to proceed by anion-abstraction mechanisms is a focus of our ongoing research efforts.

3.6 Experimental Details

3.6.1 Procedures, Materials and Instrumentation

General experimental procedures. All reactions were performed in standard, dry glassware fitted with rubber septa under an inert atmosphere of nitrogen unless otherwise described. Stainless steel syringes or cannulae were used to transfer air- and moisture-sensitive liquids. Reported concentrations refer to solution volumes at room temperature. Evaporation and concentration *in vacuo* was performed using house vacuum (ca. 40 mm Hg). Column chromatography (using a Biotage® Isolera Four™) was done using reusable cartridges filled with ZEOprep® 60 (40–63 micron) silica gel from American Scientific. Thin layer chromatography (TLC) was used for reaction monitoring and product detection using pre-coated glass plates covered with 0.20 mm silica gel with fluorescent indicator; visualization by UV light or $KMnO_4$ stain.

Materials. Reagents were purchased in reagent grade from commercial suppliers and used without further purification, unless otherwise described. 1-chloroisochroman (**2**) and catalysts **1a** were prepared according to the procedures reported previously.[13] Anhydrous solvents (toluene, *tert*-butylmethylether (TBME), CH_2Cl_2, MeOH) were prepared by passing the solvent through an activated alumina column. Triethylamine, diisopropylethylamine (DIPEA), and pyridine were distilled from CaH_2 at atmospheric pressure. Toluene-d_8 used for NMR experiments other than structure elucidation (e.g. chloroether epimerization studies, NOESY experiments, serial dilution experiments) was distilled from CaH_2 and degassed by four cycles of freezing in liquid nitrogen, evacuating the headspace under vacuum (ca. 0.5 Torr) and allowing the solvent to thaw with the flask isolated from the vacuum manifold.

Instrumentation. Proton nuclear magnetic resonance (^{1}H NMR) spectra and proton-decoupled carbon nuclear magnetic resonance (^{13}C {^{1}H} NMR) spectra were recorded at 25 °C (unless stated otherwise) on Varian-Mercury-400 (400 MHz) or Varian Unity/Inova 500 (500 MHz) spectrometers at the Harvard University nuclear magnetic resonance facility. Chemical shifts for protons are reported in parts per million downfield from tetramethylsilane and are referenced to residual protium in the NMR solvent according to values reported in the literature.[38] Chemical shifts for carbon are reported in parts per million downfield from tetramethylsilane and are referenced to the carbon resonances of the solvent. The solvent peak was referenced to 7.26 ppm for ^{1}H and 77.0 ppm for ^{13}C for $CDCl_3$, to 3.31 ppm for ^{1}H and 49.15 ppm for ^{13}C for CD_3OD, to 5.32 ppm for ^{1}H and 54.0 ppm for ^{13}C for CD_2Cl_2, and to 2.09 ppm for ^{1}H and 20.4 ppm for ^{13}C for toluene-d_8. Data are represented as follows: chemical shift, integration, multiplicity (br = broad, s = singlet, d = doublet, t = triplet, q = quartet, m = multiplet), coupling constants in Hertz (Hz). In the case of compounds containing one or more fluorine atom(s), we note that ^{13}C NMR experiments were obtained without ^{19}F decoupling.

Optical rotations were measured using a 1 mL cell with a 5 cm path length on a Jasco P-2000 digital polarimeter.

Infrared spectra were recorded using a Bruker Tensor 27 FT-IR spectrometer. Data are represented as follows: frequency of absorption (cm^{-1}), intensity of absorption (s = strong, m = medium, w = weak, br = broad). In-situ IR kinetic experiments were carried out using a Mettler

[38] Gottlieb, H. E.; Kotlyar, V.; Nudelman, A. *J. Org. Chem.* **1997**, *62*, 7512–7515.

Toledo ReactIR™ iC 10 ATR FTIR spectrometer and a 9 mm AgX probe with a SiComp (silicon-based) window.

Low-resolution mass spectrometry was measured using an Agilent 6120 Quadrupole LC/MS, samples were injected in 0.1% formic acid in methanol and bypassed the LC column en route to the MS detector. High-resolution mass spectrometry was measured using a Bruker micrOTOF-QII™ ESI-Qq-TOF mass spectrometer calibrated using an aqueous sodium formate solution (prepared via adding 1 mL of 1 M aq. NaOH in 100 mL of 1% aq. formic acid). Additional high-resolution mass spectrometry was measured at the Small Molecule Mass Spectrometry Facility at Harvard University within the Faculty of Arts and Sciences using an Agilent 6220 Time-of-Flight LC/MS.

Chiral gas chromatography (GC) analysis was performed on a Hewlett-Packard 5890 gas chromatograph using an Alltech Cyclodex β (20 m x 0.25 mm) column, chiral high performance liquid chromatography (HPLC) analysis was performed using an Agilent 1200 quaternary HPLC system with a commercially available *S,S*-Whelk-01 chiral column.

All curve fitting presented in this paper was carried out using KaleidaGraph 4.1.3.[39]

[39] KaleidaGraph Version 4.1.3 for Mac OS X, 2011, Synergy Software (http://www.synergy.com).

3.6.2. Catalyst Synthesis

Catalyst **1a** was prepared according to the published procedure.[13] $[\alpha]_D^{23}$ = +14.2º (c = 1.0, $CHCl_3$).

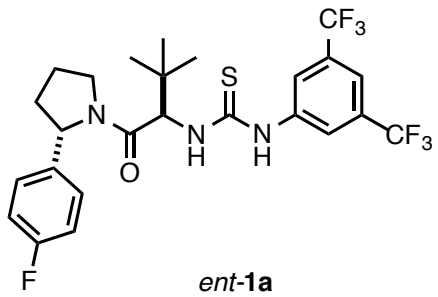

ent-**1a**

ent-**1a** was prepared by an analogous procedure, employing (+)-sparteine in place of (–)-sparteine in the arylpyrrolidine synthesis, and *N*-Boc-D-*tert*-leucine in the amino acid coupling step.[40] ^{1}H NMR (500 MHz, C_6D_6; under these conditions, *ent*-**1a** is a mixture of two rotamers in a 1:1.3 ratio, major rotamer denoted with *, minor denoted with §) δ = 8.99 (br. s, 1 H§), 7.99 (br. s, 1 H*), 7.94 (s, 2 H§), 7.78 (s, 2 H*), 7.58 (d, J=10.25 Hz, 1 H§), 7.51 (br. s, 1 H§), 7.47 (br. s, 1 H*), 7.39 (d, J=9.28 Hz, 1 H*), 6.95–7.01 (m, 2 H§, coincident with solvent ^{13}C satellite), 6.69–6.78 (m, 2 H*, 2 H§), 6.53 (t, J=8.55 Hz, 2 H*), 5.88 (d, J=7.32 Hz, 1 H§), 5.67 (d, J=10.25 Hz, 1 H§), 5.62 (d, J=9.28 Hz, 1 H*), 4.82 (d, J=7.32 Hz, 1 H*), 3.99–4.07 (m, 1 H*), 3.19–3.31 (m, 1 H*, 2 H§), 1.63–1.73 (m, 1 H§), 1.47–1.58 (m, 1 H*), 1.30–1.47 (m, 3 H§), 1.14–1.29 (m, 3 H*), 1.08 (s, 9 H*), 0.83 (s, 9 H§). $[\alpha]_D^{23}$ = −15.2º (c = 1.0, $CHCl_3$). ESI HRMS *m/z* calcd. for $C_{25}H_{27}F_7N_3OS$ ($[M + H]^+$) 550.1758, found 550.1773.

[40] Campos, K.; Klapars, A.; Waldman, J. H.; Dormer, P. G.; Chen, C.-y. *J. Am. Chem. Soc.* **2006**, *128*, 3528–3539.

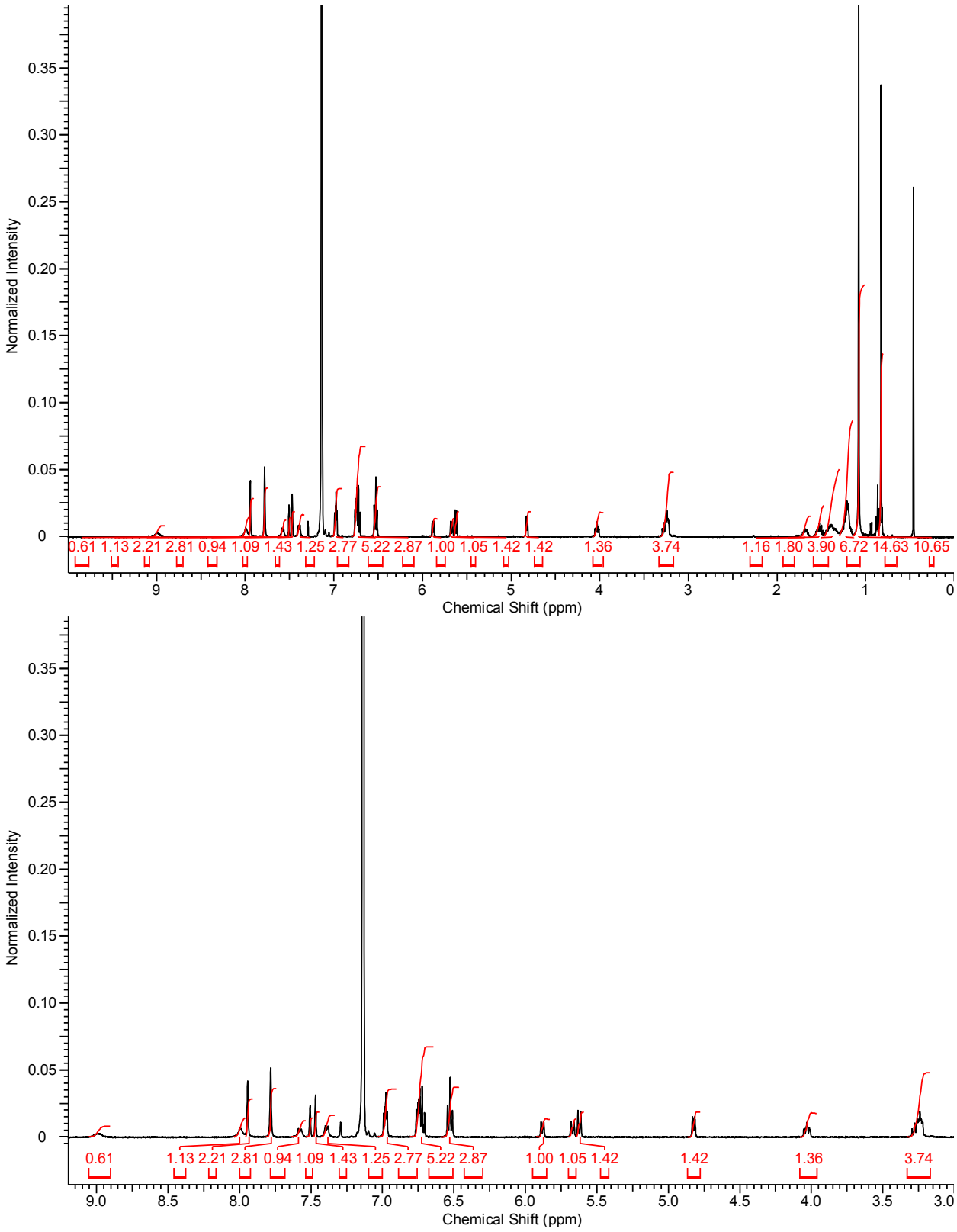

Figure 3.14. ^{1}H NMR spectrum (500 MHz, C_6D_6) of *ent*-**1a**.

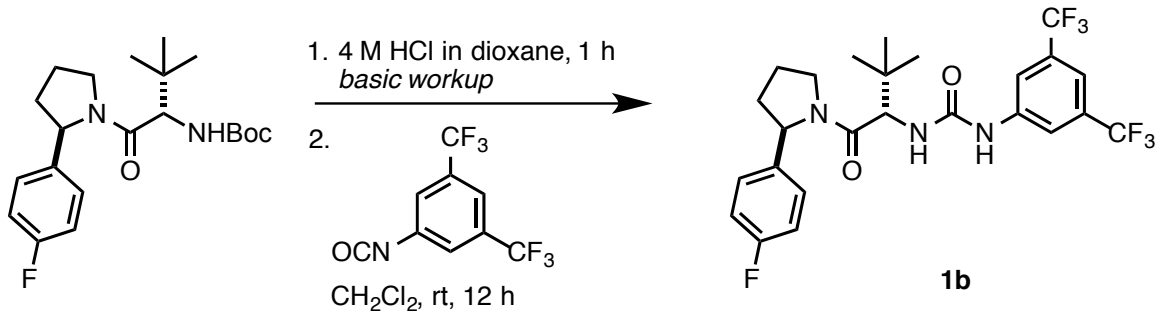

To *tert*-butyl ((*S*)-1-((*R*)-2-(4-fluorophenyl)pyrrolidin-1-yl)-3,3-dimethyl-1-oxobutan-2-yl)carbamate (470 mg, 1.24 mmol),[13] was added hydrogen chloride as a 4 M solution in 1,4-dioxane (5 mL, 16 equiv). This mixture was aged at room temperature for 1 h, and the reaction mixture was diluted with CH_2Cl_2 (30 mL) before careful addition of NaOH (30 mL of a 1M aqueous solution). The mixture was stirred rapidly, and NaOH pellets were slowly added until the pH of the aqueous layer measured to be > 12 using pH paper. The organic layer was separated, and washed with Na_2SO_4 before concentrating under reduced pressure. The residue was dissolved in 6 mL CH_2Cl_2, and 3,5-bis(trifluoromethyl)phenyl isocyanate (236 μL, 1.36 mmol, 1.1 equiv) was added with stirring. This mixture was aged for 12 h at room temperature before the solvent was removed under reduced pressure. The crude material was purified by silica gel chromatography (solvent system), yielding 510 mg of **1b** as a white powder (77% yield over two steps). ^{1}H NMR (500 MHz, $CDCl_3$; under these conditions, **1b** is a mixture of two rotamers in a 1:1.3 ratio, major rotamer denoted with *, minor denoted with §) δ = 8.44 (br. s. 1H§), 8.29–8.29 (m, 1 H*), 8.29 (s, 2 H*), 7.91 (s, 2 H§), 7.86 (s, 2 H*), 7.51 (s, 1 H*, 1 H§), 7.34 (dd, *J*=8.70, 5.04 Hz, 2 H§), 7.10 (t, *J*=8.47 Hz, 2 H§), 6.74–6.80 (m, 2 H*), 6.66–6.73 (m, 2 H*), 5.95 (app. d, *J*=10.07 Hz, 1 H*, 1 H§), 5.30 (d, *J*=6.41 Hz, 1 H§), 5.08 (d, *J*=7.33 Hz, 1 H*), 4.84 (d, *J*=9.62 Hz, 1 H*), 4.52 (d, *J*=10.07 Hz, 1 H§), 4.09–4.19 (m, 1 H*), 3.83 (d, *J*=7.33 Hz, 1 H*), 3.59–3.73 (m, 2 H§), 2.34–2.44 (m, 1 H§), 2.23–2.33 (m, 1 H*), 2.10–2.21 (m, 1 H§), 1.83–2.03 (m, 3 H*, 2 H§), 1.12 (s, 9 H*), 0.69 (s, 9 H§). ^{13}C {^{1}H} NMR (126 MHz, $CDCl_3$): d

173.3, 171.9, 162.3 (d, *J*=246 Hz), 161.4 (d, *J*=245 Hz), 155.0, 154.4, 141.3, 141.2, 139.2 (d, *J*=4 Hz), 136.3 (d, *J*=3 Hz), 132.0 (q, *J*=33 Hz), 132.0 (q, *J*=33 Hz), 128.4 (d, *J*=8 Hz), 126.4 (d, *J*=8 Hz), 123.4 (q, *J*=273 Hz), 123.3 (q, *J*=273 Hz), 118.5 (br. s.), 118.3 (br. s.), 115.8 (d, *J*=22 Hz), 115.2 - 115.5 (m), 115.0 - 115.2 (m), 114.7 (d, *J*=21 Hz), 61.9, 60.1, 57.9, 56.6, 49.0, 47.5, 35.5, 35.4, 35.0, 34.0, 26.6, 26.5, 23.0, 21.6. IR (ATR, neat): 2361 (w), 2342 (w), 1706 (m), 1646 (m), 1613 (m), 1570 (m), 1510 (m), 1442 (m), 1387 (m), 1276 (s), 1223 (m), 1175 (s), 1128 (s), 1062 (m), 949 (m), 880 (m) cm^{-1}. $[\alpha]_D^{23}$ = +81.6º (c = 1.0, $CHCl_3$). ESI MS *m/z* calcd. for $C_{25}H_{27}F_7N_3NaO_2$ ($[M + Na]^+$) 556.2, found 556.2.

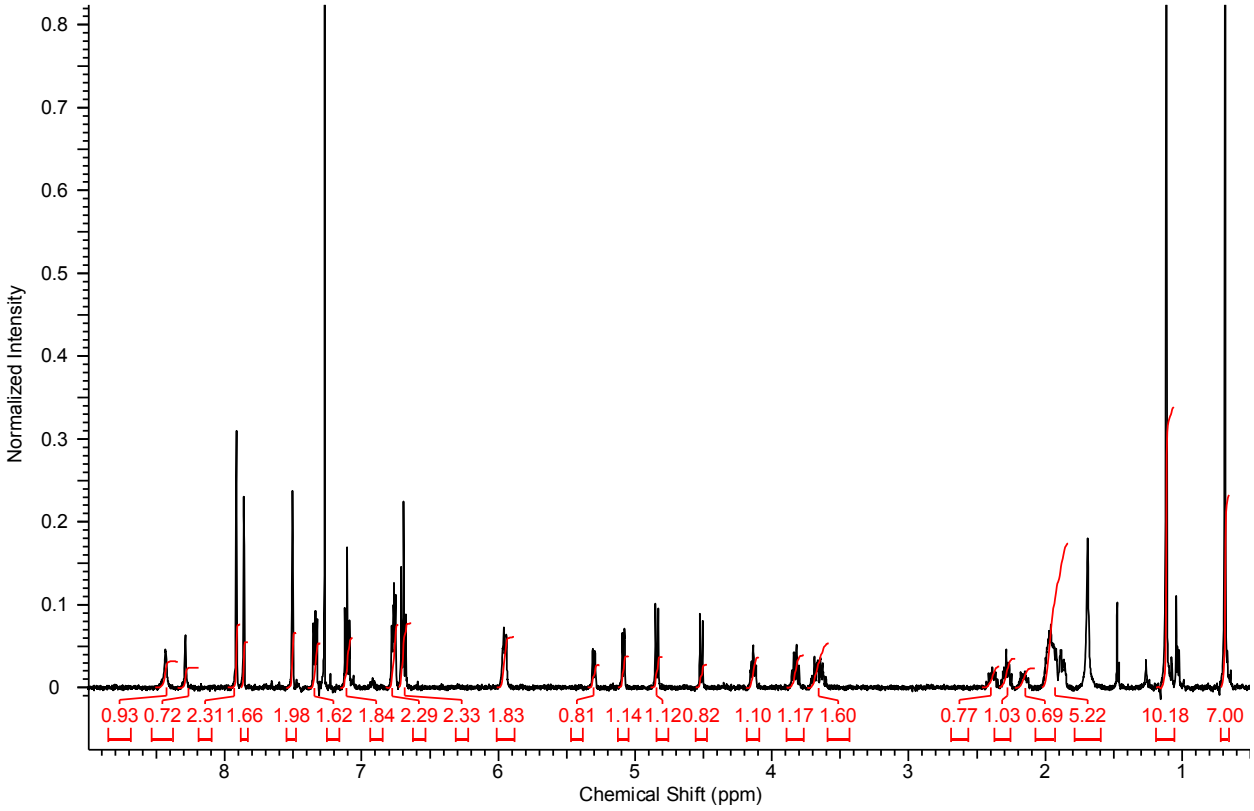

Figure 3.15. ^1H NMR spectrum (500 MHz, $CDCl_3$) of **1b**.

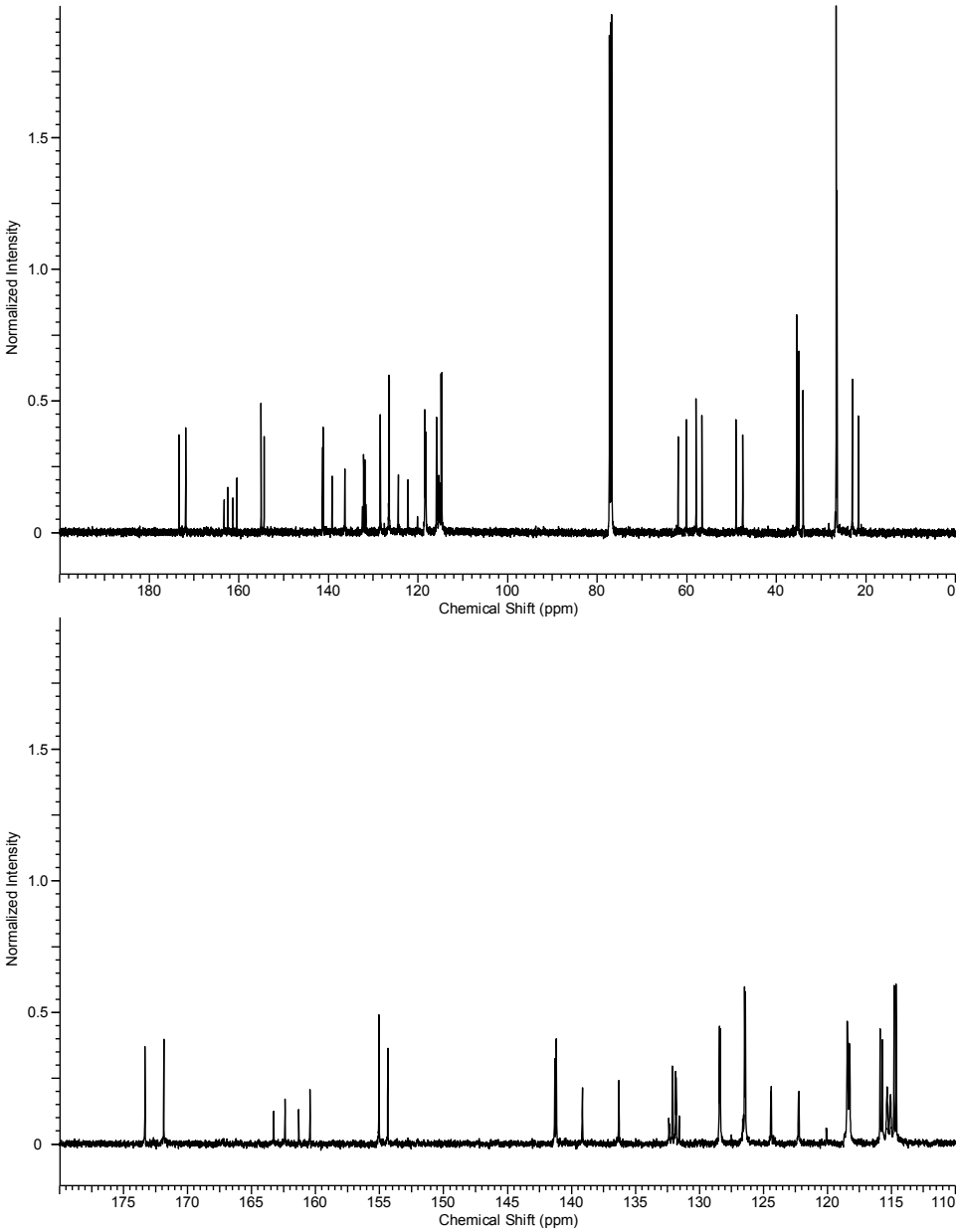

Figure 3.16. ^{13}C NMR spectrum (126 MHz, $CDCl_3$) of **1b**.

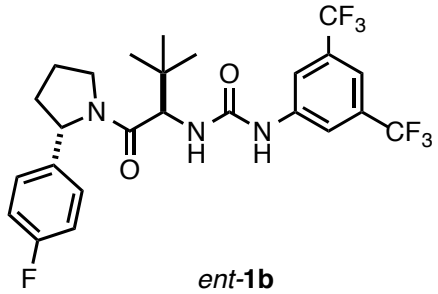

ent-**1b**

ent-**1b** was prepared by an analogous procedure to the one shown above for **1b**, employing (+)-sparteine in place of (–)-sparteine in the arylpyrrolidine synthesis, and *N*-Boc-D-*tert*-leucine in the amino acid coupling step.[40] ^{1}H NMR (500 MHz, $CDCl_3$; under these conditions, *ent*-**1b** is a mixture of two rotamers in a 1:1.3 ratio, major rotamer denoted with *, minor denoted with §): δ = 8.55 (br. s., 1 H*), 8.33 (br. s., 1 H§), 7.92 (s, 2 H*), 7.86 (s, 2 H§), 7.51 (br. s., 1 H*, 1 H§), 7.38–7.31 (m, 2 H§), 7.11 (t, J = 8.5 Hz, 2 H§), 6.79–6.71 (m, 2 H*), 6.71–6.65 (m, 2 H*), 5.97 (m, 1 H*, 1 H§), 5.30 (d, J = 6.9 Hz, 1 H§), 5.08 (d, J = 7.3 Hz, 1 H*), 4.86 (d, J = 9.6 Hz, 1 H*), 4.52 (d, J = 10.1 Hz, 1 H§), 4.10–4.19 (m, 1 H*), 3.83 (m, 1 H*), 3.73–3.58 (m, 2 H§), 2.39 (m, 1 H§), 2.28 (m, 1 H*), 2.15 (m, 1 H§), 2.04 (m, 3 H*, 2 H§), 1.13 (s, 9 H*), 0.69 (s, 9 H§). $[\alpha]_D^{23}$ = −87.2º (c = 1.0, $CHCl_3$). ESI HRMS *m/z* calcd. for $C_{25}H_{27}F_7N_3NaO_2$ ($[M + H]^+$) 534.1986, found 534.1998.

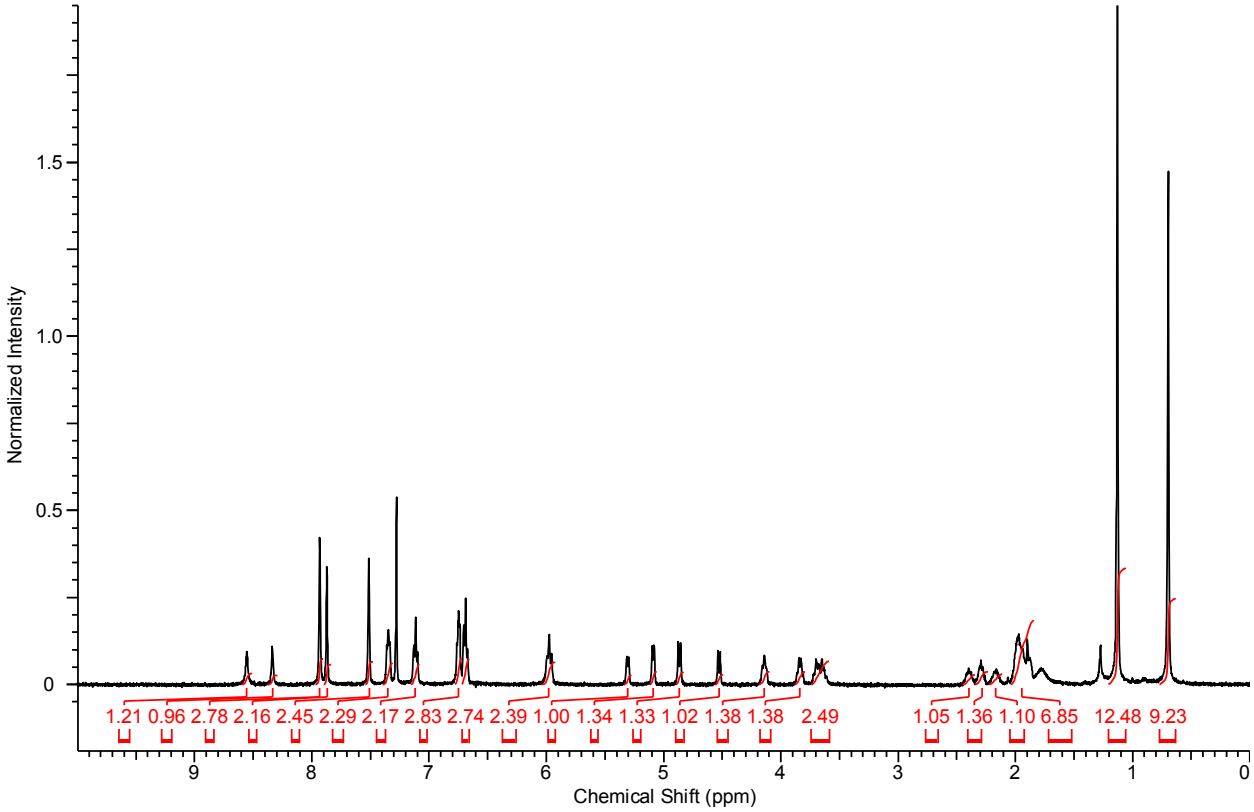

Figure 3.17. ^{1}H NMR spectrum (500 MHz, $CDCl_3$) of *ent*-**1b**.

3.6.3. Synthesis of 2-d_3

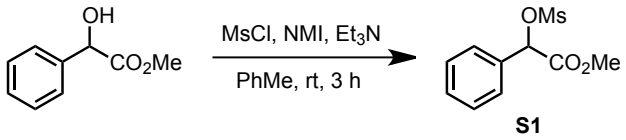

S1

S1: This procedure is a scaled up from a previously reported 1-mmol-scale procedure.[41] An oven-dried 250-mL round-bottomed flask equipped with a PTFE-coated magnetic stirbar was charged with methyl DL-mandelate (3.32 g, 20.0 mmol, 1.00 equiv), anhydrous toluene (40 mL), triethylamine (4.18 mL, 30.0 mmol, 1.50 equiv) and *N*-methylimidazole (2.39 mL, 30.0 mmol, 1.50 equiv). The flask was partially immersed in a water bath and methanesulfonyl chloride (MsCl, 2.32 mL, 30.0 mmol, 1.50 equiv) was added dropwise with rapid stirring. Addition of MsCl was accompanied by the immediate formation of a yellow precipitate and a significant exotherm: *care should be taken to add MsCl slowly*. The mixture was stirred rapidly for 3 hours before dilution with distilled water (10 mL) and ethyl acetate (40 mL). The mixture was acidified with 1 M HCl and the organic layer was washed with brine, dried over sodium sulfate and concentrated under reduced pressure to yield a pale yellow solid. This material was triturated with hexanes to yield **S1** as a white solid (4.09 g, 16.8 mmol, 84% yield). ^{1}H NMR (500MHz, $CDCl_3$) δ = 7.59–7.40 (m, 5 H), 5.95 (s, 1 H), 3.79 (s, 3 H), 3.10 (s, 3 H). ^{13}C {^{1}H} NMR (126MHz, $CDCl_3$) δ = 168.2, 132.7, 130.0, 129.0, 127.7, 78.9, 53.0, 39.4. IR (ATR, neat): 3030 (w), 2960 (w), 2938 (w), 1764 (m), 1353 (s), 1217 (m), 1174 (s), 1012 (m), 943 (s), 880 (m), 848 (m), 737 (m), 699 (m). LRMS (ES-APCI+): expected for $[M+Na]^+$: 267.0; observe 267.0.

[41] Nakatsuji, H.; Ueno, K.; Misaki, T.; Tanabe, Y. *Org. Lett.* **2008**, *10*, 2131–2134.

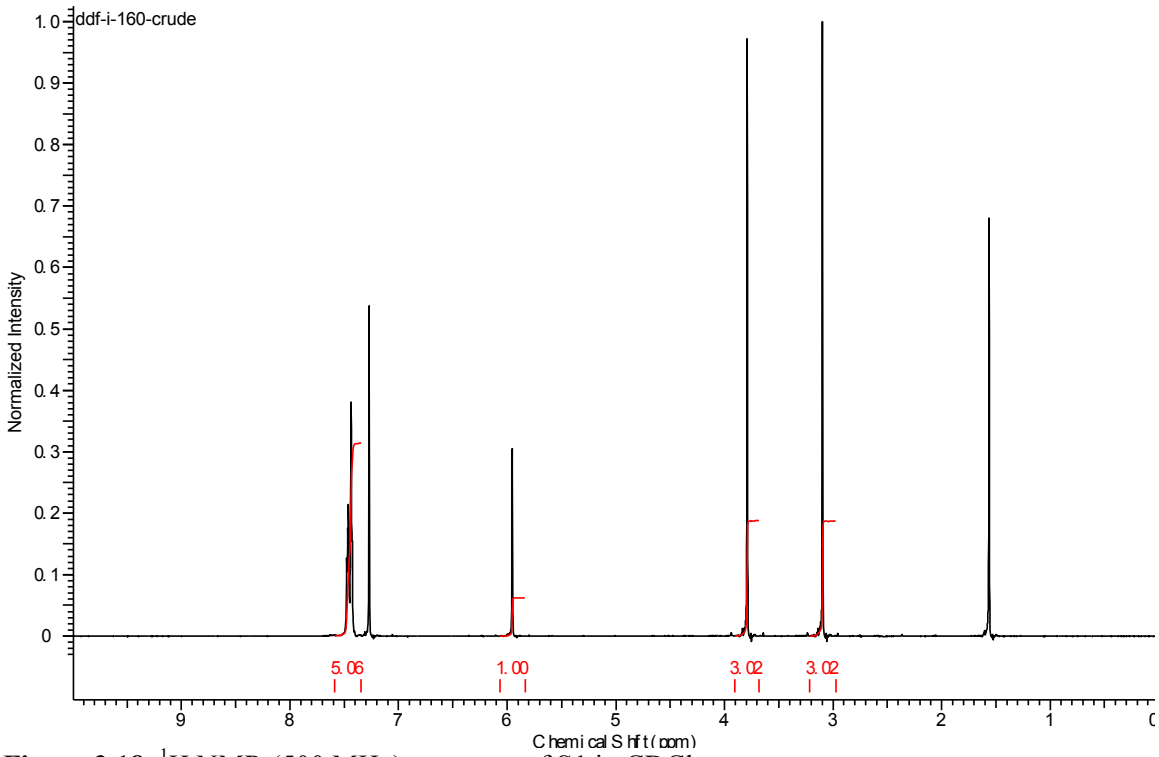

Figure 3.18. ^{1}H NMR (500 MHz) spectrum of **S1** in $CDCl_3$.

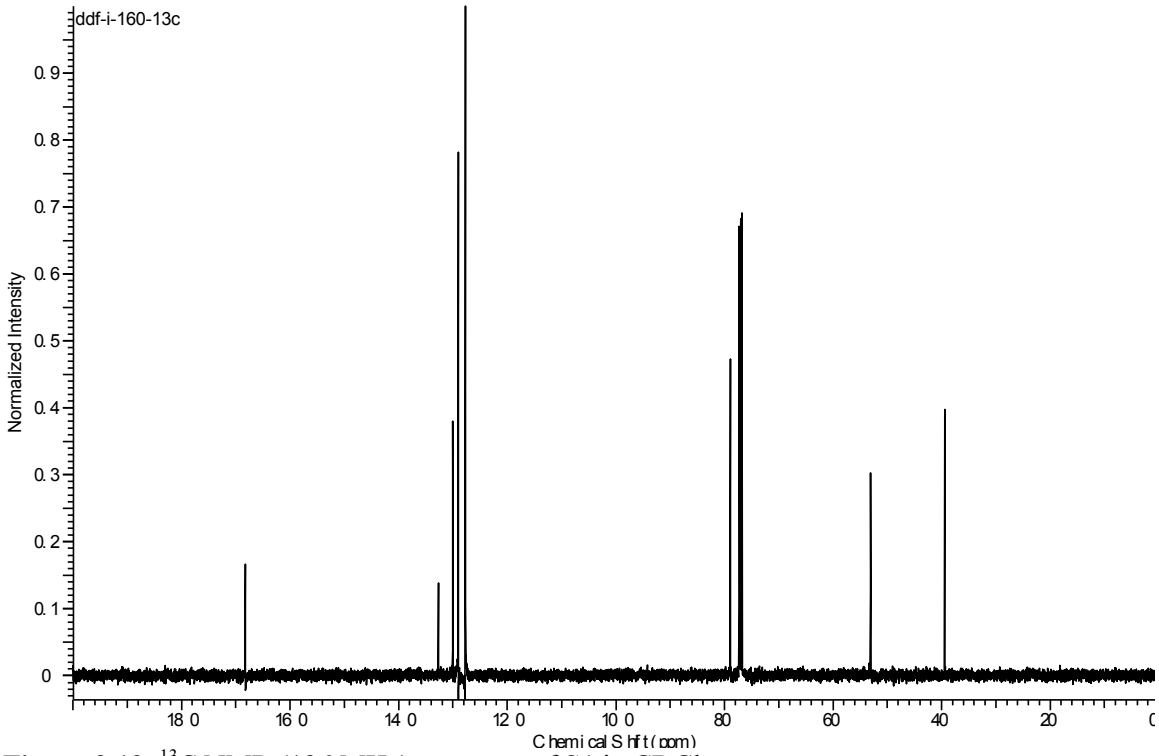

Figure 3.19. ^{13}C NMR (126 MHz) spectrum of **S1** in $CDCl_3$.

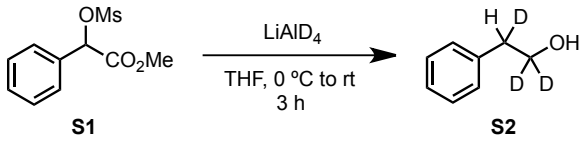

S1 **S2**

S2: An oven-dried 500-mL round-bottomed flask equipped with a PTFE-coated magnetic stirbar was charged with **S1** (6.45 g, 26.4 mmol, 1.00 equiv) and anhydrous THF (250 mL). The resulting solution was cooled to 0 ºC before lithium aluminum deuteride (2.22 g, 52.8 mmol, 2.00 equiv) was added cautiously in one portion. The reaction mixture was stirred rapidly and the ice bath was allowed to melt. After 3 h, the reaction mixture was cooled to 0 ºC and 2.2 mL DI H_2O, 2.2 mL 15% NaOH (aq) and 6.6 mL DI H_2O were added in dropwise in sequence. Stirring was continued for 30 minutes before Celite was added and the mixture was filtered through a pad of Celite. The Celite was rinsed with diethyl ether and the resulting solution was concentrated under reduced pressure. The residue was dissolved in diethyl ether. The ethereal solution was washed with brine, dried over $MgSO_4$ and concentrated under reduced pressure to yield a clear, colorless oil. This material was purified by silica gel flash chromatography (gradient elution: 20% → 50% diethyl ether in hexanes) to yield **S2** as a clear, colorless oil (2.60 g, 20.8 mmol, 79% yield). This material was sometimes accompanied by a small impurity (<5 %) that was very difficult to separate. This impurity was no longer present after the following step. ^{1}H NMR (500MHz, $CDCl_3$) δ = 7.38–7.30 (m, 2 H), 7.30–7.17 (m, 3 H), 2.86 (br. s., 1 H), 1.54 (br. s., 1 H). ^{13}C {^{1}H} NMR (126MHz, $CDCl_3$) δ = 138.4, 129.0, 128.6, 126.4, 62.9 (quin, J_{CD} = 22 Hz), 38.6 (t, J_{CD} = 20 Hz). IR (ATR, neat): 3329 (br, w), 3027 (w), 2919 (w), 2209 (w), 2290 (w), 1604 (w), 1495 (m), 1451 (m), 1127 (m), 1102 (m), 1009 (m), 739 (s), 716 (s), 697 (s). LRMS (ESI+): expected for $[M+Na]^+$: 148.1; observe 148.1.

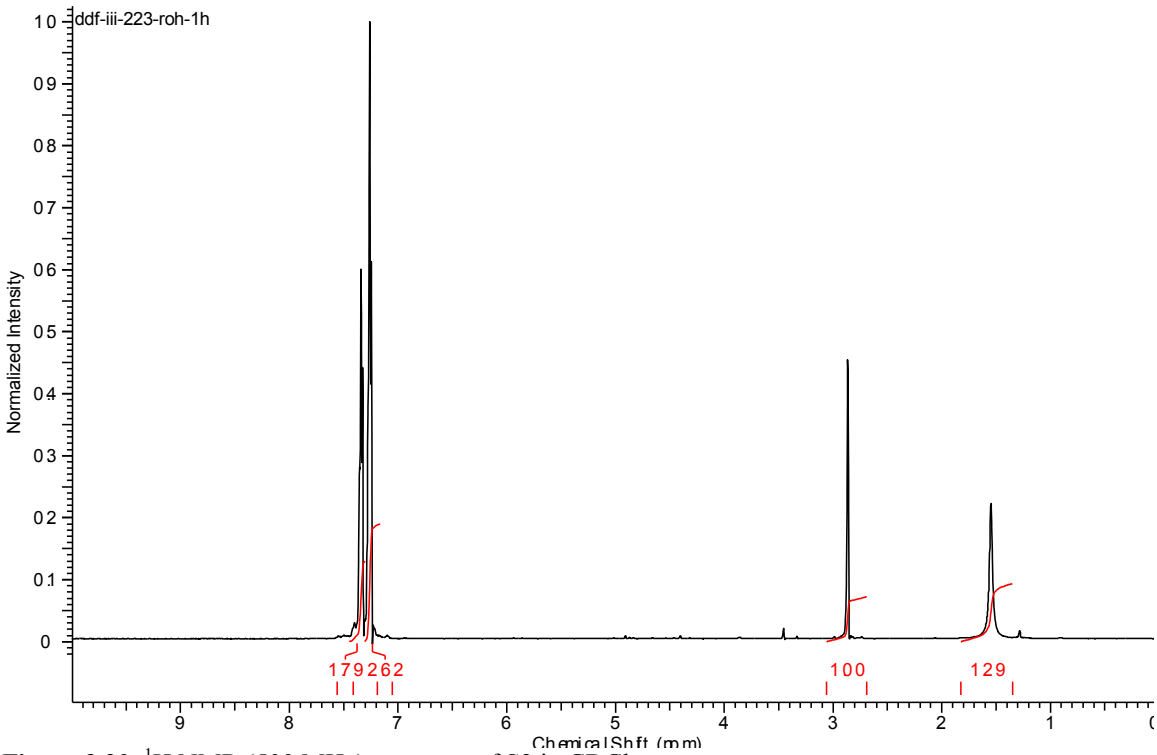

Figure 3.20. ^{1}H NMR (500 MHz) spectrum of **S2** in $CDCl_3$.

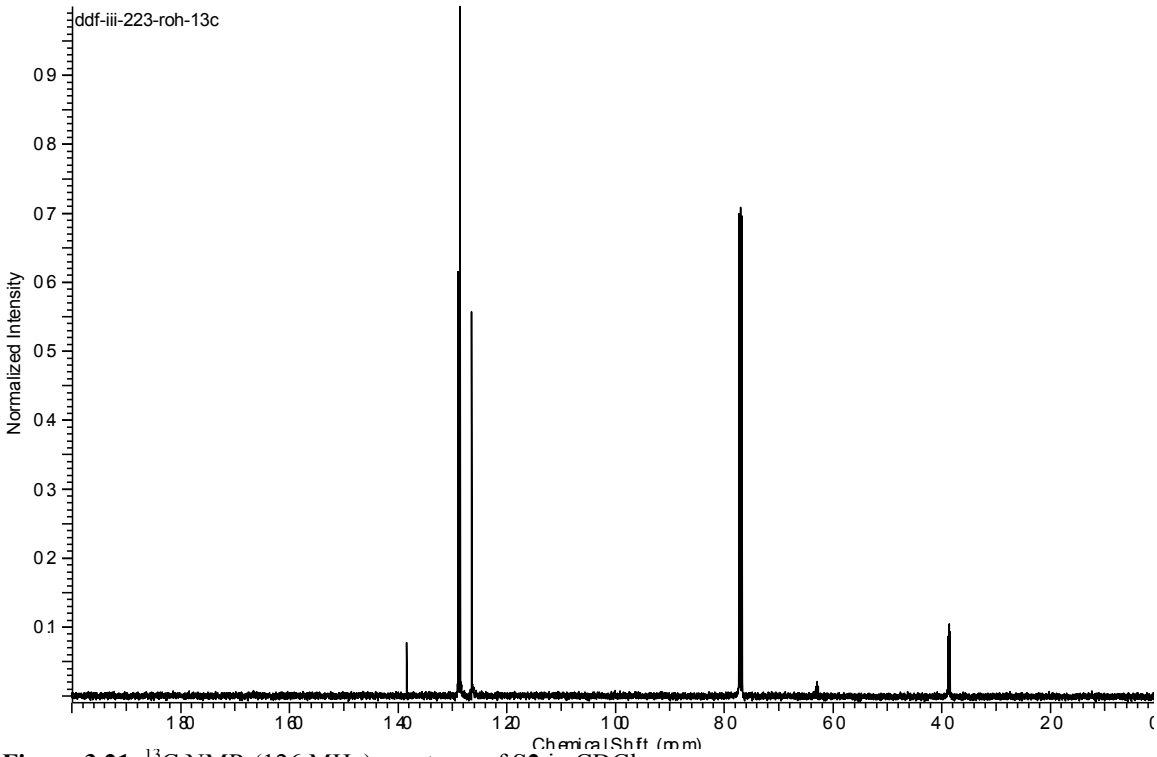

Figure 3.21. ^{13}C NMR (126 MHz) spectrum of **S2** in $CDCl_3$.

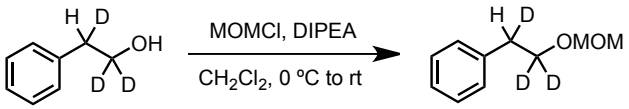

S2 **S3**

S3: An oven-dried 100-mL round-bottomed flask equipped with a PTFE-coated magnetic stirbar was charged with **S2** (2.60 g, 20.8 mmol, 1.00 equiv), anhydrous CH_2Cl_2 (40 mL) and diisopropylethylamine (10.9 mL, 62.3 mmol, 3.00 equiv). The resulting solution was cooled to 0 ºC before addition of chloromethyl methyl ether (2.37 mL, 31.2 mmol, 1.50 equiv) and the ice bath was allowed to melt. The reaction mixture was aged for 96 h (reaction may have completed earlier) before it was diluted with diethyl ether. The resulting solution was washed with 1 N HCl (aq), sat. $NaHCO_3$ (aq) and brine, was dried over $MgSO_4$ and was concentrated under reduced pressure to yield **S3** as a clear, colorless oil (3.06 g, 18.1 mmol, 87% yield). This material was >95% pure by ^{1}H NMR spectroscopy and was carried forward without further purification. ^{1}H NMR (500 MHz, $CDCl_3$) δ = 7.17–7.23 (m, 2 H) 7.09–7.17 (m, 3 H) 4.52 (s, 2 H) 3.20 (s, 3 H) 2.79 (br. s., 1 H). ^{13}C {^{1}H} NMR (126MHz, $CDCl_3$) δ = 138.8, 128.8, 128.3, 126.2, 96.3, 67.6 (quin, J_{CD} = 22 Hz), 55.1, 35.7 (t, J_{CD} = 19.5 Hz). IR (ATR, neat): 2929 (w), 2196 (w), 2089 (w), 1496 (w), 1451 (w), 1138 (m), 1114 (m), 1048 (s), 917(m), 741 (m), 698 (m). HRMS (ESI+): *m/z* expected for $[M + Na]^+$: 192.1074, observe: 192.1070.

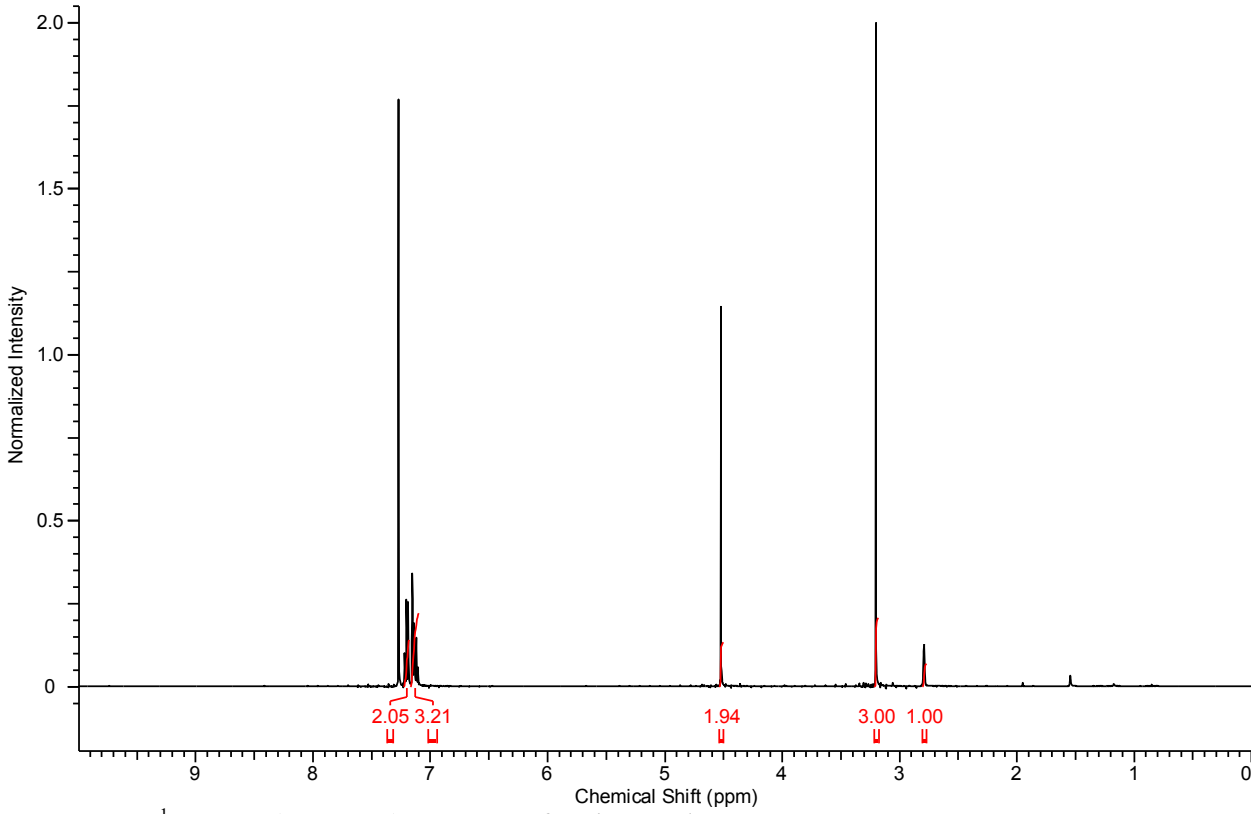

Figure 3.22. ^{1}H NMR (500 MHz) spectrum of **S3** in $CDCl_3$.

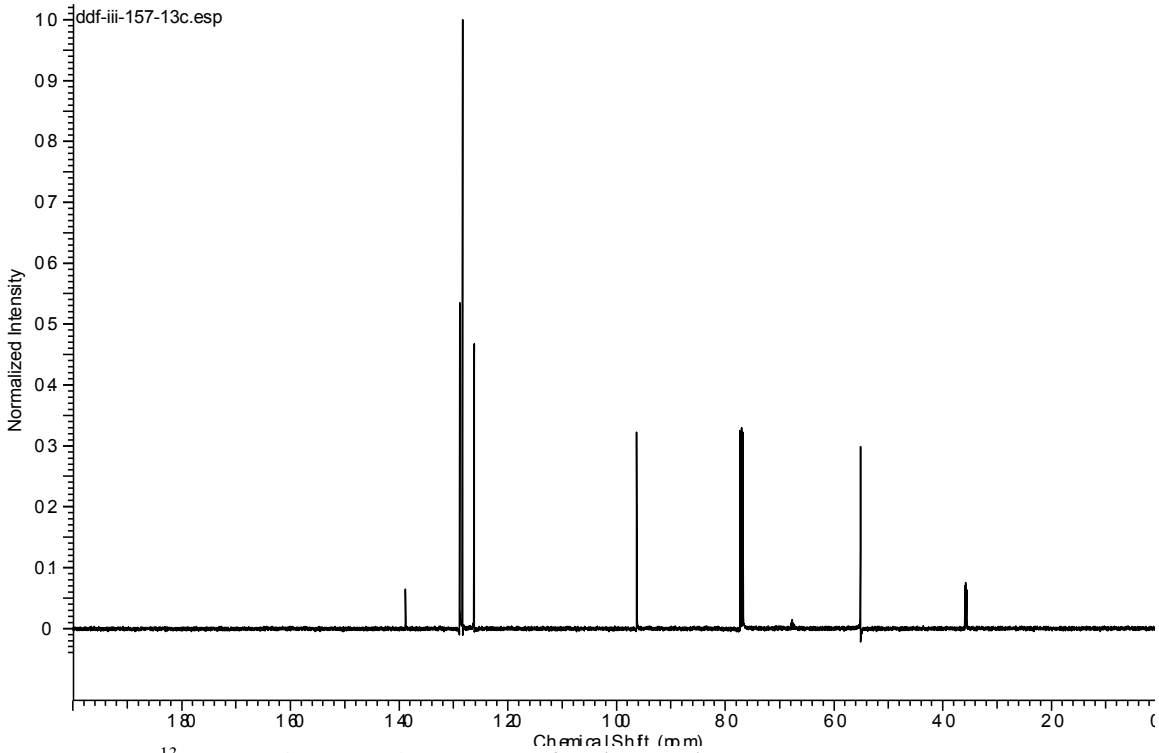

Figure 3.23. ^{13}C NMR (126 MHz) spectrum of **S3** in $CDCl_3$.

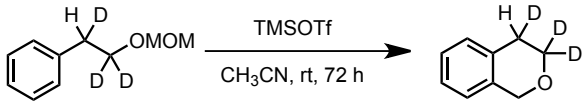

S3 **S4**

S4: An oven-dried 200-mL round-bottomed flask equipped with a PTFE-coated magnetic stirbar was charged with **S3** (3.06 g, 18.1 mmol, 1.00 equiv) and anhydrous acetonitrile (90 mL). The resulting solution was stirred rapidly while trimethylsilyl trifluoromethanesulfonate (3.27 mL, 18.1 mmol, 1.00 equiv) was added dropwise. The reaction mixture was aged for 72 h before addition of aqueous sat. $NaHCO_3$ (40 mL) and concentration under reduced pressure. The resulting slurry was diluted with diethyl ether and the organic layer was washed with brine, dried over $MgSO_4$ and concentrated under reduced pressure to yield a clear, colorless oil. This material was purified by automated flash column chromatography (100 g cartridge, 2% → 20% diethyl ether in hexanes) to yield **S4** as a clear, colorless oil (1.90 g, 13.9 mmol, 77% yield). ^{1}H NMR (500MHz, $CDCl_3$) δ = 7.25–7.07 (m, 3 H), 7.07–6.94 (m, 1 H), 4.81 (s, 2 H), 2.86 (br. s., 1 H). ^{13}C {^{1}H} NMR (126MHz, $CDCl_3$) δ = 134.9, 133.1, 128.9, 126.3, 125.9, 124.3, 67.8, 64.5 (quin, J_{CD} = 22 Hz), 27.7 (t, J_{CD} = 19.5 Hz). IR (ATR, neat): 3022 (w), 2895 (w), 2829 (w), 2220 (w), 2096 (w), 1584 (m), 1450 (m), 1367 (m), 1260 (m), 1202 (m), 1147 (m), 1098 (s), 1035 (m), 941 (m), 740 (s). LRMS (APCI+) expected for $[M - H]^+$: 136.2, observe 136.1.

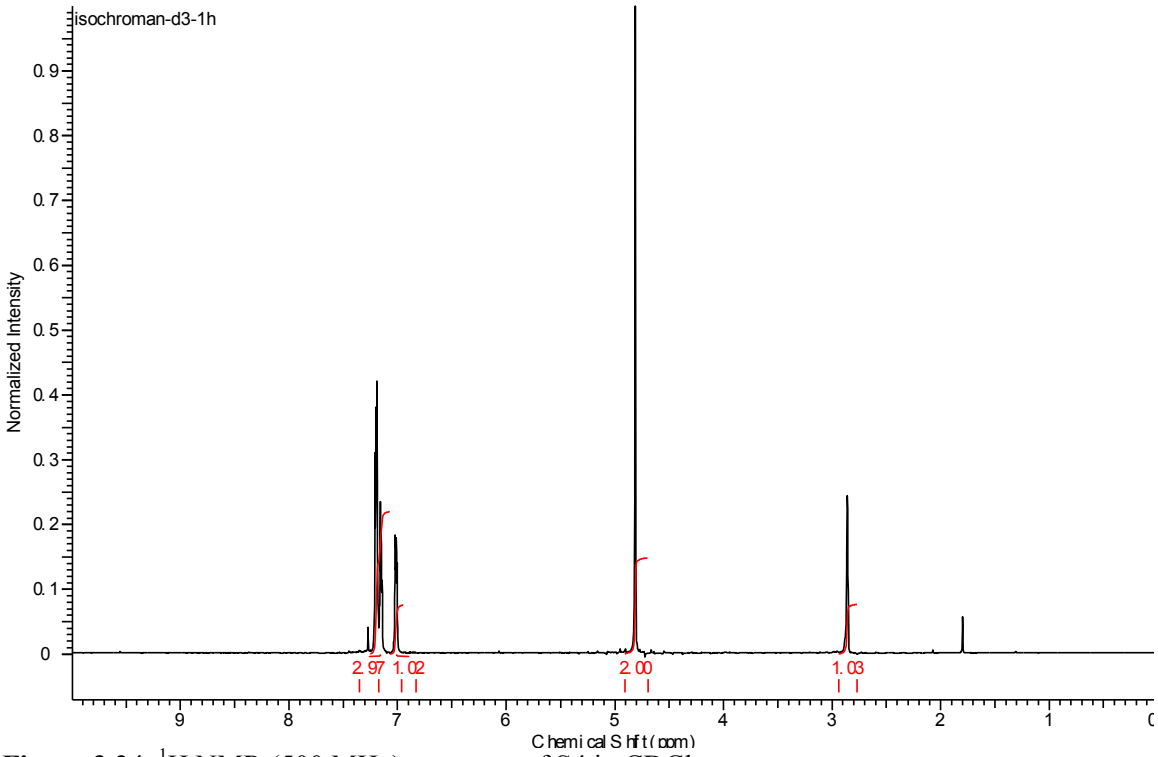

Figure 3.24. ^{1}H NMR (500 MHz) spectrum of **S4** in $CDCl_3$.

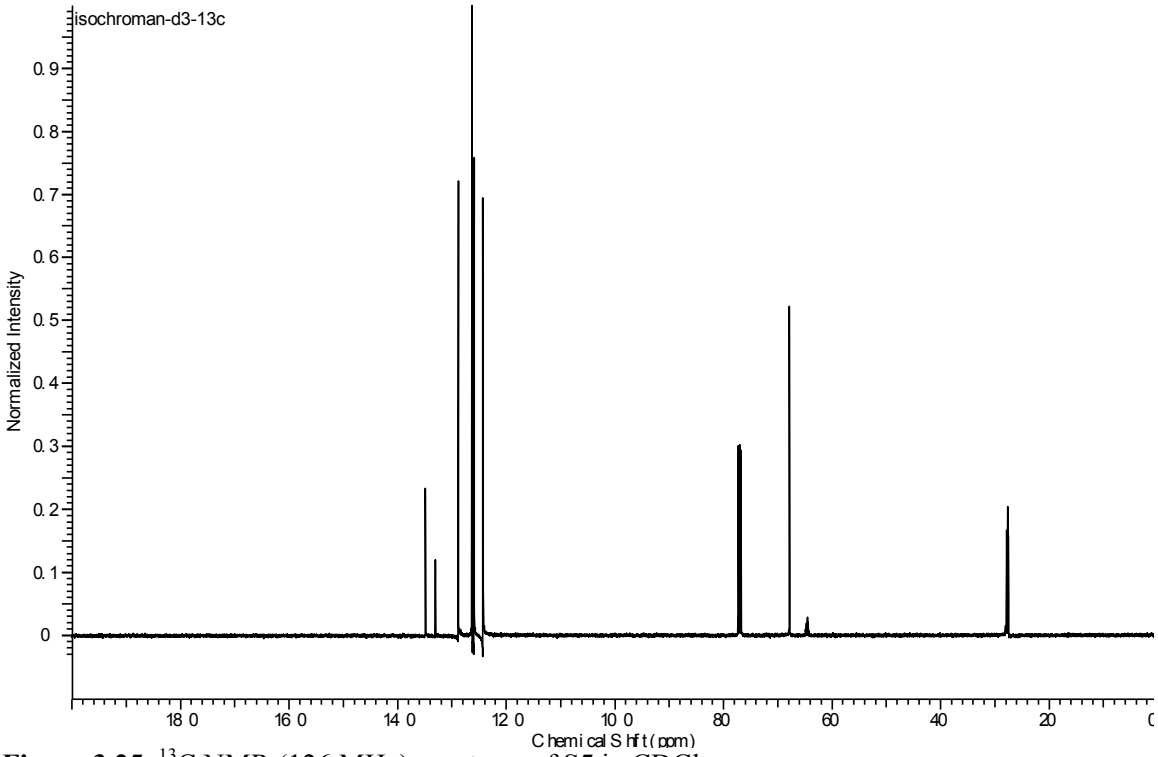

Figure 3.25. ^{13}C NMR (126 MHz) spectrum of **S5** in $CDCl_3$.

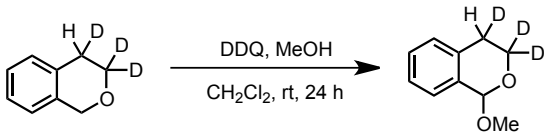

S4 **S5**

S5: An oven-dried 200-mL round-bottomed flask equipped with a PTFE-coated magnetic stirbar was charged with **S4** (1.90 g, 13.9 mmol, 1.00 equiv), methanol (0.73 mL, 18.9 mmol, 1.30 equiv) and CH_2Cl_2 (92 mL). To the resulting mixture was added 2,3-dichloro-5,6-dicyano-1,4-benzoquinone (4.09 g, 18.0 mmol, 1.30 equiv) with stirring. The reaction mixture was stirred at room temperature for 24 h before portionwise addition of sat. aqueous $NaHCO_3$. The resulting biphasic mixture was stirred rapidly, taking care to control evolution of gas. Stirring was continued until very little precipitate remained. The layers were separated and the organic layer was rinsed with sat. aqueous $NaHCO_3$ until the aqueous layer remained colorless after rinsing. The organic layer was dried over Na_2SO_4 and was concentrated under reduced pressure to yield a yellow oil. This material was purified by automated flash column chromatography (100 g cartridge, 5% → 40% diethyl ether in hexanes) to yield **S5** as a colorless oil (1.4 g, 8.4 mmol, 61% yield). The majority of the mass balance is the over-oxidized lactone form, which is more easily separated from **S5** than is **S4**. ^{1}H NMR (500 MHz, $CDCl_3$) δ = 7.28 (br. s., 3 H), 7.21–7.08 (m, 1 H), 5.50 (s, 1 H), 3.60 (s, 3 H), 3.03 (br. s., 0.5 H), 2.62 (br. s., 0.5 H). ^{13}C {^{1}H} NMR (126 MHz, $CDCl_3$; two peaks are split, presumably arising from the two diastereomers of **S5**. These peaks are denoted by *) δ = 134.5*, 134.4*, 134.2, 128.8*, 128.7*, 128.4, 127.7, 126.6, 98.1, 57.3 (quin, J_{CD} = 22 Hz), 55.6, 27.7 (t, J_{CD} = 20 Hz). IR (ATR, neat): 2888 (br. w), 2825 (w), 2230 (w), 2112 (w), 1609 (w), 1491 (m), 1455 (m), 1366 (m), 1348 (m), 1279 (w), 1259 (w), 1208 (m), 1187 (m), 1156 (w), 1093 (s), 1051 (s), 981 (m), 945 (m), 927 (m), 885 (m), 793 (w), 750 (s), 736 (s), 710 (w), 657 (w). HRMS (ESI+) expected for $[M + Na]^+$: 190.0918, observe 190.0920.

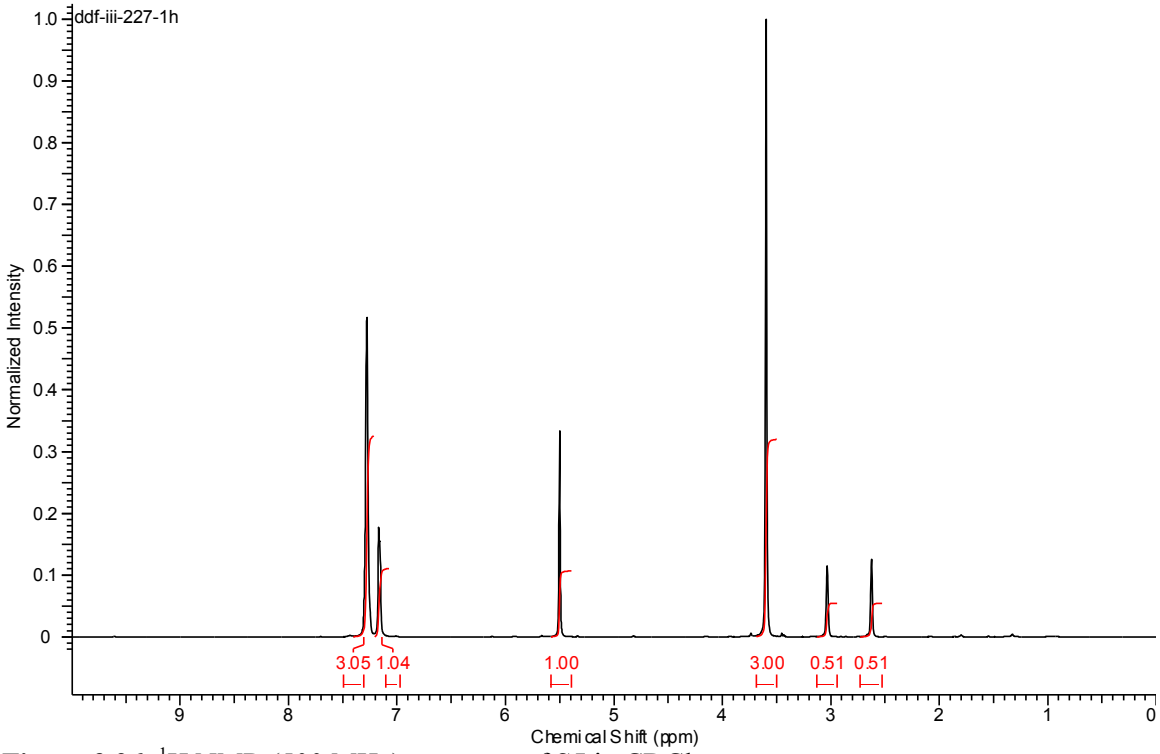

Figure 3.26. ^{1}H NMR (500 MHz) spectrum of **S5** in $CDCl_3$.

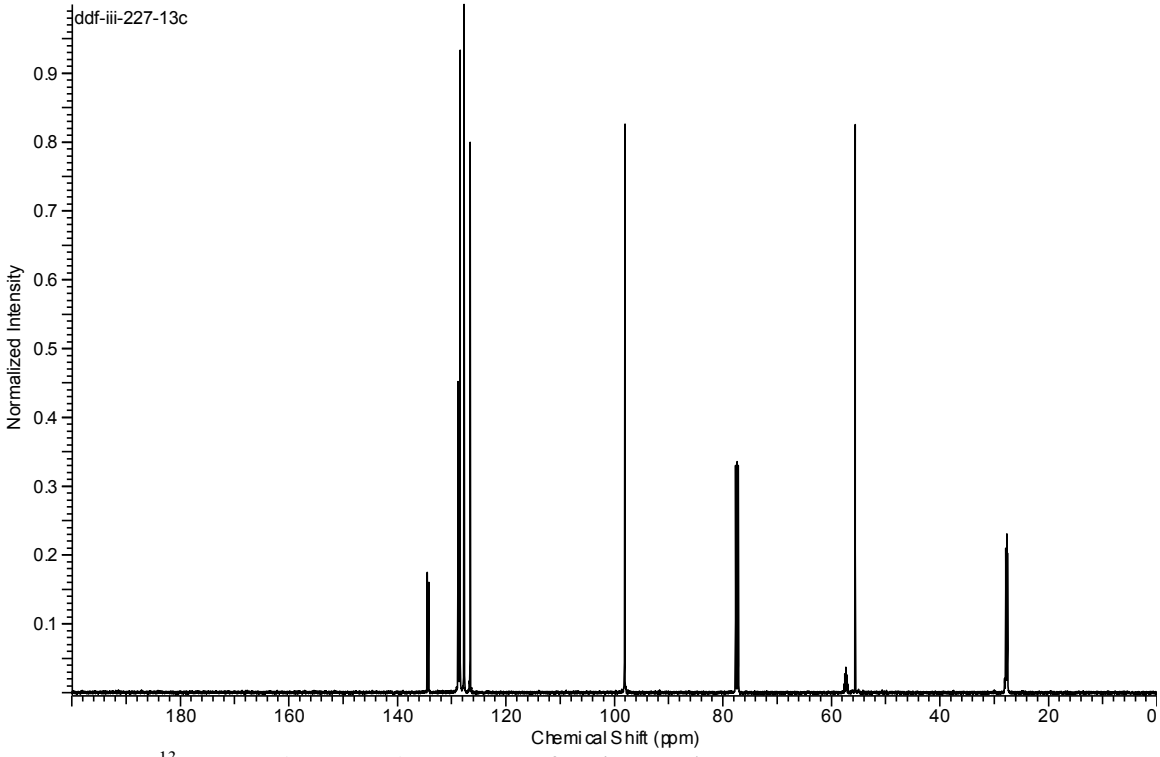

Figure 3.27. ^{13}C NMR (126 MHz) spectrum of **S5** in $CDCl_3$.

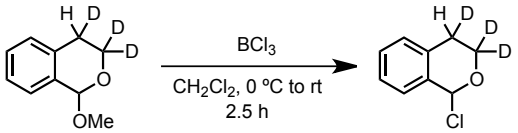

S5 **2**-d_3

2-d_3: An oven-dried 50-mL round-bottomed flask equipped with a PTFE-coated magnetic stirbar was charged with **S5** (1.65 g, 9.87 mmol, 1.00 equiv) and CH_2Cl_2 (8 mL) and cooled to 0 ºC. To the resulting mixture was added boron trichloride as a 1.0 M solution in hexane (3.95 mL, 3.95 mmol, 0.4 equiv), dropwise with stirring. As the last portion of BCl_3 solution is added, the reaction mixture becomes pale yellow in color. This color fades after a few minutes. After 30 minutes, the reaction mixture was warmed to room temperature and the mixture was aged for an additional 2 hours. Taking care to avoid exposure to air, the flask was fitted with a vacuum transfer apparatus. The flask containing the reaction mixture was cooled to −78 ºC and the system was put under vacuum (ca. 0.5 Torr). After allowing several minutes for the level of vacuum to stabilize, the reaction mixture was warmed to room temperature in air while the receiving flask was cooled to −78 ºC and the solvent was collected in the receiving flask. After vacuum transfer was complete, a yellow oil remained in the reaction flask. The vacuum transfer tube was quickly replaced with a short path distillation head fitted with a Schlenk-type receiving flask and the system was placed under vacuum (ca. 0.07 Torr). After 30 minutes, the reaction flask was heated to 95 ºC and the distillation head was gently warmed with a heat gun. In our experiments, we found that prolonged heating led to decomposition of the product, and a successful distillation was typically complete in ca. 5 min. After distillation, **2**-d_3 was isolated as a clear, colorless oil (1.42 g, 84% yield). For reproducible NMR experiments, this material was stored at −30 ºC under N_2 in an oxygen- and moisture-free inert atmosphere glove box. This material decomposes under typical mass spectrometry conditions. ^{1}H NMR (500 MHz, toluene-d_8) δ = 6.85–6.93 (m, 3 H), 6.84 (s, 1 H), 6.61 (d, J = 6.84 Hz, 1 H), 2.48 (br. s., 0.5 H) 1.80 (br.

s., 0.5 H). ^{13}C NMR (126 MHz, toluene-d_6; two peaks are split, presumably arising from the two diastereomers of **2**-*d*3. These peaks are denoted by *) δ = 135.58*, 135.54*, 132.12, 128.53, 128.37*, 128.31*, 127.23, 126.48, 93.52, 59.29 (quin, J_{CD} = 22.50 Hz) 26.26 (t, J_{CD} = 19.20 Hz).

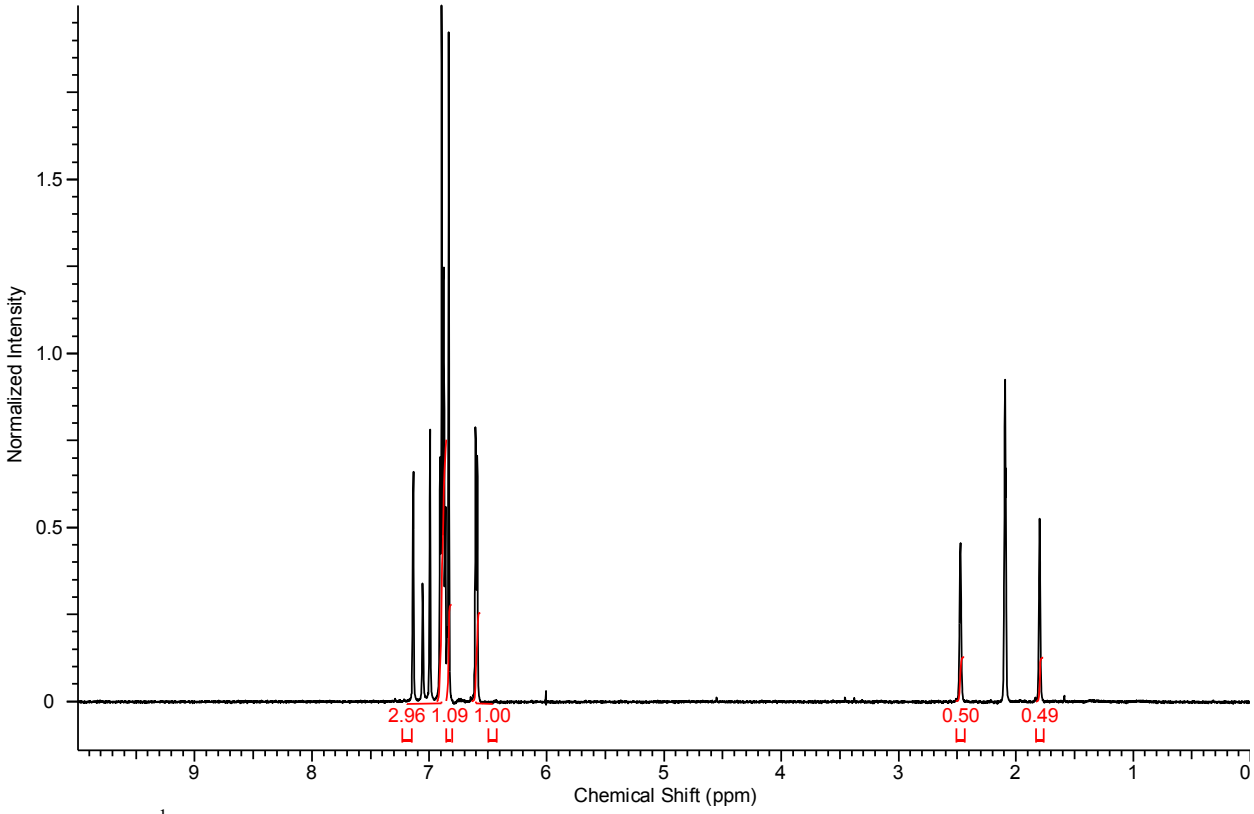

Figure 3.28. ^{1}H NMR (500 MHz) spectrum of **2**-d_3 in toluene-d_8.

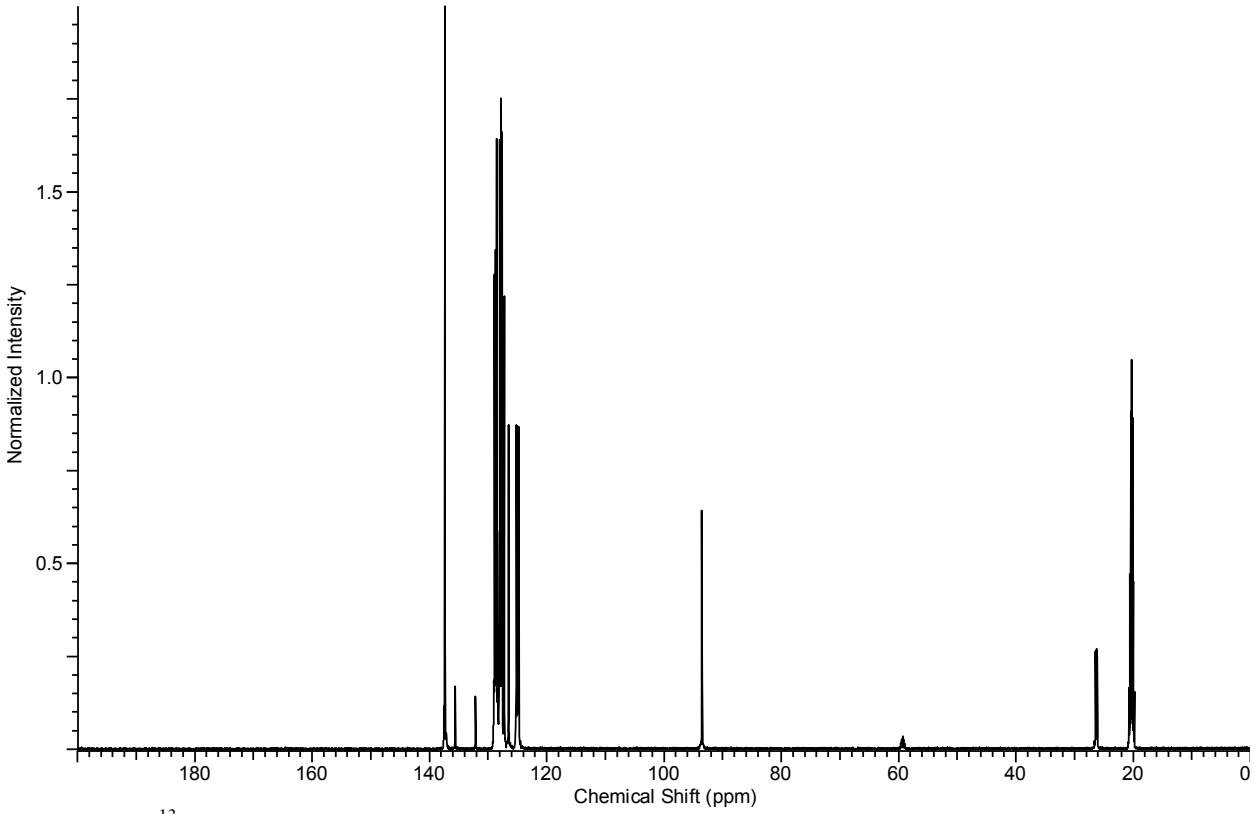

Figure 3.29. ^{13}C NMR (126 MHz) spectrum of **2**-d_3 in toluene-d_8.

3.6.4 Derivation of the rate law

Scheme 3.6. Simplified mechanism for the alkylation reaction used in this derivation. Note that substrate binding steps are combined into the rate- and e.e.-determining C–C bond-forming step.

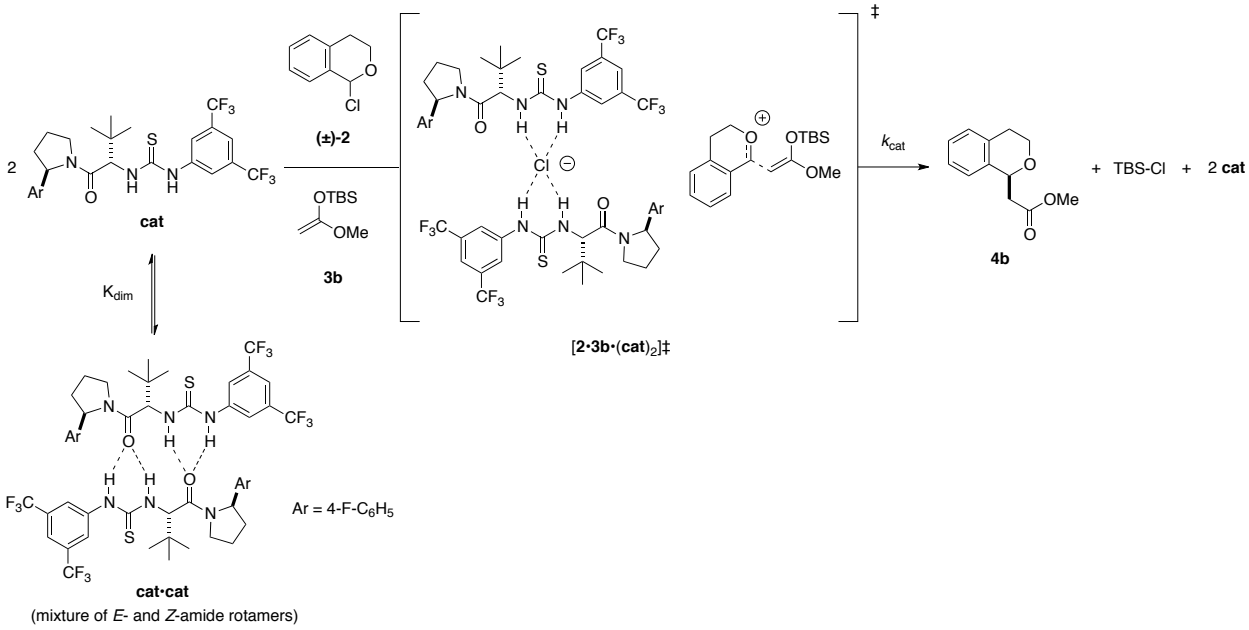

Based on Scheme 3.6, the rate of product formation should be:

$$\frac{d[\mathbf{product}]}{dt} = rate = k_{cat}[\mathbf{cat}]^2\,[\mathbf{electrophile}]^1\,[\mathbf{nucleophile}]^1 \tag{3.4}$$

The equation is more useful if we rewrite it in terms of $[cat]_T$, the total concentration of catalyst across all possible resting states. This is the amount of catalyst added to the reaction mixture, whereas [cat] only reflects the concentration of the monomer present in solution. Hence, our first task is to find an expression for [cat] as a function of $[cat]_T$.

For the self-dimerization of the catalyst equilibrium process shown above in Scheme 3.6, the equilibrium constant K_{dim} is defined by eq 3.5:

$$K_{\mathrm{dim}} = \frac{[\mathbf{cat{\bullet}cat}]}{[\mathbf{cat}]^2} \tag{3.5}$$

Rearrange:

$$[\mathbf{cat{\bullet}cat}] = K_{\mathrm{dim}}\,[\mathbf{cat}]_T \tag{3.6}$$

If [cat•cat] and [cat] are the only two resting states of the catalyst and other intermediates are present in vanishingly small concentrations:

$$[\mathbf{cat}]_T = 2[\mathbf{cat{\bullet}cat}] + [\mathbf{cat}] \tag{3.7}$$

Substitute eq 3.6 into eq 3.7:

$$[\mathbf{cat}]_T = 2K_{dim}[\mathbf{cat}]^2 + [\mathbf{cat}] \tag{3.8}$$

Rearrange to form a standard quadratic equation:

$$2K_{dim}[\mathbf{cat}]^2 + [\mathbf{cat}] - [\mathbf{cat}]_T = 0 \tag{3.9}$$

The roots of the quadratic equation can be obtained from the equation:

$$x = \frac{-b \pm \sqrt{b^2 - 4ac}}{2a} \tag{3.10}$$

where the quadratic equation in its standard form is of the form:

$$0 = ax^2 + bx + c \tag{3.11}$$

Thus, the roots of eq 3.9 are obtained from equation 3.12:

$$[\mathbf{cat}] = \frac{-1 \pm \sqrt{(1^2 + -4(2K_{dim})(-[\mathbf{cat}]_T)}}{2(2K_{dim})} \tag{3.12}$$

Simplify:

$$[\mathbf{cat}] = \frac{-1 \pm \sqrt{(1 + 8K_{dim}[\mathbf{cat}]_T)}}{4K_{dim}} \tag{3.13}$$

Because any physically meaningful solution must have [cat] > 0 and because $\sqrt{(1 + 8K_{dim}[\mathbf{cat}]_T)} > 0$, then the solution is given by equation 3.14:

$$[\mathbf{cat}] = \frac{-1 + \sqrt{(1 + 8K_{dim}[\mathbf{cat}]_T)}}{4K_{dim}} \tag{3.14}$$

Rationalize the numerator:

$$[\mathbf{cat}] = \frac{(-1 + \sqrt{(1 + 8K_{dim}[\mathbf{cat}]_T)})}{4K_{dim}} \bullet \frac{(1 + \sqrt{(1 + 8K_{dim}[\mathbf{cat}]_T)})}{(1 + \sqrt{(1 + 8K_{dim}[\mathbf{cat}]_T)})} \tag{3.15}$$

Now we have an expression for [cat] as a function of $[cat]_T$ and the equilibrium constant K_{dim}:

$$[\mathbf{cat}] = \frac{2[\mathbf{cat}]_T}{1 + \sqrt{(1 + 8K_{dim}[\mathbf{cat}]_T)}} \quad (3.16)$$

Substitute eq 3.16 into the proposed rate law for product formation (eq 3.4) in which the reaction is proposed to be second order of the catalyst (**cat**) and first order in both the **nucleophile** and **electrophile**:

$$\frac{d[\mathbf{product}]}{dt} = k_{cat}\left[\frac{2[\mathbf{cat}]_T}{1 + \sqrt{(1 + 8K_{dim}[\mathbf{cat}]_T)}}\right]^2 [\mathbf{electrophile}]^1 [\mathbf{nucleophile}]^1 \quad (3.17)$$

which simplifies to eq 3.18:

$$\frac{d[\mathbf{product}]}{dt} = k_{cat} \frac{4\,([\mathbf{cat}]_T)^2\,[\mathbf{electrophile}][\mathbf{nucleophile}]}{\left(1 + \sqrt{(1 + 8K_{dim}[\mathbf{cat}]_T)}\right)^2} \quad (3.18)$$

where **cat** is **1a** or **1b,** the **electrophile** is **(±)-2**, and **nucleophile** is any of the silyl ketene acetals (e.g., **3b** or **3c**) and **product** is corresponding product (e.g., **4b** or **4c**) depending on the silyl ketene acetal used.

If $K_{dim}[cat]_T << 1$, eq 3.18 simplifies:

$$\frac{d[\mathbf{product}]}{dt} = k_{cat}\,([\mathbf{cat}]_T)^2\,[\mathbf{electrophile}][\mathbf{nucleophile}] \quad (3.19)$$

Similarly, if $K_{dim}[cat]_T >> 1$, eq 3.18 simplifies:

$$\frac{d[\mathbf{product}]}{dt} = \frac{k_{cat}}{2K_{dim}}\,[\mathbf{cat}]_T\,[\mathbf{electrophile}][\mathbf{nucleophile}] \quad (3.20)$$

3.6.4. Kinetics of Epimerization of 2-d_3 by Selective Inversion-Recovery

All samples were prepared in an inert-atmosphere glovebox at room temperature. Stock solutions were prepared using volumetric glassware and volumes of these stock solutions were dispensed with glass syringes. The NMR tube was capped, and the cap was taped in place to slow the influx of oxygen. The 90º pulse width was recalibrated before collecting data for each new sample or temperature. Each time the temperature of the probe was changed, the temperature was calibrated with a no-D ^{1}H spectrum of a methanol standard and the "tempcal" macro in the Varian VNMR software.

The samples were locked and shimmed on the residual protium at the methyl position of the toluene-d_8 solvent. All spectra were acquired without spinning. For each sample, a standard inversion-recovery experiment was performed followed by a selective inversion-recovery experiment (Figure 3.29). In all cases the recycle delay *d1* was set to 120 s. Due to the deoxygenated solvent, a long recycle delay was necessary for reliable results. The mixing time *d2* was incremented, with typically 9–12 values of *d2* per experiment. The acquisition time *at* was fixed at 2 s in all cases. The selective inversion experiment was performed with a pure-phase I-BURP-2 inversion pulse. For each value of *d2*, a single transient was acquired with no steady-state scans (i.e. one scan, no dummy scans).

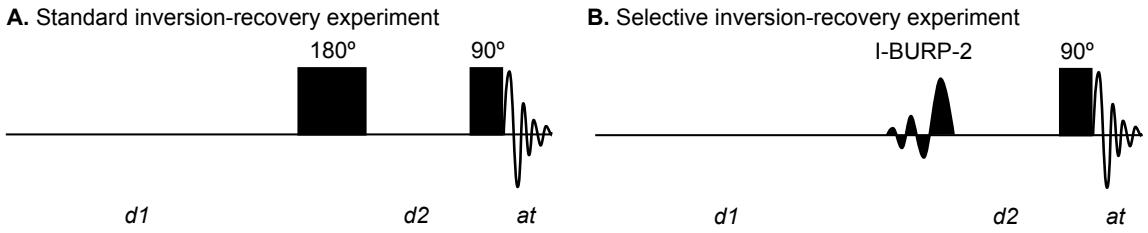

Figure 3.30. Pulse sequence schematics for the two experiments performed for each sample of **2**-d_3 with various additives and catalysts. **A**: the standard inversion-recovery experiment with square pulses. This experiment provides primarily T_1 information. **B**: the selective inversion-recovery experiment with a selective 180º pulse. This experiment provides primarily k_{obs} information.

After collecting the standard inversion-recovery data as well as the selective inversion-recovery data, the spectra were Fourier-transformed, phased and batch integrated using the ACD/Labs NMR Processor. The integral values were normalized such that the integral values were on the order of 1 (arbitrary units) and k_{obs} and T_1 were fitted with the CIFIT program according to Bain's procedure.[19]

Example data set from one sample:

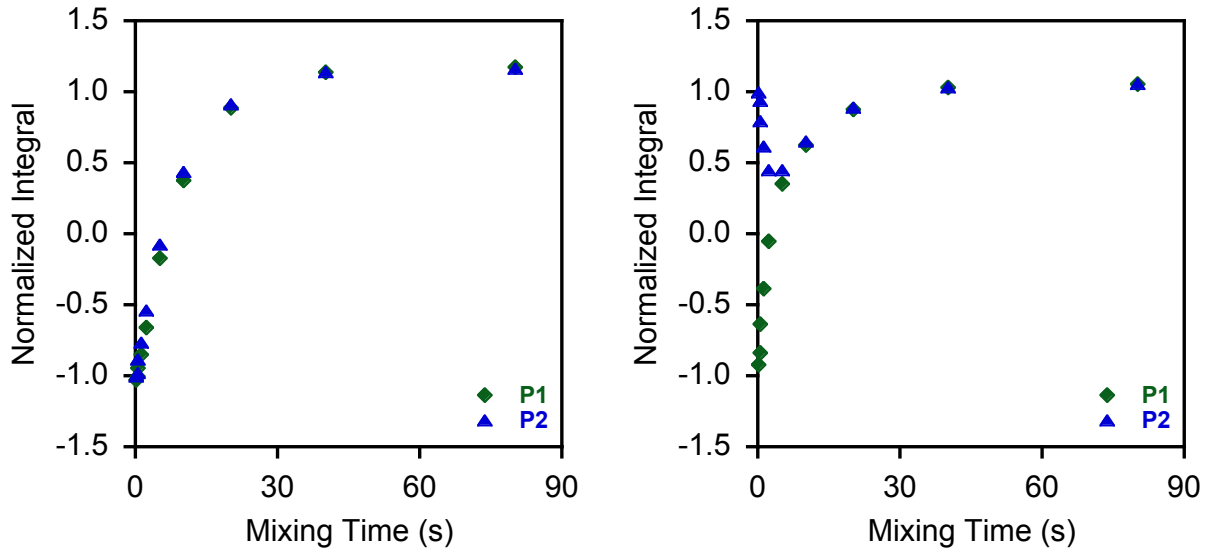

Figure 3.31. Data from standard (left) and selective (right) inversion-recovery experiment of a sample with $[\mathbf{1a}]_T$ = 10 mM, [**2**-d_3] = 100 mM in Toluene-d_8 at –40 ºC. P1 and P2 represent the two resonances that undergo chemical exchange.

Table 3.3. Normalized integration data used to generate Figure 3.30:

	Standard Inversion-Recovery		Selective Inversion-Recovery	
d2 (s)	Peak 1	Peak 2	Peak 1	Peak 2
0.1	-1.027	-1.000	-0.912	1.000
0.2	-1.003	-0.973	-0.833	0.941
0.5	-0.942	-0.885	-0.636	0.793
1	-0.844	-0.761	-0.376	0.618
2	-0.649	-0.541	-0.045	0.453
5	-0.161	-0.067	0.359	0.448
10	0.387	0.441	0.628	0.655
20	0.896	0.912	0.886	0.899
40	1.140	1.142	1.034	1.036
80	1.175	1.171	1.062	1.061

Fitting of the data shown in Table 3.3 using the CIFIT program yielded a rate constant $k_{obs} = 0.32 \pm 0.01$ s^{-1}, as well as values for $1/T_1$ for Peak 1 and Peak 2 of 0.083 ± 0.002 and 0.133 ± 0.002 s^{-1}, respectively. The uncertainty is the standard error of the fit calculated using KaleidaGraph. Each epimerization rate constant reported in this chapter was determined in this fashion.

Table 3.4. Order in **1a** and **1b**:

$[\mathbf{1a}]_T$ (mM)	k_{obs} (s^{-1})	$[\mathbf{1b}]_T$ (mM)	k_{obs} (s^{-1})
1[b]	0.021 ± 0.001	1[a]	0.008 ± 0.002
2.2[a]	0.052 ± 0.003	2.5[a]	0.046 ± 0.005
2.5[b]	0.053 ± 0.003	5[c]	0.37 ± 0.02
4.4[a]	0.124 ± 0.006	5[b]	0.255 ± 0.006
5[b]	0.098 ± 0.005	5[a]	0.40 ± 0.01
7.5[b]	0.152 ± 0.005	7.5[a]	0.55 ± 0.02
8.9[a]	0.23 ± 0.01	10[c]	0.79 ± 0.03
10[b]	0.189 ± 0.008	10[a]	0.89 ± 0.04
13.3[a]	0.32 ± 0.01	10[b]	0.87 ± 0.02
20[a]	0.46 ± 0.02	15[b]	1.35 ± 0.04
		15[c]	1.52 ± 0.04
		20[c]	1.97 ± 0.05
		20[b]	2.00 ± 0.05

Each experiment was performed on a 600 µL sample in a 5 mm NMR tube with [**2**-d_3] = 100 mM at –40 ºC in toluene-d_8. As described above, error bars represent the standard error of the fit from CIFIT. [a,b,c]The superscript letters denote experiments run using the same stock solutions.

We initially attributed the sharp drop-off of rate at low catalyst concentration to the presence of a catalyst poison in one of our reagents. To evaluate this hypothesis, we tested whether a variety of additives (potential impurities) affected the rate of epimerization of **2**-d_3 and the results are presented in Table 3.5. We ultimately concluded that the kinetic behavior was due to a change in resting state, but we include the results of our additive studies below:

Table 3.5. Summary of additive effects on the rate of epimerization of **2**-d_3.

Entry	Additive (10 mM)	H-Bond Donor (10 mM)	k_{obs} (s^{-1})
1	none	none	–0.003 ± 0.001
2	none	**1a**	0.22 ± 0.01
3	none	**1b**	1.11 ± 0.05
4	$B(OMe)_3$	none	–0.005 ± 0.001
5	$B(OMe)_3$	**1a**	0.24 ± 0.01
6	$B(OMe)_3$	**1b**	1.06 ± 0.05
7	HCl[a]	none	0.24 ± 0.02
8	HCl[a]	**1a**	0.014 ± 0.014
9	HCl[a]	**1b**	0.048 ± 0.005
10	$(octyl)_4NCl$	none	0.007 ± 0.001
11	$(octyl)_4NCl$	**1a**	–0.003 ± 0.001
12	$(octyl)_4NCl$	**1b**	–0.004 ± 0.001

[a]Generated *in situ* by creating a mixture with $[MeOH]_0$ = 10 mM and $[$**2**-$d_3]_0$ = 110 mM.

The data in Table 3.5 show that trimethyl borate does not catalyze epimerization, nor does it affect the epimerization activity of **1a** or **1b**. In contrast, HCl does catalyze epimerization, but it also inhibits catalysis by **1a** or **1b**. Finally, tetraoctylammonium chloride (a stand-in for a possible impurity resulting from the reaction of a trace amine impurity with **2**-d_3) does not catalyze epimerization, but it does inhibit catalysis by **1a** and **1b**.

3.6.5. Kinetics of Chloroether Alkylation

General Considerations

*Sample kinetic experiment using 10 mol% of **1a** and silyl ketene acetal **3a***:

An oven-dried modified flask equipped with a stir bar was attached to a hot React-IR probe that had been previously warmed with a heat gun and the system was purged with N_2. After the purge outlet was closed, the system was kept under a positive pressure of N_2 for the remainder of the experiment. Flask was allowed to cool to rt, charged with TBME (1.65 mL), then cooled to –78 °C (using a dry ice/acetone cooling bath) and after the temperature had stabilized (ca. 15–20 min) a background spectrum was acquired (600–3400 cm^{-1}). IR spectroscopy measured made use of a two-point correction baseline. To the reaction vessel was added a solution of silyl ketene acetal **3a** (165 μL, 0.300 mmol, 0.182 M in TBME; prepared by dissolving 342 mg in 1 mL of TBME), followed by 1-chloroisochroman (135 μL, 0.200 mmol, 1.48 M in TBME; prepared by dissolving 250 mg in 1 mL of TBME). The reaction was initiated by adding **1a** catalyst (50 μL, 0.020 mmol, 0.40 M in THF, prepared by dissolving 220 mg of **1a** in 1 mL of THF). Volumes of injections (dispensed using precision glass syringes) were maintained constant for all experiments, unless stated otherwise, and the amounts of reagents was altered by changing the concentration of the stock solutions used. Changing the volume of the THF catalyst solution had observable effects on the rate data. Reactions were quenched by the adding NaOMe (0.15 mL, 0.5 M NaOMe in MeOH) to the reaction mixture, which converts any remaining 1-chloroisochroman to 1-methoxyisochroman. The reaction mixture was diluted with 1 mL of 50% Et_2O in hexanes, filtered through a pipette filled with ¾ inch of silica gel on top of a plug of cotton wool using ca. 15 mL of 50% Et_2O in hexanes. The solvent was removed by rotary

evaporation under reduced pressure to give the crude residue, which was purified by silica gel chromatography (6% Et_2O in hexanes).

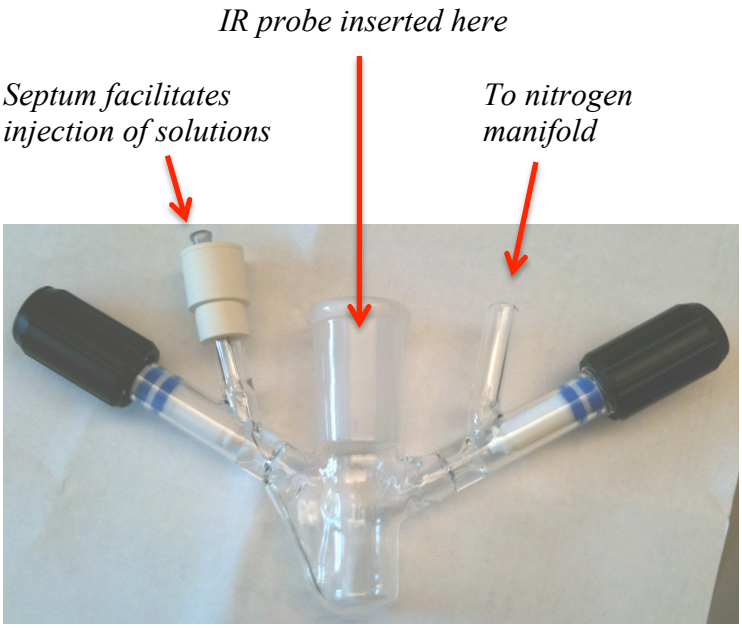

Figure 3.32. Photograph of custom-made reaction vessel used for alkylation kinetics monitored by ReactIR.

The reaction was monitored by following the consumption of the silyl ketene acetal **3** and the formation of product **4** at appropriate wavelengths (see Table S1). Spectra (with resolution of 1 cm^{-1}) were collected every 15 seconds for the first hour, then every 30 seconds for the next two hours and finally every minute for the remainder of the experiment. A two-point baseline correction was used for monitoring the peak intensities (e.g., 1800 cm^{-1} and 1550 cm^{-1} for silyl ketene acetals **3b** and **3c**).

Having determined the absorption coefficient (*e*) for **3** at –78°C in TBME which correlates the absorption intensity to the concentration of **3** (see below), the kinetics data collected above was converted to [**3**] as a function of time, and fitted to the following 7th order polynomial (using an unweighted least-squares fit; analysis was performed using KaleidaGraph Version 4.1.3[39]):

$$[\mathbf{3}] = f(t) = a_0 + a_1 t^1 + a_2 t^2 + a_3 t^3 + a_4 t^4 + a_5 t^5 + a_6 t^6 + a_7 t^7$$

The rate of consumption of **3** (–d[**3**]/d*t*) is obtained from the derivative of *f*(*t*), namely d*f*(*t*)/d*t*:

$$\frac{d[\mathbf{3}]}{dt} = \frac{df(t)}{dt} = a_1 + 2a_2 t^1 + 3a_3 t^2 + 4a_4 t^3 + 5a_5 t^4 + 6a_6 t^5 + 7a_7 t^6$$

The rates extracted from d*f*(*t*)/d*t* are valid only over the range of concentrations of **3** for which experimental data was collected. An analogous analysis using the concentration **4** at a function of time allows for determination of the rate of formation of **4** (d[**4**]/d*t*).

*Determination of absorption response factor (R_o) for **3** and **4***: The absorption intensity (*A*) was plotted as a function of concentration of **3** or **4**, the linear region of the plot was fitted with a linear least-squares fit corresponding to the equation:

$$A = R_o\,[\mathbf{c}]$$

in which *A* is the absorption intensity of the peak corresponding to compound **c**, R_o is the response factor, and [**c**] is the concentration of compound **c (**where **c** is either compound **3** or **4**). It should be noted that the absorption coefficient is temperature- and solvent-dependent and was measured at –78 °C in TBME to match the conditions of the kinetic experiments.

Scheme 3.7. Alkylation of 1-chloroisochroman (**(±)-2**) using silyl ketene actetals **3a–j**.

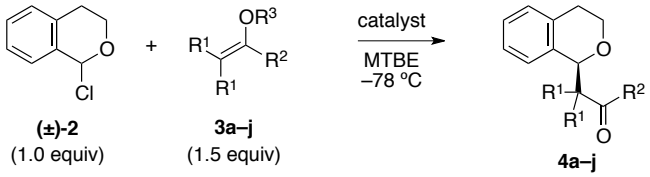

(±)-2 (1.0 equiv) **3a–j** (1.5 equiv) **4a–j**

Table 3.6. Wavelength of diagnostic IR peaks for reactions kinetics, relative rates and product ee.

Silyl Ketene Acetal	R^1	R^2	R^3	Silyl ketene acetal C=C stretch (cm^{-1})	Product C=O stretch (cm^{-1})	$-d$[**3**]/dt at [**3**] = 0.12 M (30% conversion) (x 10^{-5} M^{-1}•s^{-1})	Product ee (%)
3e	Me	OMe	$SiMe_3$	1715	1745	0.48	92
3f	Me	OMe	$SiEt_3$	1712	1745	0.97	93
3a	Me	OMe	Si(*t*-Bu)Me_2	1712	1745	0.43	94
3g	Me	OMe	Si(*i*-Pr)$_3$	1710	1745	0.36	95
3b	H	OMe	Si(*t*-Bu)Me_2	1659	1745	10.5	85
3h	H	OEt	Si(*t*-Bu)Me_2	n.d.	n.d.	n.d.	86
3c	H	O*i*-Pr	Si(*t*-Bu)Me_2	1659	1749	8.9	84
3i	H	O*t*-Bu	Si(*t*-Bu)Me_2	n.d.	n.d.	n.d.	84
3d	H	OBn	Si(*t*-Bu)Me_2	1656	1740	7.0	86
3d-d_2	D	OBn	Si(*t*-Bu)Me_2	1622	1740	7.9[b]	86
3j	H	SEt	$SiMe_3$	1608[a]	1697	2.5	81

[a] The peak at 863 cm^{-1} was used for monitoring consumption of the silyl ketene acetal in the reaction kinetics experiments. [b] Rate estimated from KIE experiments: A competition experiment with 2.5 equiv of **3d** and 2.5 equiv **3d**-d_2 afforded a measured KIE = (–d[**3d**]/dt)/(–d[**3d**-d_2]/dt) = 0.88 in which –d[**3d**]/dt) and –d[**3d**-d_2]/dt were measured at [**3d**] = 0.235 M.

Table 3.7. Rate as a function of total concentration of catalyst **1a**.

	$-d$[**3b**]/dt (x 10^{-5} M/s)			
[**1a**]$_T$ /mM	[**3b**] = 0.13 M (20% conv.)	[**3b**] = 0.12 M (30% conv.)	[**3b**] = 0.11 M (40% conv.)	[**3b**] = 0.10 M (50% conv.)
15.0	21.3	19.1	16.8	14.4
15.0	20.1	17.8	15.5	13.1
15.0	23.9	21.0	17.3	13.7
12.5	19.5	17.1	14.7	12.2
12.5	18.9	16.6	14.2	11.8
12.5	16.7	14.6	12.5	10.4
10.0	11.0	9.68	8.37	7.03
10.0	17.1	14.8	12.4	10.1
10.0	14.1	12.3	10.5	8.76
7.50	8.72	7.33	5.97	4.64
7.50	7.95	6.90	5.83	4.76
7.50	10.7	9.38	8.01	6.65
5.00	5.91	4.94	4.05	3.24
5.00	5.28	4.55	3.82	3.09
5.00	4.81	4.19	3.56	2.92
2.50	1.21	0.976	0.758	0.564
2.50	1.39	0.849	0.566	0.470
2.50	0.951	0.695	0.483	0.350
1.00	0.125	0.113	0.156	NA
1.00	0.243	0.218	0.157	NA

	$-d$[**3b**]/dt (x 10^{-5} M/s)		
[**1a**]$_T$ /mM	[**3b**] = 0.090 M (60% conv.)	[**3b**] = 0.080 M (70% conv.)	[**3b**] = 0.070 M (80% conv.)
15.0	11.9	9.27	6.48
15.0	10.7	8.09	5.39
15.0	10.1	6.81	4.12
12.5	9.69	7.17	4.68
12.5	9.33	6.76	4.09
12.5	8.25	6.03	3.77
10.0	5.68	4.32	2.95
10.0	7.71	5.44	3.39
10.0	6.99	5.25	3.60
7.50	3.40	2.31	1.45
7.50	3.68	2.60	1.58
7.50	5.29	3.96	2.71
5.00	2.53	1.90	1.33
5.00	2.38	1.70	1.12
5.00	2.29	1.68	1.10
2.50	0.408	0.301	0.232
2.50	0.346	0.292	0.257
2.50	0.285	0.224	0.154
1.00	NA	NA	NA
1.00	NA	NA	NA

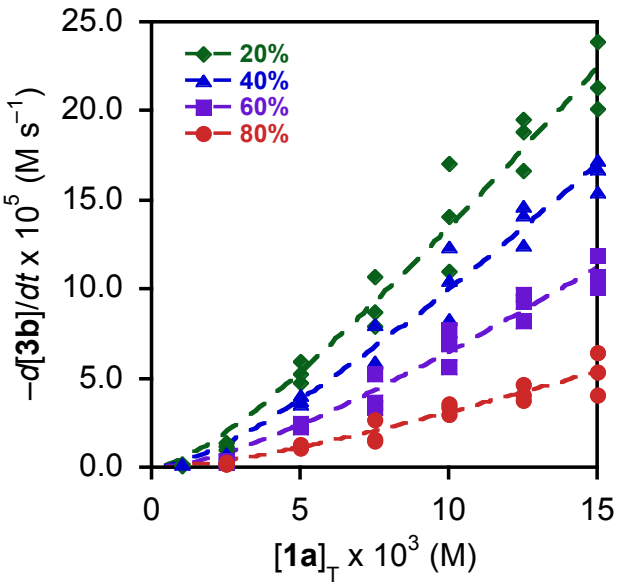

Figure 3.33. Rate as a function of total concentration of catalyst **1a**, fit to eq 3.18.

Table 3.8. Fitted parameters from Figure 3.33.

Conversion of **2** (%)	[**2**] (M)	[**3b**] (M)	$k_{cat,obs}$ [a] (M^{-1} s^{-1})	k_{cat} (× 10^2 M^{-3} s^{-1})	K_{dim} (× 10^2 M^{-1})	R^2
20	0.08	0.13	7 ± 4	7 ± 4	1.5 ± 1.0	0.97
40	0.06	0.11	4 ± 2	6 ± 2	0.9 ± 0.6	0.97
60	0.04	0.09	2 ± 1	6 ± 2	0.7 ± 0.4	0.97
80	0.02	0.07	1.0 ± 0.6	7 ± 4	0.7 ± 0.6	0.92

[a] $k_{cat,obs} = k_{cat}$ [**2**] [**3b**]

Table 3.9. Rate as a function of total concentration of catalyst **1b**.

	–*d*[**3b**]/*dt* (x 10^{-5} M/s)					
$[\mathbf{1b}]_T$ /mM	[**3b**] = 0.13 M (20% conv.)	[**3b**] = 0.12 M (30% conv.)	[**3b**] = 0.11 M (40% conv.)	[**3b**] = 0.10 M (50% conv.)	[**3b**] = 0.09 M (60% conv.)	[**3b**] = 0.08 M (70% conv.)
15.0	8.49	6.84	5.22	3.70	2.39	1.44
10.0	3.42	2.83	2.23	1.64	1.06	0.572
7.50	1.99	1.53	1.17	0.885	0.648	0.381
5.00	0.632	0.452	0.320	0.222	0.124	0.080
5.00	0.461	0.327	0.211	0.136	0.0931	NA
2.50	0.124	0.0908	0.0853	NA	NA	NA
2.50	0.123	0.0742	NA	NA	NA	NA

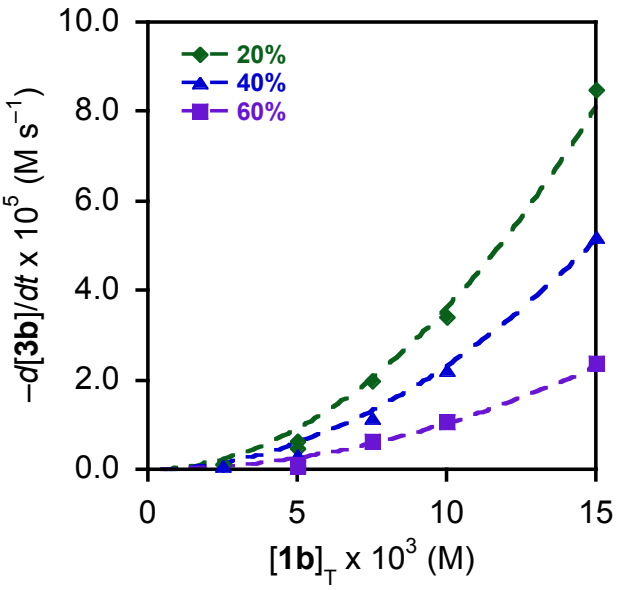

Figure 3.34. Rate as a function of total concentration of catalyst **1b**, fit to eq 3.18.

Table 3.10. Fitted parameters from Figure 3.34.

Conversion of **2** (%)	[**2**] (M)	[**3b**] (M)	$k_{cat,obs}$[a] ($\times 10^{-1}$ M^{-1} s^{-1})	k_{cat} ($\times 10^{1}$ M^{-3} s^{-1})	K_{dim} (M^{-1})	R^2
20	0.08	0.13	3.6 ± 0.7	3.5 ± 0.6	0.2 ± 3	0.99
40	0.06	0.11	2.4 ± 0.6	3.6 ± 0.8	0.8 ± 5	0.99
60	0.04	0.09	1.0 ± 0.3	2.9 ± 0.9	0.3 ± 5	0.92

[a] $k_{cat,obs} = k_{cat}$ [**2**] [**3b**]

Based on these data, we can see that these reactions are operating in the limit of no catalyst dimerization. These data are fit equally well by a simple second order kinetic dependence (eq 3.19).

Table 3.11. Rate as a function of initial concentration of **3b**.[a]

$[\mathbf{3b}]_{initial}$ (M)	$d[\mathbf{4b}]/dt$ (x 10^{-5} M/s)				
	[**4b**] = 0.01 M	[**4b**] = 0.02 M	[**4b**] = 0.03 M	[**4b**] = 0.04 M	[**4b**] = 0.05 M
0.0409	6.64	3.93	1.60	NA	NA
0.0409	8.45	5.16	1.92	NA	NA
0.0482	8.23	5.49	2.79	0.64	NA
0.0817	11.5	9.58	7.60	5.59	3.56
0.0999	9.98	8.73	7.45	6.14	4.79
0.118	13.7	11.9	10.0	8.15	6.26
0.123	12.3	10.7	8.99	7.29	5.56
0.150	11.8	10.4	8.88	7.37	5.82
0.150	14.8	12.8	10.8	8.78	6.75
0.195	17.4	15.3	13.0	10.8	8.48
0.227	18.1	15.3	12.6	9.96	7.51
0.300	20.1	17.7	15.2	12.6	10.0
0.372	22.8	19.5	16.2	12.9	9.82
0.449	18.0	15.8	13.6	11.3	8.98
0.518	19.5	16.6	13.7	10.8	7.91
0.599	7.0	6.13	5.2	4.36	3.49

$[\mathbf{3b}]_{initial}$ (M)	$d[\mathbf{4b}]/dt$ (x 10^{-5} M/s)			
	[**4b**] = 0.06 M	[**4b**] = 0.07 M	[**4b**] = 0.08 M	[**4b**] = 0.09 M
0.0817	1.66	0.64	NA	NA
0.0999	3.38	1.93	0.628	0.326
0.118	4.37	2.58	1.30	0.691
0.123	3.81	2.13	0.095	0.383
0.150	4.25	2.65	1.19	0.551
0.150	4.76	2.91	1.53	0.671
0.195	6.18	3.91	1.91	0.830
0.227	5.39	3.67	2.24	0.812
0.300	7.40	4.72	2.23	0.854
0.372	6.91	4.46	2.59	0.658
0.449	6.65	4.33	2.20	0.869
0.518	5.20	2.99	1.71	0.269
0.599	2.66	1.88	1.24	0.777

[a]All reactions run with $[\mathbf{2}]_{initial}$ = 0.10 M and $[\mathbf{1a}]_T$ = 0.01 M, in TBME at –78 °C.

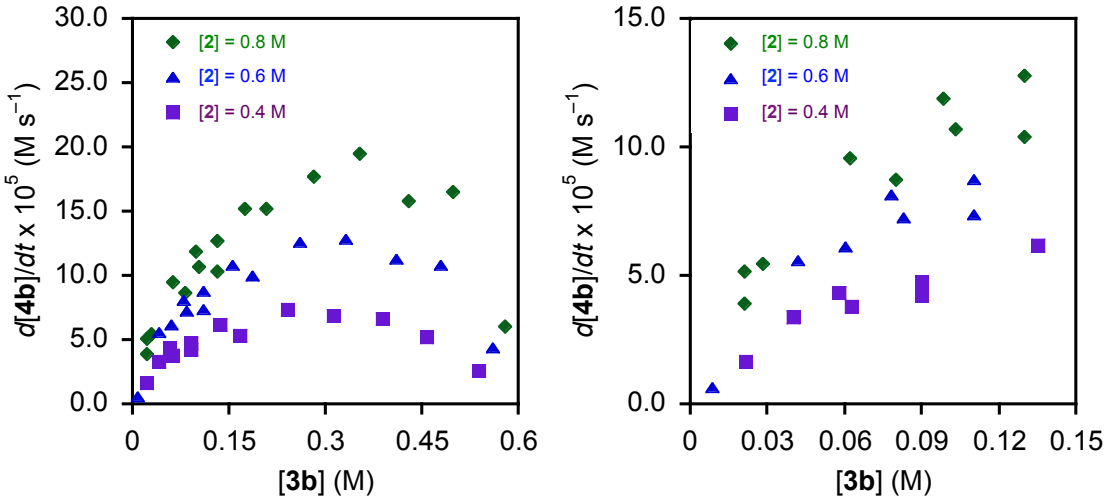

Figure 3.35. Rate as a function of [**3b**]. The dependence seems first order at low [**3b**], but deleterious effects on rate are observed at high [**3b**]. Given the fact that the reaction mixture is frozen solid at [**3b**] = 0.8 M, it seems likely that this is due to a medium effect. Regardless of the exact interpretation of the shape of the curve, it is clear that there is a positive dependence of rate on [**3b**] at low concentration, implying that **3b** is present in the turnover-limiting transition state.

Table 3.12. Rate as a function of initial concentration of **2** over the full course of the reaction.[a]

	$-d$[**3b**]/dt (x 10^{-5} M/s)				
[**2**]$_{initial}$ (M)	[**4b**] = 0.01 M	[**4b**] = 0.02 M	[**4b**] = 0.03 M	[**4b**] = 0.04 M	[**4b**] = 0.05 M
0.0500	9.10	6.55	4.02	1.73	NA
0.0780	15.0	12.7	10.4	8.02	5.58
0.100	20.4	16.1	12.4	9.54	7.19
0.100	11.8	10.4	8.88	7.37	5.82
0.200	36.3	33.0	29.6	26.2	22.8
0.297	59.7	54.4	49.2	43.9	38.6
0.371	70.5	64.7	58.8	53.0	47.0

	$-d$[**3b**]/dt (x 10^{-5} M/s)					
[**2**]$_{initial}$ (M)	[**4b**] = 0.06 M	[**4b**] = 0.07 M	[**4b**] = 0.08 M	[**4b**] = 0.09 M	[**4b**] = 0.10 M	[**4b**] = 0.11 M
0.0780	3.08	0.903	NA	NA	NA	NA
0.100	4.98	3.09	NA	NA	NA	NA
0.100	4.25	2.65	1.19	0.551	NA	NA
0.200	19.3	15.8	12.3	8.90	5.72	3.24
0.297	33.3	28.1	22.8	17.8	12.9	8.47
0.371	41.1	35.2	29.2	23.3	17.5	12.0

[a]All reactions run with [**3b**]$_{initial}$ = 0.15 M and [**1a**]$_T$ = 0.01 M, in TBME at –78 °C.

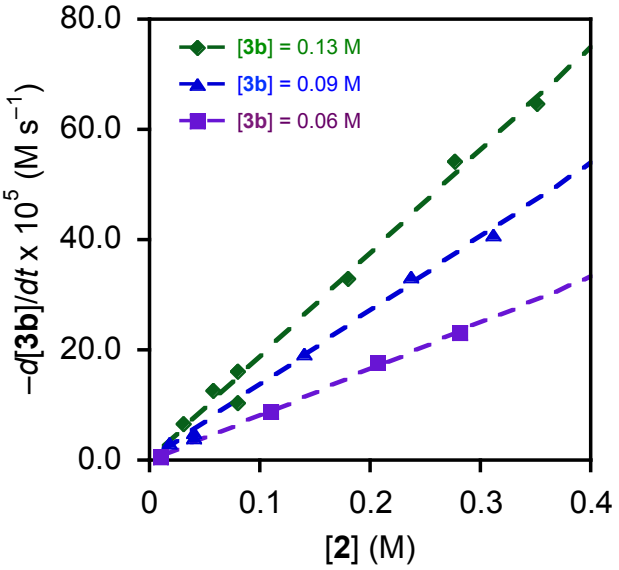

Figure 3.36. Rate as a function of [**2**]. The data were fitted to a simple linear model, showing that the reaction obeys strict first-order kinetics with respect to **2**.

"Same Excess" Experiment

This experiment (shown in Figure 3.4) was performed under slightly different conditions from the remainder of the kinetics data presented in this section. These reactions were initiated by adding neat **3b** last to a solution of **2** and **1a** in TBME at –78 ºC. Rate was determined by the appearance of the ester product **4b**. [**2**] was inferred from $[\mathbf{2}]_0$ and the amount of **4b** formed. The data are presented in Table 3.13.

Table 3.13. Data used to generate Figure 3.4. The units of the rate $d[\mathbf{4b}]/dt$ are "$\times 10^{-4}$ M^{-1} s^{-1}".

$[\mathbf{2}]_0$ = 0.10 M		$[\mathbf{2}]_0$ = 0.075 M		$[\mathbf{2}]_0$ = 0.050 M	
[**2**] (M)	$d[\mathbf{4b}]/dt$	[**2**] (M)	$d[\mathbf{4b}]/dt$	[**2**] (M)	$d[\mathbf{4b}]/dt$ ($M\ s^{-1}$)
0.0763	2.85	0.0614	2.00	0.0432	1.34
0.0674	2.49	0.0548	1.79	0.0391	1.2
0.0603	2.17	0.0491	1.60	0.0352	1.08
0.0537	1.90	0.0443	1.42	0.0319	0.962
0.0484	1.66	0.0405	1.27	0.0293	0.86
0.0439	1.44	0.0368	1.12	0.0267	0.772
0.04	1.26	0.0338	1.00	0.0246	0.688
0.0371	1.10	0.0313	0.893	0.0226	0.614
0.0341	0.967	0.0289	0.791	0.0212	0.551
0.0313	0.85	0.0269	0.707	0.0198	0.491
0.029	0.749	0.025	0.627	0.0188	0.441
0.027	0.664	0.0231	0.561	0.0173	0.394
0.0246	0.591	0.0219	0.501	0.016	0.353
0.0232	0.529	0.0201	0.447	0.0153	0.319
0.0216	0.476	0.0188	0.403	0.0142	0.286
0.0203	0.431	0.0179	0.362	0.0134	0.258
0.0189	0.394	0.0165	0.328	0.0128	0.234
0.0177	0.362	0.0155	0.297	0.0121	0.213
0.0166	0.335	0.0146	0.271	0.0112	0.195
0.0156	0.312	0.014	0.248	0.0109	0.178
0.0145	0.291	0.0131	0.229	0.0099	0.164
0.0136	0.274	0.0125	0.211	0.0096	0.152
0.0131	0.258	0.0117	0.197	0.00876	0.14
0.0119	0.244	0.0112	0.184	0.00872	0.131
0.0115	0.23	0.0107	0.173	0.00834	0.122
0.0107	0.218	0.0101	0.163	0.0084	0.115
0.01	0.206	0.00964	0.154	0.00775	0.108
0.0096	0.195	0.00909	0.146	0.00735	0.102
0.00922	0.184	0.00869	0.139	0.00702	0.0967
0.00882	0.174	0.00825	0.133	0.00664	0.0917
0.00819	0.163	0.00796	0.127	0.00608	0.0871
0.00766	0.153	0.00754	0.121	0.00619	0.0829
0.00702	0.143	0.00718	0.115	0.00589	0.0787
0.00672	0.133	0.00676	0.11	0.00571	0.0748

$[\mathbf{2}]_0$ = 0.10 M		$[\mathbf{2}]_0$ = 0.075 M		$[\mathbf{2}]_0$ = 0.050 M	
[**2**] (M)	$d[\mathbf{4b}]/dt$	[**2**] (M)	[**2**] (M)	$d[\mathbf{4b}]/dt$	[**2**] (M)
0.00658	0.123	0.00663	0.105	0.00531	0.0711
0.00616	0.114	0.0062	0.0999	0.0052	0.0675
0.0063	0.104	0.00602	0.0948	0.00503	0.0641
0.00597	0.0959	0.00575	0.0898	0.00485	0.0606
0.0055	0.0877	0.00563	0.0849	0.00499	0.0572
0.00498	0.0801	0.00543	0.0798	0.00488	0.054
0.00436	0.0732	0.00504	0.0751	0.00459	0.0507
0.00469	0.0667	0.00504	0.0702	0.00493	0.0477
0.00449	0.0612	0.00475	0.0653	0.00426	0.0445
0.00429	0.0563	0.00469	0.0608	0.00451	0.0416
0.00416	0.0521	0.00432	0.0561	0.00421	0.0388
0.00388	0.0486	0.00445	0.0519	0.00385	0.0359
0.00365	0.0459	0.00425	0.0477	0.00356	0.0334
0.00367	0.0438	0.00432	0.0435	0.00381	0.0308
0.00334	0.0423	0.00379	0.0399	0.00372	0.0284
0.00317	0.0413	0.004	0.0363	0.00326	0.0262
0.00319	0.0409	0.00376	0.0331	0.00363	0.0243
0.00299	0.0409	0.00376	0.0301	0.00386	0.0224
0.00256	0.0412	0.00345	0.0273	0.00334	0.0207
0.0022	0.0416	0.00339	0.025	0.00317	0.0192
0.0027	0.0422	0.00331	0.023	0.00344	0.0179
0.00221	0.0427	0.00304	0.0212	0.0031	0.0168
0.00217	0.043	0.00301	0.0198	0.0031	0.0158
0.00223	0.0431	0.00299	0.0187	0.00313	0.0151
0.00185	0.0428	0.00285	0.0179	0.00273	0.0145
0.00222	0.042	0.0029	0.0174	0.00317	0.0141
0.00194	0.0407	0.0027	0.0171	0.0026	0.0138
0.00254	0.0387	0.00259	0.0171	0.00311	0.0136
0.00139	0.036	0.00251	0.0173	0.00251	0.0136
0.00182	0.0327	0.00243	0.0177	0.00274	0.0136
0.00192	0.0286	0.00259	0.0182	0.00244	0.0137
0.0015	0.0238	0.00246	0.0189	0.00257	0.0139
0.00149	0.0189	0.00229	0.0196	0.00234	0.0141
0.00153	0.0134	0.00239	0.0203	0.00249	0.0142

3.6.6. NMR Assignment of Catalyst Solution Structure

Methods:

Pulse sequences used as implemented in Varian VNMR on Varian INOVA 500 spectrometers. Our assignments were made primary with 2D NOESY and TOCSY spectra. NOESY spectra were recorded using deoxygenated solvent.

Labeling System:

Each proton is lettered according to the diagram shown below. Because the catalyst is a mixture of amide rotamers, we use the convention (*E*)-A and (*Z*)-A to refer to the proton at position H_A in the *E* and *Z* rotamers, respectively.

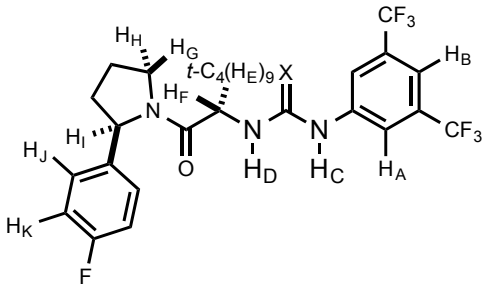

Assignment of Intermolecular nOe's:

When studying the 2D NOESY spectra shown below, it was straightforward to assign the nOe between protons of the *E* rotamer and protons of the *Z* rotamer as being intermolecular in origin. In contrast, the (*E*,*E*) and (*Z*,*Z*) homodimers also have characteristic nOe's, but because the dimers are symmetric, the nOe could theoretically arise from close contacts within one molecule of catalyst or from contacts between two molecules of catalyst. To determine whether a given nOe (NOESY crosspeak) is due to the monomer or the dimer, we consider the relevant H-H distance in the monomer and the dimer. We used DFT calculations at the B3LYP/6-31G(d,p) level of theory for this purpose. We present here the relevant distances for our analysis. A discussion of our computational methods is presented below in Section 3.6.9.

[(*Z*)-1a]$_2$: (*Z*)-A to (*Z*)-I: v. weak NOESY crosspeak observed.

Type I Dimer (Solid State)

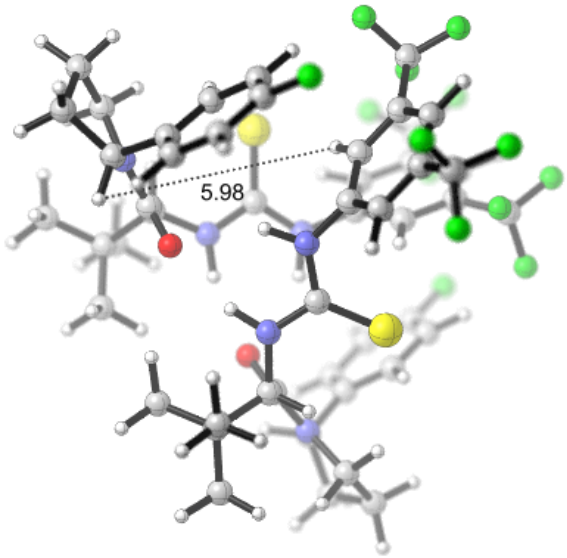

Type II Dimer (Alternate Geometry)

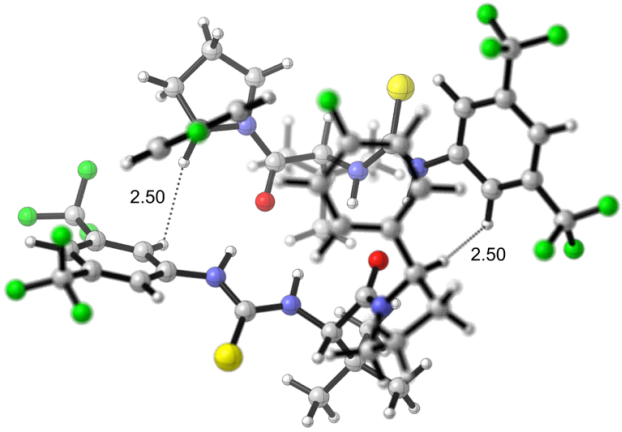

(*Z*)-1a • (*E*)-1a: (*E*)-A to (*Z*)-I: NOESY crosspeak observed.

Type I Dimer (Solid State)

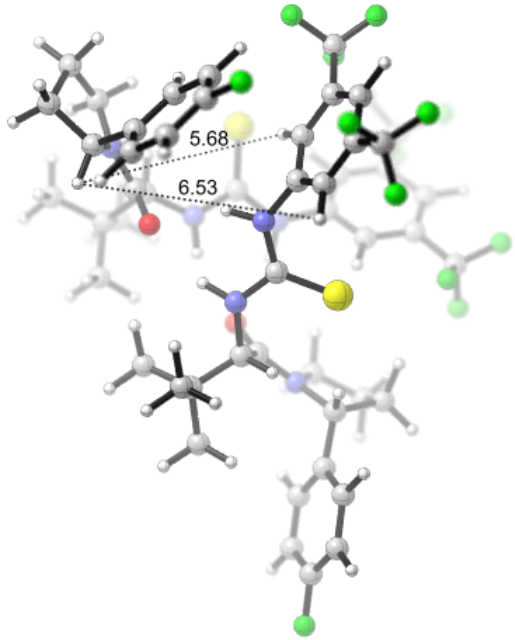

Type II Dimer (Alternate Geometry)

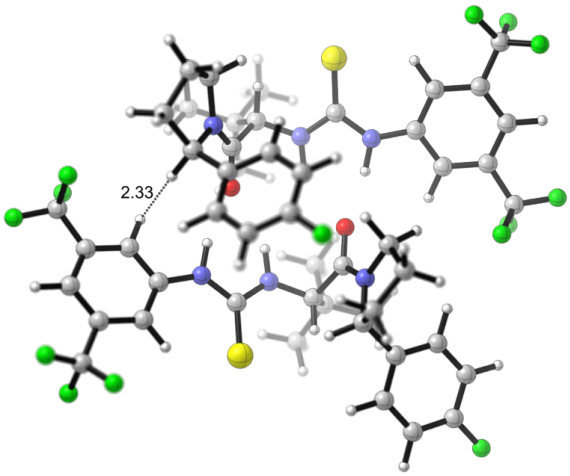

(*Z*)-**1a** • (*E*)-**1a: (*Z*)-A to (*E*)-G,H: NOESY crosspeak observed.**

Type I Dimer (Solid State)

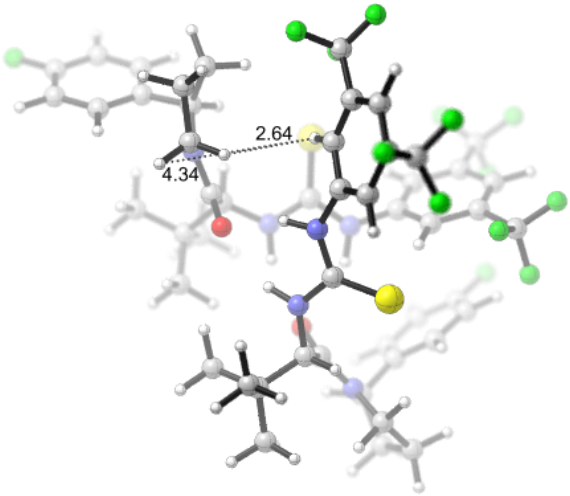

Type II Dimer (Alternate Geometry)

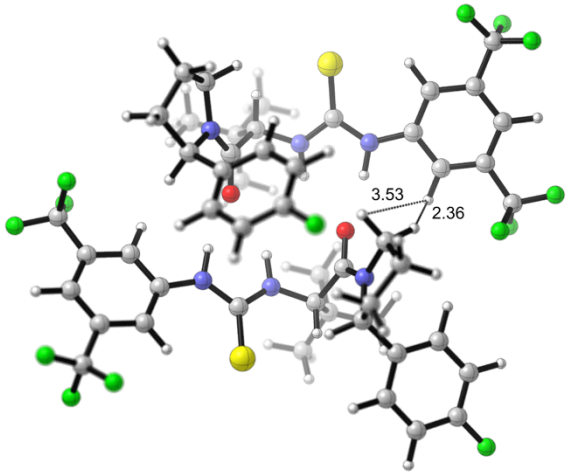

[(*E*)-**1a**]$_2$**: (*E*)-A to (*E*)-G,H: NOESY crosspeak observed.**

Type I Dimer (Solid State)

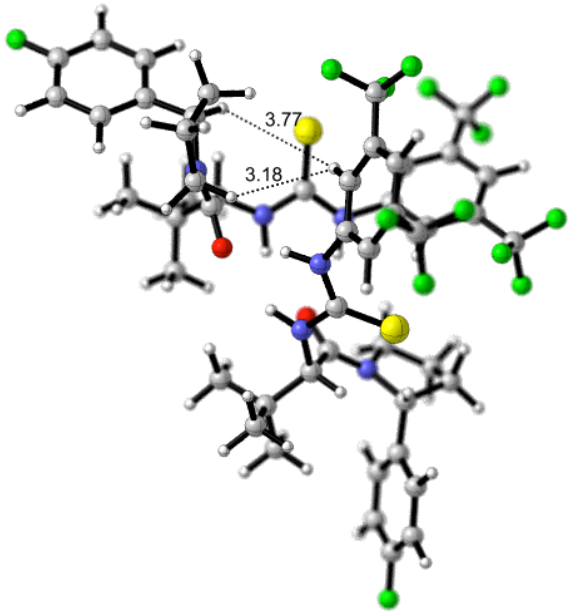

Type II Dimer (Alternate Geometry)

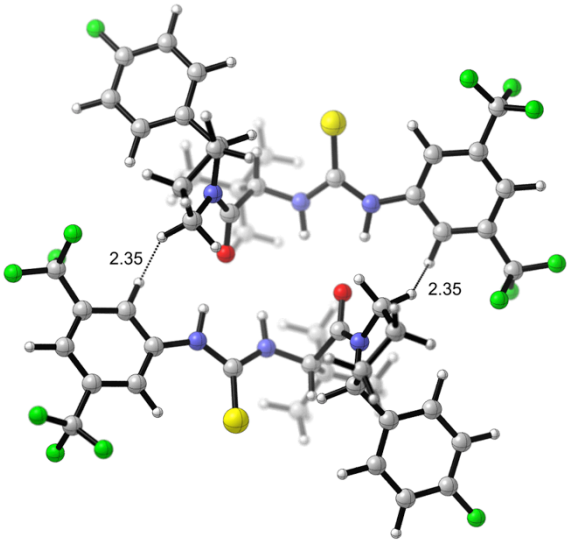

Corresponding distances in the monomeric complexes.

(a) (*E*)-1a (Gas phase DFT Geometry)

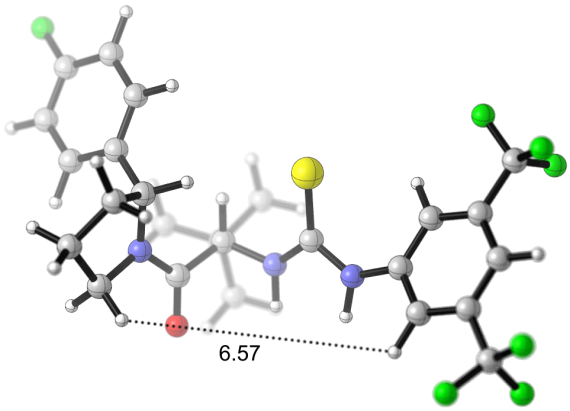

(b) (*Z*)-1a (Gas phase DFT Geometry)

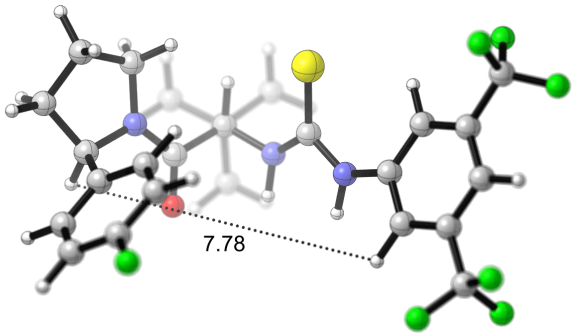

3.6.7 Assignment of the Solution Structure of Thiourea Catalyst 1a

NOESY: 10 mM, Toluene-d_8, 25 ºC, 128 increments in the indirectly detected dimension, 16 scans per increment.

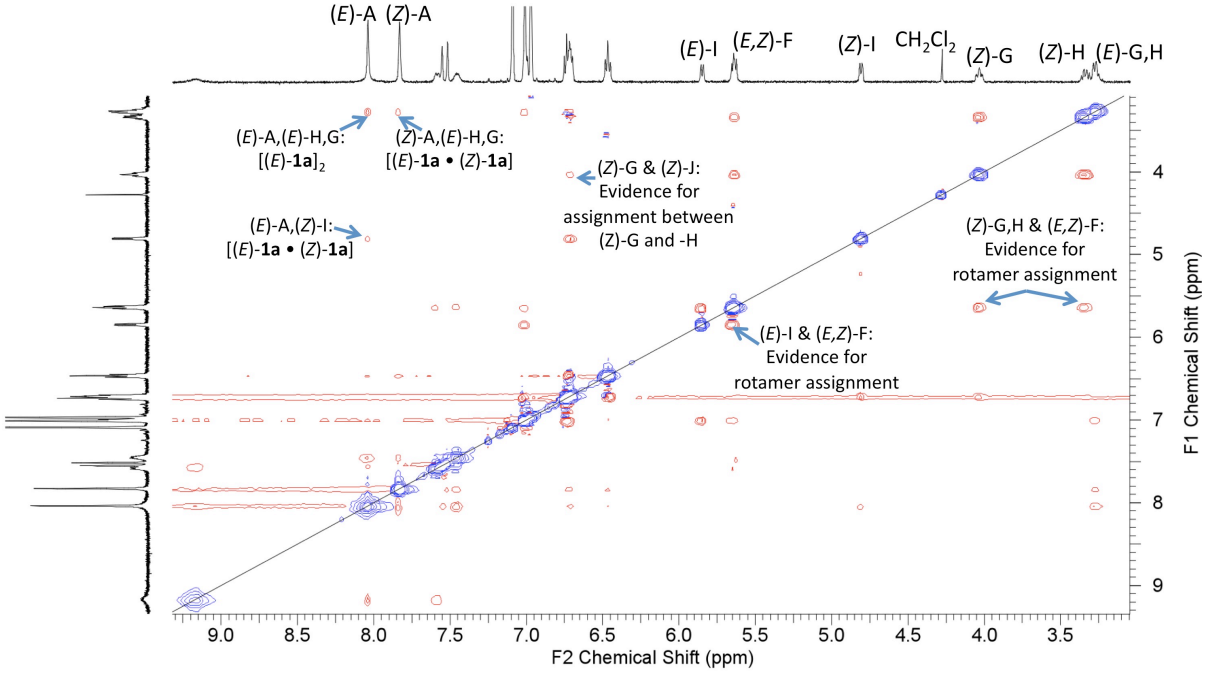

Detail:

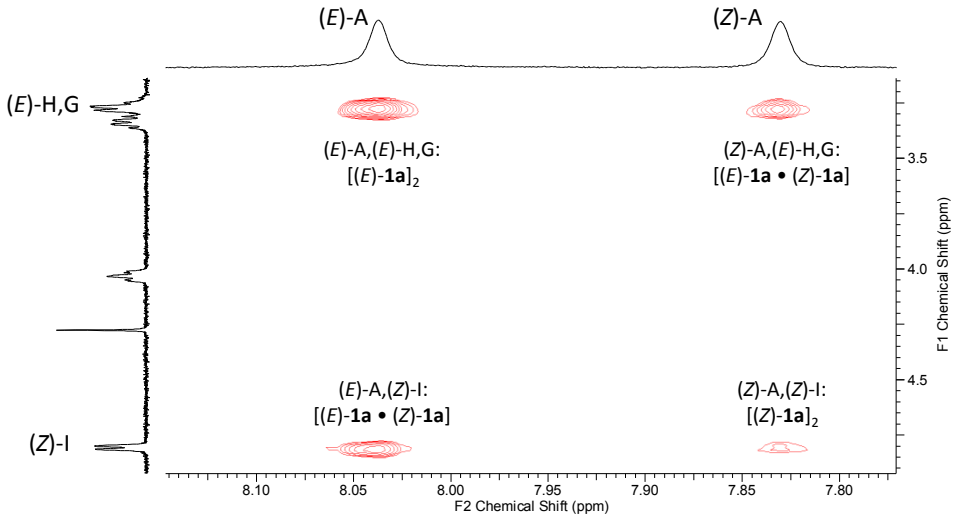

TOCSY: 10 mM, Toluene-d_8, 25 ºC,

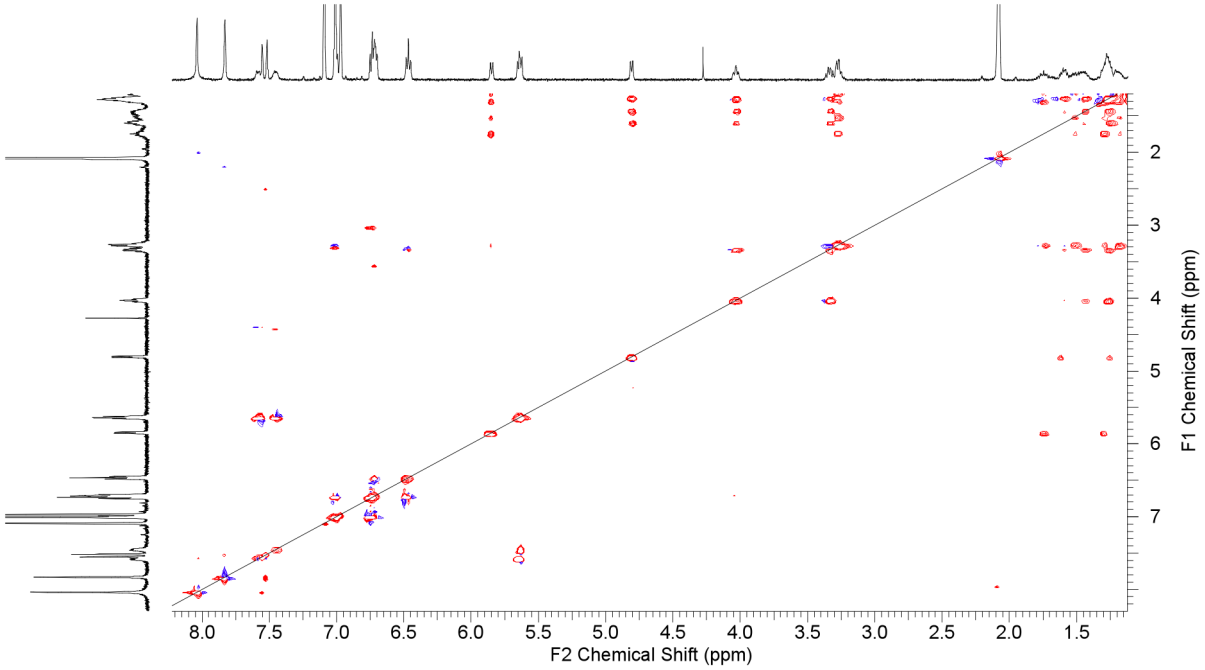

Assignment of the Solution Structure of Urea Catalyst 1b

NOESY: 10 mM, Toluene-d_8, 25 ºC,

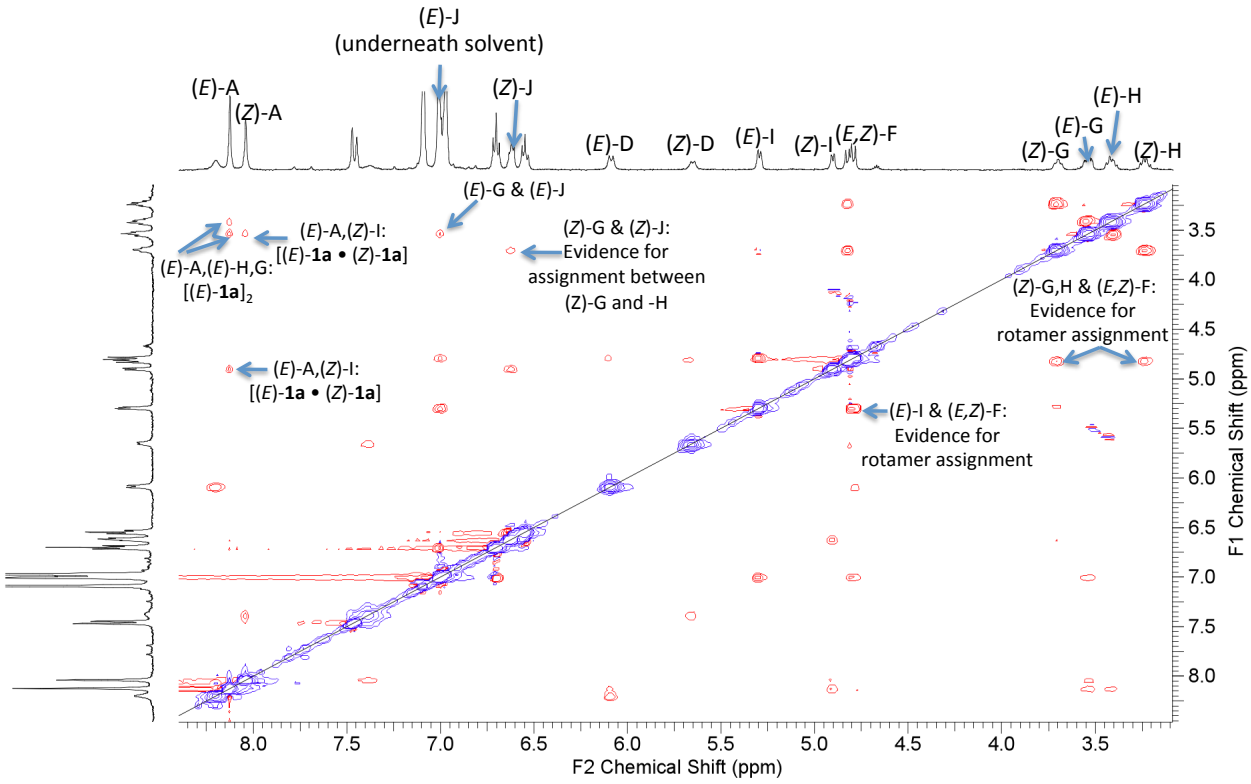

TOCSY: 10 mM, Toluene-d_8, 25 ºC,

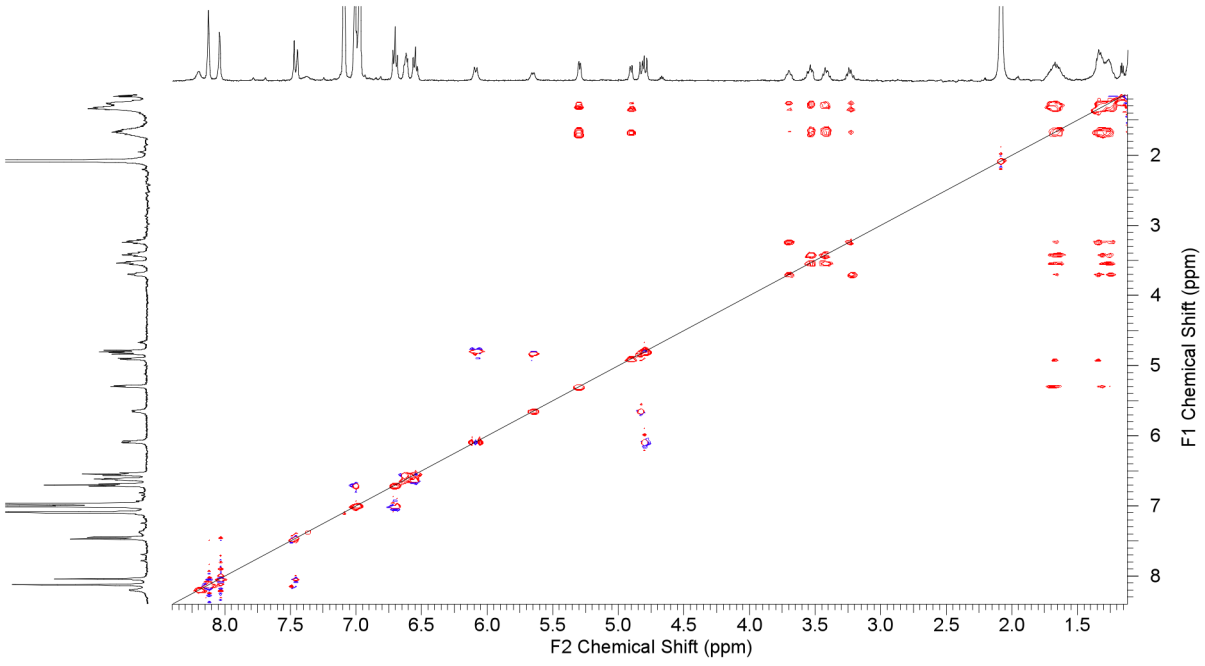

NOESY: 10 mM, Toluene-d_8, 80 ºC, 96 increments in the indirectly detected dimension, 16 scans per increment. Note that at this temperature, the major peaks are the same phase as the diagonal. These are due to chemical exchange between the amide rotamers of **1b**. For example, a cross-peak connects (*Z*)-A with (*E*)-A. This spectrum indicates that rotamer conversion occurs on the timescale of seconds at 80 ºC (the EXSY timescale). This is evidence for our assignment of the two sets of peaks present in the spectrum as amide rotamers.

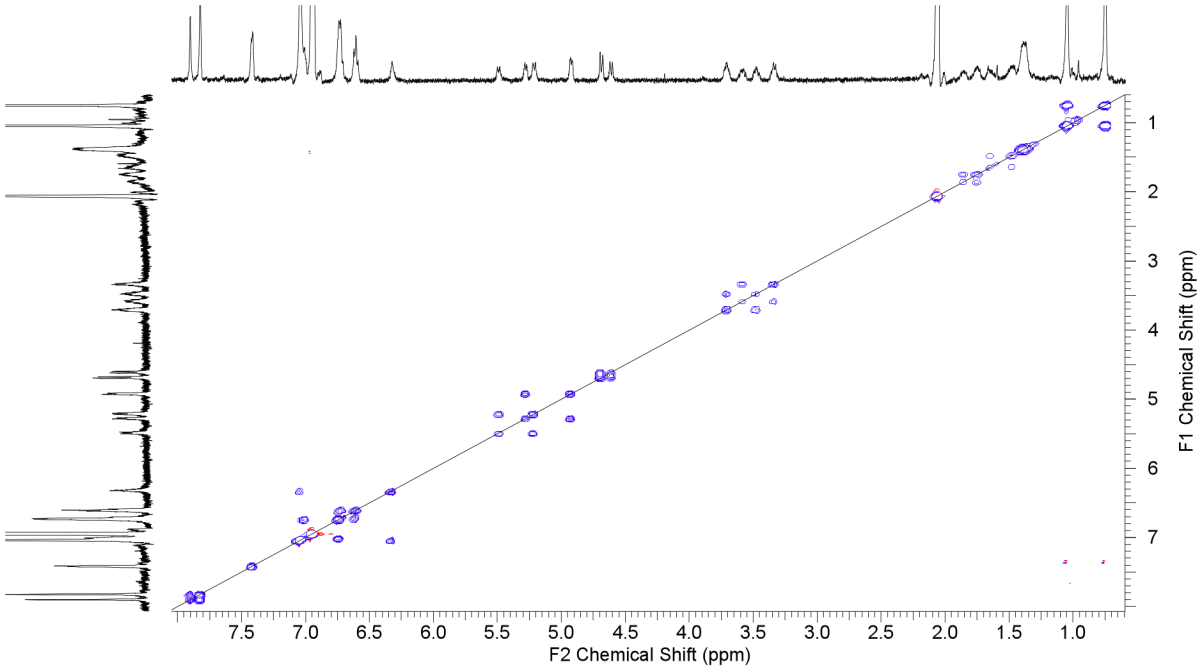

3.6.8. ^{1}H NMR Dilution Experiments

The 2D NMR spectra used to assign these 1D spectra are presented in the preceding section.

Catalyst **1a**: toluene-d_8, 500 MHz, 25 ºC

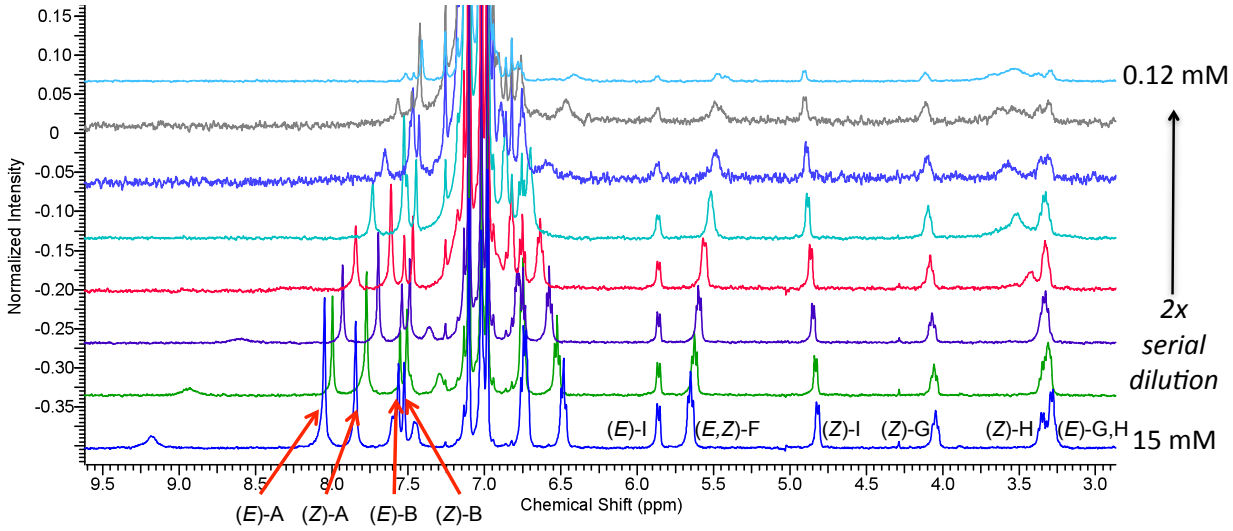

Table 3.14 Data used to generate Figure 3.11.

	Chemical Shift (ppm)			
$[\mathbf{1a}]_T$ (mM)	(*E*)-A	(*Z*)-A	(*E*)-B	(*Z*)-B
15	8.0740	7.8430	7.5630	7.5250
7.5	7.9940	7.7720	7.5520	7.5080
3.75	7.9280	7.6950	7.5410	7.4900
1.88	7.8420	7.6120	7.5250	7.4680
0.94	7.7330	7.5260	7.5070	7.4470
0.47	7.6510	7.4670	7.4850	7.4290
0.23	7.5650	7.4230	7.4740	7.4230
0.12	7.5170	7.4110	7.4640	7.4110

Catalyst **1a**: toluene-d_8, 500 MHz, –40 ºC

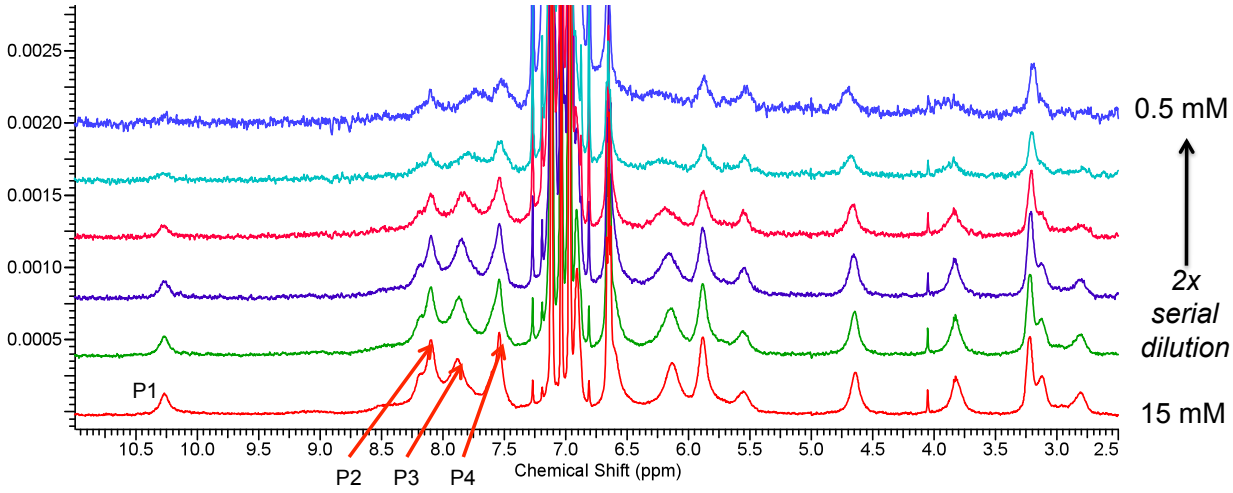

Table 3.15. Data used to generate Figure 3.12.

	Chemical Shift (ppm)			
$[\mathbf{1a}]_T$ (mM)	P1	P2	P3	P4
15	10.234	8.0610	7.8450	7.5070
7.5	10.231	8.0630	7.8320	7.5060
3.75	10.221	8.0590	7.8080	7.5060
1.88	10.235	8.0640	7.7910	7.4980
0.94	10.241	8.0660	7.7610	7.4920
0.47	10.214	8.0710	7.7120	7.4870
0.23	10.274	8.0610	ND	7.4660

Catalyst **1b**: toluene-d_8, 500 MHz, 25 ºC

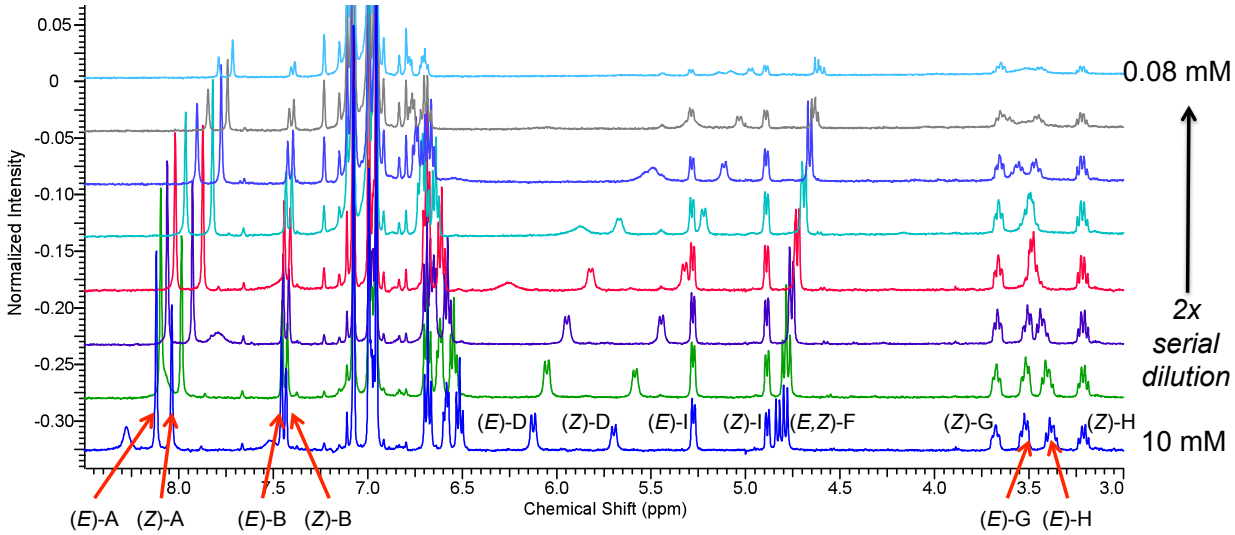

Table 3.16 Data used to generate Figure 3.11.

	Chemical Shift (ppm)			
$[\mathbf{1b}]_T$ (mM)	(*E*)-A	(*Z*)-A	(*E*)-D	(*Z*)-D
10	8.1200	8.0400	6.1200	5.7000
5.0	8.0900	7.9900	6.0500	5.5850
2.5	8.0600	7.9300	5.9450	5.4450
1.25	8.0200	7.8700	5.8200	5.3200
0.63	7.9600	7.8200	5.6700	5.2200
0.31	7.9000	7.7800	ND	5.1150
0.16	7.8400	7.7400	ND	5.0300
0.08	7.7900	7.7100	ND	4.9700

Catalyst **1b**: toluene-d_8, 500 MHz, –40 ºC

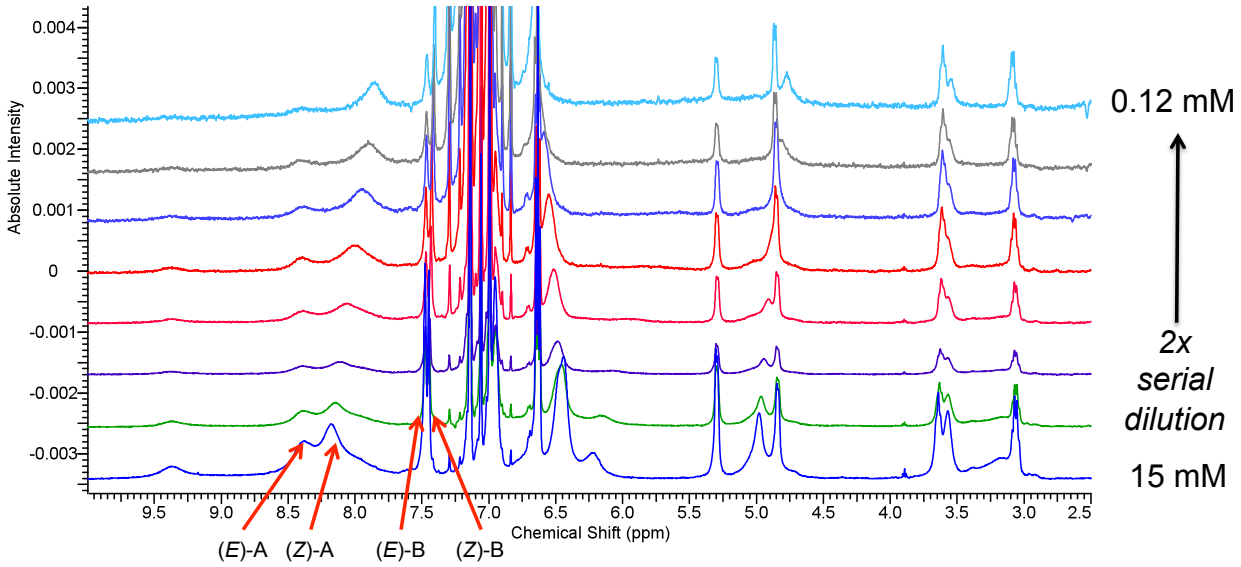

Table 3.17 Data used to generate Figure 3.12.

$[\mathbf{1b}]_T$ (mM)	Chemical Shift (ppm)			
	(*E*)-A	(*Z*)-A	(*E*)-B	(*Z*)-B
15	8.3840	8.1790	7.4780	7.4480
7.5	8.3890	8.1460	7.4760	7.4450
3.75	8.3910	8.1100	7.4740	7.4400
1.88	8.3860	8.0540	7.4700	7.4320
0.94	8.3970	7.9960	7.4700	7.4270
0.47	8.3850	7.9450	7.4660	7.4170
0.23	8.3970	7.9030	7.4660	7.4120
0.12	8.3980	7.8510	7.4610	7.4040

3.6.9 Computational Chemistry

Methods:

Calculations were performed using the Gaussian 09 program[42] on the Odyssey cluster supported by Harvard University's FAS Science Division Research Computing Group. Default geometric and SCF convergence criteria were used. In cases where SCF convergence was difficult to achieve, a quadratic convergence algorithm was employed using the keyword `SCF=(XQC,maxconventionalcycles=25)` where QC only begins after 25 cycles of the default algorithm have failed to converge on an SCF. Minima were characterized by the presence of all positive eigenvalues of the Hessian. All molecular structures were rendered in CYLView.[43] The B3LYP DFT functional[44] were used as its default implementations in Gaussian 09.

[42] Gaussian 09, Revision A.02, M. J. Frisch, G. W. Trucks, H. B. Schlegel, G. E. Scuseria, M. A. Robb, J. R. Cheeseman, G. Scalmani, V. Barone, B. Mennucci, G. A. Petersson, H. Nakatsuji, M. Caricato, X. Li, H. P. Hratchian, A. F. Izmaylov, J. Bloino, G. Zheng, J. L. Sonnenberg, M. Hada, M. Ehara, K. Toyota, R. Fukuda, J. Hasegawa, M. Ishida, T. Nakajima, Y. Honda, O. Kitao, H. Nakai, T. Vreven, J. A. Montgomery, Jr., J. E. Peralta, F. Ogliaro, M. Bearpark, J. J. Heyd, E. Brothers, K. N. Kudin, V. N. Staroverov, R. Kobayashi, J. Normand, K. Raghavachari, A. Rendell, J. C. Burant, S. S. Iyengar, J. Tomasi, M. Cossi, N. Rega, J. M. Millam, M. Klene, J. E. Knox, J. B. Cross, V. Bakken, C. Adamo, J. Jaramillo, R. Gomperts, R. E. Stratmann, O. Yazyev, A. J. Austin, R. Cammi, C. Pomelli, J. W. Ochterski, R. L. Martin, K. Morokuma, V. G. Zakrzewski, G. A. Voth, P. Salvador, J. J. Dannenberg, S. Dapprich, A. D. Daniels, O. Farkas, J. B. Foresman, J. V. Ortiz, J. Cioslowski, and D. J. Fox, Gaussian, Inc., Wallingford CT, 2009.

[43] CYLview, 1.0b; Legault, C. Y., Université de Sherbrooke, **2009** (http://www.cylview.org).

[44] (a) Becke, A. D. *Phys. Rev. A* **1988**, *38*, 3098–3100. (b) Lee, C.; Yang, W.; Parr, R. G. *Phys. Rev. B.* **1988**, *37*, 785–789. (c) Becke, A. D. *J. Chem. Phys.* **1993**, *98*, 1372–1377. (d) Stephens, P. J.; Devlin, F. J.; Chabalowski, C. F.; Frisch, M. J. *J. Phys. Chem.* **1994**, *98*, 11623–11627.

DFT-Optimized (B3LYP/6-31G(d,p) Geometries based on XRD Data for [(*Z*)-1a]$_2$:

[(*Z*)-**1a**]$_2$:

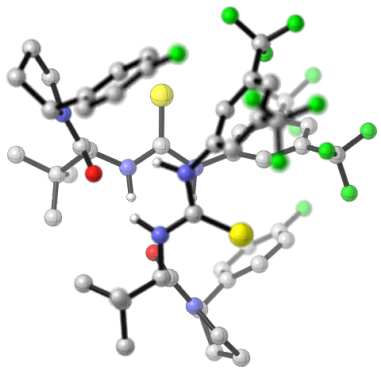

Charge: 0
Spin Multiplicity: 1
Solvation: gas phase
Electronic Energy (AU): -4609.96093843
Gibbs Free Energy at 298.150 K (AU): -4609.100790

S	0.223687	-0.116476	-3.221624
F	6.226227	-1.844134	0.772650
F	-2.325277	-5.332026	0.887271
F	-0.925173	-3.878322	1.707253
F	-3.054885	-3.671188	2.088306
O	1.891551	2.939948	-0.603310
N	3.069478	2.745854	-2.520321
N	-0.415920	2.154480	-1.910009
H	-0.800768	2.582195	-1.067986
N	-1.492106	0.283900	-1.183419
H	-1.881134	0.901507	-0.474015
C	5.637678	1.650549	0.017405
H	5.925580	2.630300	0.390549
C	6.132598	0.511407	0.649772
H	6.790510	0.576209	1.509486
C	5.758815	-0.736366	0.162219
C	4.904683	-0.871612	-0.924436
H	4.615847	-1.857256	-1.268683
C	4.409695	0.280986	-1.536943
H	3.710461	0.174347	-2.360371
C	4.777156	1.555093	-1.085243
C	4.361670	2.832887	-1.803925
H	4.287335	3.635296	-1.065562
C	5.329114	3.197419	-2.953964
H	6.365152	2.950029	-2.713567
H	5.270315	4.274135	-3.151686
C	4.773980	2.403725	-4.145541
H	5.093371	1.359529	-4.085443
H	5.101458	2.796114	-5.111351
C	3.248830	2.512493	-3.974022
H	2.715278	1.608114	-4.281658
H	2.858847	3.356573	-4.545285
C	1.902816	2.871840	-1.848038
C	0.578872	2.915082	-2.648655
H	0.722115	2.384904	-3.591368
C	-0.593428	0.816739	-2.064329
C	-1.967135	-1.058364	-1.205501
C	-2.673552	-1.538681	-2.313237
H	-2.818340	-0.901586	-3.176194
C	-3.181213	-2.834294	-2.300065
C	-2.991004	-3.662258	-1.191047
H	-3.379712	-4.672883	-1.189238
C	-2.291254	-3.174041	-0.092247
C	-1.777391	-1.872818	-0.090683
H	-1.235021	-1.499071	0.772632
C	0.036952	4.353841	-2.991314
C	-1.270209	4.186420	-3.793743
H	-2.047029	3.697239	-3.201514
H	-1.645780	5.168213	-4.101467
H	-1.110017	3.588360	-4.697295
C	-0.241292	5.187349	-1.729732
H	0.669866	5.354094	-1.150707
H	-0.641585	6.165487	-2.018362
H	-0.977515	4.714037	-1.075094
C	1.046829	5.119203	-3.867566
H	1.195107	4.629501	-4.835295
H	0.665540	6.125077	-4.070459
H	2.018959	5.232182	-3.376987
C	-4.019193	-3.324371	-3.451500
F	-3.870005	-4.652926	-3.647749
F	-5.336113	-3.105925	-3.227951
F	-3.706424	-2.701782	-4.607468
C	-2.139566	-4.020080	1.142969
S	-0.223700	-0.117047	3.221421
F	-6.226651	-1.843605	-0.772123
F	0.924687	-3.878338	-1.708023
F	3.054408	-3.671447	-2.089015
F	2.324552	-5.332392	-0.888295
O	-1.891014	2.939702	0.603647
N	-3.068911	2.745825	2.520707
N	0.416416	2.154014	1.910229
H	0.801359	2.581801	1.068286
N	1.492205	0.283332	1.183329
H	1.881458	0.900986	0.474097
C	-5.637395	1.650966	-0.016921
H	-5.925086	2.630770	-0.390089
C	-6.132544	0.511914	-0.649272
H	-6.790431	0.576836	-1.508995
C	-5.759017	-0.735926	-0.161698
C	-4.904906	-0.871332	0.924954
H	-4.616235	-1.857030	1.269190
C	-4.409679	0.281177	1.537438
H	-3.710436	0.174408	2.360843
C	-4.776886	1.555354	1.085723
C	-4.361128	2.833072	1.804376
H	-4.286693	3.635466	1.066007
C	-5.328449	3.197796	2.954461
H	-6.364540	2.950567	2.714125

H	-5.269465	4.274508	3.152143
C	-4.773381	2.404055	4.146041
H	-5.100725	2.796557	5.111850
H	-5.092974	1.359916	4.086024
C	-3.248222	2.512544	3.974427
H	-2.714802	1.608085	4.282052
H	-2.858054	3.356578	4.545631
C	-1.902258	2.871614	1.848380
C	-0.578287	2.914668	2.648950
H	-0.721568	2.384451	3.591637
C	0.593638	0.816210	2.064322
C	1.967009	-1.059019	1.205224
C	2.673208	-1.539668	2.312958
H	2.817991	-0.902767	3.176058
C	3.180609	-2.835379	2.299612
C	2.990364	-3.663110	1.190420
H	3.378849	-4.673786	1.188483
C	2.290837	-3.174564	0.091631
C	1.777234	-1.873231	0.090241
H	1.235027	-1.499213	-0.773061
C	-0.036225	4.353355	2.991682
C	1.271114	4.185773	3.793793
H	2.047769	3.696616	3.201328
H	1.646810	5.167511	4.101540
H	1.111102	3.587621	4.697316
C	-1.045878	5.118619	3.868278
H	-1.193846	4.628854	4.836023
H	-0.664574	6.124498	4.071114
H	-2.018157	5.231576	3.377990
C	0.241742	5.187026	1.730146
H	-0.669570	5.353946	1.151415
H	0.642205	6.165084	2.018813
H	0.977726	4.713745	1.075214
C	4.018335	-3.325890	3.451050
F	3.868401	-4.654355	3.647353
F	5.335373	-3.108211	3.227466
F	3.705963	-2.703094	4.607011
C	2.139052	-4.020368	-1.143741

(*Z*)-**1a** • (*E*)-**1a**:

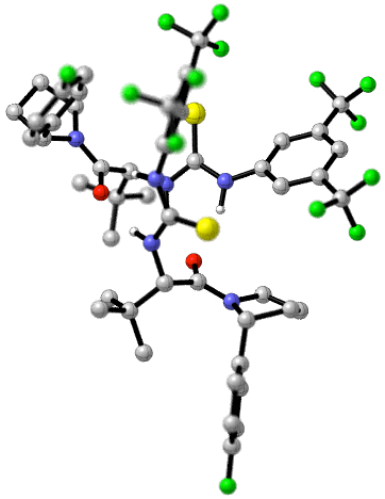

Charge: 0
Spin Multiplicity: 1
Solvation: gas phase
Electronic Energy (AU): -4609.96147851
Gibbs Free Energy at 298.150 K (AU): -4609.104329

S	-2.260738	1.435177	-2.768165
F	-5.251539	-2.346836	3.674519
F	2.170758	5.589231	1.874592
F	2.349650	3.432956	2.142059
F	3.720878	4.482970	0.824907
O	-1.159130	-2.779512	-1.542161
N	-3.215247	-2.739126	-2.480324
N	-0.424795	-0.526218	-2.952529
H	0.454750	-0.917845	-2.621581
N	0.330760	1.357463	-1.954550
H	1.148273	0.767216	-1.794958
C	-3.889575	-4.234926	0.898837
H	-3.438944	-5.205905	0.709754
C	-4.286002	-3.912201	2.195353
H	-4.149997	-4.601296	3.021617
C	-4.864606	-2.668615	2.424464
C	-5.041598	-1.745401	1.402377
H	-5.475880	-0.776184	1.613407
C	-4.627342	-2.082374	0.113408
H	-4.738120	-1.343440	-0.673632
C	-4.059534	-3.333726	-0.161632
C	-3.722548	-3.795616	-1.572997
H	-2.954947	-4.570296	-1.501570
C	-4.967049	-4.293334	-2.345265
H	-5.682267	-4.795701	-1.690811
H	-4.654196	-5.003875	-3.119219
C	-5.524850	-3.015330	-2.988462
H	-6.107784	-2.447362	-2.258407
H	-6.173250	-3.216219	-3.844700
C	-4.263759	-2.236256	-3.401452
H	-4.373036	-1.152439	-3.298383
H	-4.001248	-2.458387	-4.436930

C	-1.913083	-2.375387	-2.448881
C	-1.368353	-1.448519	-3.559383
H	-2.183209	-0.834348	-3.945480
C	-0.733074	0.738310	-2.557956
C	0.462042	2.688136	-1.506247
C	-0.079570	3.783464	-2.192322
H	-0.690591	3.625194	-3.069465
C	0.160695	5.074401	-1.725604
C	0.954728	5.302629	-0.600948
H	1.133814	6.310428	-0.247844
C	1.498471	4.208957	0.068788
C	1.241889	2.907322	-0.363605
H	1.616554	2.061976	0.205542
C	-0.699711	-2.190109	-4.782178
C	-0.265221	-1.115190	-5.800126
H	0.488790	-0.445072	-5.380401
H	0.163298	-1.593414	-6.687248
H	-1.115070	-0.504689	-6.123567
C	0.527627	-3.013088	-4.355086
H	0.258981	-3.804315	-3.651320
H	0.977821	-3.482581	-5.236243
H	1.299220	-2.393024	-3.890684
C	-1.703731	-3.132064	-5.472738
H	-2.538695	-2.578941	-5.914241
H	-1.203360	-3.662918	-6.288877
H	-2.104188	-3.888273	-4.790041
C	-0.375804	6.251034	-2.500481
F	-0.625110	7.306882	-1.695083
F	0.512228	6.671100	-3.433681
F	-1.517815	5.951522	-3.150267
C	2.423081	4.430242	1.235211
S	1.371109	-0.225430	2.391574
F	9.556100	-3.206939	1.617296
F	-3.915213	2.951397	0.154438
F	-5.513691	1.590583	0.717059
F	-5.001748	3.259401	2.017154
O	2.387039	-0.844541	-1.743501
N	4.117044	-0.328551	-0.391660
N	1.087329	-2.018746	0.395903
H	0.515833	-2.360021	-0.375014
N	-0.839335	-1.003668	1.057534
H	-1.252499	-1.526393	0.287670
C	6.432030	-1.514625	2.333851
H	5.790184	-1.301626	3.184879
C	7.608516	-2.235896	2.534023
H	7.898372	-2.592184	3.516421
C	8.418126	-2.504957	1.437060
C	8.083335	-2.077961	0.157814
H	8.737438	-2.314486	-0.674309
C	6.903141	-1.356482	-0.021489
H	6.627752	-1.040474	-1.022444
C	6.061455	-1.063385	1.059321
C	4.803216	-0.218454	0.924501
H	4.095420	-0.481660	1.713134
C	5.110373	1.296541	0.998155
H	5.933830	1.510154	1.683058
H	4.223800	1.823840	1.359668
C	5.414953	1.683174	-0.455257
H	5.263772	2.749239	-0.637661
H	6.451155	1.441067	-0.710319
C	4.435972	0.825811	-1.269731
H	4.839552	0.479400	-2.225747
H	3.512243	1.368738	-1.489597
C	3.028792	-1.076741	-0.695862
C	2.530002	-2.182695	0.265917
H	2.947803	-2.013650	1.257453
C	0.510627	-1.121895	1.239404
C	-1.723693	-0.206463	1.832218
C	-1.816019	-0.376875	3.217653
H	-1.167608	-1.084268	3.717408
C	-2.739038	0.369720	3.945301
C	-3.585225	1.277949	3.306021
H	-4.302165	1.854221	3.877309
C	-3.492510	1.433969	1.925666
C	-2.557702	0.705336	1.184081
H	-2.480909	0.851294	0.110351
C	2.887482	-3.658086	-0.135998
C	2.347450	-4.588409	0.970451
H	1.259170	-4.529732	1.053066
H	2.615908	-5.626187	0.746476
H	2.773398	-4.335280	1.947281
C	4.414674	-3.821782	-0.213343
H	4.899638	-3.577707	0.735451
H	4.659135	-4.861196	-0.455499
H	4.857331	-3.190689	-0.989272
C	2.280900	-4.069352	-1.488101
H	2.653311	-3.442009	-2.300706
H	2.556135	-5.106605	-1.708131
H	1.188821	-4.017004	-1.489515
C	-2.892668	0.123436	5.423571
F	-3.340683	1.222362	6.070031
F	-3.782133	-0.867112	5.666640
F	-1.727774	-0.243504	5.997601
C	-4.470344	2.321962	1.204805

[(*E*)-**1a**]$_2$:

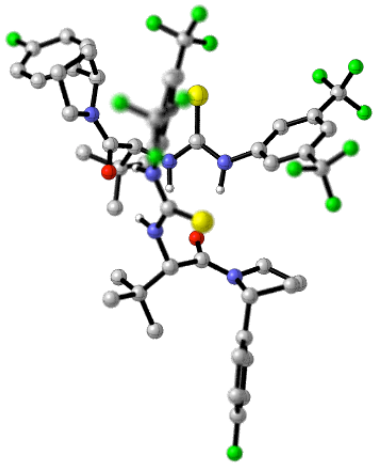

Charge: 0
Spin Multiplicity: 1
Solvation: gas phase
Electronic Energy (AU): -4609.96180125
Gibbs Free Energy at 298.150 K (AU): -4609.106837

S	-2.575706	0.737241	-2.058246
F	-9.324499	-4.347738	-1.185374
F	3.185356	5.244257	-1.614162
F	2.827532	3.832880	0.006670
F	4.266863	3.359064	-1.550055
O	-1.698721	-2.250054	1.133360
N	-3.856664	-1.614712	0.964300
N	-1.342015	-1.606918	-1.542363
H	-0.476858	-2.079311	-1.290802
N	0.052159	0.105392	-2.065308
H	0.775384	-0.570927	-1.813497
C	-6.869897	-1.681116	-1.278496
H	-6.595593	-0.839014	-1.908960
C	-7.949811	-2.483453	-1.647817
H	-8.521341	-2.289826	-2.549148
C	-8.286811	-3.559976	-0.836096
C	-7.576914	-3.854430	0.322448
H	-7.864356	-4.709859	0.924318
C	-6.502002	-3.039595	0.675344
H	-5.929859	-3.283988	1.564564
C	-6.132250	-1.942869	-0.115284
C	-5.015927	-0.983923	0.270076
H	-4.652166	-0.473202	-0.624935
C	-5.479787	0.064184	1.312745
H	-6.528449	0.334869	1.172143
H	-4.878511	0.971484	1.208591
C	-5.198818	-0.608968	2.662516
H	-5.991514	-1.320769	2.912383
H	-5.126293	0.106758	3.484955
C	-3.868915	-1.331557	2.421017
H	-3.751821	-2.258010	2.989963
H	-3.017988	-0.688671	2.669805
C	-2.697978	-2.047424	0.410701
C	-2.579081	-2.252146	-1.117420
H	-3.388995	-1.725792	-1.621209
C	-1.244135	-0.294566	-1.886365
C	0.498584	1.387368	-2.471692
C	0.024387	1.982517	-3.648741
H	-0.731707	1.483068	-4.239022
C	0.522097	3.220179	-4.042829
C	1.501550	3.873398	-3.288576
H	1.878057	4.841137	-3.596394
C	1.974494	3.271736	-2.127605
C	1.472725	2.034155	-1.708471
H	1.814431	1.595712	-0.774845
C	-2.614889	-3.745859	-1.610476
C	-2.599106	-3.724967	-3.153113
H	-1.693198	-3.250982	-3.539849
H	-2.639244	-4.748514	-3.540075
H	-3.461897	-3.181166	-3.552675
C	-1.415655	-4.562162	-1.098933
H	-1.390434	-4.596997	-0.007969
H	-1.490833	-5.589663	-1.470698
H	-0.459501	-4.164395	-1.451439
C	-3.909697	-4.428483	-1.139202
H	-4.799577	-3.911503	-1.505644
H	-3.939997	-5.454910	-1.519524
H	-3.973237	-4.481073	-0.048016
C	0.060964	3.850799	-5.331345
F	-0.138934	5.179355	-5.187748
F	0.987394	3.700525	-6.308840
F	-1.086728	3.309193	-5.784833
C	3.055608	3.935109	-1.315286
S	2.565281	0.710976	2.071993
F	9.352262	-4.359014	1.088564
F	-2.813555	3.822647	0.024728
F	-4.269828	3.320159	1.556504
F	-3.193602	5.206252	1.664477
O	1.713583	-2.197377	-1.156887
N	3.872130	-1.570370	-0.963603
N	1.346285	-1.635819	1.533623
H	0.483945	-2.109350	1.274524
N	-0.058215	0.063530	2.072532
H	-0.777214	-0.614953	1.815156
C	6.893636	-1.701227	1.268595
H	6.622257	-0.876301	1.922433
C	7.977092	-2.510904	1.609571
H	8.554404	-2.340241	2.511726
C	8.310540	-3.564678	0.767294
C	7.593444	-3.829511	-0.393762
H	7.878630	-4.667916	-1.019989
C	6.514886	-3.007448	-0.718178
H	5.937436	-3.227954	-1.610047
C	6.148887	-1.932943	0.103617
C	5.030473	-0.963364	-0.248056
H	4.666283	-0.483690	0.663797
C	5.493744	0.120762	-1.253408
H	6.541584	0.388753	-1.102390
H	4.890066	1.022669	-1.119850

C	5.215826	-0.506977	-2.625510
H	5.142948	0.236482	-3.423114
H	6.010199	-1.208390	-2.898109
C	3.887118	-1.240006	-2.410453
H	3.773439	-2.147673	-3.009694
H	3.035052	-0.591554	-2.639352
C	2.711226	-2.016878	-0.426006
C	2.586496	-2.265839	1.095414
H	3.393881	-1.753570	1.617672
C	1.240325	-0.327310	1.889579
C	-0.510223	1.340128	2.490786
C	-0.046034	1.920631	3.679026
H	0.705575	1.413558	4.268724
C	-0.547761	3.152634	4.085586
C	-1.521301	3.815083	3.331684
H	-1.901209	4.778252	3.649263
C	-1.983976	3.228280	2.158872
C	-1.478423	1.996389	1.728029
H	-1.813396	1.569675	0.786583
C	2.623264	-3.772638	1.545660
C	2.592774	-3.796849	3.088068
H	1.681208	-3.337990	3.479725
H	2.633579	-4.831205	3.445029
H	3.449359	-3.261496	3.511642
C	3.925733	-4.435767	1.067820
H	4.809887	-3.923060	1.453907
H	3.958820	-5.471094	1.422545
H	3.998173	-4.460505	-0.023764
C	1.432697	-4.579025	0.999616
H	1.418248	-4.583660	-0.092096
H	1.508461	-5.616182	1.343322
H	0.471324	-4.195336	1.353230
C	-0.099914	3.764594	5.387763
F	0.086800	5.097469	5.270717
F	-1.029578	3.585693	6.357447
F	1.050889	3.226249	5.837110
C	-3.057374	3.902509	1.345340

Alternative Geometry Located by Calculations (B3LYP/6-31G(d,p)) in the Gas Phase: Type II Dimers

[(*Z*)-**1a**]$_2$:

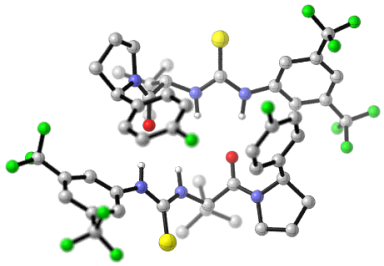

Charge: 0
Spin Multiplicity: 1
Solvation: gas phase
Electronic Energy (AU): -4609.97070747
Gibbs Free Energy at 298.150 K (AU): -4609.111634

O	1.601867	1.271634	1.529048
C	1.219006	2.450587	1.393268
C	0.001929	2.943916	2.195699
H	-0.343959	3.903220	1.812749
N	-1.084212	2.008787	1.925848
C	-2.248453	2.334746	1.289361
N	-3.012652	1.226659	1.034310
H	-2.608927	0.322718	1.287180
C	0.289890	3.137235	3.728588
H	-0.850969	1.023474	1.998094
C	1.470906	4.112561	3.901503
H	1.669659	4.271402	4.966079
H	2.393634	3.730933	3.451141
H	1.251139	5.092290	3.463868
C	-0.966097	3.753131	4.375593
H	-1.832594	3.095163	4.268042
H	-0.793785	3.912867	5.445345
H	-1.222324	4.715335	3.922513
C	0.619300	1.811850	4.436234
H	1.503272	1.330133	4.012044
H	0.805683	1.997418	5.499416
H	-0.219362	1.113029	4.372087
S	-2.692297	3.919897	0.912926
N	1.813545	3.310985	0.539147
C	1.450757	4.736729	0.326768
C	2.993007	2.916067	-0.263492
C	2.416486	5.201618	-0.773622
H	0.400805	4.835655	0.038950
C	3.632004	4.282748	-0.596619
H	3.657881	2.319018	0.363270
H	1.968357	5.049072	-1.760189
H	4.270239	4.229492	-1.480491
H	4.247587	4.612325	0.247798
H	2.658764	6.262596	-0.677060
H	1.610118	5.302788	1.249682

C	2.639217	2.106876	-1.506610
C	3.649189	1.354553	-2.122653
C	1.362852	2.113325	-2.079867
C	3.394299	0.596599	-3.263775
H	4.647851	1.351236	-1.696963
C	1.090720	1.378129	-3.234592
H	0.559566	2.676350	-1.615503
C	2.110627	0.621375	-3.795478
H	4.161862	-0.021284	-3.716181
H	0.107806	1.369555	-3.691077
C	-4.294085	1.118192	0.465953
C	-4.764498	1.921115	-0.583566
C	-5.094304	0.068737	0.932961
C	-6.011623	1.655063	-1.144796
H	-4.157753	2.734581	-0.953479
C	-6.329818	-0.197804	0.343275
H	-4.741787	-0.544100	1.755881
C	-6.805539	0.596093	-0.696779
H	-7.768961	0.396392	-1.148828
O	-1.601471	-1.270910	1.528925
C	-1.218898	-2.450031	1.393805
C	-0.001856	-2.943151	2.196414
H	0.344039	-3.902565	1.813740
N	1.084281	-2.008086	1.926326
C	2.248520	-2.334221	1.289926
N	3.012688	-1.226195	1.034522
H	2.608978	-0.322194	1.287208
C	-0.289841	-3.136043	3.729354
H	0.850950	-1.022762	1.998151
C	-1.470581	-4.111656	3.902529
H	-1.669449	-4.270076	4.967147
H	-2.393363	-3.730532	3.451848
H	-1.250429	-5.091511	3.465372
C	0.966280	-3.751372	4.376637
H	1.832566	-3.093137	4.269043
H	0.793893	-3.910927	5.446404
H	1.222876	-4.713590	3.923798
C	-0.619660	-1.810513	4.436541
H	-1.503811	-1.329223	4.012235
H	-0.805933	-1.995765	5.499797
H	0.218764	-1.111436	4.372104
S	2.692380	-3.919481	0.913972
N	-1.813724	-3.310790	0.540250
C	-1.451223	-4.736708	0.328585
C	-2.993163	-2.916055	-0.262519
C	-2.417076	-5.201958	-0.771542
H	-0.401299	-4.835988	0.040786
C	-3.632425	-4.282790	-0.594916
H	-3.657896	-2.318573	0.363982
H	-1.968963	-5.049952	-1.758200
H	-4.270707	-4.229862	-1.478772
H	-4.248010	-4.611840	0.249706
H	-2.659532	-6.262847	-0.674466
H	-1.610676	-5.302268	1.251789
C	-2.639318	-2.107559	-1.506072
C	-3.649188	-1.355319	-2.122380
C	-1.363026	-2.114607	-2.079485
C	-3.394264	-0.598020	-3.263930
H	-4.647798	-1.351548	-1.696571
C	-1.090864	-1.380074	-3.234624
H	-0.559817	-2.677592	-1.614938
C	-2.110666	-0.623378	-3.795779
H	-4.161744	0.019797	-3.716567
H	-0.108003	-1.371965	-3.691234
C	4.294132	-1.117875	0.466171
C	4.764586	-1.921102	-0.583101
C	5.094329	-0.068282	0.932902
C	6.011724	-1.655201	-1.144369
H	4.157856	-2.734676	-0.952800
C	6.329869	0.198088	0.343186
H	4.741779	0.544795	1.755628
C	6.805626	-0.596101	-0.696624
H	7.769061	-0.396530	-1.148702
C	-6.464636	2.446086	-2.344728
C	-7.081802	-1.423415	0.780788
C	6.464776	-2.446549	-2.344071
C	7.081841	1.423811	0.780401
F	-5.913643	3.672677	-2.389265
F	-6.120878	1.813845	-3.498994
F	-7.806527	2.593154	-2.371274
F	-7.062302	-1.581254	2.121489
F	-8.367993	-1.411399	0.384539
F	-6.512800	-2.545279	0.253666
F	1.833276	-0.143809	-4.877400
F	5.913748	-3.673136	-2.388321
F	6.121097	-1.814594	-3.498517
F	7.806664	-2.593665	-2.370509
F	8.368022	1.411732	0.384118
F	6.512803	2.545548	0.253043
F	7.062376	1.581953	2.121066
F	-1.833277	0.141166	-4.878147

(*Z*)-**1a** • (*E*)-**1a**:

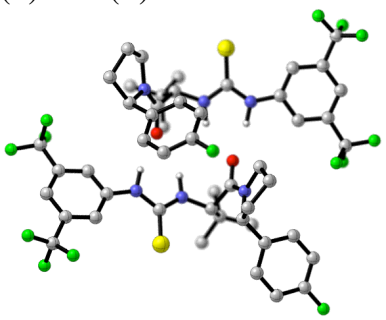

Charge: 0
Spin Multiplicity: 1
Solvation: gas phase
Electronic Energy (AU): -4609.96985776
Gibbs Free Energy at 298.150 K (AU): -4609.115538

O	1.477870	0.500006	0.969593
C	1.045313	1.636163	0.677317
C	0.000339	2.293703	1.596210
H	-0.288540	3.271423	1.216061
N	-1.188566	1.448345	1.487905
C	-2.390644	1.831700	0.963659
N	-3.219293	0.749309	0.793853
H	-2.763189	-0.156033	0.915744
C	0.475938	2.512675	3.075325
H	-1.020139	0.450101	1.581030
C	1.807929	3.286245	3.057569
H	2.116469	3.518433	4.081919
H	2.612704	2.703394	2.597463
H	1.719925	4.231764	2.514051
C	-0.593134	3.366819	3.786149
H	-1.566601	2.868489	3.787908
H	-0.299921	3.540547	4.826934
H	-0.718798	4.339513	3.301106
C	0.656873	1.196863	3.853346
H	1.422072	0.561491	3.403775
H	0.957491	1.420300	4.882457
H	-0.279334	0.632169	3.905907
S	-2.775715	3.435017	0.602299
N	1.412708	2.250619	-0.463362
C	2.241576	1.525058	-1.455194
C	0.902488	3.542100	-0.994762
C	2.288510	2.454809	-2.677573
H	3.235215	1.318608	-1.053217
C	1.044785	3.340085	-2.522059
H	-0.154003	3.648964	-0.739604
H	3.199730	3.059924	-2.659957
H	1.123447	4.293445	-3.048770
H	0.163223	2.815169	-2.901725
H	2.276586	1.892860	-3.613846
H	1.760858	0.565813	-1.672913
C	1.655986	4.755164	-0.466765
C	0.954497	5.956082	-0.290189
C	3.030401	4.734078	-0.188489
C	1.600160	7.114611	0.140372
H	-0.114582	5.984993	-0.483410
C	3.691561	5.883530	0.243904
H	3.600704	3.816157	-0.289360
C	2.964377	7.057883	0.398076
H	1.063215	8.045578	0.285083
H	4.753171	5.877134	0.465153
C	-4.569074	0.623907	0.438367
C	-5.376882	1.625860	-0.122103
C	-5.123729	-0.652201	0.642334
C	-6.694807	1.328393	-0.473907
H	-4.971294	2.614378	-0.282502
C	-6.429725	-0.935294	0.256469
H	-4.523484	-1.424262	1.112291
C	-7.235524	0.054009	-0.304925
H	-8.253195	-0.161217	-0.603102
O	-1.579829	-1.627013	0.964751
C	-1.238182	-2.802808	0.721956
C	-0.170175	-3.473903	1.601701
H	0.122082	-4.435154	1.181335
N	1.014591	-2.626645	1.501053
C	2.180494	-2.988769	0.877620
N	2.996385	-1.903184	0.695029
H	2.546034	-1.000116	0.856865
C	-0.628091	-3.742037	3.076892
H	0.846641	-1.631841	1.624963
C	-1.928905	-4.568414	3.043085
H	-2.240675	-4.818635	4.061915
H	-2.754128	-4.019798	2.575709
H	-1.792557	-5.512155	2.503105
C	0.475549	-4.564594	3.770325
H	1.424785	-4.022171	3.784628
H	0.190175	-4.775463	4.806380
H	0.646245	-5.518723	3.262382
C	-0.864988	-2.447235	3.874231
H	-1.653146	-1.834388	3.431951
H	-1.159233	-2.695867	4.899370
H	0.046668	-1.845326	3.936189
S	2.525738	-4.576917	0.420632
N	-1.724907	-3.477650	-0.339573
C	-1.475436	-4.900463	-0.683657
C	-2.640912	-2.818709	-1.300086
C	-2.143247	-5.066131	-2.056648
H	-0.404816	-5.118095	-0.708128
C	-3.265988	-4.020502	-2.044494
H	-3.408846	-2.276363	-0.746470
H	-1.426477	-4.844494	-2.853421
H	-3.611982	-3.744869	-3.042782
H	-4.129032	-4.381539	-1.475229
H	-2.506288	-6.084995	-2.210574
H	-1.944877	-5.549035	0.064269
C	-1.919124	-1.829463	-2.208055
C	-2.620559	-0.722202	-2.703625
C	-0.582792	-2.001636	-2.591161
C	-2.010986	0.199835	-3.553458
H	-3.655342	-0.565643	-2.411879

C	0.044066	-1.092356	-3.444137
H	-0.007104	-2.837319	-2.206673
C	-0.682739	-0.002934	-3.905800
H	-2.543750	1.066819	-3.928071
H	1.077828	-1.219841	-3.746610
C	4.327200	-1.757368	0.278285
C	5.151067	-2.759631	-0.256468
C	4.842402	-0.456143	0.403351
C	6.445514	-2.434782	-0.666924
H	4.774890	-3.767350	-0.359294
C	6.123551	-0.148004	-0.039758
H	4.223082	0.317701	0.844234
C	6.945770	-1.135326	-0.579583
H	7.943133	-0.899740	-0.926550
C	7.338435	-3.537008	-1.180481
C	6.571736	1.284711	0.055293
C	-6.925656	-2.348594	0.398237
C	-7.565851	2.435200	-1.015379
F	-0.067299	0.906397	-4.699582
F	7.963269	-4.177573	-0.166816
F	6.644634	-4.467548	-1.868518
F	8.302290	-3.059636	-1.999728
F	6.474170	1.759553	1.316290
F	7.841068	1.460093	-0.353442
F	5.786998	2.094336	-0.714445
F	3.599145	8.170797	0.819634
F	-8.134066	3.148338	-0.018120
F	-6.862233	3.302995	-1.772379
F	-8.571208	1.951420	-1.779127
F	-8.265420	-2.435626	0.306257
F	-6.406704	-3.148233	-0.573904
F	-6.554907	-2.895500	1.577385

[(*E*)-**1a**]$_2$:

Charge: 0
Spin Multiplicity: 1
Solvation: gas phase
Electronic Energy (AU): -4609.96814830
Gibbs Free Energy at 298.150 K (AU): -4609.113292

O	-1.782486	-0.628043	0.820659
C	-1.651607	-1.824860	0.484287
C	-0.796949	-2.761242	1.357522
H	-0.779596	-3.765861	0.939854
N	0.569278	-2.252804	1.249014
C	1.623158	-2.908595	0.673887
N	2.700316	-2.071337	0.532640
H	2.495277	-1.086280	0.709101
C	-1.291603	-2.902745	2.839707
H	0.675683	-1.254910	1.410082
C	-2.779659	-3.301396	2.828421
H	-3.122059	-3.490665	3.850859
H	-3.410393	-2.507495	2.414759
H	-2.951008	-4.211551	2.245608
C	-0.471119	-4.031677	3.495454
H	0.599447	-3.808939	3.479352
H	-0.775125	-4.155527	4.540175
H	-0.619692	-4.986843	2.982642
C	-1.112201	-1.614474	3.663178
H	-1.697420	-0.787938	3.256039
H	-1.440144	-1.792042	4.692883
H	-0.061968	-1.309612	3.707156
S	1.568583	-4.534702	0.222887
N	-2.178567	-2.284917	-0.667840
C	-2.826398	-1.341845	-1.609117
C	-1.994883	-3.635048	-1.264239
C	-3.120583	-2.185474	-2.858280
H	-3.732035	-0.917178	-1.172655
C	-2.101584	-3.329539	-2.777689
H	-0.990736	-3.999666	-1.036934
H	-4.140771	-2.578134	-2.818054
H	-2.392630	-4.213210	-3.349218
H	-1.123315	-2.996437	-3.141863
H	-3.030132	-1.598914	-3.775652
H	-2.135989	-0.515260	-1.810409
C	-3.008109	-4.660537	-0.775069
C	-2.605029	-5.998705	-0.662613
C	-4.338367	-4.332916	-0.473765

C	-3.501006	-6.993747	-0.273547
H	-1.573056	-6.266382	-0.873076
C	-5.247314	-5.315933	-0.082825
H	-4.680484	-3.304063	-0.524402
C	-4.813273	-6.633276	0.007315
H	-3.195148	-8.029756	-0.178558
H	-6.277007	-5.073005	0.155290
C	4.025676	-2.264434	0.119303
C	4.564765	-3.432485	-0.442447
C	4.858098	-1.143102	0.270662
C	5.897429	-3.440520	-0.856745
H	3.942951	-4.307609	-0.563089
C	6.173837	-1.162177	-0.179300
H	4.460903	-0.246220	0.734268
C	6.713751	-2.313660	-0.748124
H	7.736278	-2.332403	-1.101744
O	1.782502	0.628046	0.820679
C	1.651614	1.824859	0.484298
C	0.796952	2.761243	1.357527
H	0.779600	3.765861	0.939857
N	-0.569274	2.252805	1.249014
C	-1.623154	2.908596	0.673885
N	-2.700308	2.071336	0.532630
H	-2.495267	1.086276	0.709081
C	1.291601	2.902750	2.839714
H	-0.675681	1.254911	1.410086
C	2.779655	3.301407	2.828431
H	3.122051	3.490678	3.850870
H	3.410393	2.507509	2.414771
H	2.951001	4.211563	2.245618
C	0.471110	4.031678	3.495457
H	-0.599456	3.808935	3.479352
H	0.775112	4.155530	4.540179
H	0.619680	4.986844	2.982646
C	1.112202	1.614478	3.663184
H	1.697424	0.787944	3.256046
H	1.440143	1.792047	4.692890
H	0.061970	1.309612	3.707160
S	-1.568580	4.534704	0.222890
N	2.178568	2.284912	-0.667834
C	2.826403	1.341838	-1.609106
C	1.994878	3.635038	-1.264241
C	3.120583	2.185462	-2.858273
H	3.732043	0.917178	-1.172642
C	2.101579	3.329521	-2.777688
H	0.990729	3.999654	-1.036936
H	4.140769	2.578127	-2.818050
H	2.392620	4.213192	-3.349223
H	1.123311	2.996412	-3.141860
H	3.030135	1.598896	-3.775643
H	2.135999	0.515248	-1.810394
C	3.008099	4.660535	-0.775076
C	2.605014	5.998701	-0.662626
C	4.338358	4.332920	-0.473771
C	3.500987	6.993749	-0.273566
H	1.573039	6.266372	-0.873090
C	5.247302	5.315943	-0.082837
H	4.680481	3.304068	-0.524404
C	4.813255	6.633285	0.007297
H	3.195125	8.029757	-0.178582
H	6.276997	5.073021	0.155279
C	-4.025670	2.264433	0.119296
C	-4.564762	3.432486	-0.442447
C	-4.858090	1.143098	0.270650
C	-5.897426	3.440521	-0.856742
H	-3.942949	4.307611	-0.563085
C	-6.173830	1.162174	-0.179309
H	-4.460893	0.246215	0.734252
C	-6.713746	2.313660	-0.748126
H	-7.736274	2.332403	-1.101744
C	-6.967654	-0.110985	-0.073844
C	-6.483327	4.719886	-1.401091
C	6.483328	-4.719883	-1.401101
C	6.967663	0.110980	-0.073830
F	-5.688098	-7.586129	0.387898
F	5.553693	-5.481658	-2.013092
F	7.028036	-5.470094	-0.416939
F	7.465214	-4.475359	-2.298480
F	8.245592	-0.039029	-0.464829
F	6.974312	0.598326	1.185850
F	6.421975	1.089771	-0.854483
F	-6.421966	-1.089771	-0.854500
F	-6.974301	-0.598336	1.185835
F	-8.245584	0.039024	-0.464842
F	-7.465217	4.475365	-2.298468
F	-7.028033	5.470093	-0.416924
F	-5.553695	5.481665	-2.013081
F	5.688076	7.586143	0.387875

Monomeric Catalysts (B3LYP/6-31G(d,p) gas phase)

(*Z*)-1a

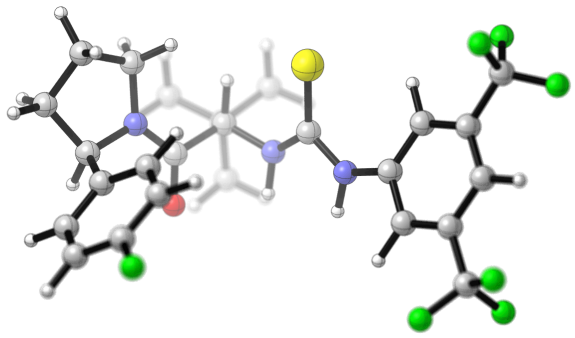

Charge: 0
Spin Multiplicity: 1
Solvation: gas phase
Electronic Energy (AU): -2304.96413243
Gibbs Free Energy at 298.150 K (AU): -2304.551718

S	0.053824	-1.972797	-1.333915
F	-1.748105	5.658045	-0.699932
F	5.808747	2.709880	0.954869
F	3.988994	2.927447	2.136890
F	5.543204	1.549119	2.772421
O	-3.179783	-0.115320	1.778570
N	-3.946087	-0.382425	-0.338809
N	-1.055020	-1.706658	1.105211
H	-1.106298	-1.143469	1.949747
N	1.067310	-0.918839	0.954778
H	0.856661	-0.608447	1.895071
C	-4.404373	3.334231	0.123272
H	-5.380970	3.340594	0.601053
C	-3.696848	4.529385	0.011919
H	-4.094799	5.465520	0.388050
C	-2.443701	4.505974	-0.589780
C	-1.885549	3.329695	-1.072030
H	-0.901052	3.349016	-1.526656
C	-2.611203	2.143222	-0.952867
H	-2.169184	1.218741	-1.310994
C	-3.878716	2.128479	-0.360113
C	-4.730804	0.866494	-0.268622
H	-5.265472	0.887057	0.685236
C	-5.702376	0.706147	-1.461979
H	-6.063587	1.668559	-1.830499
H	-6.569464	0.112510	-1.149738
C	-4.871317	-0.069459	-2.494465
H	-4.179651	0.607312	-3.005796
H	-5.479586	-0.564647	-3.255365
C	-4.090166	-1.076164	-1.636815
H	-3.113846	-1.324518	-2.062751
H	-4.659318	-2.004632	-1.512118
C	-3.226249	-0.783025	0.740159
C	-2.393401	-2.077745	0.643669
H	-2.282831	-2.403262	-0.390016
C	0.020818	-1.516318	0.285757
C	2.356937	-0.541481	0.528541
C	3.077902	-1.207092	-0.471633
H	2.635163	-2.041579	-0.994488
C	4.367078	-0.778104	-0.786578
C	4.967237	0.285962	-0.114642
H	5.971187	0.603354	-0.366630
C	4.250643	0.930366	0.892273
C	2.955435	0.528327	1.208609
H	2.404553	1.059232	1.978895
C	-2.978265	-3.272955	1.474304
C	-2.114488	-4.516867	1.189774
H	-1.072085	-4.349401	1.474653
H	-2.487210	-5.374361	1.760131
H	-2.132799	-4.783261	0.127733
C	-2.975153	-2.983514	2.988097
H	-3.544845	-2.084297	3.231744
H	-3.412907	-3.831484	3.525409
H	-1.955735	-2.854226	3.367070
C	-4.422856	-3.547410	1.014065
H	-4.465508	-3.789031	-0.053576
H	-4.831447	-4.404770	1.558401
H	-5.083023	-2.694409	1.203008
C	5.111748	-1.453535	-1.911218
F	4.875266	-0.845613	-3.094942
F	6.448208	-1.420087	-1.711236
F	4.751830	-2.746425	-2.049034
C	4.898404	2.034617	1.686459

(*E*)-**1a**

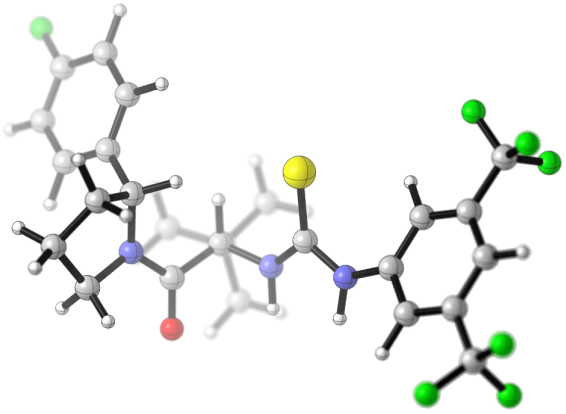

Charge: 0
Spin Multiplicity: 1
Solvation: gas phase
Electronic Energy (AU): -2304.96329425
Gibbs Free Energy at 298.150 K (AU): -2304.550712

S	-0.093848	1.276040	-0.085486
F	7.621207	2.935018	-0.563307
F	-7.085070	-1.489950	-1.564513
F	-5.568221	-3.019609	-1.226307
F	-6.815605	-2.340930	0.416884
O	2.277053	-3.058624	0.934492
N	3.157114	-1.729960	-0.671619
N	0.527689	-0.893193	1.380226
H	0.279194	-1.819567	1.710372
N	-1.676989	-0.706699	0.873065
H	-1.705168	-1.645797	1.249747
C	4.278420	1.792460	-1.374245
H	3.322132	2.204574	-1.685327
C	5.357491	2.652144	-1.173579
H	5.268238	3.722795	-1.321200
C	6.570667	2.112098	-0.763436
C	6.729301	0.749375	-0.542441
H	7.688872	0.368331	-0.210367
C	5.637710	-0.094901	-0.747838
H	5.746693	-1.156499	-0.551410
C	4.401898	0.410436	-1.172268
C	3.208175	-0.485078	-1.476770
H	2.293364	0.092515	-1.319235

C	3.226868	-1.041643	-2.924131
H	3.672917	-0.334817	-3.627135
H	2.196871	-1.235832	-3.243796
C	4.001383	-2.360488	-2.801416
H	5.078524	-2.167002	-2.774224
H	3.809476	-3.046753	-3.630064
C	3.519177	-2.927615	-1.460861
H	4.274514	-3.518570	-0.935001
H	2.634188	-3.564617	-1.570987
C	2.500366	-1.921879	0.505296
C	1.977286	-0.702807	1.292599
H	2.134660	0.226548	0.748356
C	-0.419450	-0.150637	0.747906
C	-2.931726	-0.253057	0.415245
C	-3.295022	1.099660	0.373262
H	-2.583375	1.861617	0.654680
C	-4.573254	1.452505	-0.055415
C	-5.509944	0.486739	-0.425560
H	-6.495735	0.775874	-0.767661
C	-5.148304	-0.856745	-0.359967
C	-3.868522	-1.227361	0.049734
H	-3.594849	-2.277782	0.064417
C	2.622686	-0.538922	2.714720
C	2.169629	0.820473	3.282612
H	1.079675	0.879034	3.357070
H	2.582925	0.965458	4.286470
H	2.508012	1.651036	2.654708
C	2.199922	-1.659619	3.685527
H	2.452018	-2.647203	3.294835
H	2.708284	-1.521296	4.645564
H	1.123391	-1.630260	3.887679
C	4.156344	-0.542926	2.575617
H	4.503140	0.228008	1.881369
H	4.616275	-0.345737	3.549476
H	4.527966	-1.511510	2.225968
C	-4.980518	2.905000	-0.048298
F	-5.855682	3.179310	-1.040701
F	-5.588246	3.237488	1.114412
F	-3.923679	3.728176	-0.193642
C	-6.156265	-1.926672	-0.689560

3.6.10 Nonlinear Effect Experiment

Procedure: An oven-dried 1-dram vial fitted with a magnetic stirbar and a cap with a PTFE-lined septum was cooled to –78 ºC under N_2 atmosphere in a dry ice/acetone bath. The vial was charged with catalysts **1a** and *ent*-**1a** as stock solutions in TBME according to Table 3.18 (750 µL, 0.01 mmol; stock solution prepared by dissolving 36.6 mg of **1a** or *ent*-**1a** up to 5 mL with TBME). After 5 minutes, the vial was charged with **3b** as a stock solution in TBME (125 µL, 0.15 mmol; solution prepared by diluting 452 mg **3b** to a volume of 2 mL with TBME). After 5 minutes, the vial was charged with **2** as a stock solution in TBME (125 µL, 0.1 mmol; solution prepared by diluting 270 mg **2** to a volume of 2 mL with TBME). This mixture was aged for 2 h at –78 ºC before the addition of sodium methoxide as a 0.5 M solution in methanol (0.2 mL, 0.1 mmol). This mixture was stirred for 5 min before warming to room temperature. The product was purified by silica gel chromatography as described previously.[13]

Table 3.18. Data used to generate Figure 3.7.

Entry	e.e. **1a** (%)[a]	**1a** stock solution (µL)	*ent*-**1a** stock solution (µL)	e.e. **4b** (%)[b]
1	100	750	0	84.3
2	80	675	75	82.4
3	60	600	150	78.6
4	40	525	225	66.0
5	20	450	300	42.2
6	0	375	375	3.4

[a]The preparations of **1a** and *ent*-**1a** are assumed to be enantiomerically pure. [b]Determined by HPLC analysis: (*S*,*S*)-Whelk-01, 2% IPA/hexane, 1 mL/min, observe at 210 nm.

3.6.11 Effect of Catalysts Bearing Extended Aromatic Substituents

Inspired by the work of Rob Knowles and Song Lin,[14d] we were interested in the effect of substituting larger aromatic groups on the pyrrolidine fragment of the catalyst. First, we examined the effect on the rate of alkylation of chloroether **2** with silyl ketene acetal **3**. We found that the expanse of the arene had very little effect on the rate of alkylation (Figure 3.37). We did find that the enantioselectivity was inversely correlated with the size of the arene: as arene size increases from 4-fluorophenyl to 1-napthyl, 9-phenanthryl, and 4-pyrenyl, e.e. drops from 85% to 82%, 67% and 64%, respectively. The analogous catalyst with a 2-phenylpyrroline fragment catalyzes the formation of product in 81% ee.

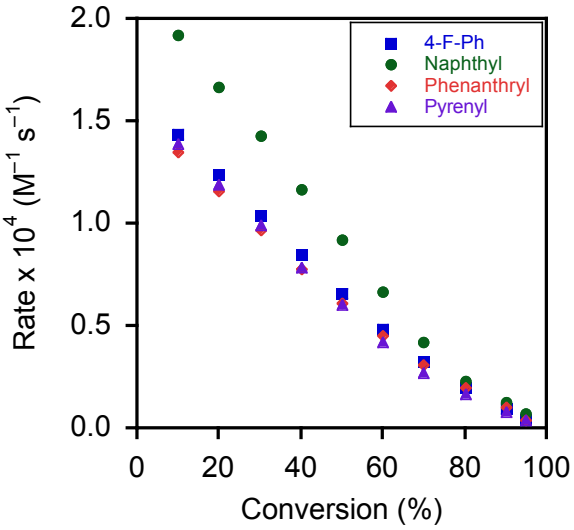

Figure 3.37. Rate of alkylation of **2** (initial concentration = 0.1 M) with **3b** (initial concentration = 0.15 M) in TBME at – 78 ºC. Reactions performed according to the procedure described above in Section 3.6.6.

On the basis of those data, we hypothesized that the larger arenes are selectively stabilizing positive charge building up in the pathway leading to the minor product, thereby leading to a decrease in enantioselectivity. Notably, the data are *not* consistent with destabilization of the pathway leading to the major product by the larger arenes; that would lead to a decrease in reaction rate with less selective catalysts. To gain more resolution on this issue,

we also measured the rate of epimerization with **2**-d_3 with catalysts bearing larger aromatic substituents. We found that while the 1-napthyl catalyst promoted epimerization at a comparable rate to **1a** (0.31 s^{-1} at 10 mM), the 9-phenanthryl catalyst was significantly faster (0.72 s^{-1} at 10 mM). This is consistent with the increased epimerization occurring *via* intermediates that are en route to the minor enantiomer of product.